IDENTIFICATION OF RECRUITED MYELOID CELLS IMPORTANT FOR THE DEVELOPMENT OF HEPATIC METASTASIS

Dr Alex Gordon-Weeks

Brasenose College

A thesis submitted to the Medical Sciences Division of the University of Oxford in partial fulfillment of the requirements for the degree of Doctor of Philosophy

Gray Institute for Radiation Oncology and Biology

Department of Oncology

University of Oxford

Trinity 2014

Word count: 36,068

ABSTRACT

IDENTIFICATION OF RECRUITED MYELOID CELLS IMPORTANT FOR THE DEVELOPMENT OF HEPATIC METASTASIS

Submitted for the degree of Doctor of Philosophy

Dr Alex Gordon-Weeks, Brasenose College, Trinity Term 2014

Hepatic metastases are a frequent cause of mortality in colon cancer patients. Many patients with hepatic metastasis have large tumour burden, signaling the need for therapies capable of down-staging metastatic disease. Research evidence indicates that immune cells promote the metastasis of various primary cancers. We wish to determine whether immune cells play a role in the promotion of hepatic colon cancer metastasis.

Using the well-characterised method of intrasplenic tumour cell injection, we developed hepatic metastases in both immunocompetent and immunoincompetent mice using a range of murine and human cancer cell lines. We analysed the immune cell infiltrates associated with hepatic metastases using flow cytometry and identified chemokines responsible for their recruitment using targeted protein arrays. The effect of immune cell depletion or inhibition of immune cell recruitment was determined using various *in-vivo* imaging techniques.

Hepatic metastases developed using the murine colon cancer cell line MC38 were associated with $CD11b^{+}/Gr1^{mid}/CCR2^{+}$ monocytes, the recruitment of which was delayed by inhibition of tumour-derived CCL2. In contrast, human HT29, HCT-116 and LoVo hepatic metastases in SCID mice were associated with infiltrates of $CD45^{+}/CXCR2^{+}$ neutrophils recruited in response to tumour-derived Macrophage Inhibitory Factor (MIF). Depletion of $Gr1^{mid}$ cells in CD11b-DTR transgenic mice delayed MC38 metastasis development, whilst neutrophil depletion using anti-Ly6G antibodies significantly inhibited the growth of HT29, HCT-116 and LoVo hepatic metastases. The neutrophils recruited to HT29, HCT-116 and LoVo hepatic metastases promoted angiogenesis, potentially through the expression of fibtroblast growth factor-2. This work demonstrates a role for myeloid cells in the development of hepatic metastasis from colon cancer and in doing so identifies various potential therapeutic targets.

ACKNOWLEDGMENTS

First, I would like to thank Professor Ruth Muschel for the continual support and advice that has been so invaluable throughout this research project. I have also been fortunate enough to be blessed with a co-supervisor in Dr Su Lim Yin (Esther) who has a remarkable eye for detail, as well as the perseverance and foresight required to help me succeed in the lab. Esther has taught me the majority of the laboratory techniques demonstrated in this thesis and it has been a pleasure to be her student. Another friend and fellow surgeon, Dr Lei Zhao helped me immensely in the first year of the DPhil, whilst Mr Michael Silva, consultant hepatobiliary surgeon at the Churchill hospital, Oxford provided guidance throughout.

The work in the first results chapter (chapter 3) is an amalgamation of work recently published. This work was performed in equal measure by Esther, Lei Zhao and myself and for this we shared joint first name authorship (Zhao et al., 2013). Although it is difficult to formally identify who was responsible for each piece of work, as often we were all working on the same experiment at once, I have attempted to indicate the relevant contributions of each person on the following page. The work presented in chapters 4 and 5 is entirely my own.

Finally, immense thanks must also go to various members of my family. First, my wife Sarah and 2-year-old son Max. They have both been a supportive influence at home and exceedingly patient during the frequent nights and weekend that I have spent in the lab. Also my parents Ruth and Phillip, who as fellow scientists, continually provide encouragement and sound advice as well as an understanding of the immense undertaking that is the DPhil. In particular, my father, who has kindly taken the time to proofread this thesis.

This project was funded in part by the Oxford Cancer Research Centre and the Royal College of Surgeons of England. Without their financial backing, it would not have taken place.

SPECIFIC ACKNOWLEDGMENTS FOR WORK PRESENTED IN CHAPTER 3

Figure 3.1 All authors contributed equally

Figure 3.2 Experiments performed by Su Lim Yin and A. Gordon-Weeks

Figure 3.3 Experiments performed by Su Lim Yin and A. Gordon-Weeks

Figure 3.4 Experiments performed by Su Lim Yin and A. Gordon-Weeks

Figure 3.5 Experiments performed by A. Gordon-Weeks

Figure 3.6 Part (a) performed by Lei Zhao, part (b) performed by Su Lim Yin, parts (c and d) performed by Lei Zhao and A. Gordon-Weeks

Figure 3.7 All authors contributed equally

Figure 3.8 All authors contributed equally

Figure 3.9 All authors contributed equally

Figure 3.10 Experiments performed by Su Lim Yin and A. Gordon-Weeks. MRI imaging performed by Dr Sean Smart.

Figure 3.11 Optimisation of DT administration to CD11b-DTR mice performed by Lei Zhao. All authors contributed equally to parts (b-e).

ABREVIATIONS AND ALTERNATIVE NOMENCLATURE

7-AAD	7-Amino-Actinomycin
AES	Amino-terminal enhancer of split (giant ring gland)
AF	Alexa Fluor
APc	Allophycocyanin
APC	Adenomatous polyposis coli (deleted in polyposis 2.5 or DP2.5)
α-SMA	α-smooth muscle actin (actin, α2, smooth muscle, aorta)
CD	Cluster differentiation
CCD	Charged coupled device
CCL	Chemokine (C-C motif) ligand
CCR	Chemokine (C-C motif) receptor
CT	Computed tomography
Ct	Cycle threshold
CXCL	Chemokine (C-X-C motif) ligand
CXCR	Chemokine (C-X-C motif) receptor
DAPI	4',6-diamidino-2-phenylindole
DMEM	Dulbecco's modified Eagle medium
DMSO	Dimethyl sulphoxide
DT	Diphtheria toxin
DTR	Diphtheria toxin receptor
ECM	Extracellular matrix
EDTA	Ethylenediaminetetraacetic acid
ELISA	Enzyme-linked immunosorbent assay
EMT	Epithelial-mesenchymal transition
ErbB1	Epidermal growth factor receptor-1 (Her1)
ERK	Extracellular signal-regulated kinase
FACS	Fluorescence activated cell sorting
FCS	Fetal calf serum
FDG-PET	Fludeoxyglucose-positron emission tomography
FGF2	Fibroblast growth factor-2 (basic fibroblast growth factor)
FSC	Forward scatter
GFP	Green fluorescent protein
GMDSC	Granulocytic myeloid-derived suppressor cells
GTPase	Guanosine triphosphatase
H&E	Haematoxylin and eosin

HCC	Hepatocellular carcinoma
HSGAG	Heparin sulphate glycosaminoglycan
HSEC	Hepatic sinusoidal endothelial cell
HSC	Hepatic stellate cell
ICAM	Intracellular adhesion molecule (CD54)
IL	Interleukin
ISO-1	(S,R)-3-(4-hydroxyphenyl)-4,5-dihydro-5-isoxazole acetic acid methyl ester
IVIS	*In-vivo* Imaging System
LLC	Lewis lung cancer
LSECtin	Liver sinusoidal endothelial cell lectin
MAPK	Mitogen-activated protein kinase
M-CSF	Macrophage colony stimulating factor
MHC	Major histocompatibility complex
MIF	Macrophage inhibitory factor (macrophage migration inhibitory factor, dopachrome isomerase or glycosylation-inhibiting factor)
MMP	Matrix metalloproteinase
MRI	Magnetic resonance imaging
NF-κB	Nuclear factor κ-light-chain-enhancer of activated B cells (nuclear factor of κ-light-polypeptide gene enhancer in B-cells or p52)
NK	Natural killer
OCT	Optimal cutting temperature
Oct4	Octamer-binding transcription factor 4 (POU domain, class 5, transcription factor 1)
PBS	Phosphate buffered saline
PE	Phycoerythrin
PECAM	Platelet endothelial cell adhesion molecule (CD31)
PECy7	Phycoerythrin-cyanine-7
PyMT	Polyoma virus middle T antigen
qPCR	Quantitative polymerase chain reaction
Ras	Rat sarcoma
RBC	Red blood cell (erythrocyte)
ROI	Region of interest
RPM	Revolutions per minute
RPMI	Roswell Park Memorial Institute medium
SEM	Standard error of the mean
shRNA	Short hairpin RNA (small hairpin RNA)

SMAD-4	Mothers against decapentaplegic homolog 4
SSC	Side scatter
STAT	Signal transducers and activators of transcription
TGF-β	Transforming growth factor-β
TIMP-1	Tissue inhibitor of matrix metalloproteinase-1
TNF-α	Tumour necrosis factor-α
TRAIL	TNF-related apoptosis-inducing ligand
VAP-1	Vascular adhesion protein-1 (amine oxidase, copper containing 3 or semicarbazide-sensitive amine oxidase)
VCAM-1	Vascular cell adhesion molecule-1 (CD106)

TABLE OF CONTENTS

LIST OF FIGURES

LIST OF TABLES

Page Nº

Chapter 2 MATERIALS AND METHODS

SUPPLEMENTARY FIGURES

CHAPTER 1. INTRODUCTION

1.1 The clinical significance of colorectal hepatic metastasis

1.1.1 The epidemiology of colorectal cancer metastasis

Worldwide, colorectal cancer is the second and third most commonly diagnosed cancer in women and men respectively and within Europe, the most common for both sexes combined (Ferlay et al., 2010). The incidence of colorectal cancer shows marked geographical variation with up to a 10-fold increase in age-standardised incidence in Europe, the USA and Australia relative to Africa and South-Central Asia (Fig. 1.1).

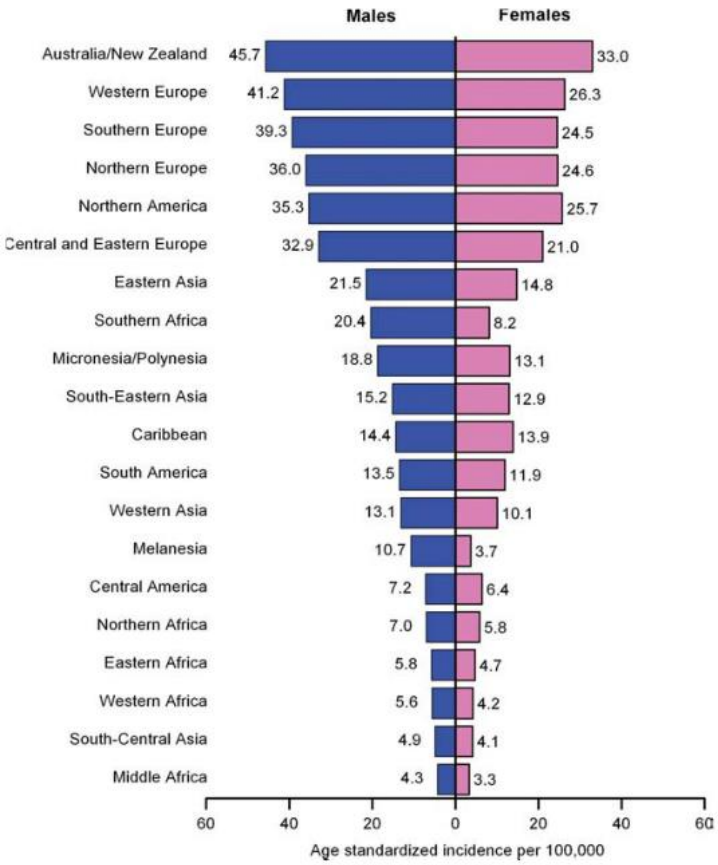

Figure 1.1 – World-wide age-standardised colorectal cancer incidence rates. Shown for women (pink) and men (blue) and demonstrating the difference in incidence between Westernised and non-Westernised regions (Jemal et al., 2011).

The median age at colorectal cancer diagnosis is 68 for men and 72 for women (Siegel et al., 2012). These epidemiological findings indicate that environmental risk factors play a key role in the aetiology of colorectal cancer. Indeed, a Western-style diet high in sugary foods (Theodoratou et al., 2013), processed meats (Chan et al., 2011) and low in fibre (Aune et al., 2011) increases colorectal cancer risk and has been proposed as an explanation for the geographical variation in colorectal cancer incidence. Given that colorectal cancer is largely a disease of the elderly population, it is likely that long-term exposure to such food is required for cancer development. Indeed, this is supported by experimental data indicating that it takes at least 17 years for benign colorectal polyps to develop into malignant growths (Jones et al., 2008). Colorectal cancer also has a strong hereditary component. Thus, once environmental differences have been taken into account, 35% of diagnoses in mono- and dizygotic twins are accounted for by hereditable genetic defects (Lichtenstein et al., 2000).

Colorectal cancer commonly metastasises to the mesenteric lymph nodes and liver, whilst metastases to the lung and brain are less common. Hepatic metastases are either diagnosed at the same time as (synchronous), or subsequent to, the diagnosis of the primary tumour (metachronous). The best available data obtained from populations in Western Europe demonstrate that approximately 15% of colorectal cancer patients have synchronous hepatic metastases (Mantke et al., 2012)(Manfredi et al., 2006) and a further 14.5% develop metachronous hepatic metastases within 5 years of the primary cancer diagnosis (Hackl et al., 2011). It should be noted that this data relies on computed tomography (CT) scanning to diagnose hepatic metastases, with more sensitive imaging modalities such as Magnetic resonance imaging (MRI) or FDG-PET being infrequently used. Given that FDG-PET has a predicted sensitivity for detecting hepatic metastasis from gastrointestinal tumours of 90%, compared to 76% and 72% for MRI and CT respectively (Kinkel et al., 2002), it is likely that such

studies have somewhat underestimated the percentage of patients who develop hepatic metastases in association with colorectal cancer.

1.1.2 Surgical resection is the gold standard treatment for patients with hepatic metastasis

Patients survive a median time of approximately 9 months in the absence of treatment for colorectal cancer liver metastasis (Stangl et al., 1994). Surgical resection is the treatment of choice as it is the only management option shown to be capable of providing long-term cure (Primrose, 2010). However, to date there has been no randomised trial of surgery versus alternative treatment for patients with operable metastasis (Garden et al., 2006). The aim of surgery for hepatic metastasis is to remove all macroscopic disease and achieve negative microscopic margins (R0 resection), whilst leaving sufficient functioning liver for survival (Abdalla et al., 2006). Resection is not possible if the metastatic burden is too large, the patient has concurrent extra-hepatic metastasis, or if the future liver remnant is of insufficient functional capacity. This is particularly important in patients who have undergone pre-operative chemotherapy, the administration of which results in impairment of normal liver function (Kooby et al., 2003)(Pawlik et al., 2007).

Typically, resection is indicated as long as 20-25% of the liver volume is predicted to remain post-operatively , or 30% in patients receiving pre-operative chemotherapy. Appropriate patient selection aided by developments in pre-operative imaging (Xu et al., 2011) and functional hepatic assessment enable a low post-operative mortality and morbidity (Ito et al., 2010), whilst 5- and 10-year cancer-specific survival rates of 36% and 23% respectively are achievable (Rees et al., 2008)(Fong et al., 1999).

1.1.3 Downstaging is an option for initially inoperable hepatic metastases

It is estimated that only about 20% of patients with colorectal cancer hepatic metastases are amenable to surgery based on currently recognised selection criteria (Penna and Nordlinger, 2002). Methods to improve operability include increasing the future liver remnant and downstaging metastatic burden. By performing staged surgery, in which hepatic metastases are resected at either side of an interval allowing for liver regeneration (Adam et al., 2000), hepatic functional reserve is increased and patients with large tumour burden become candidates for curative resection. Similar results can be obtained by occluding the portal vein to the involved hepatic lobe. This causes unilateral hepatic atrophy and compensatory contralateral hepatic lobe hypertrophy, which has the potential of increasing hepatic reserve by up to 30% (Hemming et al., 2003).

As an alternative to increasing functional hepatic reserve, chemotherapy can be used to downstage hepatic metastases. A range of chemotherapeutic regimens has been trialled in this setting, most centring around the use of 5-fluorouracil and irinotecan with or without oxaliplatin. Depending upon the selection criteria used, up to 33% of patients with initially inoperable metastases are down-staged sufficiently to enable R0 resection, with subsequent 5- and 10-year absolute survival rates of 42% and 27% respectively (Masi et al., 2009)(Barone et al., 2007)(Delaunoit et al., 2005)(Wein et al., 2001). As well as chemotherapeutic agents, biological agents such as the epidermal growth factor inhibitor Cetuximab have been used in an attempt to downstage colorectal cancer hepatic metastases. For patients whose primary tumours express the wild-type GTPase KRas, Cetuximab has shown modest benefit in metastatic downstaging, increasing the number of patients eligible for metastectomy to 7.0% from 3.7% when compared to patients treated with standard chemotherapy alone (Van Cutsem et al., 2009).

In summary, the information presented thus far identifies several hurdles that need to be overcome if increased survival is to be achieved in patients with colorectal cancer hepatic metastasis. The most important of these is to increase the number of patients categorised as having operable disease. This can be achieved through earlier diagnosis, improvements in surgical technique, or better neoadjuvant treatments aimed at downstaging disease. At present, it is unlikely that improvements in surgical technique are possible, as surgeons are already able to resect up to 80% of the liver with good early post-operative outcome. As a significant percentage of colon cancer patients present with synchronous hepatic metastases, earlier diagnosis and the development of effective treatment modalities to downstage hepatic disease are key goals for improving long-term survival. Advances in both areas will increase the proportion of patients eligible for surgery, thereby improving long-term survival. Unfortunately, biological agents such as Cetuximab – which have been developed and are administered based on characteristics of the primary tumour – have demonstrated disappointing results with regards metastatic downstaging. Furthermore, chemotherapeutic downstaging significantly impairs the functional liver remnant. Thus, a better understanding of the basic biological processes driving the survival and proliferation of metastatic cancer cells specifically within the hepatic microenvironment is required in order to identify new metastasis-specific therapeutic targets.

1.2 The biological basis of metastasis

1.2.1 Seed-soil or vascular mechanics?

The development of metastasis is a multistep process culminating in the colonisation of a distant organ, whose microenvironment is often vastly different from that of the primary tumour (Fig. 1.2). The metastatic cascade has been described as an inefficient process, as only a

small proportion of the cells that enter the circulation after being shed by the primary tumour go on to form macroscopic metastases (Chambers et al., 2002).

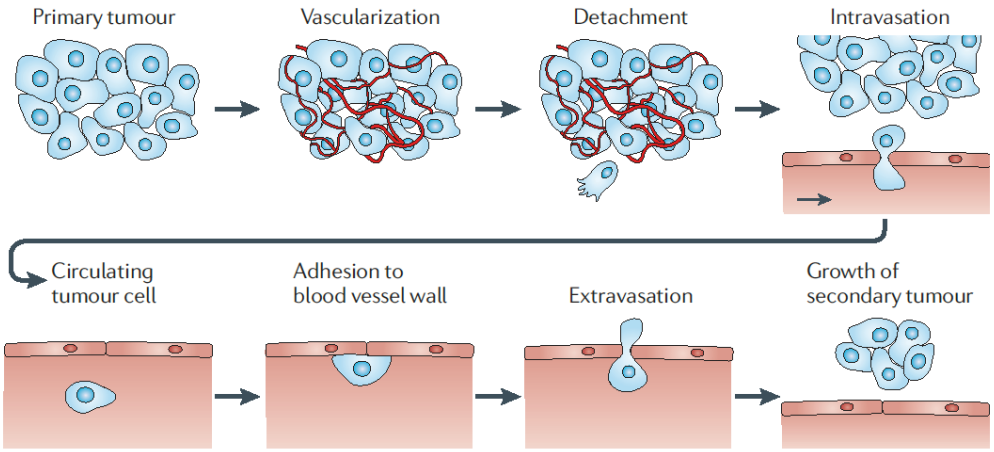

Figure 1.2 – The metastatic cascade. Multiple steps are required for tumour cells to establish metastases within a distant organ (Wirtz et al., 2011).

The rate-limiting step in the development of metastasis depends upon the cell type from which the primary tumour originates, as well as its future metastatic organ. In the liver for example, melanoma cells survive in the circulation and extravasate easily, but few extravasated cells then progress to microscopic or macroscopic metastases (Luzzi et al., 1998). In the lung, metastasising fibrosarcoma cells adhere to the endothelium before proliferating within the vessel lumen (Al-Mehdi et al., 2000), whereas the majority of melanoma and lung cancer cells that arrest within brain microcapillaries die before extravasating and are dependent upon contact with the abluminal endothelial cell surface for successful growth post-extravasation (Kienast et al., 2010) (Fig. 1.3).

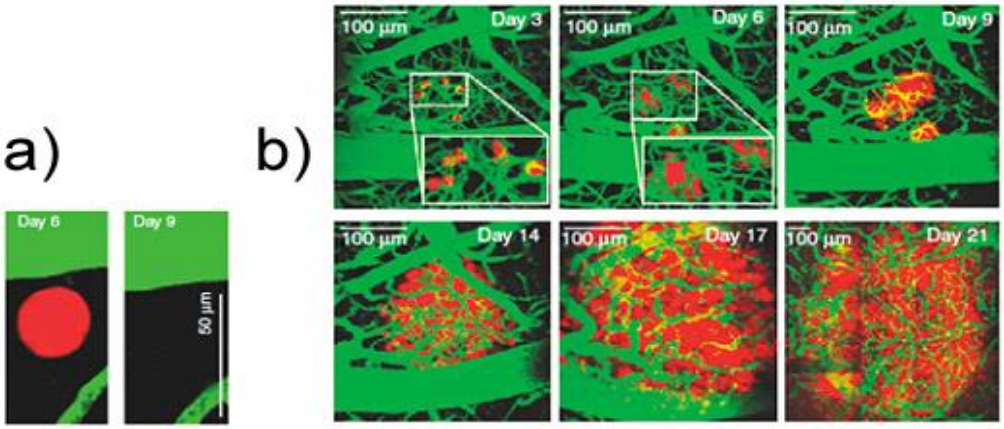

Figure 1.3 – Lung cancer colonisation of the brain. Lung cancer cells die when not in contact with the abluminal endothelial cell surface in the brain (a, the same region of the brain seen at day 6 and 9 with a red fluorescent tumour cell and vessels in green). Conversely, cells that retain endothelial contact (as demonstrated by orange staining) develop into microscopic metastases (b). Each image in (b) represents the same region of the brain (Kienast et al., 2010).

The study of the behaviour of tumour cells at different metastatic sites has promoted the understanding of factors determining metastatic organotropism: the process whereby tumour cells from certain primary cancers demonstrate a metastatic affinity for particular organs. The biology of metastatic organotropism has divided opinion amongst cancer biologists for over a century. Stephen Paget was the first to demonstrate that the distribution of metastasis in cancer patients is not random (Paget, 1889), rather, breast cancer metastasises to the liver more frequently than similarly vascularised organs such as the spleen. Thus, either specific microenvironmental factors determine an organs congeniality to circulating tumour cells, or phenotypic differences afforded to tumour cells from particular primary sites gives them a survival advantage within certain organs.

Despite the convincing nature of Paget's clinical observations, his theory was subsequently challenged by the proposal that metastatic dissemination is determined solely by mechanical factors such as an organs vascular arrangement, microvessel size and the rate at which blood flows through it (Ewing, 1919). Experiments demonstrating a correlation between the number of tumour emboli in an organ immediately following intracardiac injection of tumour cells and the number of macroscopic metastases that subsequently develop lend support to Ewing's theory (Coman et al., 1951). However, such heterotopic studies fail to take into account the ability of primary tumours to prime specific organs for metastatic dissemination by creating a conducive metastatic niche (Kaplan et al., 2005). Furthermore, it is unlikely that injection of a large number of cells directly into the vasculature accurately models basic tumour biology. More recently, a seminal study by Hart and Fidler supported Paget's 'seed and soil' hypothesis, by showing that intravenously injected B16 melanoma cells colonise ectopically implanted lung and ovarian tissue but spare similarly implanted renal tissue (Hart and Fidler, 1980). The authors were unable to demonstrate a difference in the number of radiolabelled tumour cells in the various ectopic tissues shortly following injection, effectively excluding the possibility that differences in metastatic burden between organs resulted from varying degrees of tumour cell trapping within their microvasculature.

Given these lines of experimental evidence, it seems plausible that mechanical, organ and tumour cell-specific factors determine metastatic organotropism. The seed-soil and mechanical hypotheses are not mutually exclusive and to understand the biological basis of metastasis it is therefore necessary to consider the tumour cell, as well as the mechanical and microenvironmental properties of the target organ. In organs whose vascular beds are directly connected, mechanical factors may be particularly important. The lumbar vertebral metastases of prostate cancer for example, appear prior to the development of pulmonary or hepatic metastases and this is likely the result of direct, valveless venous communications between the

prostate and vertebrae (Bubendorf et al., 2000). Other organs such as the brain are relatively protected from metastatic development by way of a specialised blood-organ barrier. For brain metastases to develop, the tumour cell therefore becomes the critical factor, as it must express proteins that facilitate adherence to the organ's endothelia and be capable of penetrating the barrier. This has been beautifully demonstrated by Joan Massague's group who compared genome-wide expression analysis of brain-metastatic and non-metastatic variants of human breast cancer cells (Bos et al., 2009). They demonstrated up-regulation of **α**2,6-sialyltransferase ST6GALNAC5 in highly metastatic cells and showed that this molecule mediated adhesion of tumour cells to brain endothelia. Alternatively, some organs provide a naturally accommodating environment for metastatic cells because of a combination of favourable mechanical and microenvironmental factors. The liver is an example of one such organ, whose low flow vascular network and relative immune tolerance make it ideal for metastatic colonisation from a range of primary cancers, particularly those of the gastrointestinal tract.

1.3 The liver as a pro-metastatic organ

1.3.1 Hepatic vascular anatomy and histology

With the exception of the skin, the liver is the largest organ in the body with functions ranging from the production of plasma proteins to metabolism and immune regulation. It receives 25% of the cardiac output, 75% of which arrives via the portal vein: a valveless vessel draining nutrient-rich blood from the intestine, omentum, pancreas, gallbladder and spleen. The remaining 25% consists of highly oxygenated blood from the hepatic artery, a branch of the celiac trunk, which divides into the right and left hepatic arteries before entering the hepatic parenchyma.

The human liver is anatomically divided into right and left lobes, demarcated by the falciform ligament anteriorly. The right and left hepatic arteries branch in a consistent enough patterns to describe 8 vascular segments (Fig. 1.4), the knowledge of which aids surgeons wishing to perform hepatic segmentectomy for malignant disease.

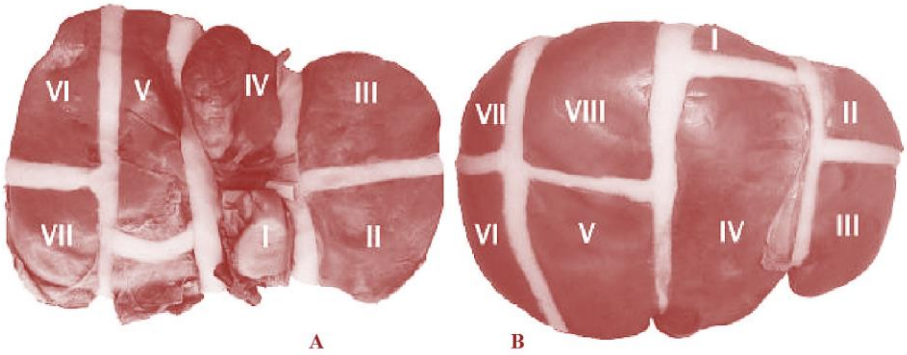

Figure 1.4 – Hepatic vascular anatomy. The liver is organised into defined vascular segments, each of which receives blood from a branch of the right or left hepatic artery, and portal vein. Seen from the posterior (A) and anterior (B) orientation demarcations have been drawn on a plastinated liver to demonstrate the vascular segments (Rutkauskas *et al*., 2006).

The hepatic acinus is the microcirculatory unit of the liver and is composed of a single portal triad (terminal branches of the hepatic artery, hepatic portal vein and biliary tree), the central acinar vein and the hepatocytes and sinusoids in-between (Fig. 1.5). Nutrients from the intestine arrive at the hepatic acinus via terminal branches of the hepatic portal vein. Hepatic portal and arterial blood mix freely in the hepatic sinusoids en-route to drainage into the central acinar vein. Central acinar veins terminate in the hepatic veins, which carry blood to the inferior vena cava. Multiple acini drain into a single central acinar vein creating a hexagonal architecture throughout the liver. The cells within the acinus are divided into three zones

numbered from 1 to 3 in the direction of blood flow. Cells in zone 1 lie along the axis between two portal triads and receive oxygenated blood and intestinal toxins first, whilst the blood in zone 3 is of relatively low oxygen tension (Fig. 1.6).

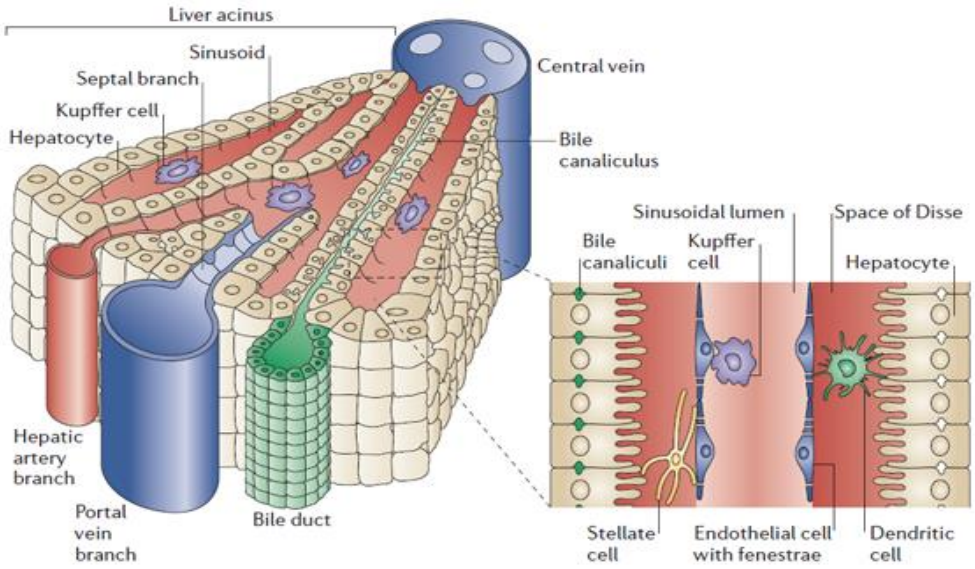

Figure 1.5 – The hepatic microcirculatory unit. The hepatic microcirculatory unit (acinus) is composed of the terminal branches of the portal vein, hepatic artery and bile duct separated from the central hepatic vein by a wedge-shaped segment of sinusoidal endothelium and hepatocytes. Magnification (right side) shows the spatial relationship between the hepatic sinusoidal endothelial cells, hepatic stellate cells, hepatocytes and Kupffer cells (Adams and Eksteen, 2006).

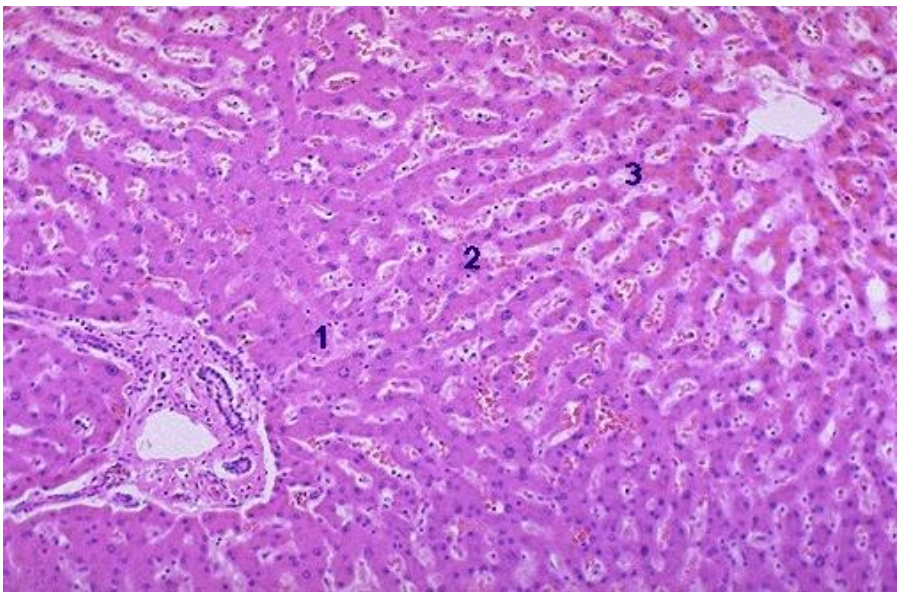

Figure 1.6 – Histology of the portal triad and hepatic acinus. H and E stained section of normal liver tissue showing the portal triad consisting of the hepatic artery, portal vein and bile duct (bottom left) and the hepatic vein (top right). Acinar zones 1 to 3 are labelled in the direction of blood flow (University of Utah, 2014).

1.3.2 Hepatic vascular physiology

Despite 30% of the hepatic volume being accounted for by blood (Lautt, 2009), the majority of this can be expelled back into the systemic circulation without adversely affecting hepatic function. This is the result of significant sinusoidal compliance and defines the liver as a major capacitance organ. Changes in hepatic blood volume are well tolerated; however, maintenance of liver function requires a steady blood flow. As the liver has no direct control over portal blood flow, maintenance of sinusoidal flow requires compensatory physiological mechanisms such as reflex arterial dilatation mediated by increased adenosine concentrations during low portal flow (Browse et al., 2003). Flow from the hepatic artery varies continually in response to changes in portal flow to ensure that sinusoidal flow remains constant (Vollmar and

Menger, 2009). Both the high degree of hepatic vascular compliance and the parallel arrangement of hepatic sinusoids ensures a low-pressure gradient of approx. 5 mmHg (compared to 115 mmHg for other organs) between the portal inflow and venous outflow (Kumar et al., 2008).

In summary, the unique anatomical and physiological features of the liver make it a low flow but vascular organ. Circulating cells travel slowly through the hepatic sinusoid giving ample time for their interaction with the sinusoidal endothelium (MacPhee et al., 1995). Whilst this system is of benefit to immune cells travelling from the circulation to the hepatic parenchyma and aids the delivery of dietary nutrients to hepatocytes, it is likely that it also facilitates the adherence of circulating tumour cells, making the liver a prime target for the development of metastasis.

1.3.3 Hepatic cellular specialisation in metastasis

The liver is composed of a multitude of cell types including the parenchymal hepatocytes and cholangiocytes, both of which are derived from the endodermal hepatoblast (Germain et al., 1988a)(Germain et al., 1988b). Non-parenchymal cells include the hepatic sinusoidal endothelia and their associated pericytes, the hepatic stellate cells, hepatic macrophages (Kupffer cells), as well as other resident and non-resident immune populations. Many studies have identified features of the hepatic cellular microenvironment that can be adapted or utilised by metastasising tumour cells to aid their passage into and proliferation within the hepatic parenchyma. Metastasising tumour cells must adhere to and then traverse the hepatic sinusoidal endothelium before colonising the hepatic parenchyma. Once the endothelial barrier has been breached, tumour cells must overcome the liver's intrinsic immune system for successful colonisation. The hepatic sinusoidal endothelial and stellate cells play

particularly prominent roles in the development of hepatic metastasis and as such, are discussed first, followed by a review of the role that various cells play in regulating the immune microenvironment within the liver.

1.3.3.1 Hepatic sinusoidal endothelial cells guard access to the hepatic parenchyma

Hepatic sinusoidal endothelial cells (HSECs) form a specialised endothelium separated from the underlying hepatocytes by the space of Disse (Fig. 1.7). HSECs contain multiple fenestrae (cell pores) of 150-175 nm in diameter grouped to form sieve plates (Fig 1.7) (Wisse, 1970) and unlike other vascular beds, do not rest upon a basement membrane. This allows mixed portal and arterial blood to traverse the HSEC layer and make contact with the underlying hepatocytes, enabling the uptake of nutrients and toxins (Enzan et al., 1997). HSECs also show functional heterogeneity throughout the sinusoid as their fenestrae decrease in diameter but increase in frequency with distance from the portal triad, increasing HSEC porosity towards the centrilobular vein (Wisse et al., 1983).

HSEC fenestrations are dynamic structures whose diameter and number alter in the face of physiological and pathological stress. This has been documented in alcohol (Ishak et al., 1991), endotoxin (Dobbs et al., 1994) and carbon tetrachloride (Martinez-Hernandez and Martinez, 1991) induced cirrhosis, all of which are pre-dated by HSEC defenestration and the appearance of a sinusoidal basement membrane. In the only published analysis of fenestration dynamics in relation to hepatic metastasis Vidal-Vanaclocha *et al*., (1990) demonstrated a reduction in fenestrae size and number within 7 days of intrasplenic melanoma or lung cancer cell injection. However, the significance of this finding – which has not been validated in humans – is unclear and as yet the factors driving de-fenestration in relation to metastasis remain unexplored.

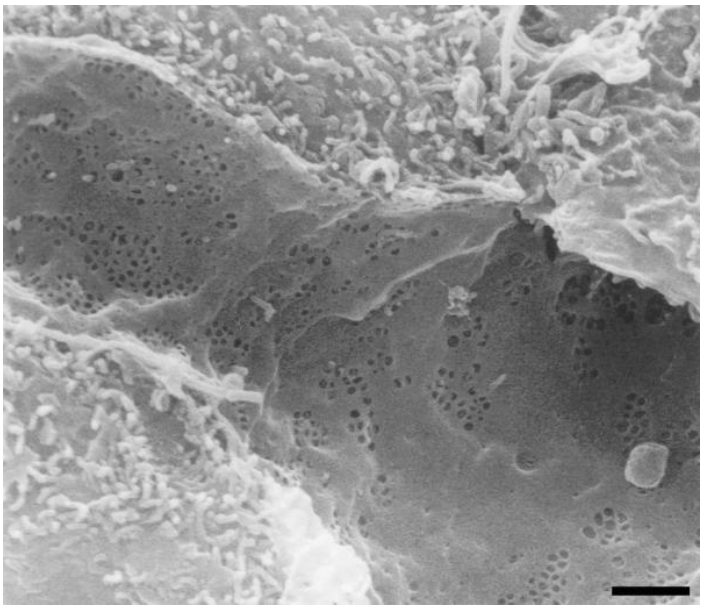

Figure 1.7 – Hepatic stellate cell fenestrae. Electron micrograph demonstrating multiple fenestrae on the HSEC surface. These allow substances to pass from the sinusoidal space into the space of Disse. Scale bar represents 1 μm (Wisse, 1970).

As well as acting as a selective sieve for macromolecules travelling between the sinusoidal lumen and space of Disse, HSECs have a high level of endocytic activity (Smedsrød et al., 1994) enabling them to scavenge circulating waste products including inflammatory proteins such as hyaluronic acid, chondroitin sulphate, heparin and collagens. This is facilitated by the expression of a wide range of scavenger receptors on the luminal surface of hepatic endothelial cells (Scoazec and Feldmann, 1991). The mannose receptor is one such scavenger receptor highly expressed by HSECs and mannose receptor knock-out mice show reduced clearance of circulating denatured collagen and a reduction in hepatic collagen deposition (Malovic et al., 2007).

With relevance to metastasis, experiments showing a correlation between mannose ligand expression on B16F1 melanoma cells and their hepatic metastatic potential point to the

ability of HSEC mannose receptors to act as docking points for circulating tumour cells (Mendoza et al., 1998). Indeed, mannose receptors are involved in the initial interaction between CT26 colon cancer cells and murine HSECs (Arteta et al., 2010). CT26 cells express interleukin (IL)-1β which stimulates the expression of hepatic mannose receptors that are then responsible for the adherence of tumour cells to the sinusoidal endothelium (Arteta et al., 2010).

As well as expressing mannose receptors, HSECs extracted from human liver express the cell-cell adhesion molecules vascular adhesion protein-1 (VAP-1), platelet endothelial cell adhesion molecule (PECAM) and intracellular adhesion molecule (ICAM) (Lalor et al., 2002). Furthermore, upon stimulation with tumour necrosis factor α (TNF-α) vascular cell adhesion molecule (VCAM) and E-selectin are also expressed by human HSECs (Lalor et al., 2002), whilst ICAM-1, VCAM-1 and E-selectin are all expressed by HSECs associated with hepatic metastases (Gulubova, 2002). VAP-1 plays an indirect role in the adhesion and transmigration of leukocytes, as its activation leads to NF-κB-dependent expression of E-selectin and VCAM (Lalor et al., 2007). Metastasising tumour cells use these adhesion molecules to adhere to the hepatic sinusoidal endothelium, whilst tumour-derived chemokines can up-regulate endothelial adhesion molecule expression. Intrasplenic inoculation of human colon cancer cells to Nu/Nu mice for example, induced TNF-α expression by Kupffer cells resulting in increased HSEC P-selectin, E-selectin, ICAM and VCAM expression (Khatib et al., 2005). HSECs also expressed TNF-α upon activation by B16F1-derived VEGF resulting in reciprocal IL-1β- and IL-18-dependent H_2O_2 production by tumour cells. This in turn up-regulated endothelial I-CAM expression, thereby enhancing tumour cell adhesion (Mendoza et al., 2001). In support of these findings, therapeutic inhibition of E-selectin and V-CAM significantly reduced the formation of orthotopic colon cancer (Khatib et al., 2002) and melanoma (Vidal-Vanaclocha et al., 2000) metastases respectively.

Given the significance of such *in-vivo* findings, attention should now be turned to an analysis of the roles played by adhesion molecules in the development of hepatic metastasis in humans. It is important to remember however, that molecules such as VCAM, ICAM and the selectins are ubiquitously expressed by both the vascular and lymphatic endothelium where they play a fundamental role in the trafficking of lymphocytes to sites of infection and inflammation. Their inhibition in humans in the hope of treating hepatic metastasis could therefore have significant adverse effects in patients already immunosuppressed, through the administration of chemotherapeutics.

On this note, HSECs express certain adhesion molecules that have not been identified in endothelial cells within other anatomical locations. Liver sinusoidal endothelial cell lectin (LSECtin) is an example of one such liver-specific adhesion molecule that modulates the interactions between HSECs and activated T-lymphocytes (Liu et al., 2004). Colon cancer cell lines LoVo and LS174T adhered to fluorescently labelled recombinant LSECtin in vitro and LSECtin$^{-/-}$ mice developed significantly smaller hepatic metastases than wild-type controls when challenged with primary patient-derived colon cancer cells (Zuo et al., 2013). Thus, the characterisation of LSECtin and the role that it plays in murine models of hepatic metastasis not only identifies it as a promising therapeutic target, but also highlights a potential mechanism for the hepatic organotropism of certain primary cancers, which may be capable of adhering specifically to LSECtin.

1.3.3.2 Hepatic stellate cell activation is a key feature of hepatic metastasis formation

Hepatic stellate cells (HSCs, also described as hepatic pericytes (Hellerbrand, 2013)), reside on the abluminal surface of the hepatic sinusoidal endothelium within the space of Disse (Fig. 1.5). Stellate cells are of mesenchymal origin (Enzan et al., 1997) and are characterised by

their expression of vitamin A (Hendriks et al., 1985). In-vitro, HSCs are contractile when stimulated by angiotensin II (Bataller et al., 2000) or endothelin I (Pinzani et al., 1996), suggesting that they play a role in the regulation of hepatic blood flow. Interestingly, rat HSCs express a range of stem cell markers including CD133 (Kordes et al., 2007), nestin (Niki et al., 1999) and Oct4 (Kordes et al., 2007) and have been shown to be capable of hepatic regeneration in murine models (Yang et al., 2008). In keeping with the expression of stem cell markers, HSCs also show significant plasticity, being capable of differentiating into endothelial and hepatocyte-like cells. Furthermore, *in-vitro* work demonstrating the up-regulation of rat stellate cell CD133, β-catenin and Wnt proteins in response to Wnt ligands produced by hepatocytes, as well as the observation that HSCs migrate towards CXCL12 expressed by HSECs have led to the suggestion that the space of Disse acts as a stem cell niche for HSCs (Sawitza et al., 2009).

HSCs are chiefly responsible for producing extracellular matrix (ECM) proteins during the development of hepatic fibrosis, and spontaneous recovery from experimentally-induced hepatic fibrosis is associated with widespread stellate cell apoptosis (Iredale et al., 1998). During the course of fibrosis, HSCs transdifferentiate into myofibroblasts expressing α-SMA (Iredale et al., 1998). Interestingly α-SMA positive myofibroblasts have also been identified in the hepatic metastatic niche (Vidal-Vanaclocha, 2008), suggesting that invading tumour cells are capable of driving the differentiation of HSCs. In return, HSCs and their myofibroblast progeny provide a stroma that is supportive for metastatic growth. Culture medium from activated HSCs promoted the proliferation and invasion of HCC cells *in-vitro* (Amann et al., 2009), whilst co-injection of HSCs with cholangiocarcinoma cells in BALB/c mice resulted in larger tumours than when cholangiocarcinoma cells alone were used (Okabe et al., 2011). To underscore the clinical relevance of HSCs in the hepatic tumour microenvironment, elevated intra-tumoural HSC numbers, determined by immunohistochemistry, independently predicted poor overall and progression-free survival in patients with HCC (Ju et al., 2009).

HSCs promote tumour growth through a variety of mechanisms including the production of pro-tumourigenic cytokines and regulation of extracellular matrix (ECM) deposition. The cytokines TGF-β, HGF and CXCL-12 were all expressed in media conditioned by activated HSCs and each supported the proliferation of colon cancer cells in vitro (Shimizu et al., 2000)(Matsusue et al., 2009). HSCs also produce ECM components such as collagen and fibronectin. These molecules enable adhesion and migration of cancer cells through integrin receptor expression on the tumour cell surface (Levental et al., 2009). As well as being directly responsible for the production of pro-tumourigenic ECM components, HSCs associated with hepatic metastases produce MMP's (Musso et al., 1997), proteins which enable the migration of tumour cells by breaking down ECM components at the invasive front (Brooks et al., 1996). HSCs therefore play a complex role in the regulation of tumour stroma. On one hand, expressing enzymes that breakdown the ECM to enable tumour cell invasion, and on the other, directly contributing to ECM formation, thus providing a scaffold for tumour growth.

1.3.4 The resident hepatic immune system

The liver's unique position downstream of the gastrointestinal venous drainage brings it into contact with both food antigens and bowel pathogens. To avoid hypersensitivity to non-harmful antigens the liver exists in a state of relative immune privilege, a feature open to exploitation by metastasising cancer cells. As well as the hepatocytes themselves, various resident cells are responsible for maintaining hepatic immunity, particularly Kupffer cells within the sinusoidal lumen and hepatic natural killer cells. Intriguingly, the human liver is also populated by haematopoietic stem cells (Crosbie et al., 1999), implying an ability to produce immune cells under appropriate conditions; a finding that may explain the phenomenon of haematopoietic chimerism and graft tolerance following hepatic transplantation (Starzl et al., 1992).

Under most circumstances hepatic immune cells act to inhibit the development of metastasis by actively destroying tumour cells. However, experimental evidence demonstrates that tumour cells exploit hepatic immune tolerance to aid liver colonisation. The role of specific hepatic immune populations in the development of liver metastases as well as the immunosuppressive role of hepatocytes is discussed below. However, it should be noted that the majority of studies published in this field rely solely on *in-vitro* data or results from animal models. Translational studies have not been performed in this area and therapies that target the relationship between metastasising cancer cells and the hepatic immune system are yet to be developed.

1.3.4.1 Hepatocytes promote lymphocyte tolerogenicity

Hepatocytes interact with T-lymphocytes via cytoplasmic projections that pass through HSEC fenestrations (Warren et al., 2006). In the resting state, hepatic MHC class I molecules in the absence of co-stimulatory molecules, enabled hepatocytes to stimulate apoptosis of $CD8^+$ T lymphocytes as they passed through the sinusoidal space (Holz et al., 2008). Hepatic inflammation resulting from viral infection or auto-immune disease, stimulates the expression of MHC class II molecules on the surface of hepatocytes (Herkel et al., 2003). However, rather than promoting immunity, in vivo evidence demonstrated that hepatocyte MHC class II molecules steer $CD4^+$ T-lymphocytes towards an anti-inflammatory, Th2 phenotype, whilst simultaneously inhibiting the production of the pro-inflammatory cytokine interferon-γ from primed Th1 $CD4^+$ T-lymphocytes (Wiegard et al., 2007). Fascinatingly, peripheral tolerance can also be mediated by hepatocytes through engulfment and lysosomal destruction of activated T-lymphocytes (Benseler et al., 2011). Given the important role that lymphocytes play in immune surveillance (Shankaran et al., 2001), it seems likely that metastasising cancer cells will gain a survival advantage within the liver as a result of hepatocyte driven T-cell interference. Greater understanding of the signalling processes through which hepatocytes control T-cell function

could identify mechanisms through which hepatic T-cell surveillance could be restored in the setting of liver metastasis.

1.3.4.2 Kupffer cells provide an important defence against metastasising cancer cells

Whilst hepatocytes appear to suppress systemic immunity - and in doing so may provide a protective niche for metastatic development - Kupffer cells offer one of the liver's first lines of defence against invading tumour cells. Kupffer cells are liver-resident macrophages; professional antigen presenting cells capable of presenting antigen to $CD4^+$ and $CD8^+$ T-lymphocytes through MHC expression (Lohse et al., 1996).

In their simplest anti-metastatic role Kupffer cells are capable of killing tumour cells through receptor-mediated phagocytosis (Bayón et al., 1996). Kupffer cells identified *in vivo* using laser scanning electron microscopy were found in close association with colon cancer cells (Timmers et al., 2004) and depletion of phagocytes using toxin-containing liposomes (Heuff et al., 1993) or administration of gadolinium chloride (Rushfeldt et al., 1999) significantly increased the formation of experimental hepatic metastases. Stimulation of Kupffer cells also appears to delay metastatic development (Williams et al., 1985), although smaller metastases are associated with delayed primary tumour development in such studies, making it difficult to determine whether treatments aimed at stimulating Kupffer cells in fact have a direct growth inhibitory effect on the tumour itself. Despite evidence showing that Kupffer cells limit hepatic metastasis, it is not clear how they recognise cancer cells, or whether Kupffer cells interact with other immune populations to inhibit cancer growth. Furthermore, convincing evidence for their anti-metastatic function has yet to be demonstrated in humans.

Interestingly, two populations of murine F4/80$^+$ Kupffer cells have been identified and each has a unique phenotype (Kinoshita et al., 2010). CD11b$^+$ Kupffer cells produce large quantities of cytokines such as TNF-α and IL-12, whilst the predominant CD68$^+$ subset is strongly phagocytic with less cytokine producing ability (Kinoshita et al., 2010). This indicates that Kupffer cell subsets may be capable of regulating other hepatic immune cells through cytokine production in response to pathogens or metastasising tumour cells. Furthermore, immune cell-derived TNF-α is capable of promoting tumour cell proliferation through NF-κB (Luo et al., 2004). For this reason, it would be interesting to study the relative contribution of different kupffer cell subsets to metastatic growth, as it is possible that, through the production of cytokines such as TNF-α, particular Kupffer cell subsets will promote rather than inhibit metastatic development.

1.3.4.3 The anti-metastatic role of resident hepatic natural killer cells

Natural Killer (NK) cells are members of the innate immune system capable of killing target cells through a variety of mechanisms. Mature NK cells (CD56$^+$) have cytotoxic ability dependent upon the exocytosis of granules containing the protein perforin, which is capable of perforating cellular membranes (Voskoboinik et al., 2006). Immature (CD56$^-$) NK cells mediate cell death through the expression of the TNF-related apoptosis-inducing ligand (TRAIL) as opposed to the expression of perforin (Zamai et al., 1998). NK cells are also capable of mediating cellular cytotoxicity indirectly by priming T-helper (Th1) lymphocytes as a result of interferon-γ expression (Martín-Fontecha et al., 2004).

NK cells identify tumour cells for destruction through the absence of MHC class I molecules on the tumour cell surface (Kärre et al., 1986), or through the expression of ligands for the Natural Killer Group 2D (NKG2D) receptor (Diefenbach et al., 2001), upregulated during

periods of cellular stress such as DNA damage (Groh et al., 1998). Evidence for the role of NK cells in tumour surveillance and tumour cell killing comes from several sources. First, patients with colorectal cancers that are infiltrated with many NK cells have a better prognosis than those with fewer NK cells both in terms of overall and disease-free survival (Coca et al., 1997). Second, reduced cytotoxicity of circulating NK cells is associated with an increased risk of cancer development (Imai et al., 2000).

Interestingly, the liver has a large population of resident NK cells which show strong *in-vitro* cytotoxicity to tumour cells (Bouwens et al., 1987). Furthermore, hepatic NK cells are capable of killing B16F1 melanoma cells through the production of perforin, whilst NK cells in the lung do not possess this ability (Ballas et al., 2013), indicating that a hepatic-specific NK cell subset provides protection against metastatic development. This is supported by the finding that TRAIL, expressed on the surface of hepatic NK cells, was responsible for cytotoxicity of fibrosarcoma cells *in-vitro*, whilst TRAIL inhibition resulted in a significant increase in their hepatic metastatic ability *in-vivo* (Takeda et al., 2001). Methods aimed at heightening the NK cell response to tumour cells within the liver may therefore be of benefit to patients with hepatic metastases.

1.4. From colon cancer to liver metastasis

For colorectal cancer cells to reach the liver they must proliferate and avoid cell death within their primary organ, invade local stromal tissue, intravasate, survive in the hepatic portal vein, adhere to the hepatic sinusoidal endothelium, extravasate and then successfully proliferate within the hepatic parenchyma. For each of these processes, colorectal cancer cells must acquire certain characteristics that will enable them to overcome protective host mechanisms and take advantage of organ-specific biology.

1.4.1 Intravasation and circulatory survival of metastatic colon cancer cells

Intravasation is the process whereby cells move from within a tissue, through the vascular basement membrane to enter a vascular lumen. Although intravasation has been assumed to represent one of the earliest steps in the metastatic cascade, there remains a relatively small volume of research literature on the subject, and factors controlling intravasation at the molecular level remain largely unstudied. Intravital imaging has demonstrated significant differences in the ability of metastatic and non-metastatic breast cancer cell lines to intravasate (Wyckoff et al., 2000), supporting the notion that this process is important for successful metastasis. Interestingly, over-expression of the Epidermal Growth Factor Receptor (ErbB1) in breast cancer cells - whilst having no effect on primary tumour growth - promoted intravasation and metastasis *in-vivo* (Xue et al., 2006), indicating that the acquisition of specific cellular factors enabling intravasation are sufficient to promote metastasis without affecting primary tumour growth.

In colorectal cancer, intravasation has been infrequently studied, not least because of the difficulties in performing intravital imaging in orthotopic models. However, a recent study using an orthotopic rectal cancer model identified the Amino-terminal enhancer of split (Aes) as an important metastasis suppressor capable of inhibiting intravasation through the inhibition of Notch signalling (Sonoshita et al., 2011). Conditional Aes knockout in germline mutant APC mice resulted in the spontaneous growth of intestinal polyps that invaded locally and intravasated, a finding not demonstrated in mice with APC mutation alone (Sonoshita et al., 2011). Again, this points to the loss or acquisition of specific molecules that endow particular subsets of colon cancer cells with metastatic potential through their ability to intravasate.

Once colorectal cancer cells invade local tributaries of the hepatic portal vein from their primary location in the bowel wall, they must survive within the circulation as they travel towards the hepatic sinusoid. Within the large, low-pressure branches of the hepatic portal vein most intravasated cells are likely to survive, however, once these cells reach the sinusoid, trauma resulting from cellular deformation and mechanical stress results in significant cancer cell death (Barbera-Guillem et al., 1993). Indeed, this has been demonstrated for fluorescently labelled HCT-116 colorectal cancer cells following intraportal injection into SCID mice, the majority of which underwent cytoplasmic destruction and death in the hepatic sinusoid within 12 hours of injection (Tsuji et al., 2006). Microenvironmental, as well as mechanical forces within the liver are capable of inhibiting metastatic dissemination. Tumouricidal nitric oxide, for example, was released within the hepatic sinusoid shortly following intramesenteric injection of B16F1 melanoma cells and inhibition of nitric oxide production resulted in a significant increase in metastatic burden (Wang et al., 2000). Although such studies do not identify the cellular source of hepatic nitric oxide, both hepatic macrophages and hepatic endothelia are potential candidates, having previously been shown to be capable of releasing H_2O_2 in response to tumour cell challenge *in-vitro* (Anasagasti et al., 1996).

1.4.2 Hepatic sinusoidal endothelial cell adhesion and extravasation in colon cancer metastasis

Melanoma and colon cancer cells visualised using intravital microscopy were shown to become trapped in hepatic sinusoids within hours of intraportal injection (Steinbauer et al., 2003)(Luzzi et al., 1998), identifying cell trapping as a possible contributory factor for metastatic development. Tumour cells also adhere to HSECs in a manner reminiscent of leukocytes adhering to activated endothelia, whereby weak interactions between endothelial selectins and immune cell glycoproteins, and subsequently ICAM- and VCAM-mediated tight adhesion constitute the first steps of extravasation (Alon and Ley, 2008).

HSECs express an array of adhesion molecules including selectins, integrins and cadherins, the expression of which is upregulated by cytokines such as IL-1β and TNF-α, both of which are expressed by colon cancer cells (Eckmann et al., 1993). Furthermore, colon cancer cells express ligands for endothelial adhesion molecules, most notably the E-selectin ligands Sialyl Lewis carbohydrate antigens A and X (Takada et al., 1993). Thus, it is likely that tumour-driven upregulation of HSEC adhesion molecules facilitates the adherence of circulating tumour cells and the retention of metastatic cells within the liver. This hypothesis is supported by *in-vivo* experiments demonstrating reduced metastasis formation following inhibition of tumour cell-HSEC interaction, as discussed above (Pages 36 and 37).

Once metastatic cancer cells have successfully adhered to the hepatic endothelium, they must leave the vascular space in a process termed extravasation. Tumour cell extravasation occurs through transcellular diapedesis, where tumour cells induce endothelial cell apoptosis as they travel through the endothelia or by paracellular diapedesis, where tumour cells move between adjacent endothelial cells to gain access to the organ parenchyma (Tremblay et al., 2008). Paracellular diapedesis of HT29 colon cancer cells occurred following ligand binding to E-selectin on the endothelial cell surface, which in turn led to activation of extracellular signal-regulated kinase (ERK) and p38-dependent actin filament retraction in the endothelial cell (Tremblay et al., 2006). Further support for the role of endothelial p38/MAPK in paracellular diapedesis of colon cancer cells comes from a recent study on the effect of the tumour derived chemokine CCL2 on endothelial permeability in the lung (Wolf et al., 2012). Selective knockout of the CCL2 receptor CCR2 on murine endothelia reduced pulmonary vascular permeability and MC38 pulmonary metastases in a p38MAPK-dependent fashion, demonstrating the importance of paracellular diapedesis in the formation of pulmonary metastasis (Wolf et al., 2012). It is not yet clear whether similar mechanisms exist for colon cancer cells metastasising to the liver and so this may be a phenomenon unique to the pulmonary vasculature.

1.4.3 Histological patterns of metastatic colonisation in the liver

Hepatic colonisation by metastasising cancer cells can be divided into microvascular, intralobular pre-angiogenic, panlobular angiogenic and lobar growth phases (Brodt, 2013). At each stage, cells of the hepatic microenvironment interact directly with tumour cells and such interactions determine whether metastasis becomes clinically evident (reaches the lobar growth phase) or succumbs to local immunity or hypoxia. The interactions between tumour cells, the hepatic sinusoidal endothelium, stellate cells and Kupffer cells, which largely define the microvascular phase of metastasis have been described above, whilst the following section focuses on the subsequent phases of metastatic growth.

The intralobular pre-angiogenic growth phase begins with cancer cells that have successfully adhered to the sinusoidal endothelium and begin to divide within the liver. Such cells may or may not have extravasated, as tumour cell division can occur within the sinusoid prior to extravasation taking place. During this phase, metastases have been suggested to develop at intrasinusoidal, perisinusoidal and periportal locations. The location of metastatic development determines the hepatic cell types with which invading tumour cells communicate and this in turn determines the histological nature of the metastatic process.

Metastases that develop at intrasinusoidal locations for example, typically show a replacement growth pattern with little disruption of the hepatic architecture (Fig. 1.8). These tumours are characterised by limited angiogenesis in their later stages, at which point the ratio of tumour to endothelial cell proliferation is higher than that for other patterns of metastatic growth (Vermeulen et al., 2001). Intrasinusoidal metastases are surrounded by HSECs and have close contact with Kupffer cells, hepatic lymphocytes and various circulating immune populations. Perisinusoidal metastases develop in the space of Disse and are therefore in close contact with the hepatic stellate cells, hepatic fibroblasts, hepatocytes and sinusoidal endothelia. They develop a desmoplastic pattern characterised by a dense fibrotic response at the liver-metastasis interface (Fig. 1.8). Metastatic cells that settle in the periportal region, in contrast typically show a pushing growth pattern whereby the hepatic architecture surrounding the tumour is lost (Fig. 1.8). Tumour cells in this location make contact with cholangiocytes, hepatic progenitor cells, hepatocytes and portal fibroblasts. The mechanisms underlying the various histological patterns of metastatic development are yet to be determined. However, they may have some clinical relevance, as anti-angiogenic agents such as endostatins have a far greater inhibitory effect on the growth of sinusoidal-type metastases than their portal type counterparts (Solaun et al., 2002), indicating that some patterns may be more amenable to pharmacological intervention than others.

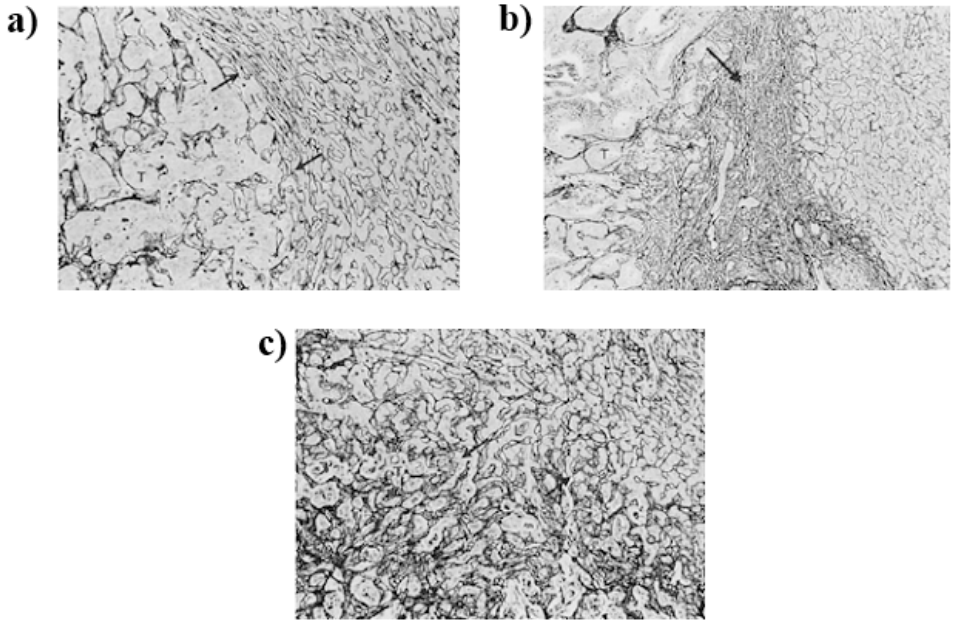

Figure 1.8 – Distinct patterns of metastatic growth within the liver. Hepatic metastases progress in three swell defined growth patterns. (a) demonstrates a pushing growth pattern, where the architecture of the surrounding liver is lost (arrows). Image (b) is an example of a desmoplastic growth pattern in which the tumour is surrounded by a dense rim of fibrotic tissue (arrow). (c) shows an example of a liver metastasis with a replacement growth pattern. Here the

architecture of the liver remains intact, making it difficult to define the liver/metastasis interface (arrow) (Vermeulen et al., 2001).

Once hepatic metastases reach roughly 300 μm, or outgrow the hepatic lobule, angiogenesis is required for further growth. Angiogenesis within hepatic metastases occurs predominantly in two histological patterns. A sinusoidal pattern, where vessels within the tumour take up an organised, concentric form, or alternatively a portal-type angiogenesis pattern characterised by a fibrous capsule and less well organised vasculature with areas of necrosis and activation of hepatic fibroblasts (Fig. 1.9) (Vidal-Vanaclocha, 2008). Angiogenesis is predated by an infiltration of VEGF-expressing HSCs (Olaso et al., 2003), likely activated in response to tumour hypoxia (Olaso et al., 1997), suggesting that cooperation between cancer cells and HSCs serves to promote metastatic angiogenesis.

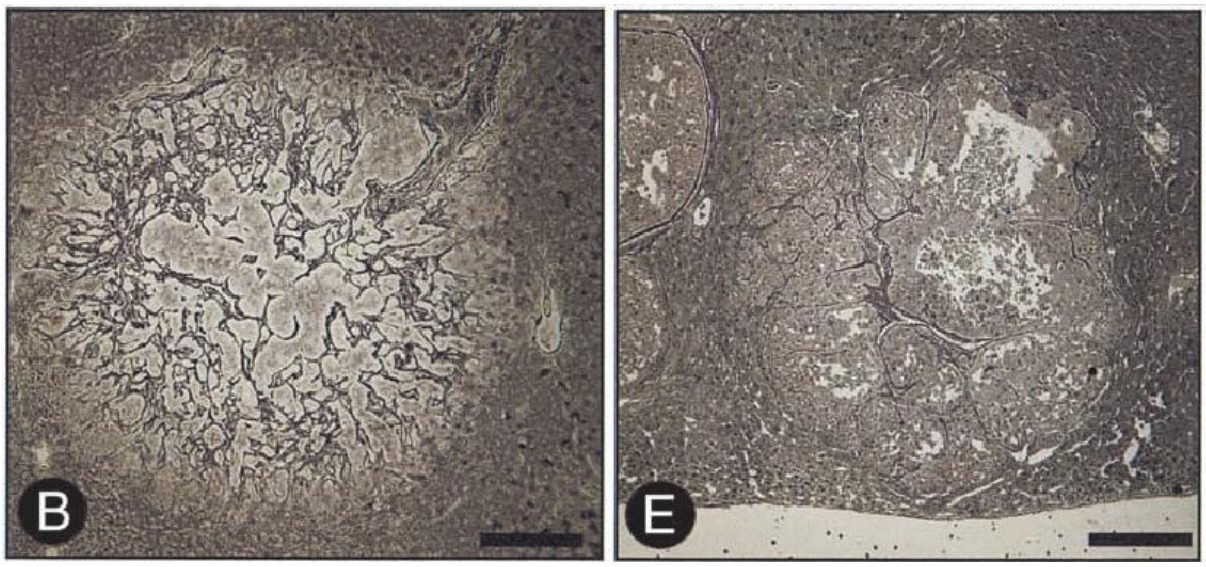

Figure 1.9 – Angiogenic development during hepatic metastasis progression. Differing angiogenic patterns are demonstrated within hepatic metastases by staining for reticulin using the Gordon-Sweets silver impregnation technique. (B) is an example of a sinusoidal-type hepatic metastasis characterised by organised, concentric vascular connections. In contrast (E) shows a portal-type metastasis

with poorly organised vasculature and areas of necrosis. Scale bars represent 100μm (Solaun et al., 2002).

To summarise, the development of successful hepatic metastasis requires specific genetic changes within tumour cells at the site of the primary tumour in order to enable local invasion and intravasation. Protective cellular mechanisms within the hepatic sinusoid must then be overcome, before tumour cells achieve sinusoidal adhesion and extravasation through interaction with specific HSEC adhesion molecules. Tumour cell proliferation within the hepatic microenvironment is then dependent upon selective communication with specific hepatic cell populations, the nature of which are not yet fully understood, but which appear to shape the morphological pattern of tumour growth. As well as relying on interactions with numerous resident hepatic cell types, emerging evidence indicates that successful liver metastasis also depends upon the development of an inflammatory reaction, typified by the recruitment of a range of circulating immune cells in response to ectopic chemokine expression by cancer cells. Thus, we finally turn our attention to the potential role of systemic immunity and in particular recruited immune cells in the development of hepatic metastasis.

1.5 The immune system and metastasis

1.5.1 The immune system can function in a tumour-promoting fashion

Historical evidence for the link between inflammation and the promotion of malignancy comes from several observations. First and foremost, inflammatory conditions such as chronic pancreatitis and ulcerative colitis are associated with an increased risk of cancer in the affected organ (Malka et al., 2002)(Ekbom et al., 1990). Furthermore, infectious agents such as *Helicobacter pylori* and *Schistosoma haematobium* cause chronic inflammation which frequently

progresses to gastric and bladder cancer respectively (Helicobacter and Cancer Collaborative Group, 2001)(Michaud, 2007). Finally, inhibition of inflammatory chemokines or their receptors leads to reduced tumour development in animal models (Balkwill, 2004), whilst anti-inflammatory drugs reduce the risk of colon cancer development in humans (Flossmann and Rothwell, 2007).

Mechanistically, inflammation and cancer have been described as being linked by intrinsic and extrinsic pathways. The extrinsic pathway involves the development of a malignancy in the setting of chronic inflammation, where inflammatory cells release factors capable of causing genotoxic stress in nearby epithelial cells, thereby promoting cancer formation (Mantovani et al., 2008). Alternatively, the intrinsic pathway stipulates that certain oncogenes are capable of driving the downstream expression of pro-inflammatory programs responsible for the recruitment of immune cells, many of which display pro-tumourigenic phenotypes. Central to such pro-inflammatory programs are chemokines, a group of proteins, which are responsible for coordinating the movement of immune cells from the bone marrow to site of tissue inflammation and which are produced ectopically by tumour cell, leading to recruitment of immune cells to the tumour microenvironment (Fig. 1.10).

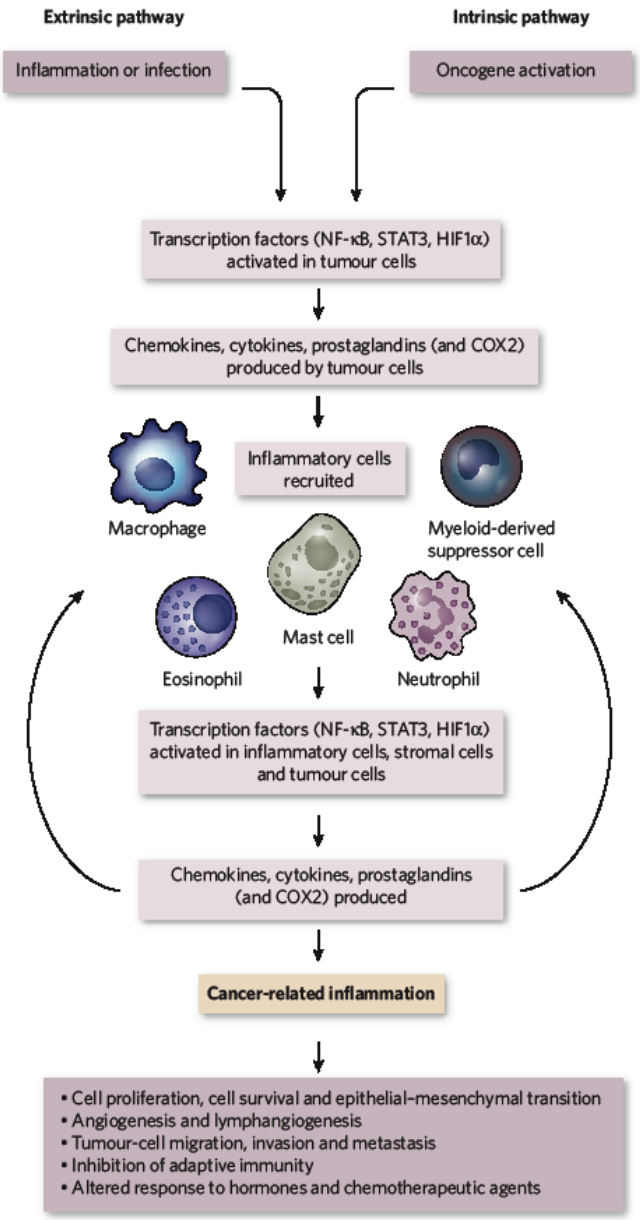

Figure 1.10 – The extrinsic and intrinsic links between inflammation and cancer. Extrinsic inflammation leads to genotoxic stress and thereby activation of oncogenes or inhibition of tumour suppressor genes. Alternatively, intrinsic gene mutation is the initiating event leading to expression of pro-inflammatory chemokines responsible for recruitment of protumourigenic inflammatory infiltrate (Mantovani et al., 2008).

Fascinatingly, it is becoming apparent that both lymphoid and myeloid cells can become pro-tumourigenic once they arrive at the tumour microenvironment. In the case of T-lymphocytes, a $CD25^+$ population of regulatory T-cells found in patients with malignant ascites secondary to ovarian cancer inhibited $CD8^+$ T-cell cytotoxicity and promoted tumour growth *in-vivo* (Curiel et al., 2004). Interestingly, naïve peripheral T-cells are converted to immunosuppressive $CD25^+$ T-cells under the influence of TGF-β (Chen et al., 2003), a cytokine

that has also been demonstrated to promote the polarisation of neutrophils from an anti-tumourigenic N1 to a pro-tumourigenic, immunosuppressive N2 phenotype (Fridlender et al., 2009). The plasticity of macrophages, as well as neutrophils is taken advantage of by developing tumours, through the expression of cytokines such as IL-4 and IL-10. Expression of these chemokines promotes the appearance of M2 (alternatively activated) macrophages capable of inhibiting tumour-specific immunity, promoting angiogenesis and driving pro-tumourigenic remodelling of the extracellular matrix (Sica et al., 2008a). Thus, a number of well-characterised immune cell types may be capable of promoting both primary tumour formation and the development of metastasis.

1.5.2 Chemokine expression in the progression of cancer

1.5.2.1 Chemokine structure and function

Chemokines are a family of cytokines with chemoattractant activity. Structural classification divides chemokines according to the number and spacing of N-terminal cysteine residues into subgroups named CC, CXC, C and CX_3C (Murphy et al., 2000). The CC and CXC subgroups have many members, each of which have two adjacent cysteines or single cysteines either side of an alternative amino acid respectively. Fractalkine (CX_3CL1) is the only member of the CX_3C subgroup (Bazan et al., 1997), whilst the C subgroup contains only lymphotactin α and β (Kelner et al., 1994) (Fig. 1.11).

Chemokines are capable of plasma membrane tethering, through direct interaction with glycosaminoglycans (Proudfoot et al., 2003). Binding to endothelial glycosaminoglycans facilitates chemokine signaling to passing leukocytes, upregulating integrin expression and thereby promoting their activation, arrest and adhesion. Meanwhile, binding of chemokines to

extracellular matrix glycosaminoglycans enables development of the chemokine gradients that are required for appropriate leukocyte trafficking (Patel et al., 2001).

Most human chemokine genes are found at two distinct chromosomal sites: 17q12 holds genes for the CC chemokines, whilst the CXC chemokines are found at 4q13.3. Despite displaying highly variable amino acid sequences, chemokines share similar tertiary protein structure (Olson and Ley, 2002). A COOH-terminus α-helix common to all CC and CXC chemokines is responsible for glycosaminoglycan interaction (Proudfoot et al., 2003), whilst receptor binding is mediated via two regions at the NH_2-terminal (Gong and Clark-Lewis, 1995).

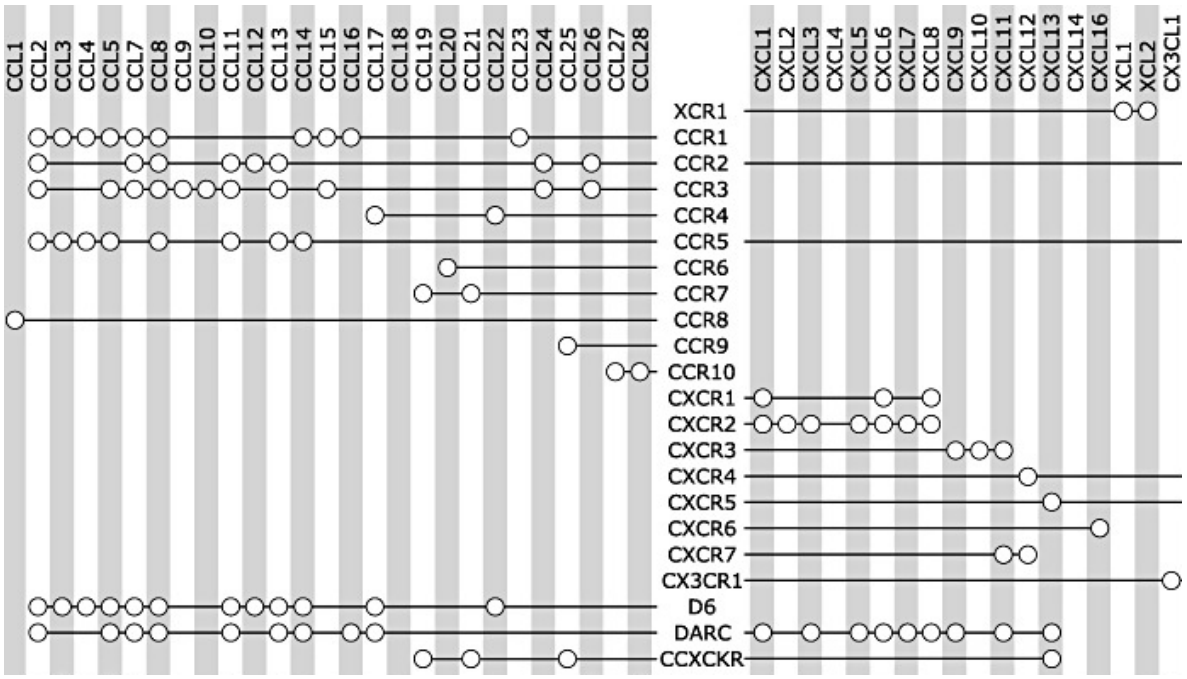

Figure 1.11 – Chemokine and chemokine receptor interactions. Known chemokine receptors (middle column) and their chemokine ligands (top row) are shown. Note that several receptors bind multiple chemokine ligands indicating a redundant system of chemokine signalling. D6, DARC and CCXCKR are decoy receptors, which bind chemokine ligands without activating cell motility pathways.

Their physiological role appears to involve the removal of excessive free chemokine from inflammatory sites (Scholten et al., 2012).

1.5.2.2 Chemokine receptor structure and function

Chemokines bind to chemokine receptors on the surface of target cells. Approximately 20 signalling and 3 non-signalling chemokine receptors have been identified to date (Allen et al., 2007), named in similarity to the chemokines but with the addition of an 'R' to indicate their receptor status (i.e. CCR, CXCR, CX_3CR1 and CXCR1) (Murphy et al., 2000). Most chemokine receptors bind multiple chemokines, but each is restricted to a single chemokine subclass. Chemokine receptors exist as 7-transmembrane repeat proteins belonging to the G-protein coupled family of receptors (Katritch et al., 2012). Mutagenesis studies demonstrate that receptors interact with chemokines through motifs at both the extracellular N-terminus, as well as various regions within the extracellular loops (sequences between two transcellular domains) (Blanpain et al., 2003)(Pease et al., 1998).

1.5.2.3 Altered chemokine expression in cancer

Intriguingly, chemokine gene expression is tightly regulated at a number of levels. CXCL8 expression in epithelial cells is driven by nuclear factor kappa-light-chain-enhancer of activated B cells (NFκB), whilst p38 mitogen activated protein kinase (MAPK) stabilises the CXCL8 mRNA transcript (Holtmann et al., 1999). Chemokine mRNAs have a short half-life such that mRNA stabilisation is a prerequisite for successful translation (Hamilton et al., 2010). In some instances, several transcription factors act in a synergistic manner to promote the transcription of chemokine genes. For example, this has been demonstrated for the expression of CCL5. Here, mutations in either the NFκB or INF-regulatory factor-3 transcription factor

binding sites within the CCL5 promoter region inhibited CCL5 expression in response to viral infection (Génin et al., 2000). Similarly, mutation of NFκB, or stimulation of specificity protein-1 (SP-1) binding sites within the CCL2 gene promoter region inhibited CCL2 expression (Ueda et al., 1994), demonstrating that binding of multiple transcription factors is required for successful gene transcription.

Importantly, NFκB is also involved in the elevated production of chemokines from cancer cells. This has most recently been demonstrated for the breast cancer cell line MCF10A expressing oncogenic mutations in the phosphoinositide 3-kinase (PI3K) gene (Hutti et al., 2012). In such cells NFκB was elevated compared to PI3K wild-type cells and this resulted in upregulation of CXCL1, CXCL2, CXCL8 and CCL2 (Hutti et al., 2012). CXCL5, CXCL8 and CXCL12 expression is also upregulated in cells with mutant p53 (Yeudall et al., 2012), a tumour suppressor gene whose mutation drives NFκB expression (Scian et al., 2005). Mutation in other oncogenes such as Ras have also been linked to the excessive production of CXCL8 (Sparmann and Bar-Sagi, 2004), whilst β–catenin expression promoted the production of CCL2 in breast cancer cell lines (Mestdagt et al., 2006). Finally, mutation in the RET oncogene in papillary thyroid carcinoma is associated with over-expression of multiple chemokines including CCL2, CCL20 and CXCL8 (Borrello et al., 2005). Thus, the oncogenic mutations that drive proliferation and inhibit apoptosis in cancer cells also promote the production of a range of chemokines capable of the recruitment of inflammatory cells to the tumour microenvironment.

1.5.2.4 The recruitment of immune cells to the hepatic metastatic microenvironment

Given the pro-tumourigenic role demonstrated for certain immune populations, as well as the fact that various cancers demonstrate ectopic chemokine expression, it appears that the recruitment of immune cells is an important feature of tumour progression. Interestingly,

Immune cells appear to be recruited to the liver during various stages of metastasis formation including the pre-metastatic phase - defined by the presence of a primary tumour without evidence of tumour cells within the hepatic parenchyma. For example, intraperitoneal colon tumours and spontaneous pancreatic cancers in mice were associated with elevated numbers of immunosuppressive $CD11b^+/Gr1^+$ cells within the liver prior to metastatic development (Connolly et al., 2010). Similarly, $VEGFR1^+$ bone marrow cells appeared in the liver before the arrival of metastatic lung or melanoma cells from their intradermal primary site (Kaplan et al., 2005). During the more advanced stages of hepatic metastasis formation, myeloid as well as lymphoid cells are again seen to support tumour growth. Thus, $CCR1^+$ myeloid cells promoted angiogenesis and the growth of spontaneous hepatic metastases following subcutaneous thymoma cell injection (Rodero et al., 2013). Meanwhile, colorectal liver metastases resected surgically displayed large infiltrates of immunosuppressive $CD4^+/Foxp3^+$ regulatory T-lymphocytes (Pedroza-Gonzalez et al., 2013). At present, it therefore appears that immune populations recruited to the hepatic microenvironment play a role in metastatic progression. Nonetheless, the chemokines involved in immune cell recruitment and the role of such immune cells within the tumour microenvironment of the liver have not been thoroughly explored.

1.6 Summary

The development of hepatic metastasis from colorectal cancer is a complex, multistep process involving interplay between the hepatic microenvironment as well as tumour and infiltrating immune cells. The ability of tumour cells to successfully metastasise to the liver is therefore dependent upon a number of important factors. An increasing body of experimental evidence indicates that tumour cells within the liver are able to recruit populations of immune cells, potentially through the expression of various chemokines. Recruited immune cells then promote the formation of a pro-metastatic microenvironment. Currently, the roles that

recruited immune cells play in this process are poorly understood, as are the mechanisms through which tumour cells in the liver drive immune cell recruitment.

1.7 Research aims

1. To determine the nature of immune cells recruited to hepatic metastases

2. To investigate the role of tumour-derived chemokines in the recruitment of immune cells to the hepatic metastatic microenvironment

3. To determine whether immune cells in the hepatic metastatic microenvironment promote or inhibit metastatic progression

CHAPTER 2. MATERIALS AND METHODS

2.1 Cell lines, lentiviral transfection and cell culture

2.1.1 Cell lines

MC38 (murine colon cancer), Lewis Lung Cancer (murine), B16F1 (murine melanoma), Pan02 (murine pancreatic cancer), HT29, HCT-116 and LoVo (all human colon cancer) cell lines were purchased from the American Type Culture Collection. MC38, LLC and B16F1 were cultured in DMEM with 10% fetal calf serum (FCS) and Penicillin/Streptomycin (100 I.U./mL) (all Sigma-Aldrich). HT29, HCT-116, LoVo and Pan02 were grown in RPMI medium (Sigma-Aldrich) supplemented with 10% Foetal Calf Serum and Penicillin/Streptomycin (100 I.U./mL). All cells were grown in a sterile incubator (Binder) with 5% CO_2 at 37°C. Cells were used at 80% confluency and kept for no more than 10 passages. All cell culture experiments were performed under sterile conditions in a laminar flow hood.

2.1.2 Lentiviral transfection

The MC38 and LLC cell lines were transfected with an expression vector carrying the green fluorescent protein (GFP) and either the puromycin or Geneticin (G418) resistance genes (pEGFP-C1, Clontech, Paolo Alto, CA). The HT29, HCT-116 and LoVo cell lines were transfected with a lentiviral plasmid carrying the genes for firefly luciferase, m-cherry and puromycin resistance (Capital Biosciences VSL-0078P). For transfection, $5x10^3$ tumour cells were spun at 3200RPM, 4°C for 30 minutes in RPMI with 8ug/ml polybrene (Sigma-Aldrich H9268) and lentiviral particles at Multiplicities of Infection of 1, 2 and 5. Following spinoculation, cells were incubated at 4°C for a further 90 minutes to increase transfection efficiency before being plated in 24-well plates and cultured at 37°C, 5% CO_2 in a sterile incubator. After 24 hours, the lentiviral supernatant was replaced with media containing the selection antibiotic at a pre-

determined concentration based on its effect on naïve, non-transfected cells. 7-10 days later highly fluorescent cells (MC38^{GFP}, LLC^{GFP}, HCT-116^{luc}, HT-29^{luc} or LoVo^{luc}) were separated from low fluorescent ones using FACS sorting. FACS sorting of fluorescent cells was performed by Mr Andrew Worth (Jenner Institute, University of Oxford) using the Legacy MoFlo MLS High-speed Cell Sorter (Beckman Coulter). Following cell sorting, MC38^{GFP+} clones were selected for using 5 μg/ml puromycin (Sigma) and LLC^{GFP+} and B16F1^{GFP+} clones using 800 μg/ml G418 (PAA Laboratories). M-cherry expressing colon cancer clones were selected for using 0.75 μg/ml puromycin.

For inhibition of CCL2 or MIF expression, cancer cell lines were further transfected with custom-made pLKO.1 lentiviral plasmids containing CCL2shRNA, MIFshRNA or a scrambled shRNA control (MISSION shRNA, Sigma-Aldrich). The technique for transfection of cell lines with these plasmids was identical to that described above for the fluorescent/luminescent genes. Five shRNA constructs were tested for each chemokine to ensure that the greatest possible inhibition of target protein - as determined by ELISA of the cell culture supernatant - was achieved. MIFshRNA plasmids contained the neomycin resistance gene and so these colonies were selected for with the antibiotic G418 (Sigma-Aldrich G8168). MC38 (GFP negative) cells transfected with lentivirus-mediated shRNA or the scrambled shRNA control were selected with 2.5 μg/ml puromycin.

To determine the degree of chemokine inhibition achieved by transfection of cell lines with shRNA-containing lentiviral particles the chemokine concentration in tumour cell-conditioned medium was determined using commercially available ELISA kits (R&D Systems DY479E and DY289E). The mean chemokine concentration for triplicate samples were normalised to the total protein content of the supernatant determined using a bicinchoninic

acid protein assay kit (Thermo Scientific 23225). The values obtained for shRNA and scrambled shRNA transfected cell lines were then compared.

2.1.3 Assessment of chemoattractant effect of MIF on SCID murine neutrophils

Single cell suspensions generated from SCID mouse bone marrow were labeled with allophycocyanin (APC)-conjugated anti-CXCR2 and phycoerythrin-cyanine-7 (PECy7)-conjugated anti-CD45 antibodies in the presence of anti-CD16/CD32 (all eBioscience). $APC^+/PECy7^+$ cells were FACS sorted using the Legacy MoFlo High Speed Cell Sorter (Backman Coulter), before being suspended in serum-free RPMI medium (ATCC) at a concentration of $5x10^5$ cells per mL. 100µl of the neutrophil cell suspension was added to the upper wells of a 96-well 3µm pore migration plate (Cell Biolabs CBA-104). This plate was then placed within a 96-well carrier plate containing serum free RPMI supplemented with 0, 20, 50, 100, 200, 400 or 800ng/mL recombinant human MIF (R&D systems). The pores within the upper well of this transwell system therefore allow neutrophils to migrate through to the lower well under the appropriate chemotactic stimuli.

After 6 hours, the upper well plate was transferred to a new lower well plate containing a cell detachment buffer (Cell Biolabs), such that transmigrated cells adherent to the undersurface of the plate became freely suspended within the lower plate. Cell-containing solutions from the two lower plates were then combined, cells within the resultant suspension were lysed and their nucleic acids fluorescently labelled by the addition of a solution containing the CyQuant® GR dye (Cell Biolabs). Following a 20-minute incubation period, the solution from each well was transferred to a new transparent, 96-well plate (nunc, Thermo Scientific) and fluorescent measurements taken using the Infinite M200 plate reader (Tecan) with the filter set to 485/538 nm.

2.1.4 Determination of effect of intrinsic MIF inhibition or ISO-1 treatment on HT29 cell apoptosis in-vitro

For the determination of tumour cell apoptosis, $3x10^5$ $HT29^{MIFshRNA}$, $HT29^{Lenti\ ctrl}$, $LoVo^{MIFshRNA}$, $HT29^{Lenti\ ctrl}$ or untransfected HT29 cells were seeded in triplicate into the wells of 6-well plates containing 3 ml culture medium. After 24 hours, untransfected cells were treated with 100 µM ISO-1 diluted in DMSO or a concentration-matched DMSO control solution. After 4 days of treatment (or in the case of lentiviral transfected cells standard culture), cell cultures were analysed for the presence of early and late apoptotic cells using a commercially available flow cytometry-based apoptosis detection kit (BD Pharmingen; 559763).

For detection of the percentage of early and late apoptotic cells, the instruction manual was followed. Briefly, cell culture supernatant was aspirated and kept aside. Cells culture plates were washed with PBS before the addition of 500 µl 1X trypsin solution (Sigma-Aldrich), followed by incubation for 10 minutes at 37°C. The cell suspension was then resupsended with 5 ml culture media containing 10% FCS and the resultant cell suspension was added to the cell culture supernatant initially kept aside from each well. This process ensured that any late apoptotic cells that had detached from the culture dish were included in the analysis. The cell suspension was then centrifuged at 1500 rpm for 5 minutes and excess media aspirated. Cell pellets were resuspended in 1X Binding Buffer at a final concentration of $1x10^6$ cells per ml. Then 5 µl each of PE Annexin V and 7-AAD were added to a 100 µl aliquot of the cell suspension before incubation for 15 minutes at room temperature in the dark. The cells were then diluted in a further 400 µl of 1X Binding Buffer before being analysed on a flow cytometer (FACS Calibur, BD Bioscience). FACS data was interpreted using FlowJo software version 7.6.5.

2.2 Animal work and associated experiments

2.2.1 Animals

Female C57BL/6 and SCID (C.B-17-SCID) mice were purchased from Charles River Laboratories (Kent, UK) and $CCR2^{-/-}$ mice from Jackson Laboratories (Bar Harbor, ME). CD11b-DTR (Diphtheria Toxin Receptor) mice were obtained from Prof. Martin Bennett (University of Cambridge, UK). All mice were used at age 6-8 weeks and were housed in a specific pathogen free facility with humidity and temperature control. Animal procedures were performed in accordance with the UK Animal Scientific Procedures Act (1986) and followed local ethics review.

2.2.2 Liver metastasis model

C57BL/6, $CCR2^{-/-}$, SCID or CD11b-DTR mice were anesthetized using vapourised isoflurane prior to administration of 0.1mg/kg buprenorphine. Following this, an incision in the upper left lateral abdominal wall was made and tumour cells in 100 µl PBS were injected into the splenic parenchyma before splenectomy was performed using electrocautery. The operative field was irrigated with water in an attempt to lyse any spilled tumour cells and the wound closed using non-soluble sutures. For the MC38, LLC and B16F1 cell lines $5x10^5$ cells were used per mouse. For Pan02, HT29, HCT-116 and LoVo cell lines $1x10^6$ cells were used per mouse. On the final day of experimentation animals underwent schedule 1 killing by means of intraperitoneal injection of 200 µL pentobarbitone. C57bl6 mice injected with MC38, LLC or B16F1 cells were killed 2 weeks following surgery whilst those injected with the Pan02 line were killed 4 weeks following surgery. SCID mice injected with HT29 or HCT-116 cells were killed 5 weeks following surgery and LoVo injected mice were killed 7 weeks following surgery.

2.2.3 Adoptive transfer experiments

Female C57BL/6-Tg(UBC-GFP)30Scha/J mice ubiquitously expressing GFP (a kind gift from Prof. Richard Cornall, Nuffield Department of Clinical Medicine, University of Oxford), were sacrificed and cell suspensions prepared from their bone marrow. Bone marrow cells (2×10^6) were transferred to tumour bearing syngeneic C57BL/6 mice at day 11 post MC38 inoculation via tail vein injection. Recipient mice were sacrificed 24 hours later and hepatic GFP^+ cells analysed by flow cytometry and immunohistochemistry.

2.2.4 Collection of murine serum

Shortly following intraperitoneal injection of sodium pentobarbital (200 mg/kg) the thoracic cage was opened and the inferior vena cava incised just superior to the diaphragm. Blood was aspirated from the thoracic cavity using a 1 ml syringe before being placed on ice for 30 minutes. Coagulated blood samples were then spun at 12000 RPM for 10 minutes at 4˚C and the serum supernatant collected, and stored at -80˚C until analysis.

2.2.5 $CD11b^+$ myeloid cell depletion experiments

CD11b-DTR mice were administered Diphtheria Toxin (DT) (7.5 ng DT/g body weight in 0.2% BSA/PBS) or BSA/PBS control, via intraperitoneal injection on days 7 and 9, and livers collected on day 12 post tumour cell inoculation. Magnetic Resonance Imaging (MRI) was performed by Sean Smart (Oxford Cancer Imaging Centre, University of Oxford) on days 6, 8 and 11 following $MC38^{GFP}$ inoculation at 4.7T using a 40 mm quadrature birdcage coil. Cardiorespiratory triggering was used to reduce motion artifact. Images obtained using the MRI were reconstructed in 3D using ITK-snap software (http://www.itksnap.org/pmwiki/pmwiki.php) and from this reconstruction, total hepatic tumour burden was determined for each mouse at the aforementioned time points.

2.2.6 Neutrophil depletion in SCID mice

To specifically deplete murine neutrophils, mice were administered 12.5ug/kg rat anti-mouse Ly6G antibody clone 1A8 (BD Biosciences 551459) or an isotype control antibody IgG2a (BD Biosciences 562302) via the intraperitoneal route. Initially, the results of antibody administration on hepatic and splenic neutrophil count were determined in naïve mice. For this experiment, SCID mice were injected with the antibody or isotype control, sacrificed 24 or 72 hours later and total organ neutrophil number determined for both the liver and spleen.

Once the effect of anti-Ly6G administration had been determined for naïve SCID mice, neutrophil depletion was performed in mice bearing hepatic HT29, HCT116 or LoVo metastases. For some of these experiments, anti-Ly6G was either started 24 hours prior to tumour cell injection (anti-Ly6G early) or 10 days following tumour cell injection (anti-Ly6G late) and was then administered every 72 hours for the remainder of the experiment. Neutrophil depletion was confirmed for at least three mice per experiment by FACS analysis of resected livers post-mortem.

2.2.7 Small molecule inhibition of systemic MIF activity

To systemically inhibit MIF activity, tumour-bearing mice were administered the small molecule antagonist of MIF, ISO-1 (Millipore) via the intraperitoneal route. ISO-1 was initially reconstituted in 100% dimethyl sulfoxide (DMSO) before being diluted in sterile water to provide a 200µl dose of 20mg/kg per mouse. Control mice were treated with a matched dose of DMSO diluted in sterile water to the same concentration as that used to reconstitute the ISO-1. All mice from this experiment were imaged without being administered treatment for the first 10 days of the experiment. On the 10th day following tumour cell injection the experimental

mice were divided into two groups such that the mean abdominal luminescent intensity was equivalent between groups. At this stage treatment with either the DMSO control or ISO-1 was started with the IP injection being repeated every 72 hours for the duration of the experiment.

2.2.8 Determination of metastatic growth kinetics in mice

For time-course experiments designed to determine the temporal relationship between neutrophil depletion and metastatic development, mice bearing luciferase-expressing hepatic metastases were imaged at various time-points following intrasplenic tumour cell injection.

For *in-vivo* imaging, mice were anaesthetised in an anaesthetic chamber using 3% vaporised isoflurane (Piramal Healthcare), before being injected with 150mg/kg Vivo-Glo™ Luciferin (Promega). The animals were immediately transferred to a CCD camera (IVIS system, Perkin Elmer), fixed in position and imaged using automatic f/stop, exposure time and binning. Mice were imaged every minute for a variable period until the signal intensity reached a plateau. At this point imaging ceased and an ROI drawn to encompass the upper abdomen and lower thorax for each mouse. The background photon flux was then subtracted from the signal within the ROI to determine the total hepatic photon flux *in-vivo*. To represent change in photon flux with time as metastases developed, the signal for each mouse at each time-point was normalised to the value obtained for the same animal at 24 hours post surgery.

Of note, some mice developed intense luminescent signals in the region of the splenic fossa. Such signals rarely declined over the first 10 days of the experiment, unlike the signals seen for tumour cells within the liver on the contralateral side of the abdomen (Fig. 3.8 to 3.10). Mice displaying such imaging characteristics had palpable tumours in the upper abdomen on

the left side within 10 days of surgery and on post-mortem examination, these were found to represent tumours well away from the liver. This indicated either operative tumour cell spillage or tumour thrombus of the splenic vein with resultant tumour growth in the splenic fossa, which was therefore considered an unrelated pathology to the development of hepatic metastasis. As such, for these mice the ROI used to determine *in-vivo* hepatic luminescence was drawn in such a way as to exclude the signal emanating from the splenic region.

2.2.9 Determination of ex-vivo luminescence in tumour-bearing murine livers

For neutrophil depletion experiments in tumour-bearing mice, total hepatic luminescence was determined post-mortem for each mouse. To determine total hepatic luminescence, mice were injected with 150mg/kg Vivo-Glo™ Luciferin 60 seconds prior to lethal injection of 100mg/kg pentobarbital. Both injections were administered via the intraperitoneal route. The liver was immediately resected via an anterior abdominal incision and transported to a CCD camera where it was imaged using automatic f/stop, exposure time and binning as determined by the device. Serial images were taken every minute for a variable period until the signal intensity reached a plateau. At this point, a region of interest (ROI) was drawn around the entire liver and the total photon flux (p/sec/cm^2/sr) determined. From this value, the background photon flux was subtracted to give the total hepatic phonon flux.

2.2.10 Isolation of neutrophils from murine livers

Following the removal of murine livers post-mortem, single cell hepatic suspensions were generated as previously described, but with particular care taken to keep the cell suspension at room temperature in an attempt to avoid activating hepatic neutrophil populations. Following the lysis of red blood cells, cell pellets from 6 tumour-bearing or 9 naïve

mice were combined by re-suspension in 2 ml of 35% (v/v) Percoll (Sigma-Aldrich) diluted in PBS. The cell suspensions were then distributed throughout 8 ml of 35% (v/v) Percoll diluted in PBS, before being centrifuged at 300G for 10 minutes at room temperature. In the resultant density gradient, hepatic immune cell populations formed a cell pellet, whilst hepatocytes, tumour cells and other non-immune cell types reside on the surface of the Percoll solution (Cotter and Muruve, 2006). Thus, the supernatant was aspirated and the remaining immune cell layer re-suspended in 1ml FACS buffer.

Next, a cell count was performed using an automated cell counter as above, before the immune cells were incubated in the appropriate concentration of anti-CXCR2 (R&D Systems) and anti-CD45 (eBioscience) FACS antibodies in the presence of anti-CD16/CD32 (eBioscience) to block Fc receptors. After a 45-minute incubation period at room temperature, excess antibody was removed by washing the cell suspension in FACS buffer. $CD45^{+}/CXCR2^{+}$ neutrophils and all other hepatic immune cells ($CD45^{+}/CXCR2^{neg}$) were then being FACS sorted and collected using a high-speed cell sorter (MoFlo™ XDP, Beckman Coulter). Operation of the cell sorter was kindly performed by Dr Drew Worth (Jenner Institute, University of Oxford). The Percoll gradient procedure and FACS protocol enabled the separation of hepatic neutrophils from other immune cell subtypes as determined by analysis of cell morphology (Fig. 2.1).

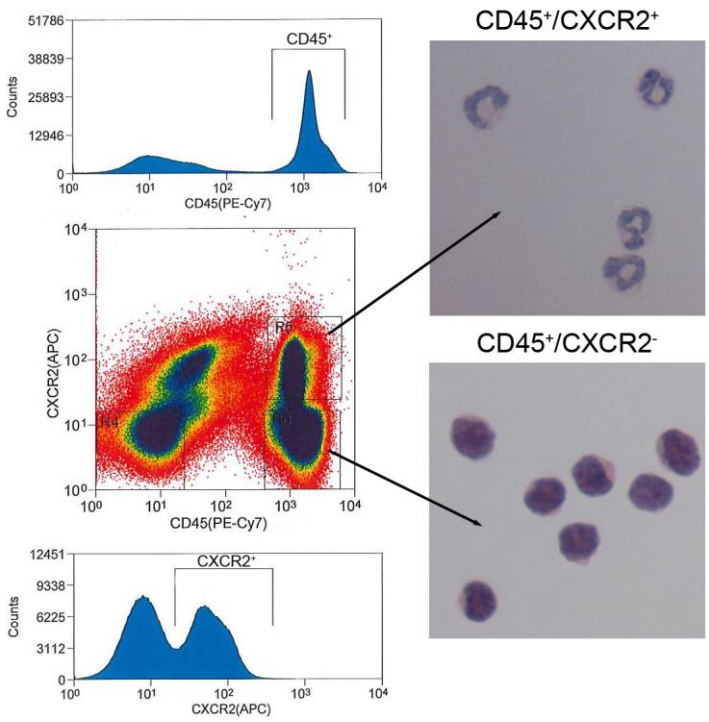

Figure 2.1 FACS sorting of hepatic neutrophils. Neutrophils were defined by their expression of both CD45 and CXCR2, as identified on flow cytometry plots (center left). These cells were polymorphonuclear (upper right panel) whereas $CD45^{+}/CXCR2^{neg}$ cells where monocytic (lower right panel).

2.2.11 Extraction of RNA from FACS sorted neutrophils

Immediately following FACS sorting, neutrophils were lysed in 300 µl Trizol reagent (Life technologies) by repetitive pipetting. After incubation at room temperature for 10 minutes 30 µl chloroform was added to the Trizol solution and the sample tubes shaken vigorously for 15 seconds. After a further 2-minute incubation period at room temperature, the samples were centrifuged at 12000 RCF for 15 minutes at 4°C. The aqueous supernatant was then transferred to a new tube containing an equal volume of isopropyl alcohol in order to precipitate the RNA. The sample was then incubated for 10 minutes at room temperature before being centrifuged again at 12000 RCF for 10 minutes at 4°C. The supernatant was then

removed and the RNA pellet washed in 75% ethanol before being centrifuged at 7500 RCF for 5 minutes. Finally, the ethanol supernatant was aspirated and the RNA pellet re-suspended in 20 µl RNase-free water (Qiagen) at 60°C for 10 minutes with regular agitation. The RNA purity and concentration was determined by analyzing 1 µl of the resultant solution on a bench-side spectrophotometer (Nano Drop 2000c Thermo Scientific).

2.2.12 Assessment of neutrophil angiogenic gene expression using qPCR

RNA samples extracted from tumour-associated and naïve neutrophils were subsequently used for the synthesis of cDNA in preparation for qPCR analysis. cDNA was synthesised using the RT^2 First Strand reverse transcription kit (SA Biosciences). Briefly, genomic DNA was eliminated from RNA samples before the addition of nucleotides and reverse transcriptase cocktail at concentrations as recommended by the manufacturer. The mixture was incubated at 42˚C for 15 minutes, after which the reaction was stopped by incubation at 95˚C for 5 minutes.

cDNA samples were then added to a qPCR master mix containing SYBR Green (SA Biosciences) before the mixture was loaded onto a commercially available 96-well PCR array plate spotted with cDNA primers specific for various angiogenic growth factors (SA Bioscience PAMM-072ZA-2). Array plates were analysed for fluorescence intensity using a qPCR machine (Stratagene Mx3005P). The thermal profile for qPCR included an initial 10 minute incubation at 95˚C followed by 40 cycles of 95˚C for 15 seconds and then 60˚C for 1 minute followed by a dissociation curve of 95˚C for 1 minute, 55˚C for 30 seconds and finally 95˚C for 30 seconds.

Following the qPCR run, melt curves were analysed for each primer and those that demonstrated multiple peaks at differing temperatures were excluded from further analysis. Further primer sets were then excluded by use of a threshold value placed in the lower third of the linear fluorescence accumulation phase as determined by observation of the log fluorescence intensity for each primer. Analysis of Ct values and fold change in gene expression between tumour-associated neutrophils and those from naïve mouse livers is discussed further below.

2.3 Flow cytometry

2.3.1 Preparation of single cell suspensions from murine tissues

Immediately following resection and under sterile conditions, whole livers or spleens were minced using a scalpel and digested at 37^{O}C in RPMI-1640 medium containing 0.05% (w/v) collagenase/dispase (Roche) and 0.01% (w/v) trypsin inhibitor (Sigma). Digested tissues were strained through a 70 μm filter into ice-cold PBS and residual red blood cells (RBC) lysed using red cell lysis buffer (Sigma). Bone marrow cells were flushed from the femurs of mice with PBS and filtered through a 70 μm cell strainer before RBC lysis as above. Blood samples were collected in 2 mg/ml EDTA and washed with PBS before RBC lysis. Finally, cell suspensions were suspended in FACS buffer (2% FCS in PBS), adjusted to 10^7 cells/ml using the NucleoCounter NC-100 automated cell counter (Chemometec) and then stained with antibodies for flow cytometric analysis.

2.3.2 Flow cytometry and flow cytometric analysis

Cells for flow cytometric analysis were stained using various fluorochrome-conjugated FACS antibodies at 4˚C for 60 minutes in the presence of anti-mouse CD16/CD32. FACS

antibodies (Table 2.1) were used at the concentration recommended by the manufacturer and were compared with matching concentrations of each isotype control. Flow cytometry was performed using a FACSCalibur flow cytometer (BD biosciences) and data analysed using FlowJo software version 7.6.5.

For experiments in which MC38^{GFP}, LLC^{GFP} or B16F1^{GFP} cell lines were used, tumour cells were gated out based on their GFP expression in order to aid the visualisation of myeloid cells. In all experiments myeloid cells were identified based on their relative forward/side scatter position as shown in Fig. 2.2.

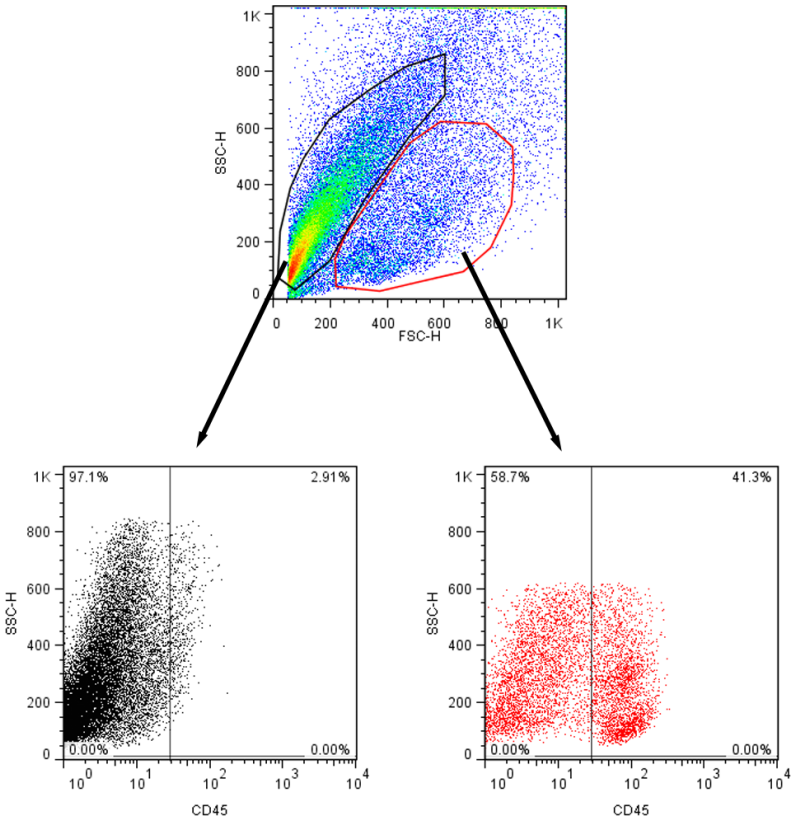

Figure 2.2 – Flow cytometric gating strategy for identification of hepatic myeloid cells. Myeloid cells were selected by creating a 'myeloid' gate (red polygon) in hepatic forward/side scatter plots shown in the upper panel. Only 2.91% of cells outside the myeloid gate are CD45$^+$

(lower left panel) indicating that the gating strategy has a high sensitivity for myeloid cells within the hepatic single cell suspension.

2.3.3 Preparation and staining of cytospun immune cells

FACS-sorted $CD45^+/CXCR2^+$ cells were suspended in 20% bovine serum albumin in PBS before being centrifuged at 500 RPM onto Superfrost Plus microscope slides (Fisher) using a Cytospin centrifuge machine (Cytospin 3, Shandon Life Sciences). Cytospun cells were then stained using a standard H&E protocol. Briefly, slides were rehydrated in distilled water before incubation in Mayer's haematoxylin (Sigma-Aldrich) solution for 4 minutes. Following a 5-minute washing step in running tap water, slides were differentiated for 5 seconds with 0.3% acid-alcohol (2800 ml ethanol, 1200 ml water and 12 ml concentrated hydrochloric acid). Slides were washed in running tap water for a further 5 minutes before being rinsed in Scotts tap water substitute. Finally, slides were incubated in Eosin (Sigma-Aldrich) for 2 minutes before being dehydrated in increasing concentrations of alcohol and then xylene (Sigma-Aldrich) for a further 2 minutes. Coverslips were mounted onto slides using Histomount (Fisher Scientific) before visualisation using bright-field microscopy.

2.3.4 Antibodies used in flow cytometry

Table 2.1 demonstrates the antibodies used in flow cytometry experiments. The antibody concentration used was as recommended by the manufacturer, with matching concentration of isotype controls used where required.

Antibody	Clone	Supplier; catalogue number
rat anti-mouse CD45 PE-Cy7	30-F11	eBioscience; 25-0451
rat anti-mouse Gr1 PE	RB6-8C5	eBioscience; 12-5931
rat anti-mouse Ly-6G PE	RB6-8C5	eBioscience; 11-5931
rat anti-mouse CD11b PE-Cy7	M1/70	eBioscience; 25-0112
rat anti-mouse CCR1 PE	643854	R and D systems; FAB5986A
rat anti-mouse CCR2 PE	475301	R and D systems; FAB5538P
rat anti-mouse CCR3 AF647	TG14	BioLegend; 129401
hamster anti-mouse CCR4 PE	2G12	BioLegend; 131204
hamster anti-mouse CCR5 PE	HM-CCR5	eBioscience; 12-1951-81
rat anti-mouse CXCR2 APC	242216	R and D systems; FAB2164P
rat anti-mouse CXCR3 APC	CXCR3-173	eBioscience; 17-1831-80
rat anti-mouse CXCR4 APC	2B11	eBioscience; 12-9991-81
rat anti-mouse CXCR5 APC	SPRCL5	eBioscience; 17-7185-80
rat anti-mouse CXCR6 APC	221002	R and D systems; FAB2145A
rat anti-mouse CXCR7 APC	734110	R and D systems; FAB7167A
rat anti-mouse TIE2 PE	TEK4	eBioscience; 12-5987-82
rat IgG2a isotype control APC	N/A	eBioscience; 17-4321-81
rat IgM isotype control APC	N/A	eBioscience; 17-4341
rat IgG2b isotype control APC	N/A	eBioscience; 17-4031-81
hamster IgG isotype control APC	eBio299Arm	eBioscience; 17-4888-81
rat IgG2b isotype control PE	N/A	eBioscience; 12-4031-81
rat IgG2a isotype control AF647	N/A	eBioscience; 51-4321-80
hamster IgG isotype control PE	eBio299Arm	eBioscience; 12-4888-81
rat IgG2a isotype control PE	N/A	eBioscience; 12-4321-42
rat IgG2a isotype control AF647	N/A	eBioscience; 51-4321-80

rat IgG2b isotype control PE	N/A	eBioscience; 12-4031-81
rat IgG2b isotype control APC	N/A	eBioscience; 17-4031-81
rat IgG2b isotype control AF647	N/A	eBioscience; 51-4031-80
rat IgG2c isotype control PE	N/A	BioLegend; 400707
rat IgG1 isotype control PE	N/A	eBioscience; 12-4301-81
rat IgG1 isotype control APC	RTK207	BioLegend; 400412
rat IgG2b isotype control PE-Cy7	N/A	eBioscience; 25-4031-82
hamster IgG isotype control PE	eBio299Arm	eBioscience; 12-4888-81
hamster IgG isotype control APC	eBio299Arm	eBioscience; 17-4888-81
hamster IgG isotype control AF647	eBio299Arm	eBioscience; 51-4888-80

Table 2.1 – Antibodies used in flow cytometry experiments.

2.4 Chemokine measurement

2.4.1 Determination of relative cytokine expression in tumour cell conditioned medium

Relative cytokine expression by the MC38, LLC and B16F1 cell lines were assayed using the Proteome Profiler Mouse Cytokine Array (R&D Systems, ARY006). Tumour cell culture-conditioned medium was obtained from MC38, LLC and B16F1 cells by plating $0.2x10^6$ cells per well in 12-well plates and collecting culture medium after 48 hours. Culture medium (1mL), obtained from at least 3 wells per cell line was incubated for 1 hour at 21°C with a panel of murine-specific, biotinylated chemokine/cytokine antibodies before incubating the mixture with a nitrocellulose membrane pre-spotted with chemokine/cytokine antibodies. After an overnight incubation at 4°C the membranes were washed and then incubated with Streptavidin Alexa Fluor 700® conjugate (Life Technologies S-21383) diluted 1:750 in PBS for 1 hour at 21°C. The membranes were then visualised on the ODYSSEY® CLx infrared imaging system (LI-COR) set to detect signals at 700 nm at a resolution of 168 um. Images of nitrocellulose membranes

taken using the LI-COR were analysed using custom made software (Danny Allen, Oxford Cancer Imaging Centre, University of Oxford), which quantifies the signal intensity at each antibody location relative to its negative control value. Values obtained from tumour cell conditioned media were then normalised to the values obtained fromcontrol, cell-free media.

2.4.2 Determination of relative chemokine expression in tumour-bearing mouse serum

To simultaneously determine the concentration of multiple human chemokines in mice with HCT-116, HT29 or LoVo hepatic metastasis relative to splenectomised control mice, serum was analysed using proteome profiler arrays containing human-specific antibodies raised against various chemokines and cytokines (R and D systems ARY005 and ARY017 (both human-specific). 350 μl of test serum pooled from 5 mice was analysed as per the method described for the detection of murine cytokines from tumour cell conditioned medium.

2.4.2 Determination of absolute chemokine concentration in mouse serum

Murine CCL2 and human MIF concentration in mouse serum was determined using commercially available sandwich ELISA kits (R&D Systems DY479E and DY289E respectively). Protocols were followed as per the manufacturer's instruction. Briefly, 96-well plates were coated for 24 hours at room temperature with the appropriate antibody before blocking with 1% bovine serum albumin for 2 hours at room temperature. Following removal of the blocking serum, samples diluted 10-fold in PBS were added to the wells and the plates incubated at room temperature for 2 hours. The plates were then washed in PBS containing 0.05% Tween-20 (Sigma-Aldrich), before the addition of a biotin-conjugated antibody targeting the chemokine of interest. Following a further washing step the wells were incubated in streptavidin-horseradish-peroxidase, before the addition of a solution containing 3,3',5,5'-

Tetramethylbenzidine (Sigma-Aldrich). After 20 minutes the chromogenic reaction was stopped by the addition of 2N hydrochloric acid. The optical densitiy of each well was determined by visualisation using an Infinite M200 plate reader (Tecan) set to 450 nm.

Samples from each mouse were plated in triplicate and at least 10 samples from each tumour type and control were analysed. Following subtraction of the average optical density obtained from blank wells, the mean value for each sample was determined by reference to a standard curve created using a known concentration of the recombinant chemokine being measured.

2.4.3 Determination of MIF concentration in human serum from cancer patients and healthy volunteers

Frozen serum samples from 30 healthy patients, 90 patients with various stages of primary colorectal cancer and 30 patients with hepatic metastases were obtained from the Oxford Radcliffe Biobank (http://orb.ndcls.ox.ac.uk/). The concentration of MIF in each sample was determined using the same commercially available sandwich ELISA kit as per that used for detection of human MIF in tumour-bearing SCID mice (R and D systems DY289E). The protocol followed was identical to that described for the determination of MIF concentration in murine serum samples.

2.5 Immunohistochemistry

2.5.1 Analysis of adoptively transferred cells (for Fig. 3.5)

Livers from tumour-bearing mice following the adoptive transfer of GFP^+ bone marrow cells were resected and placed immediately in Optimal Cutting Temperature (OCT) compound (Tissue Tek) before snap freezing in liquid nitrogen. 12 μm sections were cut from frozen tissue blocks using a Bright Cryostat and mounted on Superfrost Plus microscope slides (Fisher). Sections were counterstained with 4',6-diamidino-2-phenylindole before being mounted with glass coverslips and visualised using a laser scanning confocal microscope (LSM710, Carl Zeiss).

2.5.2 Analysis of tumour-associated neutrophils, vessels, apoptotic or proliferating cells and FGF-2 (for Fig. 4.2 and 5.6 to 5.11)

Tissue sections were prepared as described in 2.2.6.1. For the staining of neutrophils in normal and tumour-bearing mouse livers, tissues were brought to room temperature and then rehydrated in PBS before being fixed in 4% paraformaldehyde for 10 minutes. For the detection of proliferating cells tissues were then incubated in PBS with 0.01% Tween-20 (Sigma-Aldrich) to permeabilise cell membranes. This step was not performed for the immunohistochemical analysis of neutrophils, vessels, apoptotic cells or FGF-2. Following incubation in 10% goat or donkey serum for 30 minutes depending upon the species in which the secondary antibody was produced, tissues were incubated in the appropriate concentration of primary antibody or its isotype control. Incubation of all primary antibodies was performed at room temperature for 2 hours.

After the removal of the primary antibody by washing in PBS, Alexa Fluor-conjugated secondary antibodies (Life Technologies) at a final concentration of 8 ug/ml diluted in PBS were added and slides were incubated for 1 hour at room temperature. After a final washing step, sections were counterstained with 4',6-diamidino-2-phenylindole (DAPI) (Vectashield) before being mounted with glass coverslips and visualised using a laser scanning confocal microscope (LSM710, Carl Zeiss).

For the co-staining of neutrophils and FGF-2, tissues were rehydrated and fixed in ice cold acetone as opposed to paraformaldehyde. Subsequently the tissues were incubated in the anti-Ly6G antibody followed by the anti-FGF2 antibody before the addition of secondary antibodies.

2.5.3 Analysis of tumour-associated neutrophils and MIF expression in human hepatic metastases (for Fig. 5.12)

For the staining of human hepatic tissue from patients with colorectal metastases, 12 um fresh-frozen tissue sections were supplied mounted on glass slides by the Oxford Radcliffe Biobank. Tissues stained with antibodies to MIF, were fixed for 10 minutes in 4% paraformaldehyde diluted in PBS, whilst those stained with the CD66b antibody were fixed in ice-cold acetone for 10 minutes prior to rehydration. Following fixation tissues were blocked for 30 minutes in serum from the species of the secondary antibody before being incubated in the primary antibody for 2 hours at room temperature. The antibody was removed by washing slides in PBS before addition of the secondary antibody, which was incubated at room temperature for 1 hour. The washing stage was repeated before counterstaining tissues with DAPI and mounting with glass coverslips.

2.5.4 Assessment of apoptosis in tumour tissues

Hepatic metastases from ISO-1 and DMSO control-treated HT29 tumour-bearing mice, as well as those from mice bearing $HT29^{MIFshRNA}$ and $HT29^{Lenti\ ctrl}$ tumours where analysed for the presence of apoptotic cells. Following the preparation of tissue sections in the standard way described above apoptotic cells were detected using a commercially available fluorescent

apoptosis detection kit (Apoptag®, Millipore; S7160). The protocol was followed as per the manufacturer. Briefly, tissue sections were fixed in 1% paraformaldehyde solution in PBS for 10 minutes at room temperature. Following washing in PBS sections were incubated in ice-cold ethanol:acetic acid 2:1 for 5 minutes at -20°C. Next, 75 µl Equilibration Buffer was added to the sections, which were incubated for 30 seconds at room temperature. Then, 55 µl of TdT enzyme was added and the sections incubated for 1 hour at 37°C. After the application of Stop Buffer, tissues were incubated in 65 µl of anti-digoxigenin peroxidase conjugate for 30 minutes at room temperature. Finally, tissues were washed again in PBS before cover slips were mounted with vectashield mounting medium containing DAPI. Tissues were viewed using a laser scanning confocal microscope (LSM710, Carl Zeiss) or epifluorescence microscopy (Carl Zeiss).

2.5.5 Antibodies used for immunohistochemistry

Table 2.2 demonstrates the antibodies used in immunohistochemistry experiments.

Antibody	Clonality	Supplier; catalogue number	Dilution
rat anti-mouse Ly6G	Monoclonal	Biolegend; 127602	5 µg/ml
rabbit anti-mouse CD146	Polyclonal	ABCAM; ab75769	1.6 µg/ml
rat anti-mouse CD31	Monoclonal	ABCAM; ab7388	1 µg/ml
rabbit anti-human Ki67	Monoclonal	Vector; VP-RM04	
mouse anti-bovine FGF2	Monoclonal	Millipore; 05-118	10 µg/ml
mouse anti-human MIF	Monoclonal	ABCAM; ab55445	5 µg/ml
mouse anti-human CD66b	Monoclonal	Acris; SM1154P	20 µg/ml
rat IgG	Polyclonal	ABCAM; ab18407	5 µg/ml
mouse IgG	Monoclonal	ABCAM; ab18443	10 µg/ml
rabbit IgG	Polyclonal	ABCAM; ab172730	11 µg/ml

goat anti-rabbit Alexa Fluor 488	Polyclonal	Life technologies; A-11008	8 μg/ml
donkey anti-mouse Alexa Fluor 546	Polyclonal	Life technologies; A-10036	8 μg/ml
goat anti-mouse Alexa Fluor 488	Polyclonal	Life technologies; A-11001	8 μg/ml
donkey anti-rat Alexa Fluor 488	Polyclonal	Life technologies; A-21208	8 μg/ml
donkey anti-rabbit Alexa Fluor 546	Polyclonal	Life technologies; A-10040	8 μg/ml

Table 2.2 – Antibodies used in immunohistochemistry

2.6 Statistical analysis

Statistical analyses were performed using GraphPad Prism. The number of animals used in each experiment is indicated in the relevant figure legends. Data derived from animal studies are presented as mean ±SEM, as is that from *in-vitro* work. In such experiments, mean values are compared using the unpaired Student's *t* test (two-tailed). For luminescence data, which was not normally distributed, median values obtained *in-vivo* were compared using the Mann-Whitney U test. When comparing tumour growth curves constructed using luminescence data, abdominal luminescence was measured on a weekly basis and median values compared at the final time-point for each group. Mean *ex-vivo* hepatic luminescence was compared using the Students T-test. Correlation coefficients (i.e. between serum CCL-2 concentration, tumour burden and $Gr1^{mid}$ cell infiltrate) were calculated using the non-parametric Spearman correlation coefficient. Throughout the figures, the following symbols represent significant *p* values: *p=0.01 to 0.05, **p=0.001 to 0.01, ***p<0.0001.

For flow cytometry data presented in chapter 3, the number of immune cells identified in tumour-bearing and control livers is indicated as a percentage of the total cells counted

within the liver. This data is obtained directly from flow cytometry data using the FlowJo software. In contrast, the total $CXCR2^{+}$ and $CXCR2^{neg}$ cell counts presented in bar graphs in chapters 4 and 5 indicate the total number of a particular cell type in the organ of interest. This was calculated from the total number of cells obtained from harvested organs and the percentage of cells analysed in the flow cytometry sample that represent the cell of interest. Here, the total number of cells obtained from each organ was quantified using an automated cell counter (Chemometec, NucleoCounter NC-100). This method was used to account for the presence of colon cancer cells in tumour-bearing livers, which represent up to 50% of the total flow cytometry cell count. Thus, simply presenting the percentage of cells of interest within a sample would significantly underestimate the true cell count in tumour-bearing mouse livers which contain a significantly higher total cell number than naïve control livers.

For the analysis of difference in absolute chemokine values for tumour-bearing and naïve mice data is presented as the mean ±SEM and compared using the Students T-test. For the analysis of serum MIF concentration in healthy control subjects and patients with colon cancer, the Mann-Whitney U test was used to compare median values, as the data for patients with metastatic disease was not normally distributed.

For the qPCR data presented in chapter 5, fold change in RNA expression was determined for neutrophils FACS sorted from tumour-bearing mice relative to neutrophils FACS sorted from naïve mice. For each comparison neutrophils obtained from 6 tumour-bearing mice were pooled and compared to those pooled from 9 naïve mice. For fold change calculations, the $2^{-\Delta\Delta Ct}$ or comparative Ct method was used. Here, the Ct value for each gene of interest was normalised to a panel of house keeping genes (HPRT, GUSB and GAPDH) for that sample. Following this, the difference in normalised values for naïve and tumour-associated neutrophils

were determined to give the ΔΔCt value for each gene of interest from which $2^{-\Delta\Delta Ct}$ was calculated.

For the statistical analysis of proliferation and apoptosis, as well as vessel density in tissue samples from tumour bearing mice, microscopy images were analysed using freely available imaging software (Image J; http://imagej.nih.gov/ij/). For quantification of proliferating and apoptotic cells, red, green and blue channels from microscopy images were separated and a black/white threshold generated for each. An ROI was drawn around metastatic foci and the number of proliferative, apoptotic and DAPI positive cells calculated within the ROI using the Image J software. This information enabled the percentage of proliferative or apoptotic cells to be determined as a percentage of the total number of cells within metastatic deposits. For quantification of metastatic vascularity a similar approach was used however rather than performing cell counts the area of CD31 or CD146 staining was determined and expressed as a percentage of the ROI area. In the analysis of microscopy images the number of tumours imaged is indicated in the figure legend and scale bars in images represent 40 μm unless stated otherwise.

CHAPTER 3: CD11b^{+}/CCR2^{+} MONOCYTES PROMOTE HEPATIC METASTASIS FORMATION

3.1 Introduction

3.1.1 Basic monocyte biology

Monocytes are a highly plastic, circulating leukocyte subset capable of differentiating into macrophages and dendritic cells at sites of tissue inflammation in response to inflammatory stimuli. Monocytes arise from bone marrow common myeloid progenitor cells in a process dependent upon the cytokine macrophage colony stimulating factor (M-CSF) (Wiktor-Jedrzejczak and Gordon, 1996)(Ryan et al., 2001). Various subsets of circulating monocytes have been defined in man and mouse based on the expression levels of various cell surface markers. In mice, circulating 'inflammatory' monocytes strongly express Ly6C and are dependent upon the expression of the chemokine receptor CCR2 for recruitment to tissues during infection (Kurihara et al., 1997)(Serbina and Pamer, 2006). A second population of 'resident' murine monocytes expressing high levels of CX_3CR1 has also been documented (Geissmann et al., 2003). This subset patrols the lumen of small blood vessels and is capable of rapid tissue infiltration, acting as a first responder in response to acute infection (Auffray et al., 2007).

A similar designation has been assigned to human monocytes, where CD14^{++}/CD16^{-}/CCR2^{+} inflammatory 'classical' monocytes are recruited from the bone marrow to sites of infection. CD14^{dim}/CD16^{++} and CD14^{+}/CD16^{+} 'non-classical' and 'intermediate' monocytes respectively (Passlick et al., 1989)(Ziegler-Heitbrock et al., 2010) have also been demonstrated in human blood and the non-classical subset appear to patrol the blood vessel lumen, as per the Ly6G^{low} murine subset (Cros et al., 2010). Interestingly, both Ly6C^{+} and Ly6C^{low} monocytes can

differentiate into dendritic cells, whilst in non-inflammatory states circulating Ly6C^{+} monocytes return to the bone marrow and differentiate into the Ly6^{low} subset (Geissmann et al., 2003).

CCL2 is expressed by most human cells during inflammation (Shi and Pamer, 2011) and is the primary chemokine responsible for chemotaxis of CCR2^{+} inflammatory monocytes (Serbina et al., 2008). As well as CCL2 however, CCL7 acts as a ligand for CCR2 and lack of CCL2 or CCL7 inhibited CCR2^{+} monocyte recruitment to sites of infection (Jia et al., 2008). CCR2^{+} monocytes also express other chemokine receptors. Thus, tissue resident, inflammatory monocytes expressed CCR1 and CCR5 (Kaufmann et al., 2001), whilst circulating monocytes expressed CXCR2 and migrated towards the inflammatory chemokine MIF (Bernhagen et al., 2007). Nonetheless, CCR2 expression is required for monocytes to move from the bone marrow into the circulation, whereas it is not required for their movement form the circulation into inflamed tissue (Serbina and Pamer, 2006). It is likely that as monocytes mature from their progenitor state in the bone marrow, through their circulating inflammatory state and finally become tissue macrophages, their chemokine receptor expression profile changes, enabling them to respond to a variety of different chemokines expressed within the various microenvironments in which they reside. Such plasticity enables monocytes to respond to various different stimuli and fine-tune their response appropriately.

3.1.2.Expression of monocyte chemoattractants in colon cancer

Expression of various monocyte chemoattractants – most notably CCL2 - has been widely studied in solid tumours (Balkwill, 2004). Interestingly, analysis of CCL2 expression in patients with various stages of colon cancer has demonstrated conflicting results. Thus, immunohistochemical staining demonstrated a correlation between CCL2 expression level in primary colorectal cancer and disease stage (Yoshidome et al., 2009), however in a similar study

a reduction in the tumour:normal tissue CCL2 ratio predicted poor outcome in primary colon cancer patients following curative resection (Watanabe et al., 2008). Finally, there was no difference in the serum CCL2 concentration in blood taken from 99 colon cancer patients compared with 98 age-matched healthy volunteers (Krzystek-Korpacka et al., 2013). In the only study to date to analyse the expression of alternative CCR2 ligands in colon cancer patients, Cho et a., (2012) demonstrated elevated CCL7 levels in hepatic metastases compared with tissue taken from primary colon tumours or normal colonic mucosa (Cho et al., 2012).

At the present time, the relationship between the expression of monocyte chemoattractants and colon cancer development or prognosis is therefore unclear. This may be because of differences in the populations analysed in each study, or the techniques employed to detect CCL2 (ranging from immunohistochemical staining to determination of serum concentrations using ELISA). Alternatively, it may simply imply that there is significant heterogeneity in the colon cancer chemokine expression profile between individuals, such that larger patient cohorts are required to identify chemokine expression trends in relation to disease stage. This view is supported by the analysis of colon cancer samples for the presence of multiple chemokines, which demonstrated significant variability in the mRNA expression profile of both CCL and CXCL chemokines between patients (Erreni et al., 2009).

3.1.3 Monocyte involvement in metastatic progression

The presence of monocytes in various primary and metastatic tumours has been well documented (Mantovani et al., 2008). The involvement of monocytes in the progression of primary cancer to malignancy was first clearly demonstrated by crossing transgenic mice susceptible to breast cancer with those carrying a recessive null mutation in the M-CSF gene (Lin et al., 2001). Interestingly, M-CSF absence did not affect primary tumour growth, but

significantly delayed the formation of pulmonary metastasis. Furthermore, primary tumours in M-CSF$^{-/-}$ mice displayed reduced monocyte infiltration, indicating that monocyte recruitment to the primary tumour promotes its metastatic potential (Lin et al., 2001). More recently, inflammatory monocytes were identified in the lungs of mice during the development of breast cancer metastasis (Qian et al., 2011). Their recruitment to the metastatic site, where they were identified in direct communication with tumour cells, was dependent upon both tumour-derived and stromal CCL2 (Qian et al., 2011). These studies clearly implicate monocyte recruitment in the progression of primary to metastatic cancer, however the mechanisms through which infiltrating monocytes promote this progression remain poorly understood.

With relevance to the development of hepatic metastasis, spontaneous colon cancers developed in APC/SMAD-4 mutant mice were infiltrated with immature myeloid cells expressing CD34 and CCR1 (Kitamura et al., 2007). APC/SMAD-4 tumours expressed high levels of the CCR1 ligand CCL9. Furthermore, homozygous CCR1 deletion in APC/SMAD-4 mutant mice abrogated myeloid cell infiltration and was associated with a significant reduction in the ability of colon tumours to invade the bowel wall (Kitamura et al., 2007). Extension of this work demonstrated recruitment of the same myeloid cell population to the liver in the setting of orthotopic hepatic metastasis (Kitamura et al., 2010). shRNA targeting tumour-derived CCL9 significantly reduced the hepatic CCR1^{+} cell infiltrate and inhibited metastatic development, confirming that this myeloid population contributed to multiple steps in the metastatic cascade (Kitamura et al., 2010).

Importantly, a pro-metastatic role for human CCR1^{+} myeloid cells recruited through CCL15 - a human functional homologue of murine CCL9 – has also been demonstrated in human colon carcinoma. Itatani *et al* (2013) found an inverse relationship between expression of the

tumour-suppressor SMAD-4 and CCL15 in human colon cancer cell lines. Inhibition of SMAD-4 in tumour cell lines resulted in elevated CCL15 expression. This in turn promoted their metastatic potential in an intrasplenic-injection assay, through increased recruitment of myeloid cells expressing CCR1 and CD11b (Itatani et al., 2013). Given their expression of CCR1, such tumour-associated immune populations are likely to represent inflammatory monocytes. However, in the aforementioned experimental studies using various colon cancer models and human samples, the authors fail to adequately characterise the morphology or cell surface receptor expression pattern of the immune cell type recruited to the tumour microenvironment. Thus, a pro-metastatic role for monocytes in the liver is yet to be demonstrated; a surprising observation given their important role in the progression of pulmonary metastasis from breast cancer (Qian et al., 2011)(Lin et al., 2001).

In summary, studies have demonstrated an important, pro-tmourigenic role for monocytes in the metastatic progression of various solid tumours. However, the nature of immune cells recruited to the hepatic metastatic microenvironment and the factors leading to their recruitment are not fully understood. The analysis of further sets of cell lines in murine hepatic metastasis models is required to gain a broader understanding of the mechanisms behind immune cell recruitment and function in the hepatic metastatic microenvironment.

3.2 Aims

1. To determine whether murine colorectal cancer hepatic metastases are associated with immune cell infiltrates

2. To characterise immune cells associated with hepatic metastases and determine the mechanisms through which they are recruited

3. To determine whether immune populations recruited to murine colorectal cancer hepatic metastases are pro- or anti-metastatic

3.3 Results

3.3.1 Myeloid cell populations are increased in the murine tumour bearing liver

To determine whether hepatic colon cancer metastases are associated with alterations in myeloid cell numbers, $MC38^{GFP}$ tumours were developed in syngeneic C57BL/6 mice and hepatic myeloid cell populations quantified using flow cytometry. Within 14 days of intrasplenic $MC38^{GFP}$ injection large hepatic metastases had developed (Fig. 3.1a). Analysis of single cell hepatic suspensions for the archetypal murine myeloid cell markers CD11b and Gr1 (Ly6G/Ly6C) identified three $CD11b^{+}$ populations with variable Gr1 expression ($Gr1^{low}$, $Gr1^{mid}$ and $Gr1^{high}$) in both tumour bearing and control livers (Fig 3.1b). The development of hepatic metastasis was associated with a significant increase in the number of hepatic $Gr1^{mid}$ cells and a smaller, insignificant increase in the $Gr1^{low}$ population compared to the livers of control, splenectomised mice (Fig 3.1c). There was no difference in the number of hepatic $Gr1^{high}$ cells between tumour bearing and normal livers.

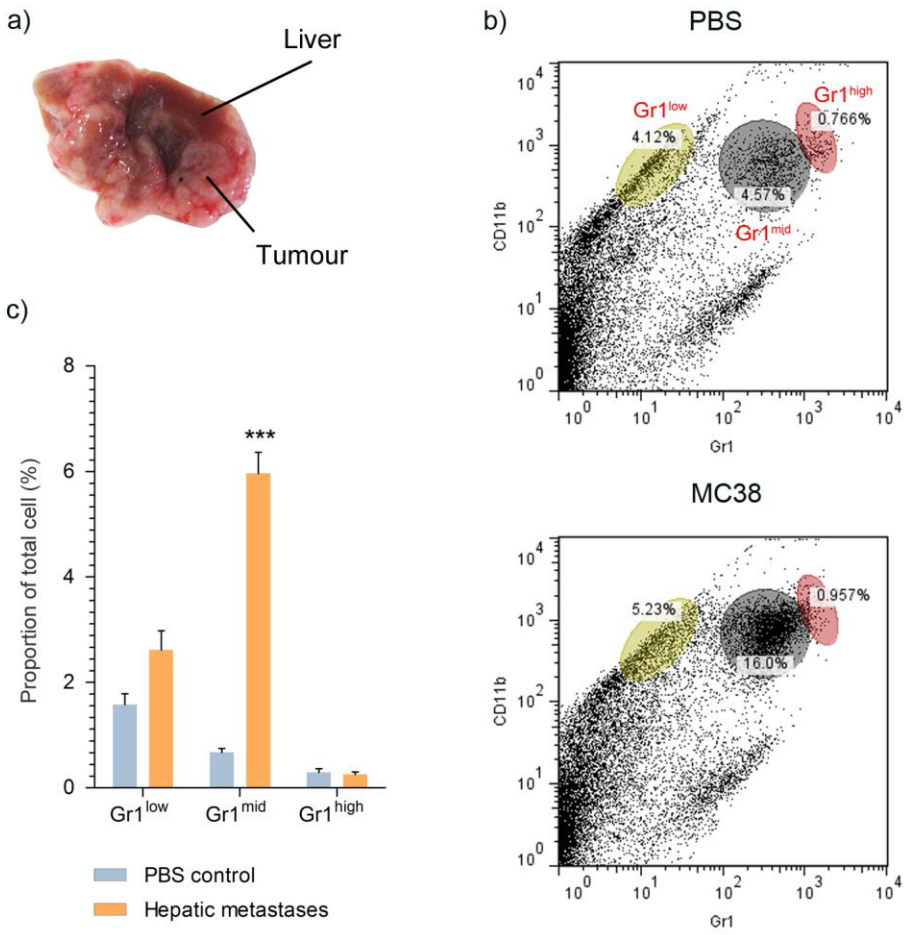

Figure 3.1. Myeloid cell populations are expanded in the murine tumour-bearing liver

a) Tumour-bearing liver 14 days following intrasplenic $MC38^{GFP}$ injection.

b) Flow cytometric comparison of hepatic single cell suspensions from intrasplenic PBS and $MC38^{GFP}$ inoculated mice demonstrating 3 distinct $CD11b^{+}$ myeloid populations expressing Gr1 at low (green), moderate (black) or high (red) levels.

c) Comparison of the total hepatic $Gr1^{low}$, $Gr1^{mid}$ and $Gr1^{high}$ cells as a percentage of total liver cells from tumour bearing mice (orange) and PBS controls (blue).

Data in (b) represents results from 3 separate experiments each with at least 5 mice.

3.3.2 Morphological features and cell-surface expression patterns of tumour-associated myeloid subsets

Analysis of H&E stained $CD11b^+$ cells FACS sorted from tumour bearing murine livers revealed $CD11b^+/Gr1^{mid}$ and $CD11b^+/Gr1^{low}$ cells to be of mononuclear morphology with vacuolated cytoplasm (Fig 3.2a). In contrast, $CD11b^+/Gr1^{high}$ cells were highly granular, polymorphonuclear cells (Fig 3.2a).

FACS analysis of cell surface marker expression was performed for the $Gr1^{low}$, $Gr1^{mid}$ and $Gr1^{high}$ cells identified in tumour bearing livers (Fig 3.3c). CD45 was expressed by $Gr1^{low}$, $Gr1^{mid}$ and $Gr1^{high}$ cells confirming their haematopoietic origin. $Gr1^{low}$ and $Gr1^{mid}$ cells strongly expressed Ly6C, whereas $Gr1^{high}$ cells expressed lower levels of Ly6C. $Gr1^{mid}$ cells expressed F4/80, whilst CD11c and CD206 expression was demonstrated in a proportion of the $Gr1^{low}$ cells (Fig 3.2c). $Gr1^{low}$, $Gr1^{mid}$ and $Gr1^{high}$ cells did not express CD3, CD4, B220 or NK1.1, excluding the possibility that they were T, B or NK cells respectively (Fig 3.2c).

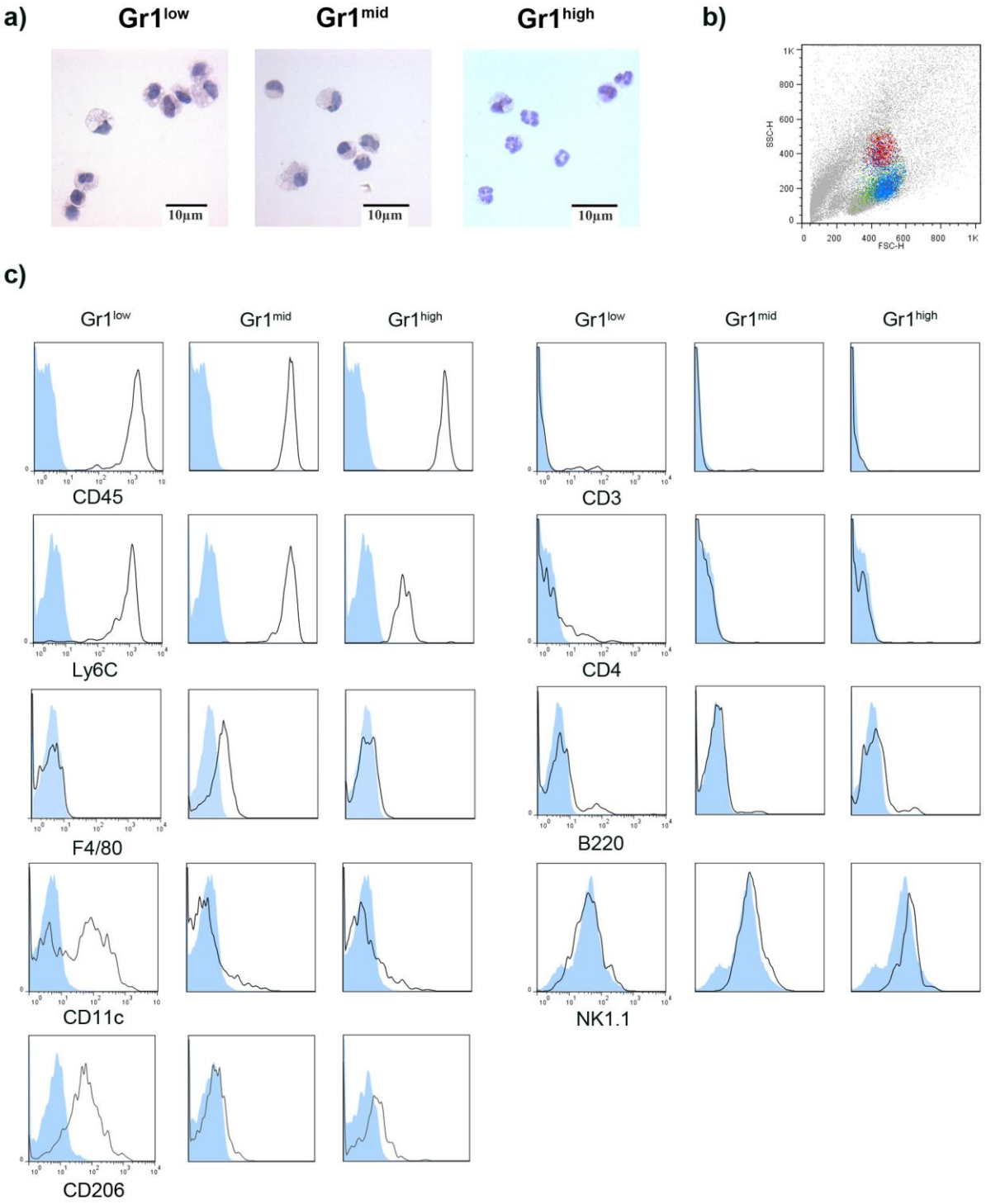

Figure 3.2. Specific morphological features and cell-surface expression patterns define tumour-associated myeloid subsets

a) H and E staining of cytospun CD11b$^+$ myeloid populations sorted from tumour-bearing liver (a).

b) Back gating of Gr1^{low} (green), Gr1^{mid} (blue) and Gr1^{high} (red) populations to demonstrate their positions on the forward scatter/side scatter (FSC/SSC) axes.

c) Histograms representing expression of cell surface molecules (black) compared to isotype controls (blue) in myeloid populations from tumour-bearing livers.

Gr1^{low} and Gr1^{mid} populations strongly expressed the chemokine receptor CCR2 and to a lesser extent CCR5 (Fig 3.3a). A subset of Gr1^{low} cells also expressed CCR4. Previous studies have identified specific inflammatory cells recruited to the metastatic niche using a range of markers including VEGFR1 (Kaplan et al., 2005), CCR1 (Kitamura et al., 2010) and Tie2(De Palma et al., 2005). Of note, these proteins were not detected in the hepatic metastasis-associated Gr1^{mid} population identified in tumour bearing livers (Fig 3.3b).

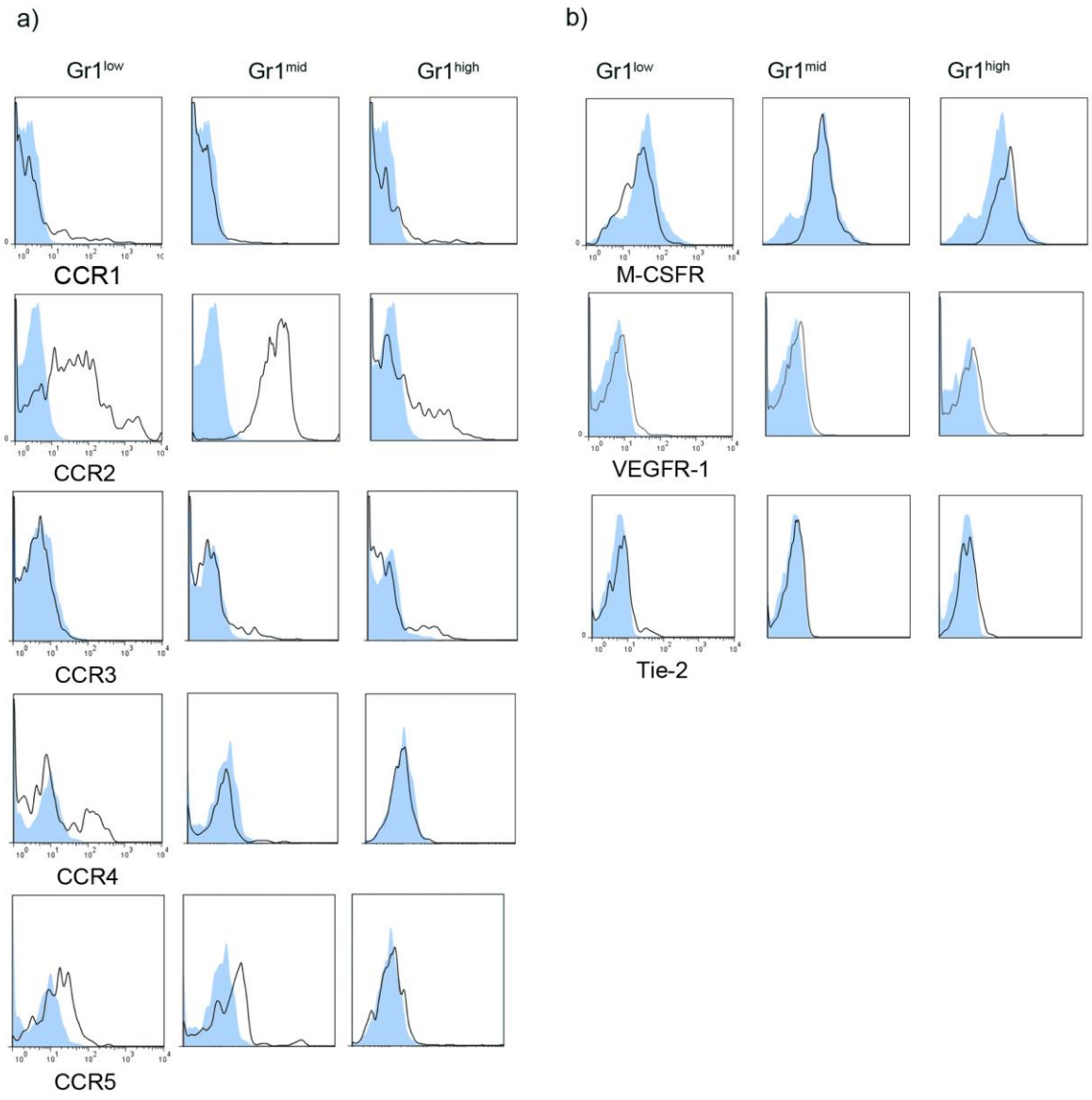

Figure 3.3. Chemokine receptor expression pattern in metastasis-associated myeloid subsets

a) Expression of chemokine receptors in the $Gr1^{low}$, $Gr1^{mid}$ and $Gr1^{high}$ myeloid subsets from tuomour-bearing liver (black) and their respective isotype controls (blue).

b) Expression of chemokine receptors shown to be of importance for tumour-associated immune cell identification by other research groups (see text for relevant references).

3.3.3 Metastasis-associated Gr1^{mid}/CCR2^{+} cells are recruited from the bone marrow

To determine whether Gr1^{mid} cells are recruited to the metastatic niche Gr1^{low}, Gr1^{high} and Gr1^{mid} cells were analysed in murine liver, blood and bone marrow at different time points following the development of hepatic metastasis (Fig. 3.4). Hepatic and circulating Gr1^{mid} cells increased with time in tumour bearing mice, whilst in bone marrow, Gr1^{mid} cells decreased after initially rising from day 0 to 5 (Fig. 3.4b). Gr1^{low} cell numbers increased in the liver, but this increase only occurred during the last 2 days of observed metastatic growth, by which time tumour cells accounted for 30-40% of the total hepatic cell population (Fig. 3.4a). The number of Gr1^{low} cells did not change with time in the bone marrow or blood.

Gr1^{high} cell numbers were elevated at 5 days following surgery in all tissue compartments before declining again on subsequent days. This may represent an early, non-specific inflammatory response to surgery rather than to the presence of tumour cells, as we noticed a similar increase in hepatic Gr1^{high} cells in the control splenectomised mice at this time point also (not shown). At 14 days, circulating Gr1^{high} cell numbers had risen again but remained at their baseline level in the bone marrow and liver.

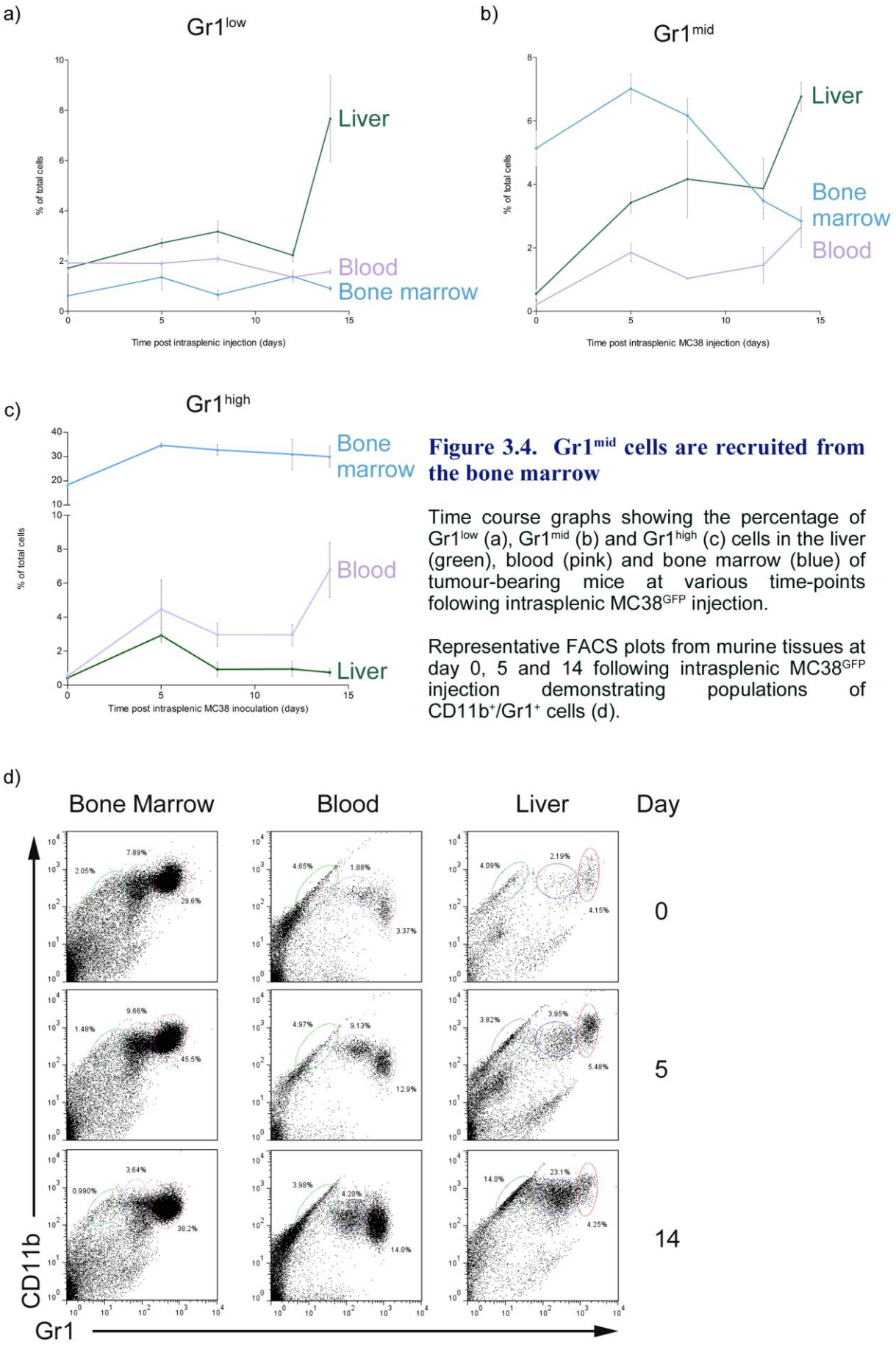

Figure 3.4. Gr1^{mid} cells are recruited from the bone marrow

Time course graphs showing the percentage of Gr1^{low} (a), Gr1^{mid} (b) and Gr1^{high} (c) cells in the liver (green), blood (pink) and bone marrow (blue) of tumour-bearing mice at various time-points folowing intrasplenic MC38^{GFP} injection.

Representative FACS plots from murine tissues at day 0, 5 and 14 following intrasplenic MC38^{GFP} injection demonstrating populations of CD11b^{+}/Gr1^{+} cells (d).

To provide further evidence that bone marrow $Gr1^{mid}$ cells move to the liver in response to metastatic development, adoptive transfer experiments were performed. Un-sorted bone marrow cells from mice ubiquitously expressing GFP were injected into the tail vein of mice bearing MC38 hepatic metastases or control splenectomised mice at day 11 following intrasplenic MC38 injection (Fig. 3.5). Tumour bearing livers were examined for the presence of GFP^+ bone marrow cells 24 hours later.

Within 24 hours of tail vein injection, GFP^+ bone marrow cells could be detected in the murine liver (Fig. 3.5a). The majority of GFP^+ bone marrow cells found in tumour bearing livers were $CD11b^+/CCR2^+$ or $CD11b^+/F4/80^+$ (Fig. 3.5b), therefore resembling the $Gr1^{mid}$ subtype. Furthermore, there were a significantly greater number of GFP^+ cells in the livers of tumor-bearing mice compared to non-tumour bearing control animals (Fig. 3.5c).

Histological examination of liver from tumour-bearing mice 24 hours following adoptive transfer of GFP^+ bone marrow was performed to determine the spatial relationship between metastases and recruited bone marrow cells. GFP^+ cells were seen within hepatic metastases and at the border between the invading adenocarcinoma and normal liver (Fig. 3.5d).

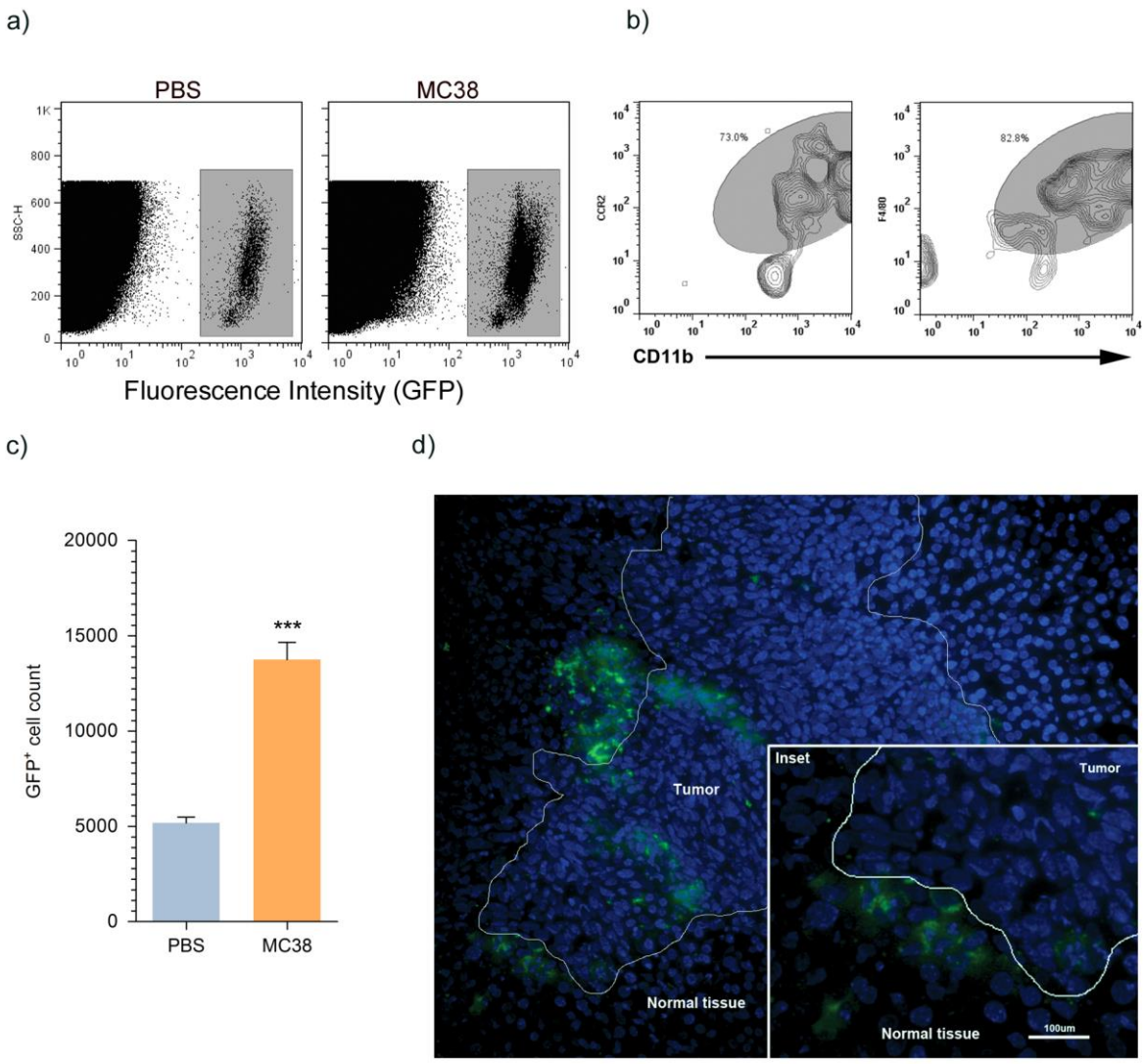

Figure 3.5. Bone marrow immune cells expressing CD11b, CCR2 and F4/80 accumulate in the tumour-bearing liver

a) Analysis of hepatic single cell suspensions 24 hours following adoptive transfer of $2x10^6$ unsorted GFP^+ bone marow cells into PBS control or tumour-bearing (MC38) mice.

b) Analysis of CD11b, CCR2 and F4/80 expresion in GFP^+ cells sorted from tumour-bearing liver following adoptive transfer as per figure (a).

c) Comparison of total hepatic GFP^+ cell count folowing FACS analysis of entire liver populations in PBS-injected (blue) and tumour bearing (orange) mice following adoptive transfer of GFP^+ bone marow cells.

d) Identification of GFP^+ cells close to hepatic metastases within 24 hours of adoptive transfer.

3.3.4 The chemokine CCL2 and receptor CCR2 are required for Gr1^{mid} cell recruitment to the hepatic metastatic microenvironment

To assess the possible tumour-derived chemokines involved in the recruitment of Gr1^{mid}/CCR2^{+} cells to the metastatic microenvironment, MC38 cell culture supernatant was analysed using a chemokine protein array. Cell culture supernatants from two commonly used murine cancer cells lines (B16F1 and LLC) were simultaneously analysed in order to determine whether findings in the MC38 cell line were unique. Both the LLC and B16F1 cell lines are capable of forming hepatic metastases within 2 weeks following intrasplenic injection in C57BL/6 mice.

CXCL1 and CCL2 levels in MC38- and LLC-conditioned medium were elevated when normalised to cell-free media alone (Fig. 3.6a). Interestingly, this was not the case for the B16F1 melanoma cell line: the culture-conditioned medium from these cells showed elevated levels of CXCL10 and CCL5 but not CCL2 (Fig. 3.6a). Quantitative analysis using ELISA for murine CCL2 demonstrated that MC38- and LLC-conditioned media were enriched with CCL2 compared to that from the B16F1 cell line (Fig. 3.6b).

CCL2 is well recognized as being important for the chemotaxis of macrophages (Matsushima et al., 1989) and is the non-cognate chemokine for the receptor CCR2 (Zlotnik and Yoshie, 2012). Furthermore, over-expression of CCL2 leading to CCR2^{+} monocyte recruitment has been demonstrated in several inflammatory diseases including atherosclerosis (Boring et al., 1998) and multiple sclerosis (Huang et al., 2001). As previously discussed, CCL2 expression has also been demonstrated to be of importance for the recruitment of tumour-promoting inflammatory monocytes to the metastatic microenvironment of the lung (Qian et al., 2011).

Despite this work, the CCL2-CCR2 axis has not yet been linked to the recruitment of immune cells in the setting of colorectal liver metastasis.

Thus, to further explore the relationship between tumour derived CCL2 expression and $Gr1^{mid}/CCR2^{+}$ cell recruitment, we simultaneously analysed the serum CCL2 concentration, tumour burden and number of hepatic $Gr1^{mid}/CCR2^{+}$ cells at various time-points following MC38 tumour cell injection (Fig. 3.6c and d). There was a significant correlation between serum CCL2 concentration and hepatic $Gr1^{mid}/CCR2^{+}$ cell count with time following MC38 cell injection ($R=0.67$, $p=0.025$). There was also a significant correlation between serum CCL2 concentration and hepatic $MC38^{GFP+}$ cell count ($R=0.89$, $p=0.002$).

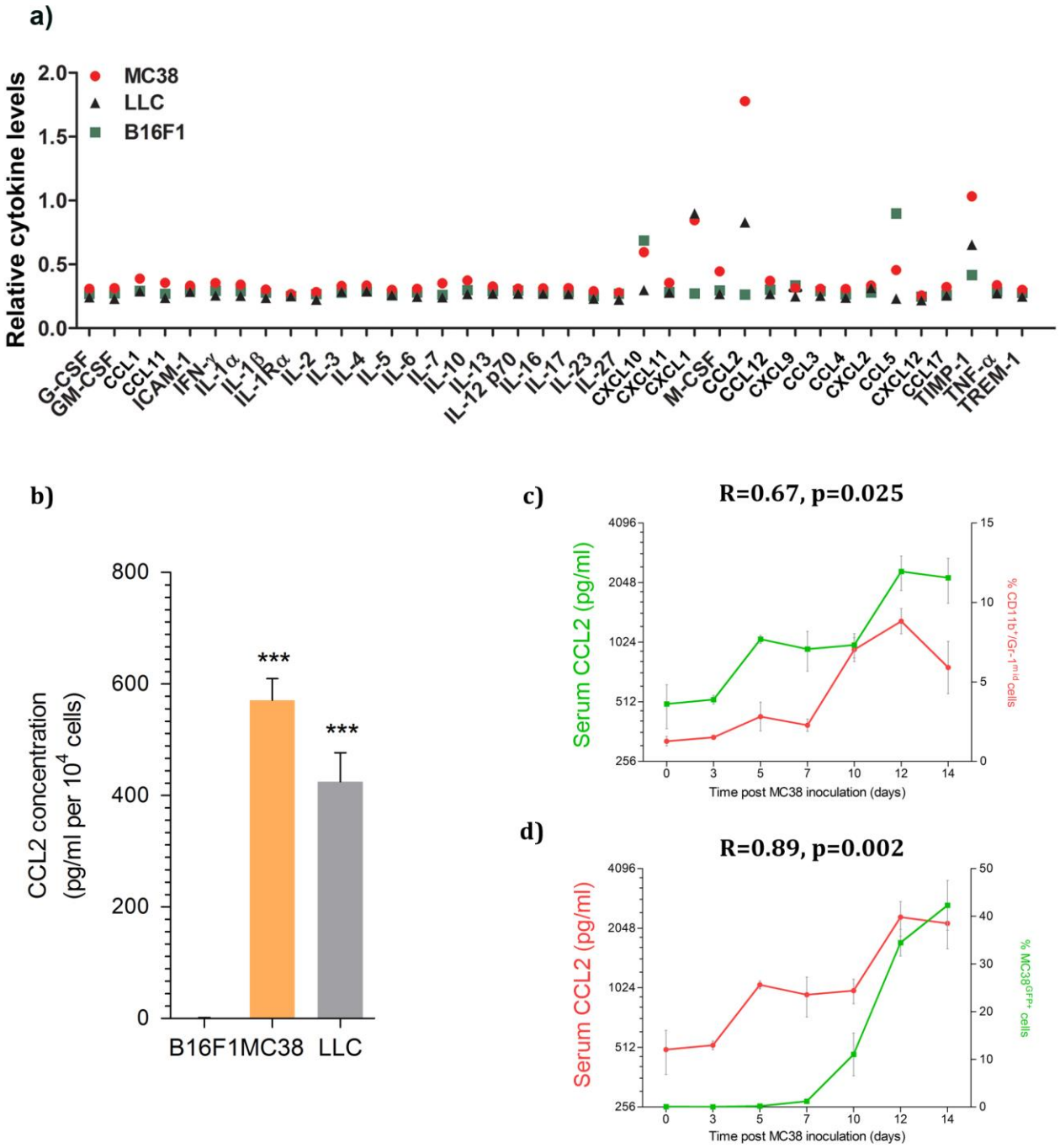

Figure 3.6. Tumour cell chemokine profiles determine myeloid recruitment pattern

a) Relative expression of multiple chemokines and cytokines determined by chemokine array performed on culture supernatant from 3 cell lines capable of forming murine hepatic metastases.

b) Quantitative of CCL2 concentration in the supernatants from the same cell lines.

c-d) Graphs of the correlation between serum CCL2 and hepatic $Gr1^{mid}$ cell numbers in MC38 tumour-bearing mice and between serum CCL2 and hepatic $MC38^{GFP+}$ cell numbers, with the Pearson's correlation coefficient (R) and p-value (p) given above each set of curves.

Data in (b) represents results from 3 independent experiments. Data in (c) and (d) represents results pooled from 3 separate experiments each from at least 4 mice.

Given the correlation between serum CCL2 concentration and $Gr1^{mid}$ cell recruitment and that the B16F1 cell line expressed CCL2 at a significantly lower level than the LLC or MC38 cell lines, we reasoned that B16F1 hepatic metastases would not be associated with $Gr1^{mid}$ cells *in-vivo*. In confirmation of this hypothesis, the livers of mice bearing B16F1 metastases had a significantly smaller number of $Gr1^{mid}$ cells than those of MC38 and LLC metastases (Fig. 3.7a-b).

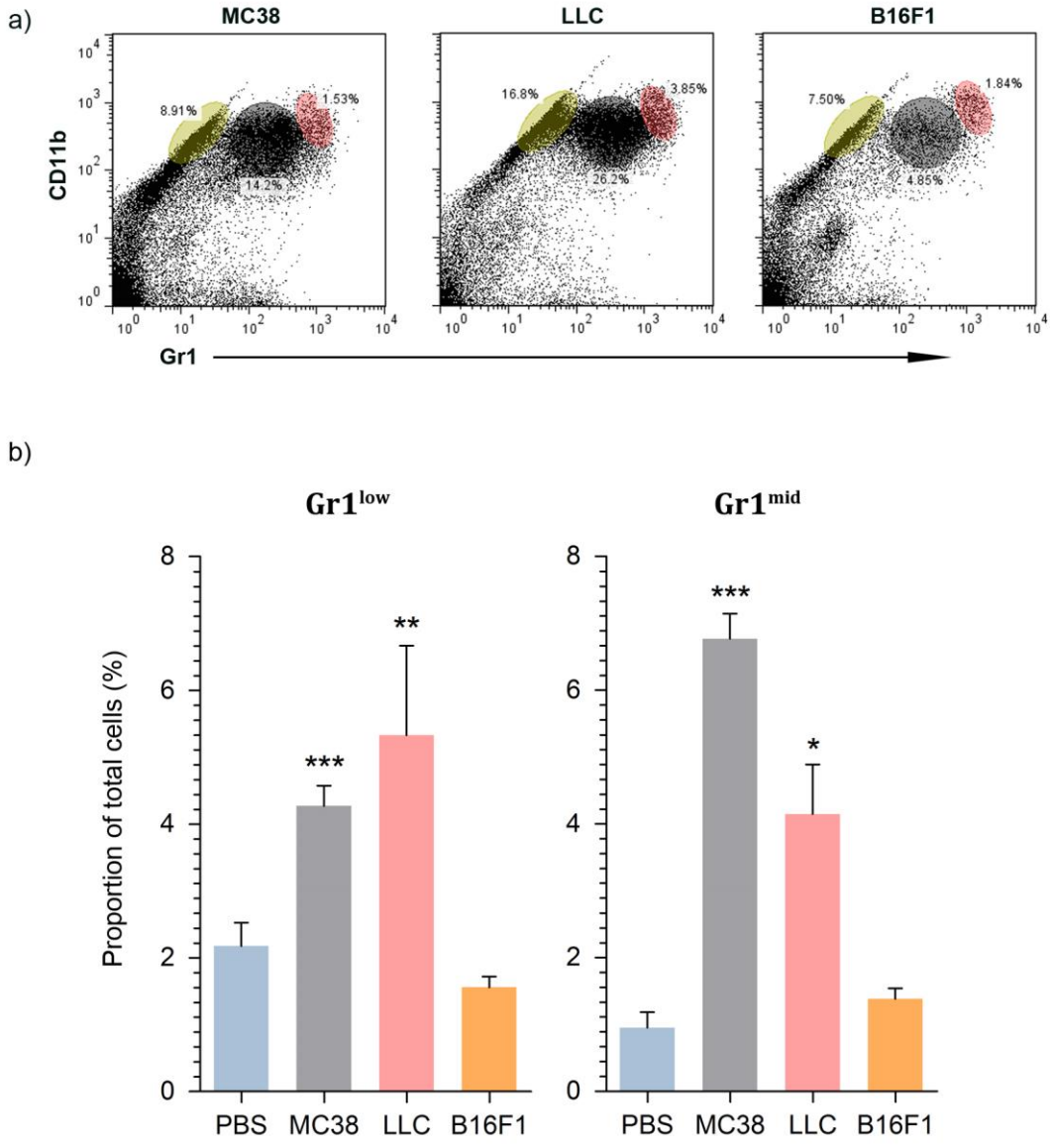

Figure 3.7. Chemokine profile of metastatic cell lines determines myeloid recruitment pattern

a) Flow cytometric analysis of hepatic cell suspensions 14 days following intrasplenic inoculation of colon ($MC38^{GFP}$), lung (LLC^{GFP}) or skin ($B16F1^{GFP}$) cancer cells.

b) Analysis of cumulative results for hepatic $Gr1^{low}$ and $Gr1^{mid}$ cells in mice bearing MC38, LLC or B16F1 tumours.

Data in (b) represents results from 3 separate experiments each with at least 3 mice.

To provide further evidence for the importance of the CCL2/CCR2 axis in the recruitment of $Gr1^{mid}/CCR2^{+}$ cells in this setting, we developed MC38 hepatic metastases in mice expressing a homozygous null mutation for the CCR2 receptor ($CCR2^{-/-}$). These mice have previously been shown to display impaired $CCR2^{+}$ monocyte trafficking from the bone marrow into the circulation in the setting of bacterial infection (Serbina and Pamer, 2006). In keeping with this observation, we found that livers from tumour bearing $CCR2^{-/-}$ mice contained significantly fewer $Gr1^{low}$ and $Gr1^{mid}$ cells than the livers from tumour-bearing wild-type mice (Fig. 3.8a-c). Interestingly, despite impaired hepatic $Gr1^{mid}$ cell recruitment, $CCR2^{-/-}$ mice displayed only a modest, insignificant reduction in tumour burden when compared with their wild-type counterparts, as determined by hepatic $MC38^{GFP+}$ cell count (Fig. 3.8d). In tumour-bearing $CCR2^{-/-}$ mice, serum CCL2 concentration was significantly higher than that in tumour-bearing wild type mice (Fig. 3.8e).

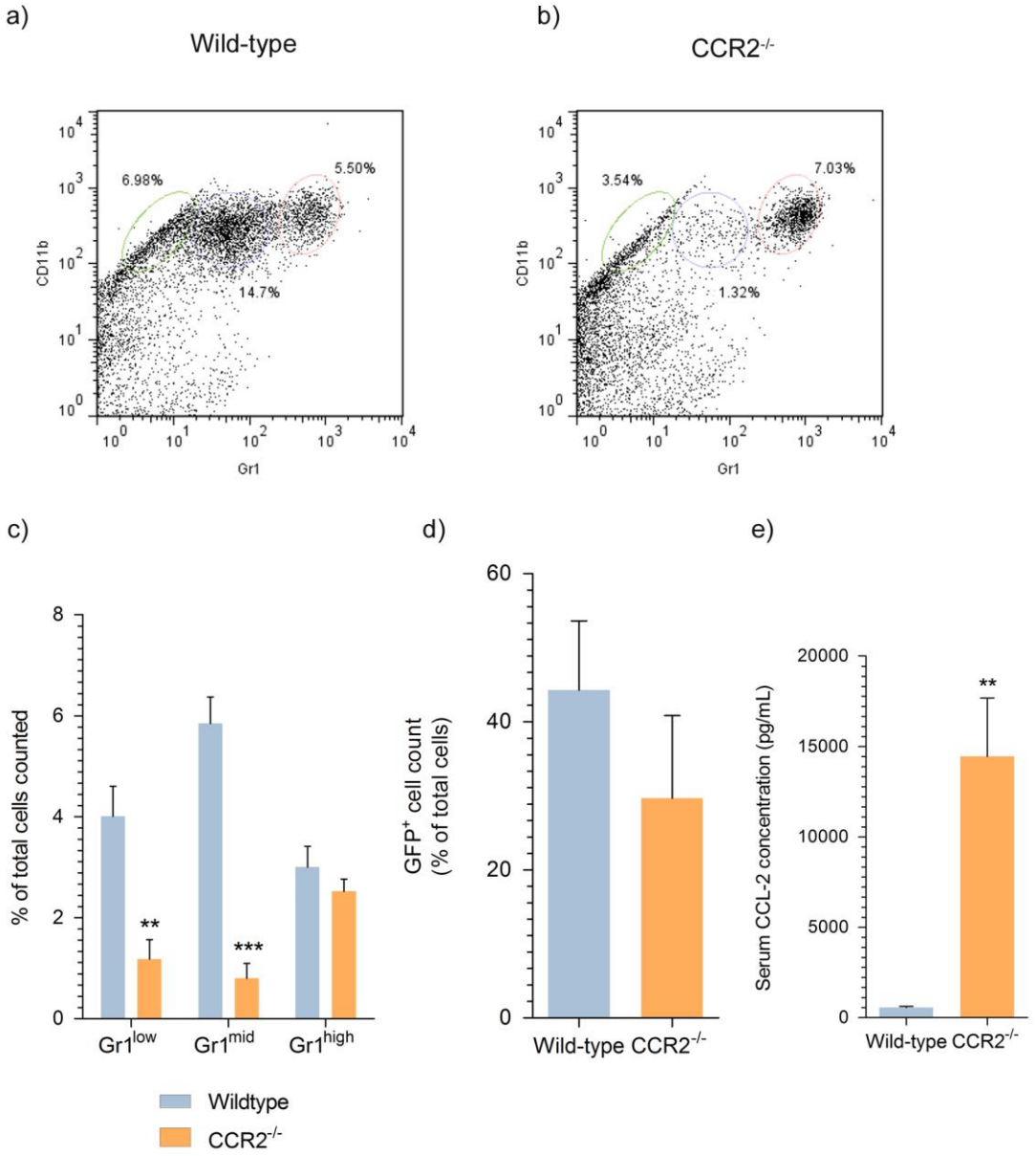

Figure 3.8. CCR2 depletion inhibits Gr1^{low} and Gr1^{mid} recruitment to hepatic metastases

a-b) Representative flow cytometry plots from the livers of MC38 tumour-bearing C57Bl6 wild-type or C57Bl6-CCR2$^{-/-}$ mice.

c-d) Collated data showing the percentage of Gr1^{low}, Gr1^{mid} and Gr1^{high} cells in tumour bearing mouse livers from wild-type (blue) and CCR2$^{-/-}$ mice (orange). Comparison of the total hepatic MC38^{GFP+} cells in wildtype and CCR2$^{-/-}$ mice 14 days following intrasplenic injection of MC38^{GFP+} cells.

e) Comparison of the serum CCL2 concentration in MC38^{GFP+} tumour-bearing wild-type and CCR2$^{-/-}$ mice.

Data in (c), (d) and (e) represents results from 2 separate experiments each from 4 mice per group.

Although MC38 cells expressed CCL2, it is conceivable that an alternative chemokine-producing cell population within the tumour microenvironment is responsible for $Gr1^{mid}$ cell recruitment. To test whether tumour-derived CCL2 was sufficient to recruit $Gr1^{mid}$ cells, CCL2 in MC38 cells was knocked down by transfecting cells with plasmids containing CCL2-shRNA ($MC38^{CCL2\text{-}shRNA}$) or a lentiviral control ($MC38^{lenti}$), and the recruitment of $Gr1^{mid}$ cells in their respective hepatic metastases determined. CCL2 expression was reduced by at least 50% in $MC38^{CCL2\text{-}shRNA}$ cells compared to wild-type cells, as determined by ELISA of the culture supernatants from each cell line (Fig. 3.9a). At days 6 and 9 there was a significant reduction in the metastasis associated $Gr1^{mid}$ population in mice inoculated with the $MC38^{CCL2\text{-}shRNA}$ cells compared to their lentiviral controls (Fig. 3.9b), but at no time was there a significant difference in $Gr1^{low}$ cell numbers. Furthermore, by day 9, tumour burden was lower in the animals inoculated with $MC38^{CCL2\text{-}shRNA}$ cells relative to animals administered $MC38^{lenti}$ cells (Fig. 3.9c). By day 13, however, there was no significant difference in hepatic $Gr1^{mid}$ or $MC38^{GFP+}$ cell numbers between the two groups. Similarly, serum CCL2 was significantly lower in mice inoculated with the $MC38^{CCL2\text{-}shRNA}$ compared to the $MC38^{lenti}$ cells at the first two time-points only (Fig. 3.9d).

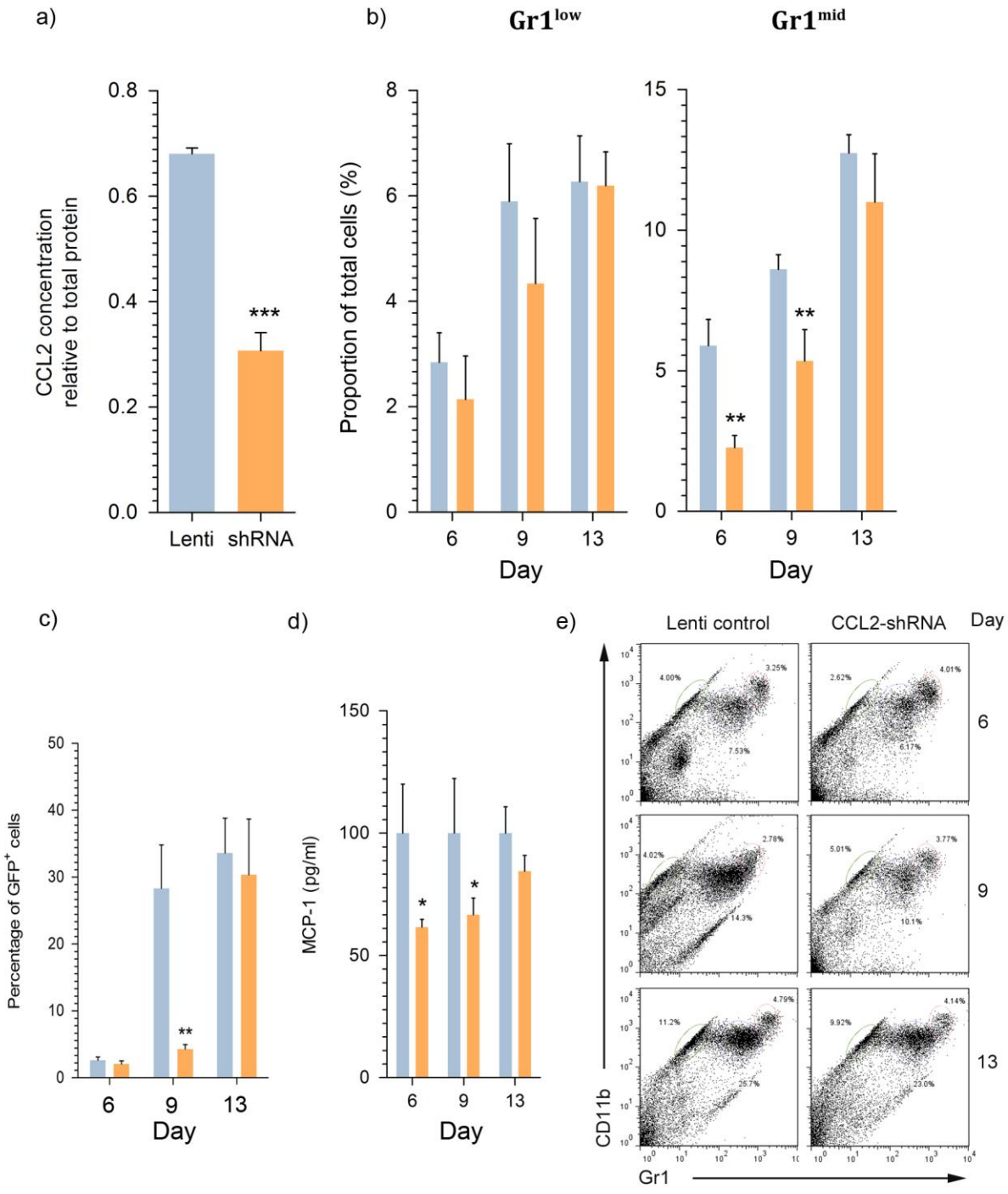

Figure 3.9. Inhibition of the chemokine CCL2 delays metastatic progression

a) Relative CCL2 concentration in the cell culture supernatant of MC38^{lenti} and MC38$^{ccl2\text{-}shRNA}$ cell lines.

b) Comparison of hepatic Gr1^{low} and Gr1^{mid} cell counts at sequential timepoints following intrasplenic injection of MC38^{lenti}(blue) or MC38$^{CCL2\text{-}shRNA}$ (orange) cells. X-axes denote time following intrasplenic injection in days.

c) Analysis of hepatic MC38 cell counts at the same time-points (same colour scheme applies).

d) Murine CCL2 concentration in the serum of mice bearing MC38^{lenti} (blue) or MC38$^{CCL2\text{-}shRNA}$ (orange) hepatic metastases normalised to lentiviral control values.

e) Representative FACS plots from mouse livers in mice bearing MC38^{lenti} (left) or MC38$^{CCL2\text{-}shRNA}$ (right) hepatic metastases at 6, 9 and 13 days post intrasplenic tumour cell injection.

3.3.5 Depletion of Gr1^{mid} cells delays the progression of hepatic colon cancer metastases

We next sought to determine the effect of selective ablation of the Gr1^{mid} cell population on MC38 metastatic growth. For this purpose we made use of a transgenic mouse line expressing the human DT receptor under the control of the CD11b promotor region (Fig. 3.10a)(Duffield et al., 2005). Integral to this system is the reduced binding affinity of DT to the murine DT receptor relative to that of the human receptor (Naglich et al., 1992). As a result, administration of DT to wild-type mice produces no adverse effects. Conversely, administration of DT to CD11b-DTR mice significantly depletes hepatic F4/80^{+} macrophages, without affecting splenic B-cells or peritoneal T-lymphocytes (Duffield et al., 2005).

To assess the effect of Gr1^{mid} cell depletion on tumour growth, DT or a vehicle control solution was administered to tumour bearing mice 7 and 9 days following intrasplenic inoculation of MC38 cells. Hepatic tumour burden was monitored by MRI at 6, 8 and 11 days following tumour cell injection (Fig. 3.10b,c) and the livers of mice were subsequently harvested and analysed using flow cytometry (Fig. 3.11). DT-treated mice developed significantly slower growing hepatic metastases compared to vehicle control mice (Fig. 3.10d). Analysis of tumour-bearing liver, showed that mice treated with DT had macroscopically smaller tumours (Fig. 3.11a) and significantly fewer hepatic MC38^{GFP+} cells than control mice (Fig. 3.11b). Furthermore, DT-treated mouse livers had significantly reduced numbers of Gr1^{low} and Gr1^{mid} cells, but the number of Gr1^{high} cells remained unaltered (Fig. 3.11c). Administration of DT had no effect on hepatic CD3e^{+} T-cell or CD19^{+} B-cell numbers (Fig. 3.11d,e).

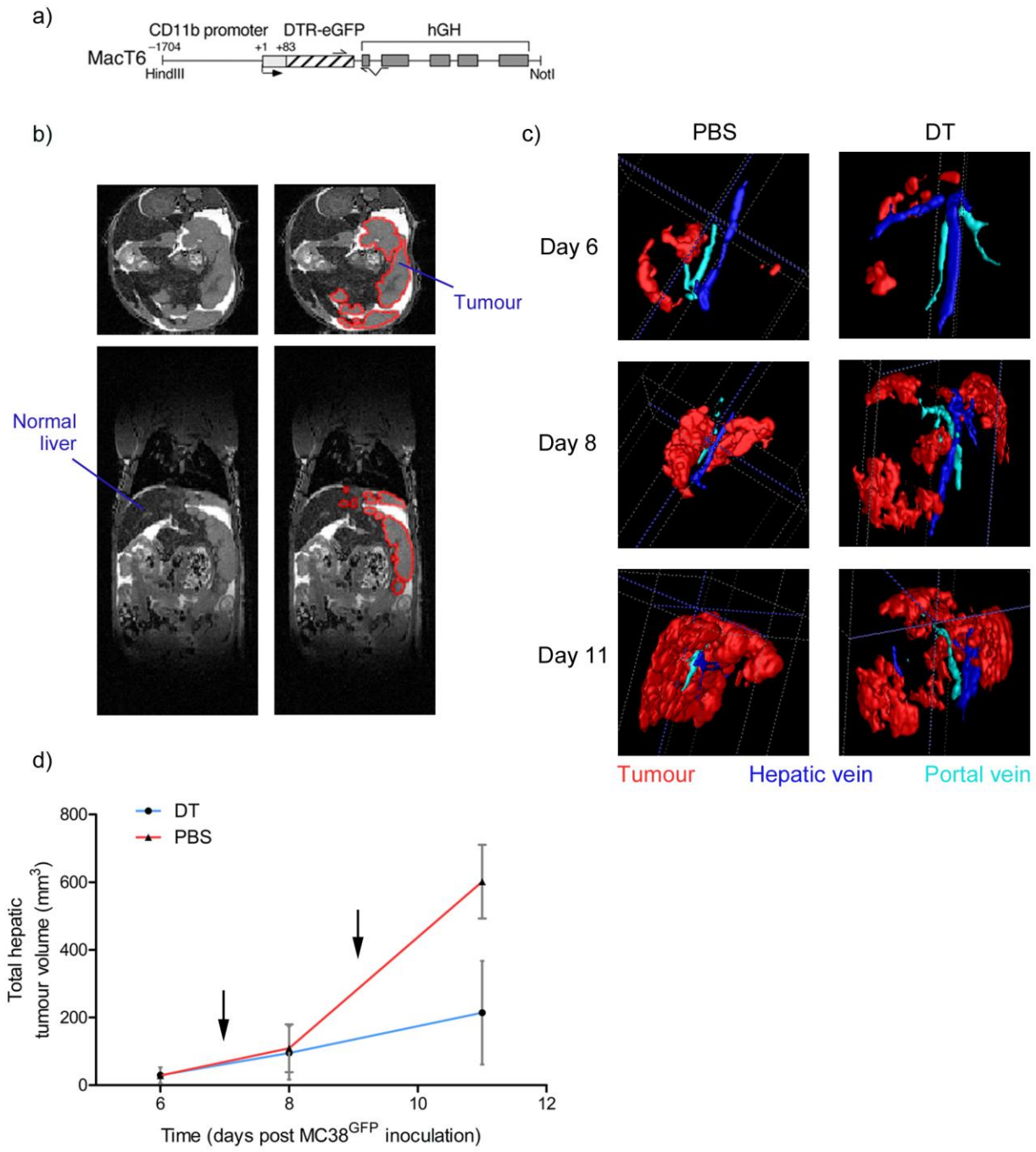

Figure 3.10. Diphtheria toxin administration to CD11b-DTR mice reduces the progression of hepatic colon cancer metastases

a) The CD11b-DTR transgene showing the DTR-eGFP fusion gene inserted between the human CD11b promoter and the human growth hormone (hGH) sequence which provides splicing and polyadenylation sequences (from Duffield *et al,* 2005).

b) Representative MRI images taken from a mouse with hepatic metastases demonstrating multiple metastatic foci within the liver highlighted in red.

c) Analysis of serial MRI images using the ITK-Snap software enabled metastases to be reconstructed, labelled and their volumes calculated.

d) Progression of total hepatic tumour volume in DT and PBS treated mice. Arrows indicate DT administration.

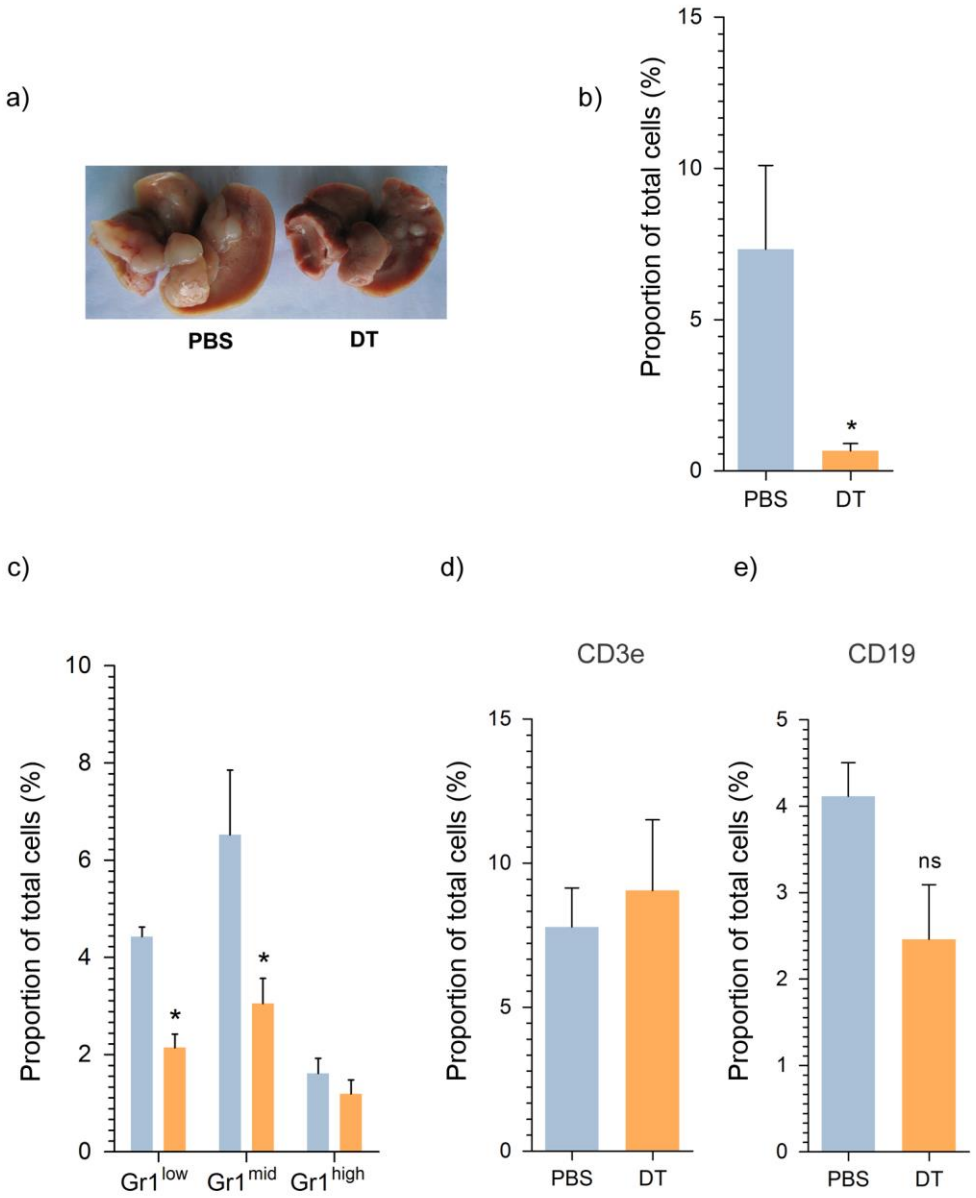

Figure 3.11. DT depletes hepatic Gr1^{mid} and Gr1^{low} cells and inhibits metastasis formation in CD11b-DTR mice

a) Hepatic metastases in DT and vehicle control-treated (PBS) mice.

b) Confirmation of macroscopic findings with FACS analysis of hepatic MC38^{GFP+} cell counts in tumour bearing livers from vehicle control and DT-treated mice.

c-e) Hepatic Gr1, CD3e and CD19 populations in vehicle control (blue) and DT-treated (orange) mice 13 days following intrasplenic tumour cell injection.

Data in (b-e) represents results from 3 separate experiments, each of at least 3 mice.

3.4 Discussion

3.4.1 Identification of hepatic metastasis associated myeloid cells

In this chapter, we have demonstrated an increase in the number of hepatic $CD11b^{+}/Gr1^{mid}$ myeloid cells in mice with MC38 liver metastases relative to naïve, control mouse livers. Several myeloid cell types were identified in the livers of both tumour bearing and naïve mice, each of which were defined based upon their relative expression of Gr1. That differential Gr1 expression identified unique myeloid cell populations was demonstrated by the different morphological appearance of $Gr1^{high}$, $Gr1^{mid}$ and $Gr1^{low}$ cells, their well-defined forward- and side-scatter flow cytometry profiles and the fact that each population expressed unique cell surface antigens. This provides validation for the gating strategy used to classify hepatic myeloid cell populations based on their Gr1 expression level.

The Gr1 epitope is found within Ly6C and Ly6G proteins (Fleming et al., 1993) and was identified in our FACS analysis using the anti-Gr1 antibody clone RB6-8C5. Previous analysis of murine bone marrow has demonstrated that neutrophils stain strongly with RB6-8C5 using flow cytometry ($Gr1^{high}$), whereas cell populations staining with intermediate ($Gr1^{mid}$) RB6-8C5 reactivity are predominantly monocytes (Hestdal et al., 1991). This is in similarity to our findings for the analysis of $Gr1^{mid}$ and $Gr1^{high}$ cells in tumour-bearing murine livers, which bear morphological resemblance to monocytes and neutrophils respectively. Bone marrow $Gr1^{low}$ cells have previously been shown to be enriched for myeloblasts with significant colony forming capacity (Hestdal et al., 1991). Interestingly, we found $Gr1^{low}$ cells to express CD11c and CCR5: molecules typically expressed by myeloid-type dendritic cells (Lee et al., 1999). Furthermore, the histological appearance of the hepatic $Gr1^{low}$ cells bears similarity to that of dendritic cells. Given that circulating monocytes can differentiate into dendritic cells (Zhou and Tedder, 1996)(Randolph et al., 1999) and that the $Gr1^{mid}$ and $Gr1^{low}$ populations share the expression of

certain cell surface markers, it is possible that the $Gr1^{mid}$ population is capable of differentiating into its $Gr1^{low}$ counterpart once within the metastatic microenvironment.

The ability of $Gr1^{mid}$ cells to differentiate into $Gr1^{low}$ cells is supported by the fact that although hepatic $Gr1^{low}$ cell numbers increased in the later stages of metastatic development, their numbers did not change in the circulation or bone marrow. If the $Gr1^{low}$ cells travelled to the metastatic niche directly from the bone marrow one would expect their numbers to fall in the bone marrow as they rose in the circulation and liver. If $Gr1^{low}$ cells differentiate from $Gr1^{mid}$ cells once in the liver, then one would not expect to see a change in circulating or bone marrow $Gr1^{low}$ cell numbers, in parallel with our results. In support of this theory, $CD11b^{+}/Gr1^{mid}$ splenocytes expressing CCR2 are capable of differentiating into $Gr1^{low}$ cells in the presence of a range of murine tumours (Ugel et al., 2012), demonstrating both the plasticity of $Gr1^{mid}$ cells and the ability of tumour-derived factors to drive myeloid cell differentiation. Interestingly, recent unpublished work from our laboratory demonstrates that GFP-labeled, tumour-derived $Gr1^{mid}$ cells differentiated into $Gr1^{low}$ and $Gr1^{mid}$ cells upon adoptive transfer back to tumour-bearing mice. Thus, $Gr1^{mid}$ cell appear to be highly plastic, a phenotype driven in part by the tumour microenvironment.

3.4.2 Tumour-specific recruitment of $CCR2^{+}$ monocytes through CCL2 expression

The $Gr1^{mid}$ cells present at elevated numbers in the livers of MC38 tumour-bearing mice expressed CCR2, a chemokine receptor required for the egress of monocytes from the bone marrow (Serbina and Pamer, 2006). Interestingly, $Gr1^{+}/CD11b^{+}/CCR2^{+}$ cells designated 'inflammatory monocytes', were found to promote tumour cell extravasation in the lungs of mice carrying PyMT-derived breast cancers in a CCL2-dependent fashion (Qian et al., 2011). Indeed, inflammatory $CCR2^{+}$ monocytes represent a specific monocyte subset that migrate to

inflamed tissues in preference to CCR2^{-} resident monocytes (Geissmann et al., 2003). Given their shared cell surface receptor expression profile and monocytic morphology, the Gr1^{mid} cells identified in MC38 hepatic metastases and the aforementioned inflammatory monocyte population recruited to lung metastases are a similar cell type.

Interestingly, although our data cannot exclude the possibility that Gr1^{mid} cells promote the extravasation of tumour cells in the liver as they do in the lung (Qian et al., 2011), our findings point to a role for Gr1^{mid} cells later, during the growth phase of hepatic metastasis. Thus, hepatic Gr1^{mid} cells rose from day five following MC38 injection (Fig 3.6), by which time tumour cells would have successfully extravasated from within the sinusoid (Martin et al., 2010)(Auguste et al., 2007) and started dividing in the hepatic parenchyma. Furthermore, depletion of Gr1^{mid} cells from day 7 following MC38 injection inhibited metastatic growth in CD11b-DTR mice indicating that even if Gr1^{mid} cells promote the extravasation of cancer cells in the liver, they also play a significant role in subsequent phases of metastatic development.

As myeloid cells originate in the bone marrow, it is likely that the Gr1^{mid} cells found in association with hepatic metastases are also of bone marrow origin. This belief is supported by the fact that Gr1^{mid} cells expressed the pan haematopoietic marker CD45 and that their numbers rose in murine tumour bearing liver, whilst simultaneously falling in the bone marrow. This data suggests that Gr1^{mid} cells exit the bone marrow and move via the circulation to the tumour bearing liver.

The ability of Gr1^{mid} cells to travel from the circulation to the liver, specifically in response to the presence of hepatic metastases is evidenced by our adoptive transfer

experiments. Here, a greater proportion of adoptively transferred GFP$^+$ bone marrow cells were found in tumour bearing livers compared to naïve livers, indicating that they move to the liver as a result of the presence of the tumour. It could be argued that as the tumour bearing liver is likely to have a greater vasculature and blood volume, we have simply measured differences in the number of GFP$^+$ cells within the hepatic vasculature rather than in cells that have passed into the hepatic parenchyma in response to the presence of metastases. However, this scenario is unlikely given that on immunohistochemical analysis adoptively transferred GFP$^+$ cells were identified in close association with hepatic metastatic deposits.

Evidence for the ability of hepatic metastases to selectively recruit Gr1^{mid} cells over other myeloid populations comes from analysis of the cell surface markers expressed by transferred GFP$^+$ bone marrow cells found within the tumour bearing liver. Thus, the majority of GFP$^+$ cells in tumour bearing livers were CD11b$^+$/F4/80$^+$ or CD11b$^+$/CCR2$^+$ indicating that they were of the Gr1^{mid} subtype. This is despite the fact that the majority of adoptively transferred cells will have been Gr1^{high}, given that this is the most prevalent population within unsorted bone marrow (Fig 3.5d and (Hestdal et al., 1991)). This strongly suggests that circulating Gr1^{mid} bone marrow cells preferentially move into the tumour microenvironment within the liver over other bone marrow myeloid populations.

As the research of others has demonstrated a role for tumour-derived chemokines in the recruitment of immune cell populations to the metastatic niche (Qian et al., 2011)(Kitamura et al., 2010)(Itatani et al., 2013), we profiled culture conditioned medium from various murine tumour cell lines to determine their relative expression of various chemokines. Expression of the CCR2 ligand CCL2 by MC38 cells identified it as the likely chemokine responsible for CCR2$^+$/Gr1^{mid} cell recruitment to MC38 hepatic metastases. This is further supported by the

correlations observed between serum CCL2 concentration, hepatic tumour burden and hepatic $Gr1^{mid}$ cell numbers, indicating that MC38 cells produce CCL2 *in-vivo* and that this in turn leads to $Gr1^{mid}$ cell recruitment. Furthermore, the B16F1 melanoma cell line did not express CCL2 and formed hepatic metastases without $Gr1^{mid}$ cell infiltration, whilst LLC cells did express CCL2 and their metastases were associated with elevated $Gr1^{mid}$ cell numbers. Whilst these findings support the role of tumour-derived chemokines in the recruitment of immune cells to the metastatic niche, they also demonstrate that certain tumour types (e.g. melanoma) develop hepatic metastases without an associated myeloid infiltrate.

The role of MC38-derived CCL2 in the recruitment of $Gr1^{mid}$ cells to the liver as demonstrated by the aforementioned, circumstantial evidence is conclusively proven by our analysis of $MC38^{CCL2shRNA}$ and $MC38^{lenti\text{-}ctrl}$ tumour bearing livers; the former demonstrated a significantly lower $Gr1^{mid}$ cell infiltrate at days 6 and 9 following tumour cell injection. The role of CCL2 in the recruitment of $CCR2^{+}$ monocytes to the metastatic niche is supported by the research of others, which has demonstrated the importance of this chemokine-receptor pair in the recruitment of monocytes to murine melanoma (Huang et al., 2007), breast (Qian et al., 2011) and prostate cancers (Loberg et al., 2007). However, it is interesting to note that in our experiments CCL2 knock down provided only a transient reduction in hepatic metastasis-associated $Gr1^{mid}$ cells, the numbers of which were equivalent in tumour bearing livers from $MC38^{CCL2shRNA}$ and $MC38^{lenti\text{-}ctrl}$ injected mice at day 13 (Fig 3.9b).

This finding likely results from the relatively poor inhibition of CCL2 that was obtained using the shRNA construct. Thus, we were only able to achieve a 50% reduction in CCL2 expression in $MC38^{CCL2shRNA}$ relative to $MC38^{lenti\text{-}ctrl}$ cells. CCL2 production by $MC38^{CCL2shRNA}$ cells was therefore still relatively high and so it may be possible for the metastases developed using

these cells to express enough CCL2 to achieve maximal hepatic $Gr1^{mid}$ recruitment. In keeping with this possibility, we found little difference in the serum CCL2 concentration of mice 13 days following $MC38^{CCL2shRNA}$ or $MC38^{lenti\text{-}ctrl}$ inoculation. This data also raises the possibility that CCL2 shRNA-transfected cells regain the ability to express CCL2 in-vivo, potentially through loss of the transfected shRNA construct as may occur once the cell line is no longer under antibiotic selection.

3.4.3 Importance of CCR2 in the recruitment of bone marrow $Gr1^{mid}$ cells

As well as demonstrating the importance of tumour-derived CCL2, our experiments using $CCR2^{-/-}$ mice highlight the role of CCR2 expression in the recruitment of $Gr1^{mid}$ cells to the metastatic niche. Thus, hepatic metastasis-associated $Gr1^{mid}$ cell numbers were reduced in the livers of $CCR2^{-/-}$ mice, indicating that CCR2 expression in $Gr1^{mid}$ cells is required for their recruitment to the tumor bearing liver. Importantly, CCR4 also acts as a receptor for CCL2, however, the $Gr1^{mid}$ cell population did not express this receptor, which is therefore unlikely to play a role in the movement of $Gr1^{mid}$ cells from the bone marrow in tumour bearing mice.

Although tumour-bearing livers from $CCR2^{-/-}$ mice contained fewer $Gr1^{mid}$ cells than their wild-type controls, there was no difference in the hepatic tumour cell number between these groups of animals. This may indicate that $Gr1^{mid}$ cells are not important for the development of hepatic metastasis formation. Alternatively, if one assumes that $Gr1^{mid}$ cells are important for the growth of MC38 hepatic metastases, the data in $CCR2^{-/-}$ mice could indicate that alternative growth-promoting attributes develop in the face of $Gr1^{mid}$ cell absence in $CCR2^{-/-}$ mice. For example, the serum CCL2 in $CCR2^{-/-}$ tumour bearing mice was significantly elevated compared to wild-type controls; presumably, because in wild-type mice CCR2 binds and internalises circulating CCL2, reducing its concentration relative to that in $CCR2^{-/-}$ animals.

Interestingly, CCL2 has been shown to promote prostate cancer PC-3 cell proliferation directly in a manner dependent on tumour cell CCR2 expression (Loberg et al., 2006). We have not yet analysed whether MC38 cells express CCR2, or whether CCL2 is capable of driving MC38 proliferation, however if this is the case as it is for PC-3 cells then this may explain the lack of tumour inhibition seen in $CCR2^{-/-}$ mice challenged with MC38 cells.

3.4.4 Evidence for the pro-metastatic role of hepatic $Gr1^{mid}$ cells

Inhibition of tumour-derived CCL2 in $MC38^{CCL2shRNA}$ reduced serum CCL2 concentration in tumour bearing mice, which in turn reduced metastatic growth. Furthermore, tumours in $MC38^{CCL2shRNA}$ injected mice had fewer $Gr1^{mid}$ cells for the time points at which CCL2 remained inhibited. Taken together, these findings implicate $Gr1^{mid}$ cells in the CCL2-driven promotion of metastatic development. Nonetheless, the association between elevated CCL2, increased tumour-associated $Gr1^{mid}$ cell count and larger metastases does not prove a causal relationship between $Gr1^{mid}$ cells and metastatic progression. As previously mentioned, CCL2 is a pleotropic chemokine capable of promoting tumour growth through the direct stimulation of angiogenesis (Stamatovic et al., 2006)(Salcedo et al., 2000) as well as tumour cell proliferation (Loberg et al., 2007). As such, CCL2 is capable of promoting the progression of MC38 hepatic metastases independently of the presence of $Gr1^{mid}$ cells.

Thus, to conclusively demonstrate that $Gr1^{mid}$ cells promote metastatic development, we analysed the development of hepatic metastases following the administration of DT to CD11b-DTR transgenic mice. DT treatment resulted in a significant reduction in tumour growth demonstrated through both serial magnetic resonance imaging and assessment of ex-vivo hepatic tumour cell number, providing strong evidence that myeloid cells play a growth-promoting role in the hepatic metastatic microenvironment.

This data bears one caveat however. Specifically, that although the administration of DT to CD11b-DTR mice depleted myeloid cells, whilst sparing cells of the lymphoid lineage (Fig 3.11d-e), it was not specific with regards its effect on $Gr1^{+}$ cell subtype. Thus, in tumour-bearing mice administered DT, we found a reduction in hepatic $Gr1^{low}$ and $Gr1^{mid}$ cells, with the $Gr1^{high}$ population being unaffected. Given that CD11b is expressed by each of these cell types, this result is puzzling, as one would expect the DT to ablate all cells expressing CD11b. The reasons behind this finding are unclear, but may stem from the fact that $Gr1^{high}$ neutrophils typically have a shorter life expectancy and higher bone marrow turn over than $Gr1^{mid}$ monocytes (cronkite and fliedner, 1964). Thus, it is possible that the hepatic neutrophil pool had become replenished within the three days between the final DT dose and the ex-vivo hepatic FACS analysis, a process that is likely to take longer for $Gr1^{mid}$ cells.

Given that the administration of DT to CD11b-DTR mice depleted both $Gr1^{low}$ and $Gr1^{mid}$ cells, we cannot be certain whether its anti-metastatic effect resulted from $Gr1^{mid}$ or $Gr1^{low}$ depletion or a combination of the two. It is clear that the depletion of $Gr1^{low}$ and $Gr1^{mid}$ cells that takes place following DT administration caused a greater, more sustained inhibition of metastatic growth than the knockdown of CCL2 in MC38 cells. One might assume that this is because DT administration depletes both $Gr1^{mid}$ and $Gr1^{low}$ cells, whereas CCL2 inhibition only inhibits $Gr1^{mid}$ cell recruitment. This would lead to the conclusion that the $Gr1^{low}$ population plays an important role in metastatic growth. This however seems unlikely when it is considered that $Gr1^{low}$ cell numbers only rise once hepatic metastases are well established. If $Gr1^{low}$ cells had an important pro-metastatic role one would expect to find them elevated in the tumour bearing liver earlier in metastatic development. Indeed, there is a more plausible explanation for the greater metastatic inhibitory effect of DT administration in CD11b-DTR mice when compared to tumour-derived CCL2 inhibition.

Thus, the administration of DT to CD11b-DTR mice is likely to cause a sudden, significant loss of $Gr1^{+}$ cells. This is quite different from the effect of CCL2 inhibition, in which the gradual accumulation of $Gr1^{mid}$ cells over time is delayed. This distinction becomes important when considering the potential pro-metastatic function of $Gr1^{mid}$ cells at the metastatic niche. Indeed, significant evidence demonstrates that myeloid cells are capable of supporting the growth and maintenance of tumour vasculature (Murdoch et al., 2008). If $Gr1^{mid}$ cells are similarly involved in the development of vessels within MC38 metastases, their sudden loss at the metastatic site (for example following the administration of DT to CD11b-DTR mice) could impair angiogenesis and/or lead to the regression of established tumour vessels. The later scenario, in particular would dramatically inhibit metastatic growth. In contrast, the delay in $Gr1^{mid}$ cell recruitment that occurs because of CCL2 inhibition in $MC38^{CCL2shRNA}$ cells may just slow vessel development rather than effecting formed vessels and as such would have a lesser inhibitory effect on metastatic growth.

CHAPTER 4. $CD45^+/CXCR2^+$ Neutrophils Promote Hepatic Metastasis Development in Mice

4.1 Introduction

4.1.1 Basic neutrophil biology

It is well recognised that neutrophils play a key role in the acute inflammatory response. They are the first leukocyte on the scene at sites of inflammation (Mantovani et al., 2011) and can specifically target and kill invading pathogens through multiple mechanisms. These include phagocytosis, the release of proteolytic enzymes (Häger et al., 2010) and the formation of neutrophil extracellular traps: structures composed of extruded DNA and neutrophil granule proteins, capable of trapping and lysing circulating microbes (Brinkmann et al., 2004). Unstimulated, neutrophils survive in the circulation for up to 10 hours (Athens et al., 1961)(McMillan and Scott, 1968). However, *in-vitro*, neutrophil lifespan increased 4-fold in response to interleukin-1β, TNF-α, granulocyte-macrophage colony stimulating factor (GM-CSF) and granulocyte-CSF (Colotta et al., 1992), indicating that neutrophil phenotype is dramatically altered by the presence of particular cytokines.

Neutrophil egress from their site of production in the bone marrow is tightly regulated by the opposing actions of various chemokines and their cell surface receptors. In steady state conditions CXCL12 expression by bone marrow stromal cells enables retention of neutrophils through agonism of their CXCR4 receptor (Balabanian et al., 2005). During episodes of inflammation, elevated circulating G-CSF simultaneously inhibits neutrophil CXCR4 expression and CXCL12 production in the bone marrow, releasing neutrophils into the circulation (Lévesque et al., 2003)(Kim et al., 2006). Movement of neutrophils from the bone marrow into the circulation is also promoted by CXC chemokines such as CXCL1, CXCL2 and CXCL8 (Eash et

al., 2010) (Kolaczkowska and Kubes, 2013), each of which contain the ELR (Glu-Leu-Arg) tri-peptide motif. Importantly, the ELR motif is required for CXC chemokine-receptor signaling and in particular for chemotaxis of neutrophils (Clark-Lewis et al., 1991)(Gerber et al., 2000).

4.1.2 Neutrophils in cancer development

Interestingly, various clinical studies have demonstrated significant neutrophil infiltrates within various primary cancers including those of the cervix, lung, liver and colon (Rao et al., 2012)(Ilie et al., 2012)(Carus et al., 2013)(Xiao et al., 2014), whilst cancer patients frequently express high circulating and tissue CXC chemokine levels compared to health controls (Cheng et al., 2014)(Doll et al., 2010)(Divella et al., 2013)(Cheng et al., 2011). Interestingly, neutrophilia predicts poor outcome and metastasis in colorectal cancer patients, suggesting that the expression of neutrophil chemoattractants serves to promote an aggressive phenotype through neutrophil recruitment (Rao et al., 2012)(Walsh et al., 2005)(Halazun et al., 2008). Nonetheless, studies demonstrating a correlation between ELR^+ CXC chemokine expression and tumour neutrophil infiltration are scarce. Thus, whilst the degree of tumour neutrophil infiltration showed a strong correlation with tissue CXCL5 concentration in patients with cholangiocarcinoma (Okabe et al., 2012) and hepatocellular carcinoma (Zhou et al., 2012), no such correlation has been demonstrated for primary or metastatic colon cancer.

This hypothesis is supported by a growing body of experimental data, which links tumour cell-derived expression of neutrophil chemoattractants to neutrophil infiltration and stimulation of cancer growth (Fridlender and Albelda, 2012). For example, $myeloperoxidase^+$ neutrophils were found to infiltrate lung tumours expressing CXCL1, CXCL2 and CXCL8 in a subcutaneous model, whilst antagonism of CXCR2 inhibited neutrophil infiltration and delayed tumour growth (Tazzyman et al., 2011). Similarly, tumours developed in spontaneous and

inflammation-driven models of colonic neoplasia expressed high levels of various ELR$^+$ CXC chemokines which are responsible for the CXCR2-dependent recruitment of tumour growth-promoting neutrophils (Jamieson et al., 2012)(Katoh et al., 2013).

4.1.3 Neutrophils in the promotion of cancer metastasis

The ability of neutrophils to promote the development and growth of primary tumours raises the question as to whether they may also facilitate metastatic development. In a recent study of the melanoma microenvironment, neutrophils were found within cutaneous tumours repeatedly exposed to intense ultraviolet radiation (Bald et al., 2014). In this model, tumour-associated neutrophils promoted melanoma angiotropism, tumour cell intravasation and the formation of lung metastasis, whilst their depletion inhibited metastasis formation (Bald et al., 2014). Intriguingly, neutrophils have also been identified in the hepatic metastatic microenvironment, where they appeared to promote metastatic development (Spicer et al., 2012). In this setting, activated neutrophils were responsible for the production of neutrophil extracellular traps (Brinkmann et al., 2004). Adhesion of tumour cells to neutrophil extracellular traps within the hepatic circulation aided their survival, thus promoting metastatic development (Cools-Lartigue et al., 2013).

Thus far, the clinical and experimental evidence presented indicates that neutrophils are capable of promoting various stages of colon cancer development and metastasis. Nonetheless, we failed to identify a significant neutrophil infiltrate in association with MC38 hepatic metastases, despite the fact that MC38 cells expressed the neutrophil chemoattractant CXCL1 (Figure 3.6). Given the significant heterogeneity that exists between cancer patients, both at the genetic and microenvironmental levels, it is possible that MC38 hepatic metastases alone are not representative of human disease.

Furthermore, although prior studies have identified a role for neutrophils in the trapping of circulating tumour cells within the vasculature (Cools-Lartigue et al., 2013)(Huh et al., 2010a), it is not yet clear whether neutrophils might also promote the progressive growth of hepatic metastasis. This distinction is particularly important in the clinical setting, given that a significant proportion of colorectal cancer patients present with synchronous hepatic metastases. Therefore, understanding the mechanisms that regulate the progressive growth of hepatic metastasis may help to identify new treatment options aimed at downstaging hepatic metastasis and improving operability. With this in mind, we next turn our attention to an analysis of the immune cells associated with a range of human colon cancer hepatic metastases developed in SCID mice.

4.2 Aims

1. To determine whether liver metastases are associated with hepatic neutrophil accumulation

2. To determine whether tumour-associated neutrophils support the growth of hepatic metastasis

4.3 Results

4.3.1 Human hepatic metastases recruit Gr1^{high} cells expressing the chemokine receptor CXCR2

To determine whether human hepatic metastases are associated with myeloid cell infiltration, the human colon cancer cell lines HT29, HCT116 and LoVo were injected via the intrasplenic route into SCID mice. Tumour-bearing livers were then analysed by flow cytometry 5-7 weeks later. Injection of HCT-116 and HT-29 cells consistently resulted in hepatic metastases within 5 weeks whereas the LoVo cell line developed macroscopic metastases within 7 weeks (Fig. 4.1 a-d).

Interestingly, the livers of tumour-bearing SCID mice contained a significantly elevated number of Gr1^{high} cells compared to naïve, splenectomised control mice (Fig. 4.1 a-e). Such cells were found to be polymorphonuclear when examined in C57bl6 mice (Chapter 3) and are therefore likely to represent granulocytes. Immunohistochemical analysis of livers from tumour-bearing SCID mice demonstrated high numbers of cells expressing the murine neutrophils marker Ly6G within the hepatic metastases from HT29, HCT-116 and LoVo cell lines (Fig. 4.2). This is in contrast to the findings presented in Chapter 3, where livers bearing MC38^{GFP} tumours were associated with high levels of Gr1^{mid} monocytes that expressed low levels of Ly6G.

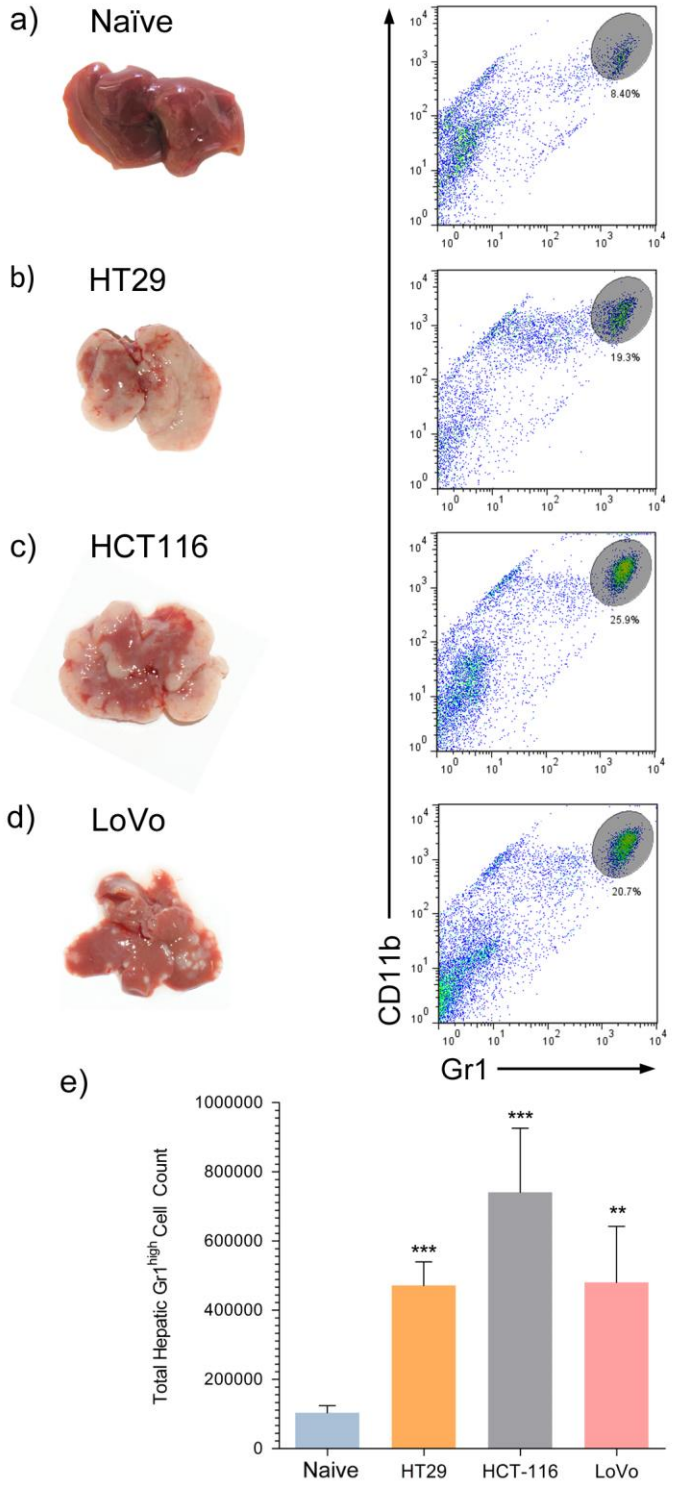

Figure 4.1 Liver metastases derived from human colon cancer cell lines are associated with elevated hepatic CD11b^{+}/Gr1^{high} cell number

a-d) Livers from naïve SCID mice (a) or SCID mice bearing HCT116, HT29 or LoVo metastases (b-d), with the CD11b^{+}/Gr1^{high} population indicated in adjacent hepatic flow cytometry plots (grey oval). Indicated percentages were calculated using the total myeloid cell number as the denominator.

e) Total hepatic CD11b^{+}/Gr1^{high} cell count in naive and tumour-bearing livers. P-value symbols indicate mean value compared with naïve liver.

Data in (e) represents results from a single experiment with at least 3 mice per cell line.

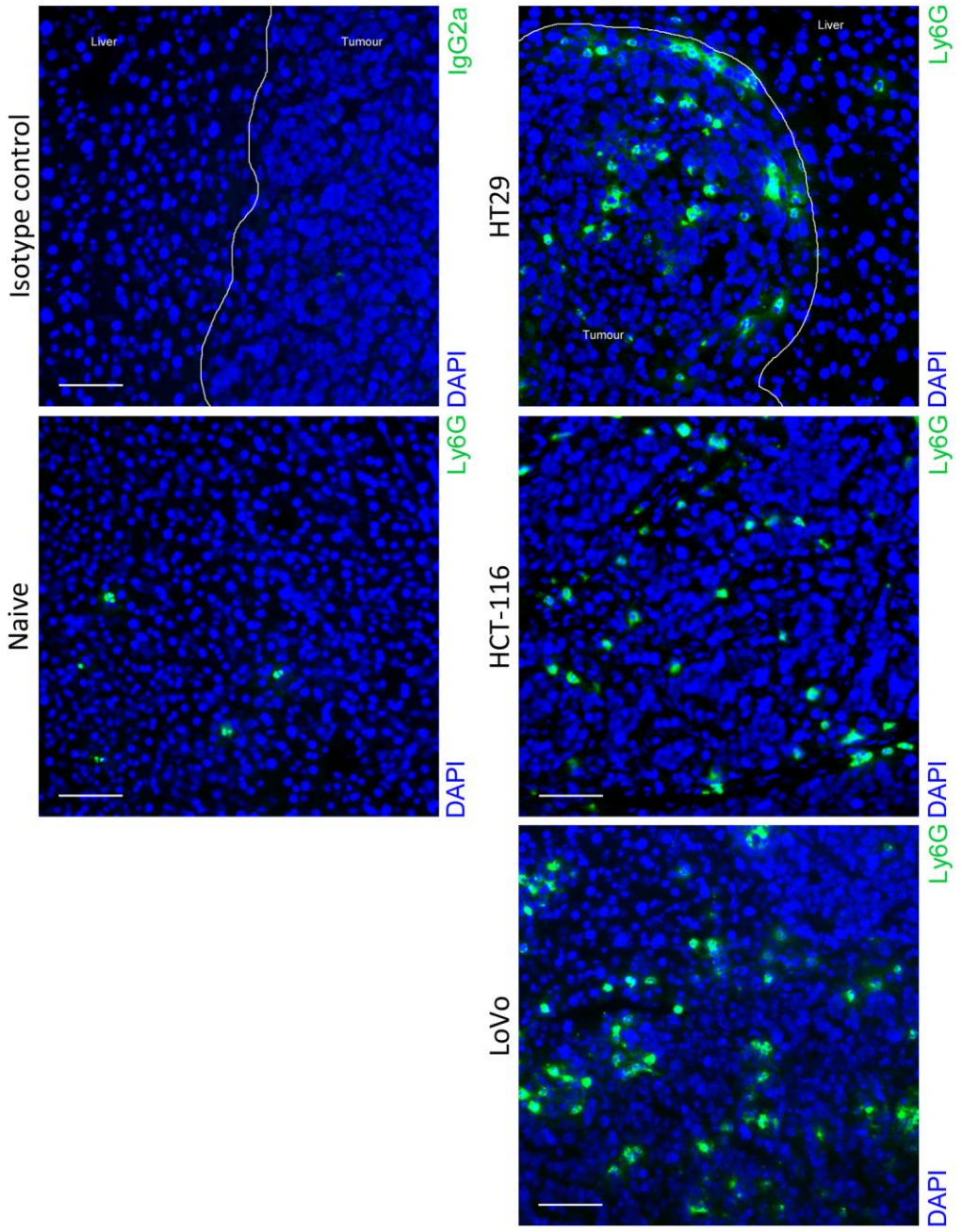

Figure 4.2 Localisation of Ly6G$^+$ neutrophils in naive and tumour-bearing murine livers

Immunolabelling of naïve and tumour-bearing mouse livers for Ly6G (1A8) or IgG2a (both green). Tissues are counterstained with DAPI.

Multiple tumours from 3 mice per cell line were imaged.

To confirm that $Gr1^{high}$ cells were neutrophils, they were back-gated to determine their forward/side scatter characteristics (Fig. 4.3a,b). $Gr1^{high}$ cells (in red, Fig. 4.3b) were of larger size and granularity than the $Gr1^{mid}$ or $Gr1^{low}$ population (seen in blue and green respectively, Fig. 4.3b). Furthermore, they expressed the murine neutrophil marker Ly6G and the chemokine receptor CXCR2 (Fig. 4.3c). Notably, CXCR2 is the major chemokine receptor expressed by both murine and human neutrophils (Bozic et al., 1994)(Thomas et al., 1991) and has been shown to be responsible for neutrophil recruitment during the development of experimentally induced ischemia-reperfusion injury in the murine liver (Kuboki et al., 2008)(Van Sweringen et al., 2013). Importantly, FACS sorted $CD45^{+}/CXCR2^{+}$ cells from HCT-116 tumour-bearing livers demonstrated multilobular nuclei (Fig. 4.3d), indicating that this cell surface marker pattern defines tumour-associated neutrophils.

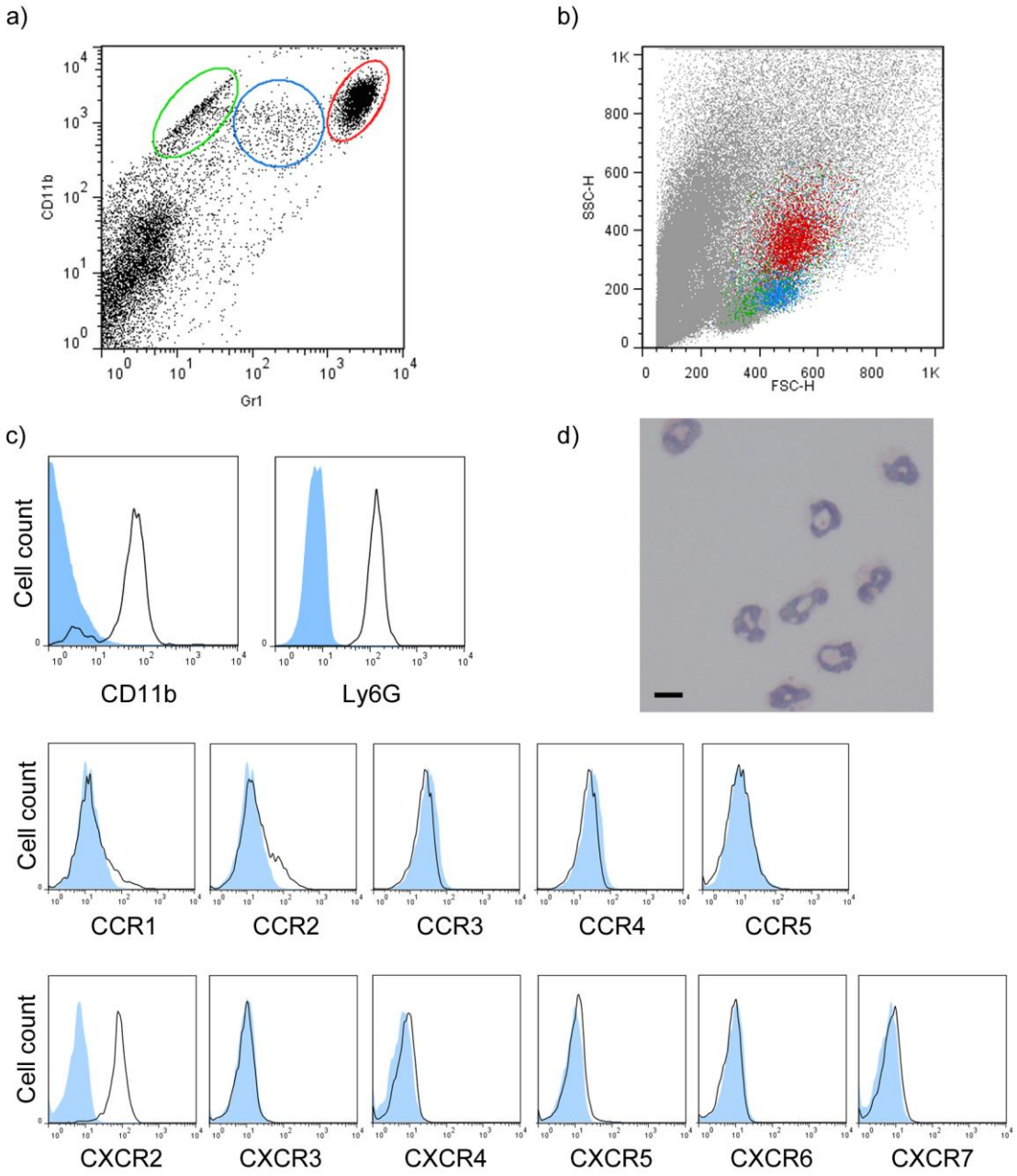

Figure 4.3 Morphological characterisation and chemokine receptor expression profile of tumour-associated neutrophils

a) FACS plot of $Gr1^{low}$ (green), $Gr1^{mid}$ (blue) and $Gr1^{high}$ (red) populations in a liver from a mouse injected with HCT-116 cells.

b) FSC/SSC back gating of $Gr1^{low}$ (green), $Gr1^{mid}$ (blue) and $Gr1^{high}$ (red) cells from (a).

c) Histograms demonstrating the expression of various cell-surface antigens identified using FACS antibodies (black curves) or an isotype control (blue) in tumour-associated $Gr1^{high}$ cells.

d) H&E staining of hepatic $CD45^{+}/CXCR2^{+}$ cells FACS sorted from HCT-116 tumour-bearing mice. Scale bar represents 10 μm.

4.3.2 $CXCR2^+/CD45^+$ neutrophils are associated with hepatic metastases

The Gr1 antigen is not found in humans, but CXCR2 is common to both murine and human neutrophils. In confirmation of the findings when assessing $Gr1^{high}$ cell numbers, the livers of mice bearing HT29, HCT-116 and LoVo metastases were infiltrated with significantly higher numbers of $CD45^+/CXCR2^+$ neutrophils than control splenectomised SCID mice (Fig. 4.4a,b).

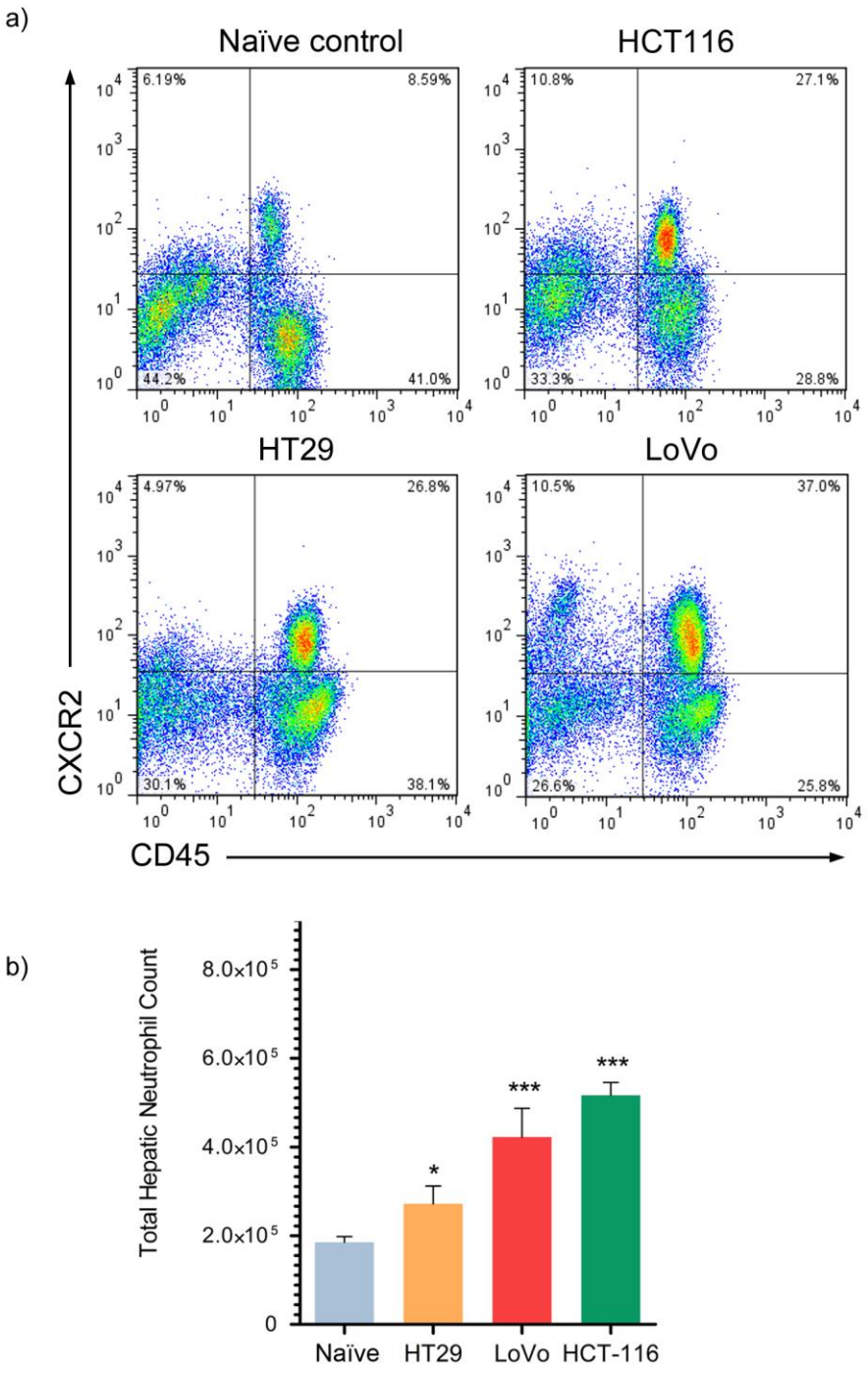

Figure 4.4 Elevated CXCR2⁺/CD45⁺ neutrophil count in mouse livers bearing human colon cancer metastases

a) Hepatic flow cytometry plots from naïve or tumour-bearing mice stained with anti-CD45 (X-axis) and anti-CXCR2 (Y-axis) antibodies. Indicated percentages were calculated using the total myeloid cell number as the denominator.

b) Total hepatic CXCR2⁺/CD45⁺ cell count in the livers of naïve and tumour-bearing mice. P-value symbols indicate mean value compared with naïve liver.

Data in (b) represents results from 2 separate experiments each with at least 5 mice per group.

4.3.3 CD45$^+$/CXCR2$^+$ neutrophil numbers are increased in the livers of immune competent mice bearing hepatic metastases

As Gr1^{high} neutrophils were not found at elevated numbers in MC38, B16F1 or LLC hepatic metastases in C57Bl6 mice, we questioned whether the neutrophil infiltration seen in SCID mice bearing hepatic colon metastases was solely the result of immunodeficiency in this model. As well as the aforementioned tumour types, pancreatic cancer also commonly metastasises to the liver in humans. Furthermore, the murine pancreatic cancer cell line Pan02 forms hepatic metastases in orthotopic mouse models (Arnold et al., 2010)(Yan et al., 2006), whilst primary pancreatic tumours developed using Pan02 cells are infiltrated with neutrophils expressing Gr1 and MMP9 (Arnold et al., 2008). We therefore inoculated C57Bl6 mice with Pan02 cells via the intrasplenic route (Fig. 4.5a) and analysed the resultant hepatic metastases for the presence of CD45$^+$/CXCR2$^+$ neutrophils.

Importantly, as identified for the human colon cancer cell lines in SCID mice, livers bearing Pan02 metastases were associated with an elevated number of neutrophils as defined by their CD11b$^+$/Gr1^{high} or CD45$^+$/CXCR2$^+$ expression, when compared to naïve C57Bl6 livers (Fig. 4.5b,c). Furthermore, Ly6G$^+$ neutrophils were identified in large numbers within Pan02 hepatic metastases (Fig. 4.5d).

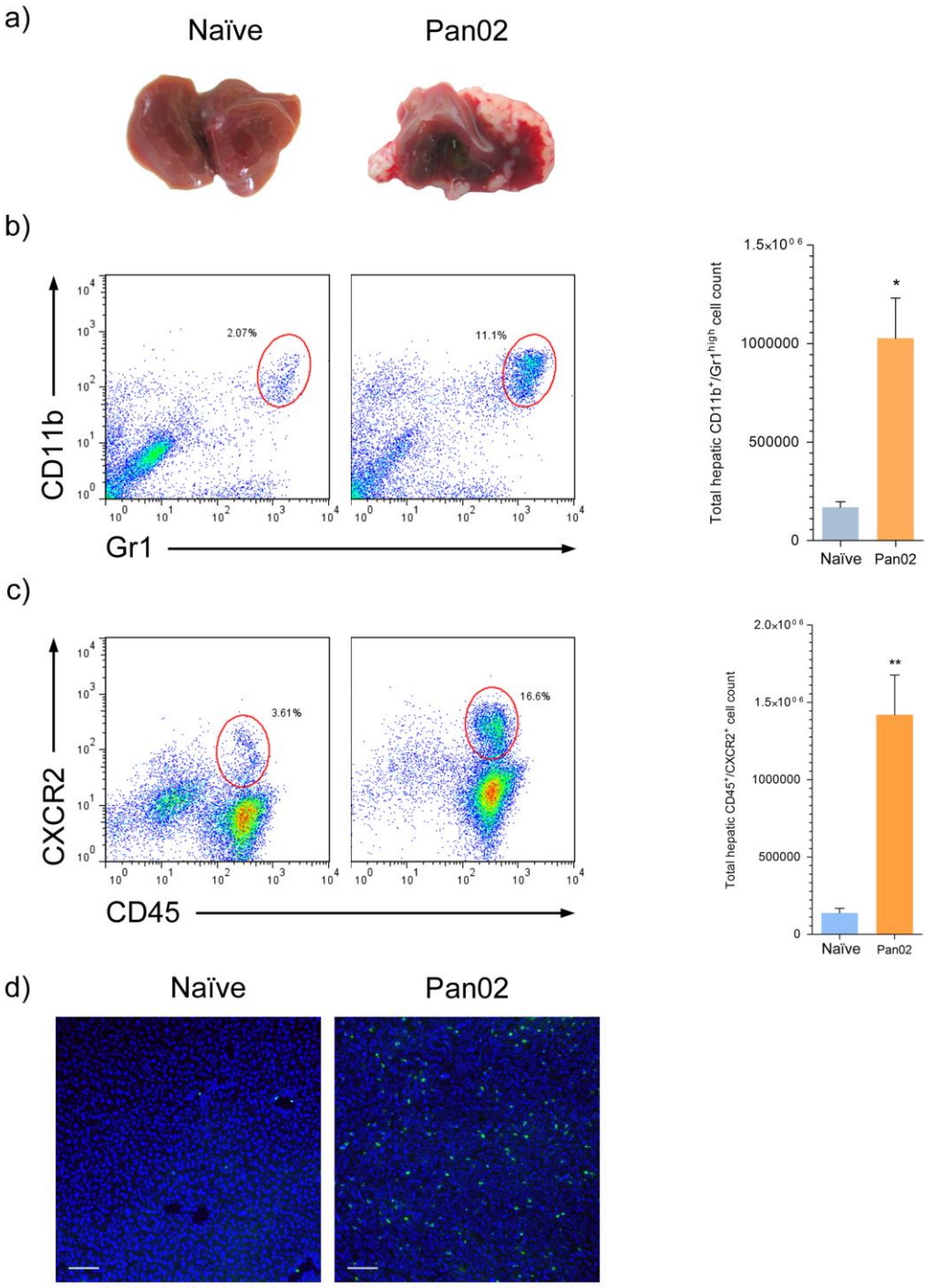

Figure 4.5 Elevated neutrophil count in Pan02 hepatic metastasis

a) Naïve C57bl6 mouse liver and C57bl6 liver with Pan02 pancreatic metastases.

b) Hepatic FACS plots and bar graph from naïve (left) and tumour-bearing (right) mice demonstrating $CD11b^{+}/Gr1^{mid}$ cells within the red circle. Indicated percentages were calculated using the total myeloid cell number as the denominator.

c) Hepatic FACS plots and bar graph from naïve (left) and tumour-bearing (right) mice demonstrating $CD45^{+}/CXCR2^{+}$ cells within the red circle. Indicated percentages were calculated using the total myeloid cell number as the denominator.

d) Staining of naïve and Pan02 metastasis-bearing livers for Ly6G (1A8) (green). Tissues are counterstained with DAPI.

Data in (b) and (c) represent results from two experiments each of 5 mice per group.

4.3.4 Anti-Ly6G antibody clone 1A8 systemically depletes neutrophils in SCID mice

To understand whether the neutrophils associated with hepatic colon cancer metastases are pro- or anti-metastatic, an experimental model for the specific depletion of neutrophils in SCID mice was developed. Previous research has demonstrated that the anti-Ly6G antibody (clone 1A8) depletes circulating murine granulocytes with high specificity over other myeloid populations in C57Bl6 mice (Daley et al., 2008). Thus, to determine whether the anti-Ly6G antibody systemically depletes neutrophils in SCID mice, 12.5 μg anti-Ly6G or an isotype control antibody (IgG2a) were administered to experimental animals via the peritoneal route. The murine liver and spleen were then harvested after 24 and 72 hours for flow cytometric analysis of myeloid populations (Fig. 4.6 and 4.7).

Within 24 hours of treatment - and for at least 72 hours after - there was a significant reduction in total splenic and hepatic $CD45^+/CXCR2^+$ cell count for mice given anti-Ly6G compared to those administered IgG2a (Figs 4.6a,b and 4.7a,b). Furthermore, anti-Ly6G administration had no effect on the total $CD45^+/CXCR2^-$ cell count in either organ (Figs 4.6b and 4.7b). Given that all haematopoietic cells express CD45, this data indicates that anti-Ly6G administration does not affect other cells of haematopoietic origin within the liver.

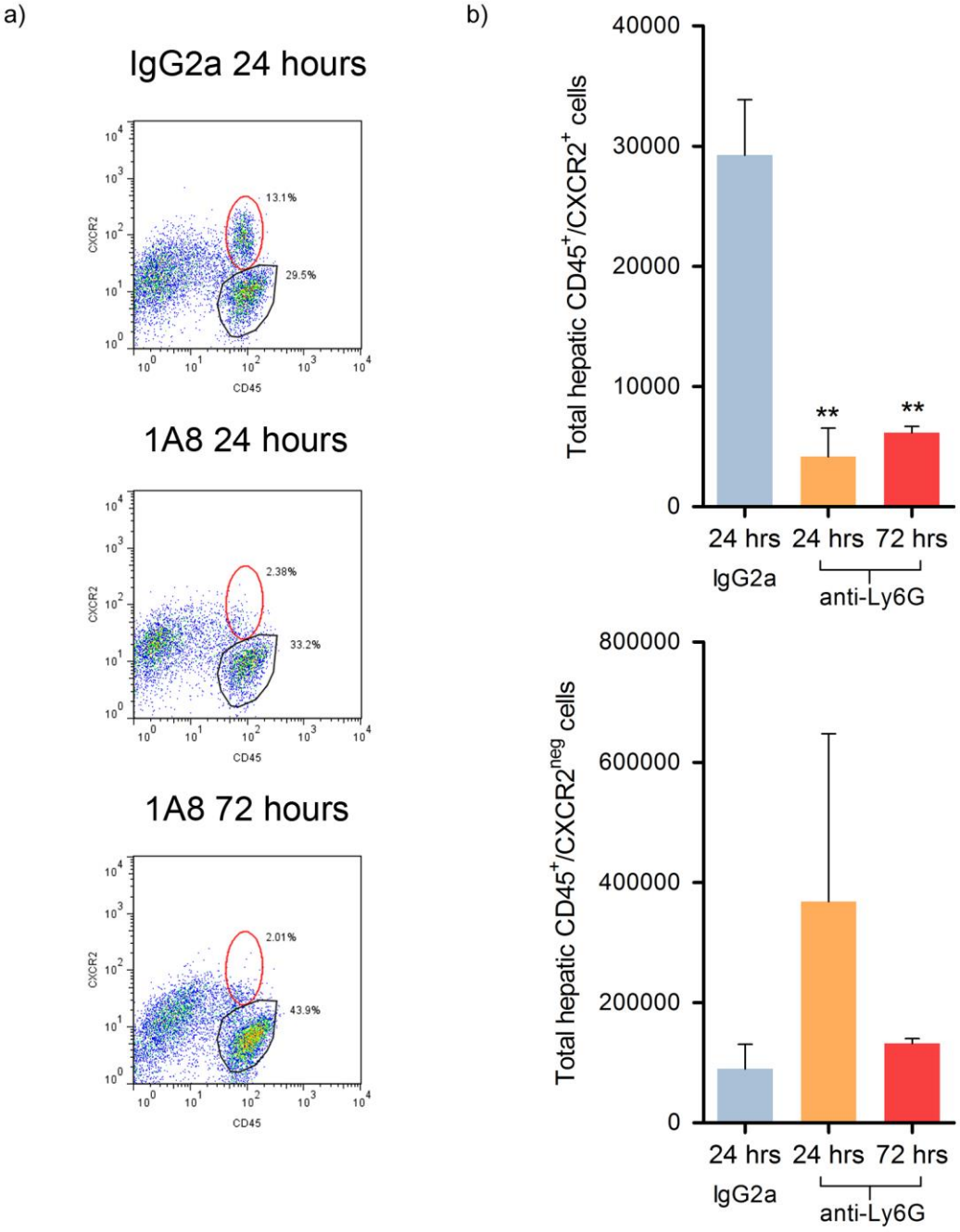

Figure 4.6 Rat anti-Ly6G (1A8) specifically depletes murine hepatic neutrophils

a) Flow cytometry plots of murine hepatic single cell suspensions 24 hours following isotype control antibody administration (IgG2a), or 24 and 72 hours following anti-Ly6G (1A8) administration. The red oval identifies $CD45^+/CXCR2^+$ neutrophils, whilst the black polygon identifies all other haematopoietic ($CD45^+/CXCR2^{neg}$) cells.

b) Corresponding bar graphs of flow cytometric data taken from multiple mice showing total hepatic $CD45^+/CXCR2^+$ cells (top) and other haematopoietic ($CD45^+/CXCR2^{neg}$) cells (bottom). P-value symbols indicate mean value compared with IgG2a-treated mice.

Data in (b) represents results from a single experiment with 5 mice per group.

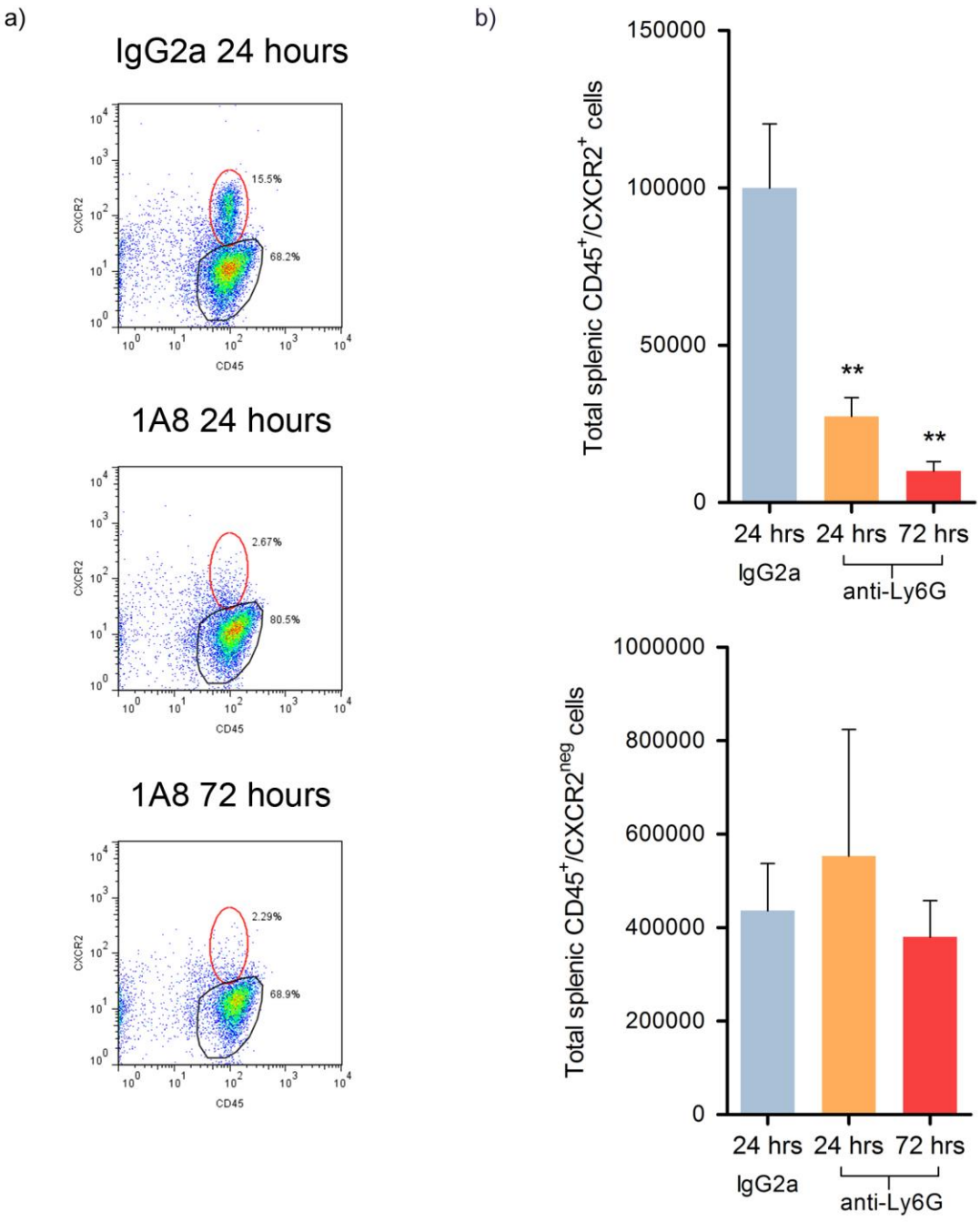

Figure 4.7 Rat anti-Ly6G (1A8) specifically depletes murine splenic neutrophils

a) Flow cytometry plots of murine splenic single cell suspensions 24 hours following isotype control antibody administration (IgG2a), or 24 and 72 hours following anti-Ly6G (1A8) administration. The red oval identifies $CD45^+/CXCR2^+$ neutrophils, whilst the black polygon identifies all other haematopoietic ($CD45^+/CXCR2^{neg}$) cells.

b) Corresponding bar graphs of flow cytometric data taken from multiple mice showing total splenic $CD45^+/CXCR2^+$ cells (top) and other haematopoietic ($CD45^+/CXCR2^{neg}$) cells (bottom). P-value symbols indicate mean value compared with IgG2a-treated mice.

Data in (b) represents results from a single experiment with 5 mice per group.

4.3.5 Neutrophil depletion inhibits the development of hepatic colon cancer metastasis in SCID mice

To determine the effect of $CD45^+/CXCR2^+$ cells on metastatic growth, $HT29^{luc}$, $HCT\text{-}116^{luc}$ and $LoVo^{luc}$ hepatic tumours were developed in mice treated with the anti-Ly6G antibody or its isotype control. For $HT29^{luc}$ and $HCT\text{-}116^{luc}$-injected mice, anti-Ly6G antibody was injected 24 hours prior to (early), or 10 days following (late), intrasplenic tumour cell injection and then injections continued 72-hourly until the end of the experiment. These experimental groups enabled differentiation of the effect of neutrophil depletion at the early (initiation) and late (growth) phases of metastatic development. We chose not to perform an analysis of the effect of late neutrophil depletion in mice injected with $LoVo^{luc}$ cells due to both financial and time constraints. Thus, $LoVo^{luc}$ metastases grew significantly slower than $HT29^{luc}$ and $HCT\text{-}116^{luc}$ tumours and thus mice injected with $LoVo^{luc}$ cells required more doses of the relatively expensive, affinity-purified anti-Ly6G antibody throughout the course of tumour growth.

Using *in-vivo* luminescence imaging (Figs 4.8a, 4.9a and 4.10a), abdominal luminescence intensity was measured during the development of liver metastases. Strong luminescence signals were detected for all mice within 24 hours of tumour cell injection. However, for all cell lines there was a marked decline in luminescence signal within the first 10 days following intrasplenic tumour cell injection indicating that the majority of tumour cells passing into the hepatic circulation failed to survive (Figs 4.8b, 4.9b and 4.10b). After this time, luminescence signal increased steadily as hepatic metastases developed. For the purpose of this experiment, metastases that formed following intrasplenic tumour cell injection can therefore be thought of as developing in 2 phases; an initiation phase, where only a select population of tumour cells survived within the hepatic sinusoid followed by a growth phase where those cells that have survived developed into micro- and macroscopic metastases.

For all colon cancer cell lines, there was a significant reduction in luminescence intensity at the final time point in mice depleted of neutrophils 24 hours prior to intrasplenic tumour cell injection compared to control, IgG2a-treated mice (Figs 4.8b, 4.9b and 4.10b (orange curves)). For mice with HT29^{luc} or LoVo^{luc} metastases, luminescence intensity reached a baseline that was independent of the presence of neutrophils. However, for mice with HCT-116^{luc} metastases early neutrophil depletion resulted in a significant reduction in the luminescence signal over the first 7-10 days (Fig. 4.9b (orange line)).

Interestingly, depletion of neutrophils 10 days post intrasplenic tumour cell injection onwards delayed the growth of HT29^{luc} and HCT-116^{luc} metastases, to the same extent with which early neutrophil depletion delayed tumour growth (Figs 4.8b and 4.9b respectively (purple line)).

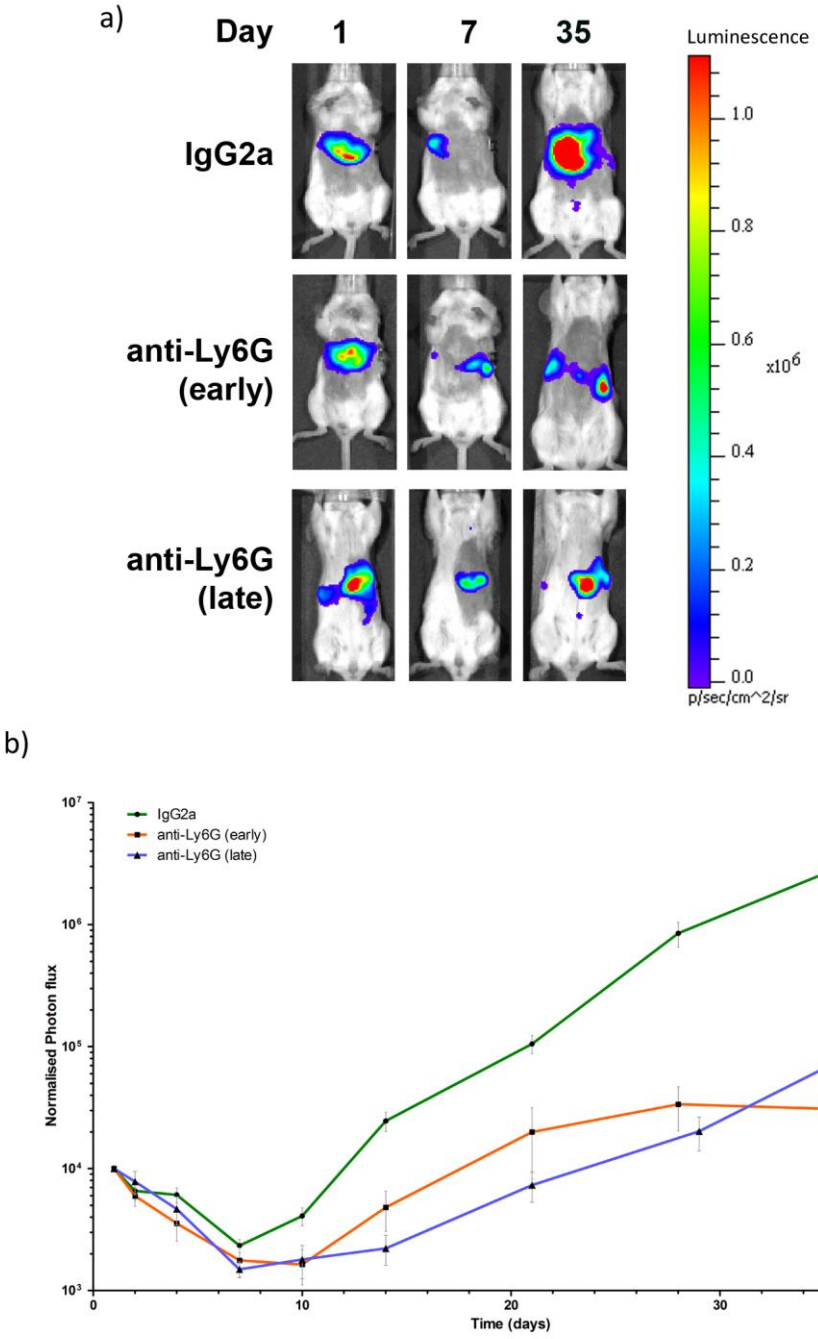

Figure 4.8 Neutrophil depletion inhibits the colonisation phase of HT29 hepatic metastasis development

a) Luminescence images of HT29 tumour-bearing mice treated with IgG2a, anti-Ly6G starting 24 hours prior to tumour cell injection (anti-Ly6G early) or anti-Ly6G starting 10 days following tumour cell injection (anti-Ly6G late).

b) Growth curves generated from luminescence data in mice treated with IgG2a (green), anti-Ly6G starting 24 hours prior to tumour cell injection (orange), or anti-Ly6G starting 10 days following tumour cell injection (purple). X-axis indicates time in days following intrasplenic tumour cell injection and Y-axis, the total abdominal photon flux relative to the value obtained at day 1 post tumour cell injection.

Data in (b) represents results from a single experiment of at least 8 mice per group.

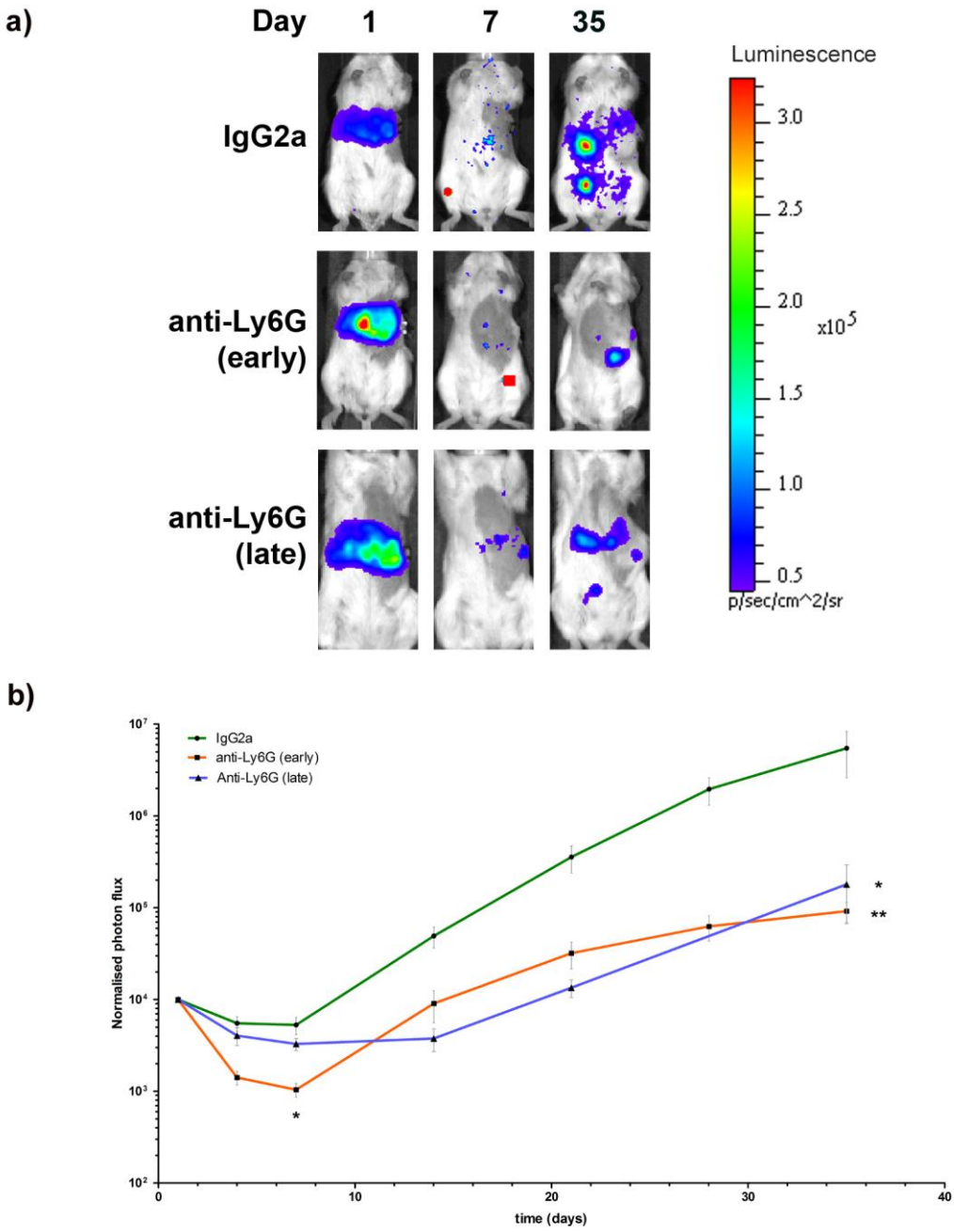

Figure 4.9 Neutrophil depletion inhibits the colonisation phase of HCT-116 hepatic metastasis development

a) Luminescence images of HCT-116 tumour-bearing mice treated with IgG2a, anti-Ly6G starting 24 hours prior to tumour cell injection (anti-Ly6G early) or anti-Ly6G starting 10 days following tumour cell injection (anti-Ly6G late).

b) Growth curves generated from luminescence data in mice treated with IgG2a (green), anti-Ly6G starting 24 hours prior to tumour cell injection (orange), or anti-Ly6G starting 10 days following tumour cell injection (purple). X-axis indicates time in days following intrasplenic tumour cell injection and Y-axis, the total abdominal photon flux relative to the value obtained at day 1 post tumour cell injection.

Data in (b) represent results from 3 experiments with at least 10 mice per group.

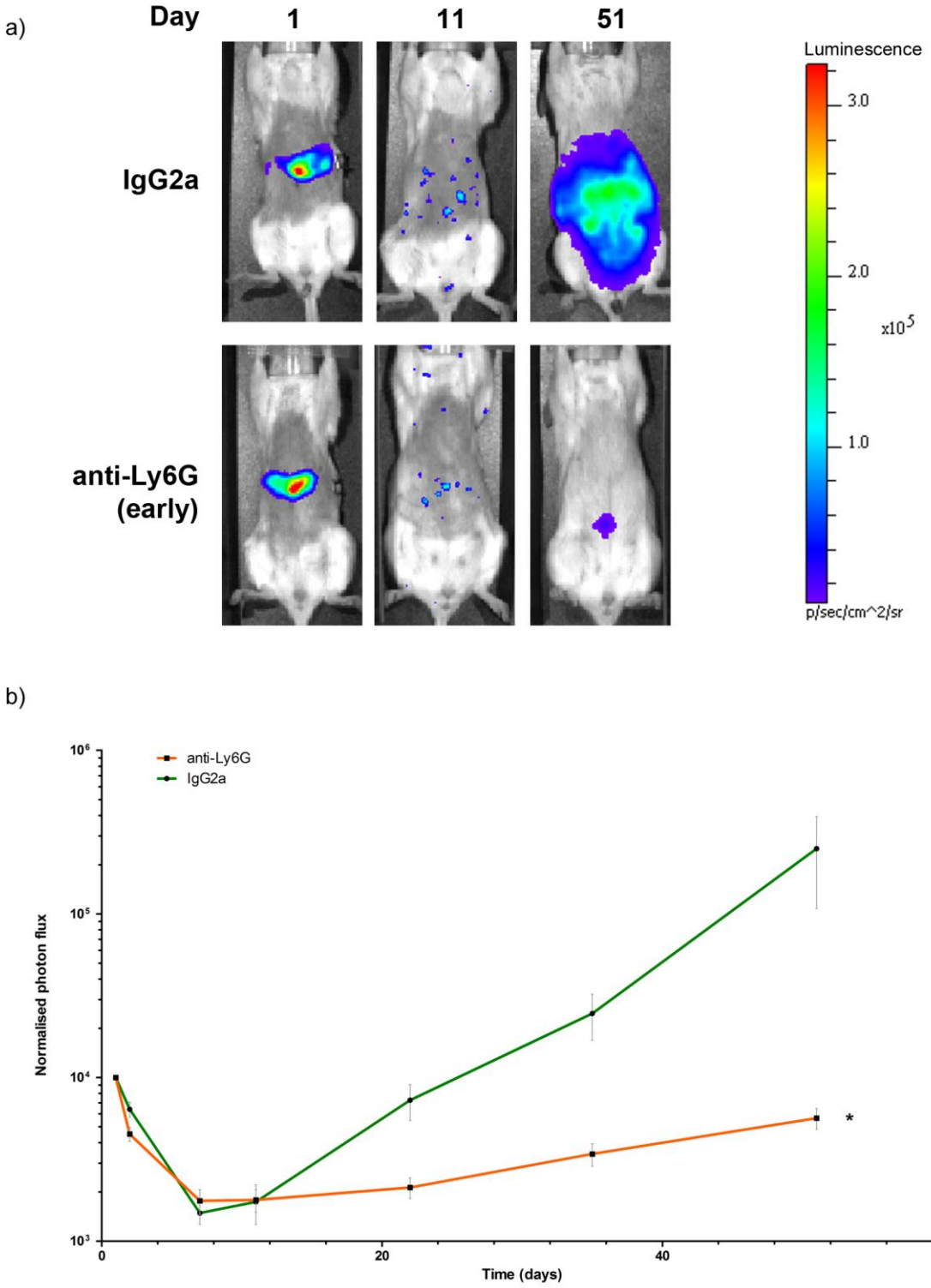

Figure 4.10 Neutrophil depletion inhibits the colonisation phase of LoVo hepatic metastasis development

a) Luminescence images of LoVo tumour-bearing mice treated with IgG2a or anti-Ly6G starting 24 hours prior to tumour cell injection.

b) Growth curves generated from luminescence data in mice treated with IgG2a (green), anti-Ly6G (orange). X-axis indicates time in days following intrasplenic tumour cell injection and Y-axis, the total abdominal photon flux relative to the value obtained at day 1 post tumour cell injection.

Data in (b) represents results from a single experiment of at least 8 mice per group.

At 5-7 weeks following intrasplenic tumour cell injection, murine livers from the neutrophil depletion experiments were harvested and hepatic tumour burden quantified. Macroscopically, metastatic burden was dramatically reduced for each cell line in mice administered anti-Ly6G prior to tumour cell injection (Figs 4.11a, 4.12a and 4.13a). For $HT29^{luc}$ and $HCT\text{-}116^{luc}$ injected animals, tumour burden also appeared reduced when anti-Ly6G was started from day 10 onwards compared to control IgG2a-treated mice (Figs 4.11b and 4.12b respectively).

The macroscopic findings were confirmed by comparing mean total hepatic luminescence *ex-vivo* between groups of experimental animals. There was a significant reduction in total hepatic luminescence for mice treated with the anti-Ly6G antibody from 24 hours prior to tumour cell injection, compared to IgG2a-treated mice for all three cell lines tests. For the $HT29^{luc}$ and $HCT\text{-}116^{luc}$ cell lines, there was also a significant reduction in hepatic luminescence intensity in mice given anti-Ly6G from day 10 onwards compared to isotype control-treated mice (Figs 4.11c and 4.12c respectively).

Flow cytometric analysis confirmed successful long-term neutrophil depletion in these experiments, as the number of $CD45^{+}/CXCR2^{+}$ cells were significantly lower in the livers of mice treated with anti-Ly6G at 5-7 weeks post intrasplenic tumour cell injection compared to IgG2a-treated animals (Figs 4.11d,e, 4.12d,e and 4.13d,e). For mice with $HT29^{luc}$ and $HCT\text{-}116^{luc}$ metastases, there was no significant difference in total hepatic $CD45^{+}/CXCR2^{neg}$ cell numbers between tumour-bearing mice treated with anti-Ly6G or IgG2a, confirming the specificity of the anti-Ly6G antibody (Figs 4.11f and 4.12f).

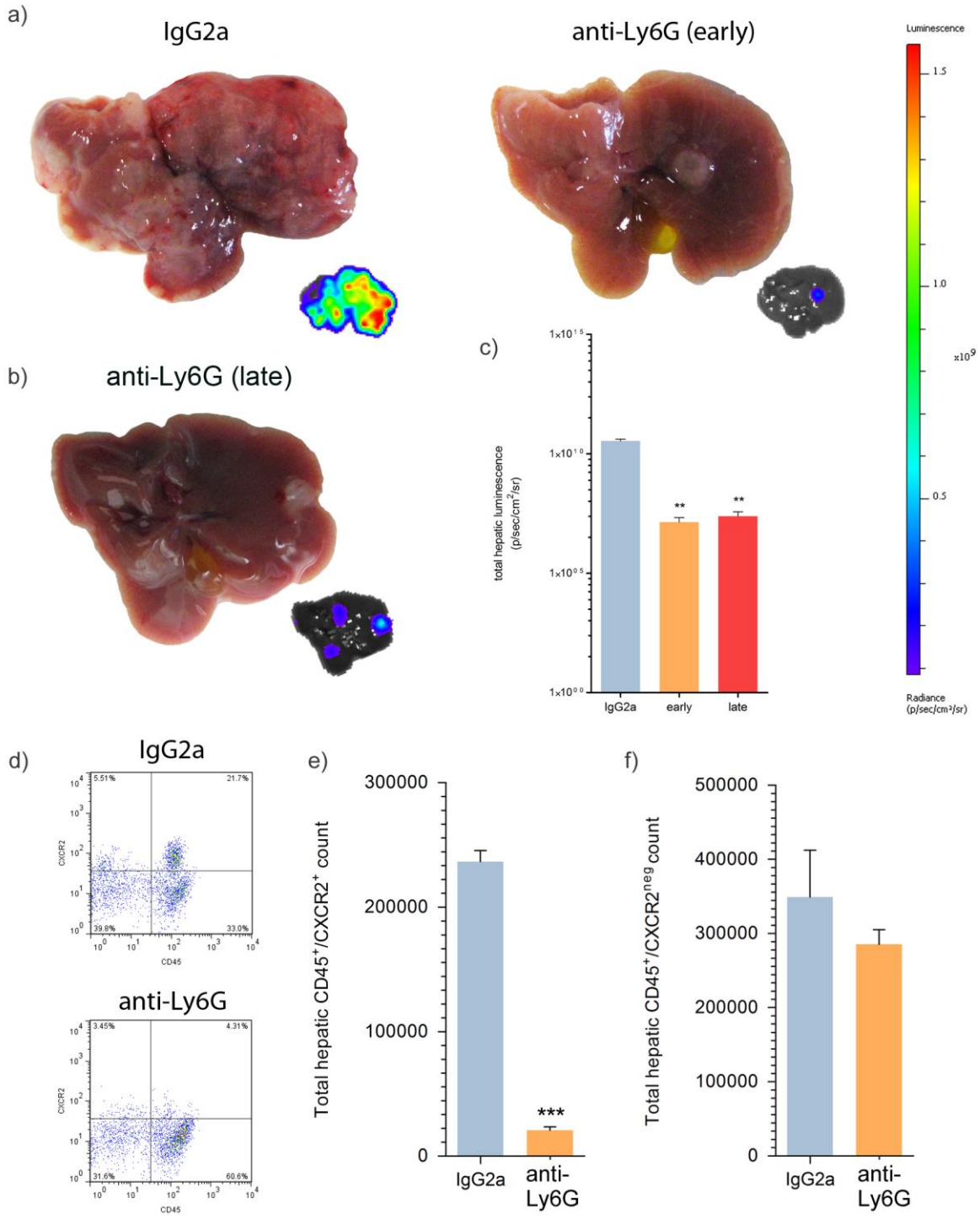

Figure 4.11 Neutrophil depletion inhibits HT29 hepatic metastasis development

a-b) Livers from HT29^{luc} inoculated SCID mice treated with IgG2a, or anti-Ly6G either throughout the experiment (a), or from day 10 post intrasplenic tumour cell injection (b).

c) *Ex-vivo* total hepatic luminescence 5 weeks following intrasplenic HT29^{luc} inoculation for mice treated with IgG2a, anti-Ly6G throughout the experiment (early), or anti-Ly6G from day 10 following tumour cell injection (late).

d) Hepatic FACS plots from IgG2a and anti-Ly6G treated HT29^{luc} metastasis-bearing mice

e-f) Total hepatic CD45^{+}/CXCR2^{+} and CD45^{+}/CXCR2^{neg} cell counts in IgG2a and anti-Ly6G-treated tumour-bearing mice.

Data in (c) represent results from a single experiment of at least 8 mice per group.

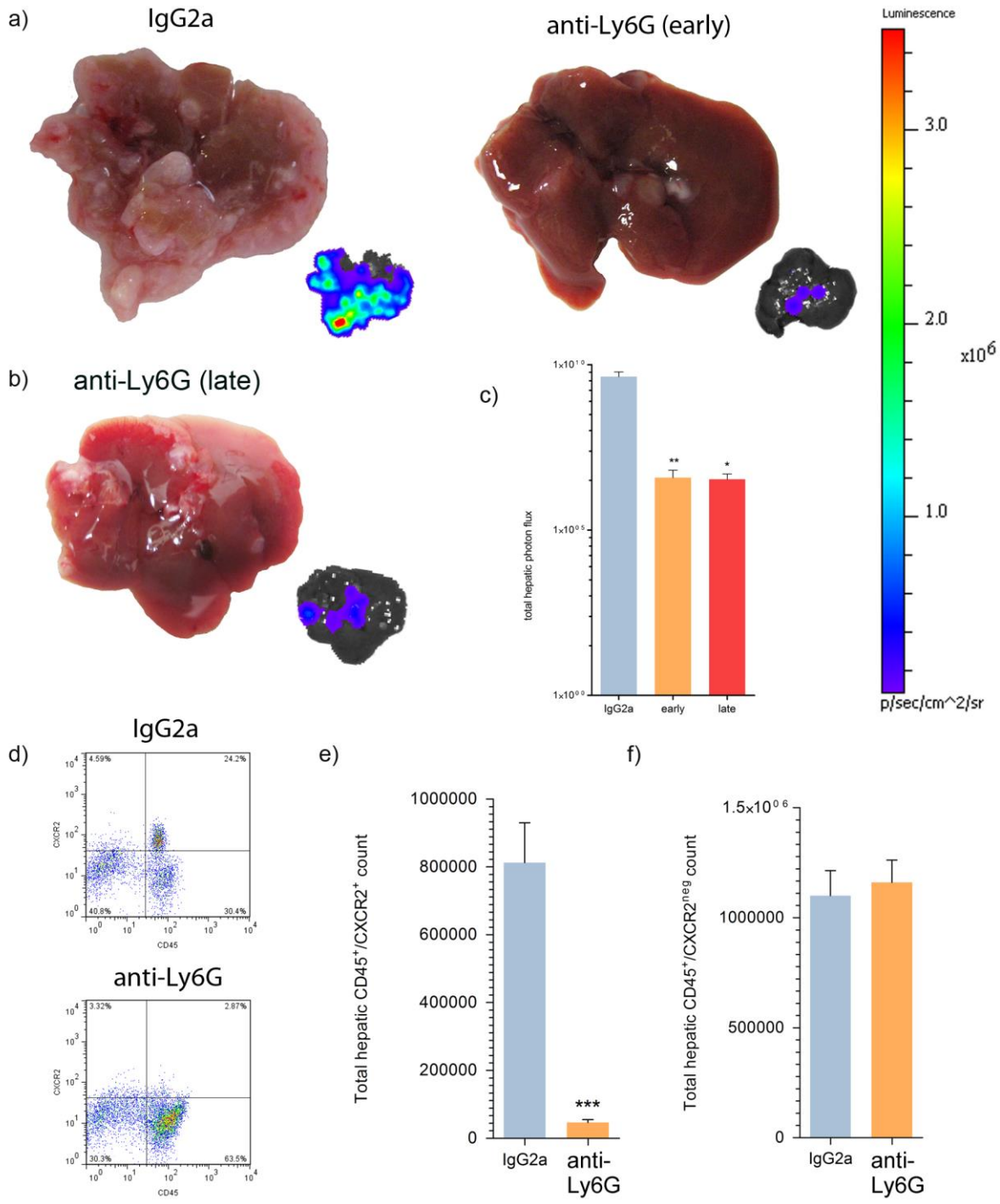

Figure 4.12 Neutrophil depletion inhibits HCT-116 hepatic metastasis development

a-b) Livers from HCT-116^{luc} inoculated SCID mice treated with IgG2a, or anti-Ly6G either throughout the experiment (a), or from day 10 post intrasplenic tumour cell injection (b).

c) *Ex-vivo* total hepatic luminescence 5 weeks following intrasplenic HCT-116^{luc} inoculation for mice treated with IgG2a, anti-Ly6G throughout the experiment (early), or anti-Ly6G from day 10 following tumour cell injection (late).

d) Hepatic FACS plots from IgG2a and anti-Ly6G treated HCT-116^{luc} metastasis-bearing mice

e-f) Total hepatic CD45^{+}/CXCR2^{+} and CD45^{+}/CXCR2^{neg} cell counts in IgG2a and anti-Ly6G-treated tumour-bearing mice.

Data in (c) represent results from 3 experiments with at least 10 mice per group.

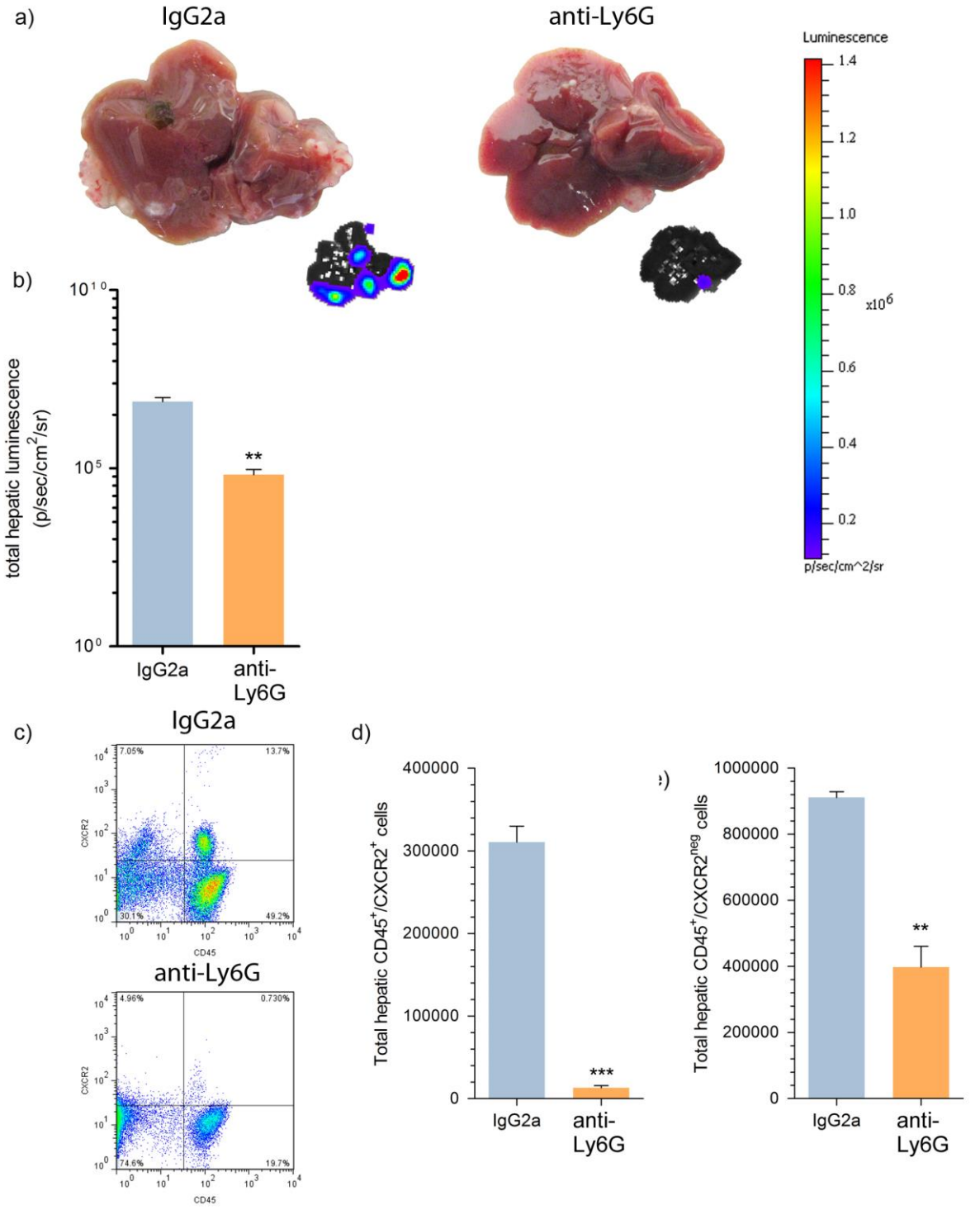

Figure 4.13 Neutrophil depletion inhibits LoVo hepatic metastasis development

a) Livers from LoVo^{luc} inoculated SCID mice treated with IgG2a, or anti-Ly6G.

b) *Ex-vivo* total hepatic luminescence 7 weeks following intrasplenic LoVo^{luc} inoculation for mice treated with IgG2a or anti-Ly6G throughout the experiment.

c) Hepatic FACS plots from IgG2a and anti-Ly6G treated LoVo^{luc} metastasis-bearing mice

d-e) Total hepatic CD45^{+}/CXCR2^{+} and CD45^{+}/CXCR2^{neg} cell counts in IgG2a and anti-Ly6G-treated tumour-bearing mice.

Data in (b) represent results from a single experiment of 8 mice per group.

4.4 Discussion

4.4.1 Neutrophil infiltration within hepatic metastases

The results presented in this chapter clearly demonstrate that neutrophils are found at higher numbers in tumour-bearing compared to naïve livers. The common leukocyte antigen CD45, which is expressed by all haematopoietic cells (Thomas, 1989) and the chemokine receptor CXCR2 were used to define hepatic neutrophils. This enabled us to identify a distinct population of cells that demonstrate various neutrophil-specific features, including large size, granularity and a multilobular nucleus. Furthermore, the increase in neutrophil count that occurs in association with the development of HT29, HCT-116 and LoVo hepatic metastases is not a feature specific to tumours developing in immune-compromised SCID mice. Even in the presence of normal T- and B-cell function, we were able to demonstrate a striking elevation in hepatic neutrophil count in association with Pan02 hepatic metastases.

The elevated neutrophil count seen in tumour-bearing livers may result from prolongation of neutrophil lifespan, increased neutrophil recruitment to the metastatic niche or both. The recruitment of neutrophils and the prolongation of their lifespan could be driven by chemokines and cytokines expressed by the tumour cells or their associated stromal cells. CXC chemokines are expressed by a range of different cancers including those of the colon and it is conceivable that the colon cancer cell lines used in our model may express factors that influence neutrophil behavior and activity. The fact that neutrophils were found within hepatic metastases for all cell lines (Fig. 4.2) points to their specific accumulation at the metastatic niche, potentially in response to tumour-derived factors.

The human colon cancer cell lines used throughout this chapter were chosen as they have been extensively studied in the research literature and had previously been shown to form hepatic metastasis in SCID mice. Furthermore, they represent the range of mutations seen in colon cancer, with the HT29 cell line being microsatellite stable and the HCT-116 and LoVo cell lines showing evidence of microsatellite instability (Kleivi et al., 2004). LoVo and HT29 cells both have mutant APC, whilst HCT-116 cells are wild-type APC but β–catenin mutant (Ilyas et al., 1997). Furthermore, HT29 cells carry BRAF and p53 mutations, whilst LoVo and HCT-116 cells both carry KRAS mutations but are wild-type for BRAF and p53 (Ahmed et al., 2013). Finally, these cell lines were developed from colon cancers at different disease stages: HT29 taken from a grade I Dukes C primary tumour, LoVo taken from a lymph node metastasis in a patient with grade IV colon cancer and HCT-116 from a primary, Dukes stage D colon cancer. This selection of cell lines therefore represents a broad range of colon cancer sub-types likely to reflect the heterogeneity of disease in the population.

4.4.2 The pro-metastatic effect of neutrophils in the hepatic metastatic microenvironment

One overriding conclusion from this study is that neutrophils play a pro-metastatic role within the hepatic metastatic microenvironment. In hepatic tumours generated from the $HT29^{luc}$ and $HCT\text{-}116^{luc}$ cell lines, neutrophil depletion from day 10 post tumour cell injection onwards was sufficient to significantly inhibit metastatic growth. This data in particular highlights the importance of neutrophils in the growth phase of hepatic metastasis, a finding that is of relevance to the clinic, where colon cancer patients frequently present with synchronous hepatic metastases and would therefore significantly benefit from therapies aimed at slowing disease progression.

Elements of our data are also in support of the proposed role of neutrophils in the promotion of liver metastasis demonstrated using lung cancer cells (Spicer et al., 2012). In this setting, neutrophils promoted the adherence of tumour cells to the hepatic sinusoidal endothelia and their depletion through administration of a single dose of anti-Gr1 antibody 24 hours prior to tumour cell injection was sufficient to significantly inhibit tumour growth (Spicer et al., 2012). Indeed, the initiation phase of HCT-116^{luc} metastatic growth was highly dependent on the presence of neutrophils, as their depletion significantly reduced the abdominal luminescence signal over the first 10 days following tumour cell injection. Interestingly, this was not the case for HT29^{luc} metastases, the initiation of which occurred to an equal degree independent of neutrophil presence. This difference indicates that cell specific characteristics are at last in-part responsible for determining the mechanisms through which tumour cells survive within the hepatic metastatic microenvironment. This may again have clinical relevance as the data implies that prophylactic neutrophil inhibition could inhibit the progression to hepatic metastatic disease in some patients (i.e. those whose tumours depend upon neutrophils for intra-sinusoidal survival), but not others.

In our study, neutrophil depletion has an apparent abrupt effect on tumour growth. When anti-Ly6G treatment was started on day 10, it delayed the growth of both HCT-116 and HT29 metastases within 4 days, as indicated by the reduced abdominal luminescent signal following antibody administration (purple lines, Figs 4.9 and 4.10 days 10 to 14). This suggests that neutrophils play a role in the promotion of tumour cell proliferation, as ablation of neutrophils prevented metastatic growth. This may result either from a direct effect on the tumour cell, or through indirect effects such as promotion of the angiogenic switch, as has been demonstrated for neutrophils recruited to primary pancreatic cancers (Nozawa et al., 2006).

The growth curves of anti-Ly6G (late) treated mice are, however, not in keeping with the possibility that neutrophils prevent the apoptosis of tumour cells. If this were the case metastatic burden and therefore the abdominal luminescence signal would decline following neutrophil depletion. Importantly, a subset of neutrophils termed granulocytic myeloid-derived suppressor cells (GMDSC) were found to infiltrate the liver during the development of B16F1 and LLC subcutaneous tumours (Ilkovitch and Lopez, 2009), whilst GMDSC promoted hepatic metastasis development following intravenous injection of breast cancer cells (Mauti et al., 2011). GMDSC inhibit antigen-driven cytotoxic T-lymphocyte function and thereby prevent tumour cell apoptosis (Movahedi et al., 2008). Unfortunately, in our experimental model the use of SCID mice precludes the analysis T-cell function. However, it is conceivable that neutrophils associated with colon cancer hepatic metastasis would similarly behave in a T-cell suppressive manner and their depletion in the immune-competent setting, may therefore have an even greater effect than that seen here for SCID mice.

Currently, our attempts to demonstrate a similar role for neutrophils in the development of pancreatic metastasis using the Pan02 cell line are at an early stage. However, the data generated from Pan02 tumours demonstrates the propensity of neutrophils to infiltrate hepatic metastases in the presence of a competent immune system. Interestingly, primary pancreatic tumours that show significant neutrophil infiltration are of a prognostically poor histological subtype (Reid et al., 2011), indicating that neutrophils promote pancreatic cancer progression. However, the role of neutrophils in the development of hepatic metastases from pancreatic cancer has not been studied. Furthermore, whilst we have demonstrated that neutrophils infiltrate Pan02 hepatic metastases, it remains to be seen whether neutrophil depletion will inhibit intrahepatic Pan02 growth as it did for the growth of metastatic human colon cancers.

In summary, this Chapter has demonstrated the pro-metastatic effect of neutrophils in the hepatic microenvironment. In the following Chapter, we will present data from experiments designed to determine the tumour-derived chemokines responsible for neutrophil recruitment to the metastatic niche, as well as the mechanisms through which neutrophils promote liver metastasis.

CHAPTER 5: MIF Recruits Pro-angiogenic Neutrophils to the Hepatic Metastatic Microenvironment

5.1 Introduction

5.1.1 Neutrophils in the promotion of tumour angiogenesis

Neutrophils promote metastasis through multiple mechanisms. These include immune suppression (Fridlender et al., 2009), induction of EMT (Liang et al., 2014)(Toh et al., 2011), ECM breakdown (Ardi et al., 2007)(Ardi et al., 2009)(Bekes et al., 2011), stimulation of angiogenesis (Tazzyman et al., 2013) and the promotion of extravasation (Spicer et al., 2012)(Huh et al., 2010b). Our data suggests that neutrophils are important for the early stages of metastasis for some cell lines and universally important later in metastatic growth. It therefore seems plausible to hypothesise that hepatic metastasis-associated neutrophils promote processes such as angiogenesis or ECM regulation, which become important during the growth phase of metastatic development.

Neutrophils have been linked to angiogenesis in a range of tumour types. Several studies have documented an association between the degree of tumour-associated neutrophil infiltration and vessel density (Jablonska et al., 2010)(Lu et al., 2012)(Bald et al., 2014), whilst in primary tumours, neutrophils appear to reside in close proximity to developing blood vessels (Mentzel et al., 2001). Co-injection of neutrophils alongside tumour cells in a subcutaneous implantation model promoted angiogenic growth, possibly due to direct differentiation of immune cells into endothelia (Yang et al., 2004). Furthermore, subcutaneous murine tumours refractory to treatment with anti-vascular endothelial growth factor (anti-VEGF) monoclonal antibodies were highly infiltrated with $CD11b^{+}/Gr1^{+}$ neutrophils (Shojaei et al., 2007). Systemic neutrophil depletion through injection of depleting antibodies delayed tumour growth, whilst

neutrophils isolated from anti-VEGF-refractory tumours expressed higher levels of a range of angiogenic factors relative to neutrophils from anti-VEGF-sensitive tumours (Shojaei et al., 2007), suggesting that tumour-associated neutrophils promote angiogenesis and thereby escape from anti-VEGF treatment. Indeed, neutrophils may be capable of promoting angiogenesis through both direct and indirect means. Direct promotion of angiogenesis involves the expression of neutrophil-derived soluble factors capable of promoting blood vessel growth, whilst indirect mechanisms involve breakdown of the ECM by neutrophil proteases and thereby the release of angiogenic growth factors sequestered within the ECM.

5.1.2 Direct promotion of angiogenesis

VEGF expression has been demonstrated in the circulating neutrophils of healthy volunteers (Kusumanto et al., 2003)(Taichman et al., 1997) and it is upregulated in the neutrophils from patients with inflammatory conditions such as rheumatoid arthritis (Kasama et al., 2000). In a Matrigel sponge angiogenesis assay, CXCL-1-stimulated neutrophils promoted angiogenesis through their expression of VEGF-A (Scapini et al., 2004). Furthermore, TNF-α promoted the expression of VEGF by cultured neutrophils (Webb et al., 1998)(McCourt et al., 1999), whilst the culture supernatant from TNF-α-treated neutrophils stimulated endothelial cell proliferation and tubule formation in an effect that was reversed by the administration of an anti-VEGF antibody (McCourt et al., 1999). In the setting of cancer progression, INF-β inhibited the expression of VEGF by tumour-associated neutrophils recruited to melanoma and fibrosarcoma (Jablonska et al., 2010). In INF-$\beta^{-/-}$ mice, tumour-associated neutrophils expressed high levels of VEGF, whilst tumour-associated neutrophils cultured in the presence of INF-β expressed lower levels of VEGF than control neutrophils. Depletion of neutrophils in INF-$\beta^{-/-}$ mice resulted in smaller, poorly vascularised tumours compared to those developed in INF-$\beta^{-/-}$ mice, providing a direct link between neutrophils and the promotion of tumour angiogenesis (Jablonska et al., 2010). The highly angiogenic factor FGF2 is also expressed by neutrophils. In

an experimental study of hind-limb ischaemia, $Gr1^+$ neutrophils expressing FGF2 infiltrated isachemic muscle, whilst antibody-mediated neutrophil depletion delayed angiogenesis within affected limbs (Tashiro et al., 2012). In this study, although neutrophils clearly promoted angiogenesis, it is not clear whether this result was dependent upon their production of FGF2 or through some other mechanism. Finally, elevated expression of multiple ELR^+ CXC chemokines was demonstrated in tumour-associated neutrophils relative to those from naïve mice (Fridlender et al., 2012). Given the pro-angiogenic role for ELR^+ CXC chemokines (Strieter et al., 1995), it is tempting to propose that neutrophils drive angiogenesis through the production of such factors, however, this remains to be formally demonstrated.

It is therefore evident that neutrophils are directly responsible for the production of angiogenic factors both *in-vitro* and *in-vivo*. Nonetheless, it would be premature to claim that tumour-associated neutrophils promote angiogenesis *in-vivo* through the production of angiogenic molecules. The evidence for neutrophil-derived angiogenic factors in the promotion of angiogenesis - let alone tumour angiogenesis - is limited to a few experimental studies. There has been no analysis of the expression of angiogenic factors by neutrophils from cancer patients and the relative contribution by different cell types within the tumour microenvironment to pro-angiogenic molecule abundance has not been studied. The only studies demonstrating elevated angiogenic factor expression by tumour-associated neutrophils analysed RNA expression (Fridlender et al., 2012)(Shojaei et al., 2007), with no study conclusively demonstrating the expression or secretion of angiogenic proteins by tumour-associated neutrophils. In conclusion, whilst neutrophils may promote vessel formation *in-vivo* through the expression of angiogenic factors (McCourt et al., 1999), the relevance of such findings for tumour biology is unclear.

5.1.3 Indirect promotion of angiogenesis

Upon activation, neutrophils strongly express several proteases, including matrix metalloproteinases (MMPs), heparinases and elastases, all of which are capable of degrading specific extracellular matrix proteins. During wound healing, the expression of such enzymes by activated neutrophils promotes tissue re-modeling (McCarty and Percival, 2013) and has been proposed to stimulate angiogenesis through the release of ECM-bound angiogenic factors (Vlodavsky et al., 1990). Indeed, multiple angiogenic factors are sequestered within the extracellular matrix, allowing for the regulation of angiogenesis through the cleavage of ECM proteins and thereby the release of bound angiogenic factors.

FGF2 is an example of one such pro-angiogenic factor sequestered within the ECM through its ability to bind directly to heparin sulphate glycosaminoglycans (HSGAGs) (Moscatelli, 1987)(Maccarana et al., 1993)(Bashkin et al., 1989). Furthermore, proteolytic enzymes, such as heparinase, modulate the local FGF2 concentration by controlling its release from HSGAGs. This has been demonstrated by *in-vitro* experiments, where ECM derived from corneal endothelial cells is deposited onto culture dishes before denudation of the cell layer. Treatment of the ECM with heparinase or heparitinase promoted the release of FGF2 which was in turn responsible for the promotion of endothelial cell proliferation (Bashkin et al., 1989)(Flaumenhaft et al., 1989). As an extension to this work, the addition of neutrophil-conditioned cell culture supernatant resulted in an increase in the release of bound FGF2 from ECM-coated plates and this effect was reversed by addition of a heparinase inhibitor (Ishai-Michaeli et al., 1990). Thus, neutrophils can indirectly modulate the concentration of available FGF2 through the production of enzymes responsible for ECM degredation. However, although it is possible that neutrophils promote angiogenesis through the action of heparinase on ECM HSGAGs, such a mechanism has not yet been demonstrated for this enzyme using *in-vivo* cancer models.

In similarity to FGF2, various VEGF isoforms (particularly $VEGF_{206}$ and $VEGF_{189}$) bind to HSGAGs and thus become sequestered within the ECM (Houck et al., 1992)(Houck et al., 1991). Furthermore, *in-vitro*, HSGAG-bound VEGF isoforms become soluble through proteolytic cleavage of matrix proteins by heparinase (Houck et al., 1991). Interestingly, both soluble and HSGAG-bound VEGF are biologically active, as both are able to promote endothelial cell proliferation (Park et al., 1993). As well as heparinase, MMPs are capable of modulating the release of ECM-bound VEGF. The action of MMP3 on ECM-bound VEGF resulted in either release of the intact protein or release of VEGF fragments which themselves are pro-angiogenic (Lee et al., 2005). Interestingly, such VEGF fragments promoted capillary dilation in existing tumour vessels, whereas the intact VEGF protein promoted angiogenesis (Lee et al., 2005), indicating that different forms of VEFG lead to different vascular outcomes and that this process is controlled through proteolysis of both the ECM and VEGF.

Importantly, MMP9 expression has been demonstrated in tumour-associated neutrophils from patients with hepatocellular carcinoma (Kuang et al., 2011) and colon cancer (Nielsen et al., 1996) using immunohistochemical staining. Furthermore, tumour-derived chemokines such as macrophage inhibitory factor (MIF) are capable of promoting the expression of MMP9 in neutrophils (Dumitru et al., 2011). Using an *in-vivo* chorioallantoic membrane angiogenesis model, neutrophils were found to promote vessel formation in a manner dependent upon their expression of MMP9 (Ardi et al., 2007). Furthermore, tumour-associated neutrophils recruited to heterotopic fibrosarcoma and prostate carcinomas promoted angiogenesis through the expression of MMP9 (Bekes et al., 2011). Indeed, CXCL8 inhibition reduced the tumour-associated neutrophil infiltrate and in turn delayed tumour angiogenesis in an effect that was reversed by the administration of recombinant MMP9 (Bekes et al., 2011). Nonetheless, in this study, no clear link was made between the expression of

MMP9 by tumour-associated neutrophils and VEGF availability. As such, it is not clear whether the pro-angiogenic effect of MMP9 in this setting is mediated through VEGF availability or alternative mechanisms.

In summary, neutrophils may be capable of promoting angiogenesis through a variety of mechanisms that include both the direct expression of pro-angiogenic factors and their release from sequestration within the ECM. However, the studies conducted to date in this field with relevance to cancer are limited. Given that tumour cells as well as other tumour stroma-associated cell subsets are capable of producing high levels of heparinase, MMP's and various pro-angiogenic factors (Zajac et al., 2013)(Roomi et al., 2009)(Hofmann et al., 2000), it remains to be seen whether neutrophils provide a meaningful contribution to the pool of such factors within the tumour microenvironment. Currently there is no available research evidence demonstrating a link between neutrophil infiltration to hepatic colon cancer metastases and the promotion of angiogenesis.

5.2 Aims

1. To identify potential tumour-derived chemokines responsible for neutrophil recruitment to the hepatic metastatic microenvironment

2. To determine whether neutrophils play a role in the promotion of angiogenesis within the hepatic metastatic microenvionment

5.3 Results

5.3.1 The sera of tumour-bearing SCID mice contain human neutrophil chemoattractants

To determine whether HCT-116, HT29 or LoVo cells express chemokines capable of recruiting neutrophils *in-vivo*, chemokine and cytokine expression was analysed in serum samples from tumour bearing and naïve mice using human-specific protein arrays. Mice with hepatic metastases from all three cell lines demonstrated elevated levels of circulating human neutrophil chemoattractants relative to splenectomised control mice (Fig. 5.1).

Specifically, serum from mice bearing HCT-116, HT29 and LoVo tumours demonstrated elevated levels of human Macrophage Inhibitory Factor (MIF), whilst HCT-116 and LoVo-bearing mice also demonstrated elevated levels of human Midkine (Fig. 5.1). Of note, Midkine has been shown to be capable of neutrophil chemoattraction (Takada et al., 1997), whilst MIF is a non-cognate ligand for $CXCR2^{+}$ monocytes (Bernhagen et al., 2007) and a potent chemoattractant for neutrophils (Dumitru et al., 2011). Mice with LoVo hepatic metastases also demonstrated high levels of CXCL8, a chemokine well known to play a role in the chemoattraction of neutrophils (Yoshimura et al., 1987).

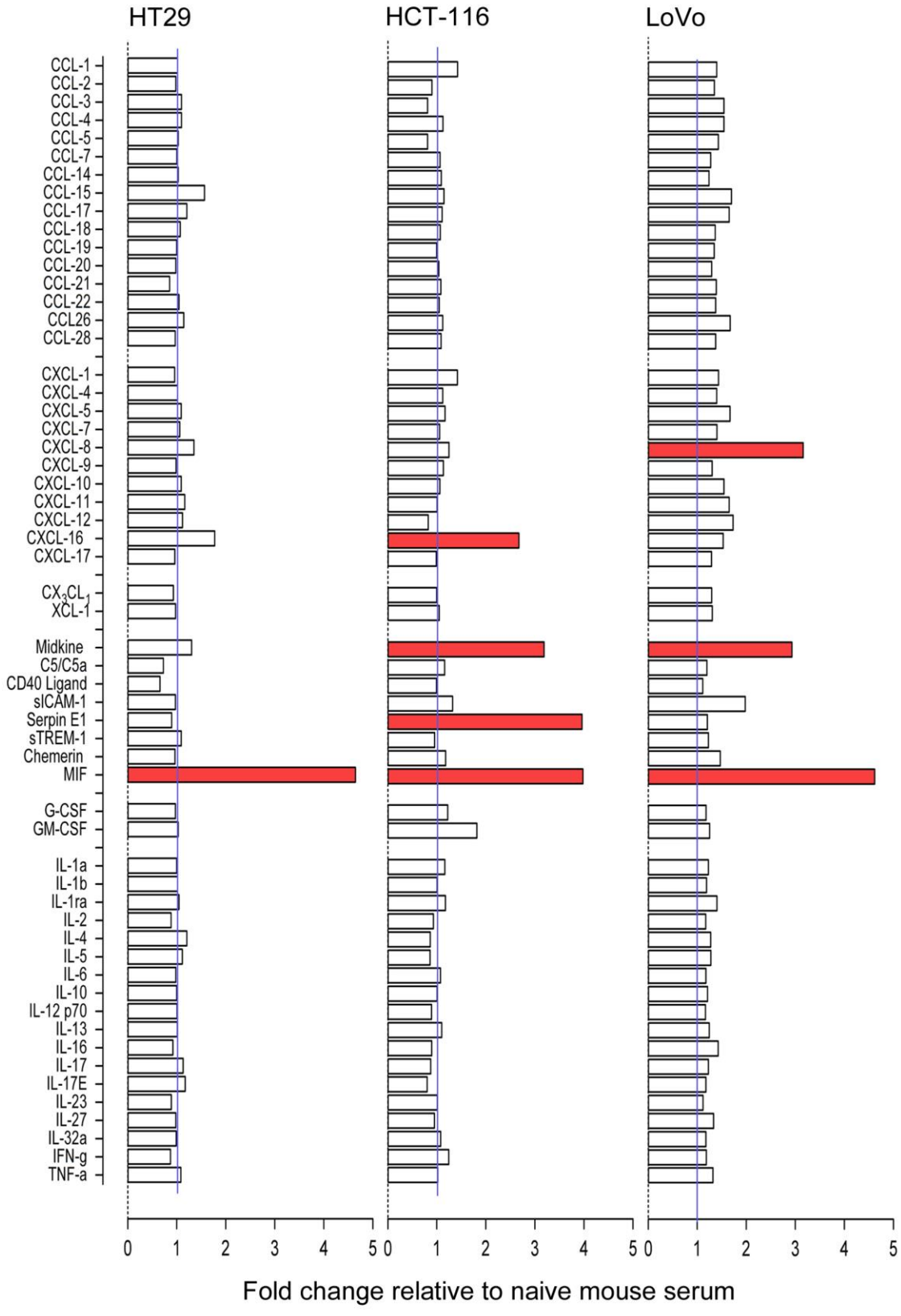

Figure 5.1 Serum from mice with hepatic metastases contains high levels of human MIF

Relative human chemokine levels in the serum of tumour bearing mice. Expression levels are normalised to that of splenectomised, non-tumour-bearing mice (purple line, arbitary value of 1) and those chemokines elevated greater than 2-fold above the value obtained for control mice are shown in red.

Data derived from pooled serum from at least 6 mice per condition.

Given that MIF expression was elevated in mice bearing metastases from all 3 cell lines and that MIF has been linked to the recruitment of neutrophils in the progression of head and neck cancer (Dumitru et al., 2011), we focused our attention on the possible role of this chemokine in neutrophil recruitment to the hepatic metastatic microenvironment. Thus, ELISA was performed to determine the absolute serum concentration of human MIF in naïve mice and those bearing HT29, HCT-116 and LoVo hepatic metastases. As expected, the concentration of serum MIF in mice bearing HT29, HCT-116 and LoVo metastases was significantly elevated when compared to control mice (Fig. 5.2a).

To confirm the ability of MIF to recruit neutrophils, $CD45^{+}/CXCR2^{+}$ bone marrow-derived cells were FACS sorted from SCID mice and their migration assessed in response to increasing concentrations of recombinant MIF. Neutrophils showed a dose-dependent response in migration to increasing MIF concentration (Fig. 5.2b).

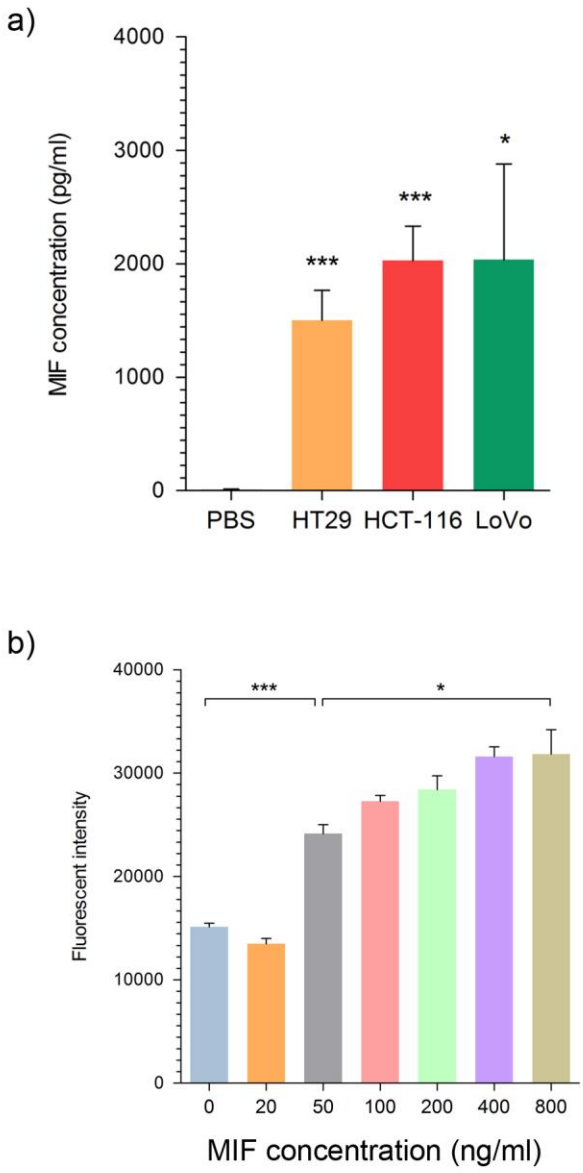

Figure 5.2 MIF is a chemoattractant for CXCR2$^+$ neutrophils and is over-expressed in tumour-bearing mice

a) Mean serum MIF concentration in control (PBS) mice and those bearing HT29, HCT-116 or LoVo hepatic metastases (5-10 mice per group with mice sacrificed at 5 weeks following tumour cell injection).

b) Effect of increasing MIF concentration (X-axis) on the migration of CD45$^+$/CXCR2$^+$ bone marrow cells (where fluorescent intensity is proportional to total migrated cell count).

5.3.2 Inhibition of tumour-derived MIF affects cell apoptosis

We next wished to determine whether MIF was directly involved in the recruitment of neutrophils to the tumour microenvironment. Thus, tumour-derived MIF was inhibited by transfecting HT29^{luc} and LoVo^{luc} cells with a lentivirus containing short hairpin RNA targeting the MIF transcript. Lentiviral transfection resulted in a 10-fold and 3-fold reduction in MIF expression in HT29^{luc} and LoVo^{luc}-conditioned medium respectively, compared to media from cells transfected with an empty vector control lentivirus, indicating successful inhibition of MIF expression (Fig. 5.3a).

Importantly, as well as acting as a chemoattractant, MIF promotes cell survival in an autocrine manner through interaction with p53 (Mitchell et al., 2002). We therefore analysed the effect, of MIF inhibition on apoptosis in both MIF knockdown HT29 and LoVo cell lines, as well as untransfected HT29 cells treated with the MIF inhibitor ISO-1 (Lubetsky et al., 2002). Apoptosis was assessed by staining cultured cells with Annexin V and 7-Amino-Actinomycin (7-AAD). Annexin V binds to cell membrane phospholipid phosphatidylserine molecules which become displayed on the outer leaflet of the plasma membrane during the early stages of apoptosis. During the later stages of apoptosis or in necrotic cells, the plasma membrane becomes permeable to vital dyes such as 7-AAD. Thus early apoptotic cells are Annevin V positive, 7-AAD negative whilst late apoptotic or necrotic cells are Annexin V positive, 7-AAD positive.

As expected, MIF knockdown in both HT29 and LoVo cells promoted apoptosis (Fig. 5.3b and c). Notably, LoVo displayed had a higher percentage of apoptotic cells than the HT29 line, in keeping with the fact that we consistently find that LoVo cells have a longer doubling time and grow slower *in-vivo* than HT29 cells. Whilst MIF inhibition resulted in an increase in both early

and late apoptotic LoVo cells, we only noticed an increase in late apoptotic HT29^{MIFshRNA} cells compared to the HT29$^{lenti\ ctrl}$ cells. The reason for this difference is unclear, however, the data suggests that whatever induced apoptosis in HT29^{MIFshRNA} cells, was not present at the time of analysis (otherwise there would have been an elevation in early apoptotic cells as well), and is therefore unlikely to be related to MIF inhibition, which remains constant throughout the culture process. Interestingly, treatment of HT29 cells with ISO-1 did not appear to promote tumour cell apoptosis, although there was a trend towards increases in both early and late apoptotic cells upon ISO-1 treatment compared to controls (Fig. 5.3b and c).

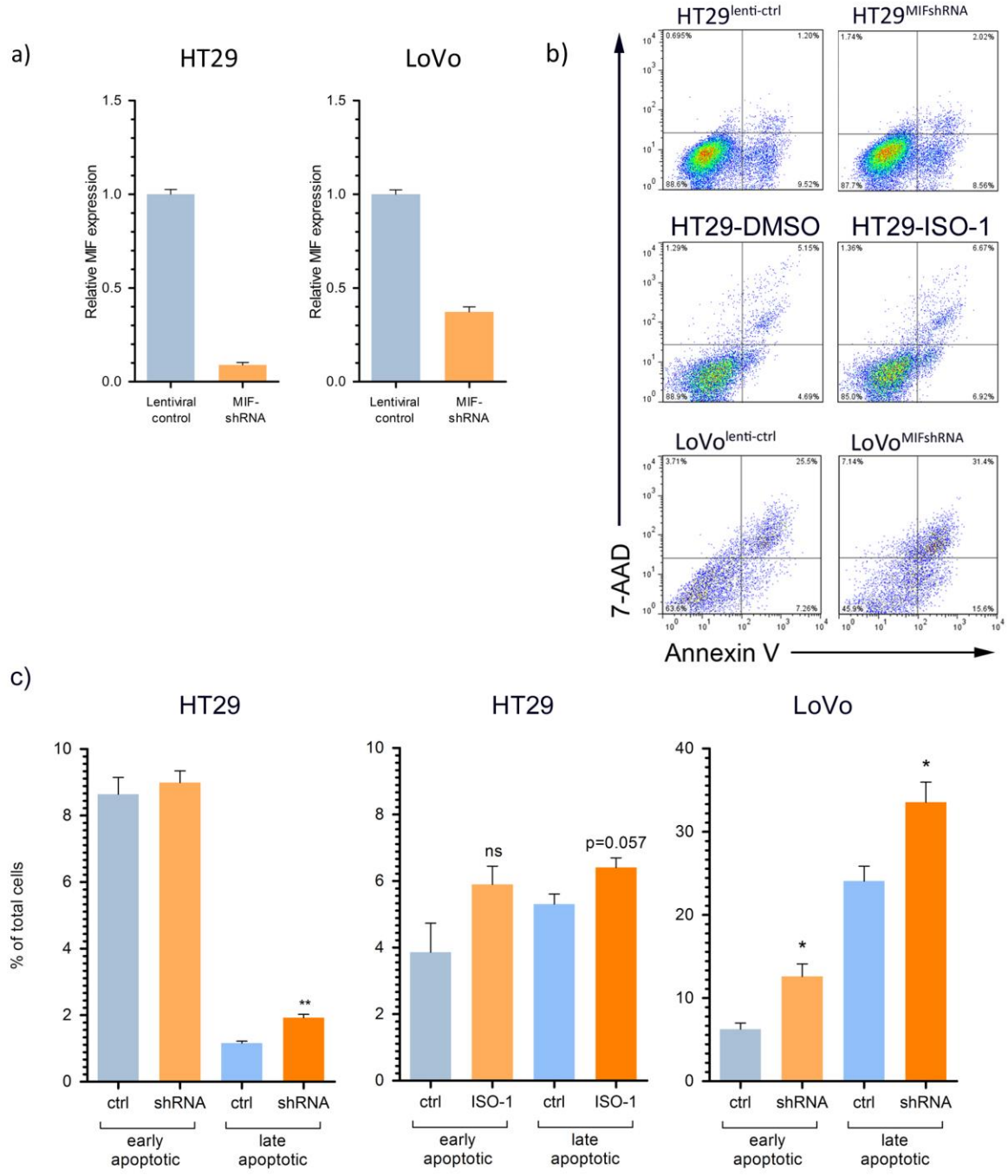

Figure 5.3 *In-vitro* effect of MIF inhibition on HT29 and LoVo cell apoptosis

a) Relative MIF expression in the cell culture supernatant of lentiviral control (blue) and MIF-shRNA (orange) lentiviral transfected HT29 and LoVo cells. Values are normalised to the total protein content of the cell culture supernatant.

b) FACS plots of Annexin V^+ (early apoptotic) and Annexin V^+/7-AAD^+ (late apoptotic) cells in lentiviral control and MIF-shRNA lentiviral transfected HT29 and LoVo cell lines and HT29 cells treated with 100 µM ISO-1 or a DMSO control.

c) Graphical representation of data in (b).

Data presented in (a) and (c) were obtained from triplicate analyses.

5.3.3 MIF inhibition delays metastatic growth in-vivo

We next wished to determine whether inhibition of tumour-derived MIF reduced neutrophil recruitment *in-vivo* and in turn inhibited metastatic growth in the liver. To determine whether this was the case, the ability of the $HT29^{MIFshRNA}$ and $HT29^{lenti\text{-}ctrl}$ cell lines to form hepatic metastases was compared. The $LoVo^{MIFshRNA}$ and $LoVo^{Lenti\text{-}ctrl}$ cell lines were not used for further analysis, as they could not be cultured to sufficient number for *in-vivo* use due to their high degree of apoptosis.

By week 8, mice injected with $HT29^{MIFshRNA}$ cells had significantly reduced hepatic metastases compared with mice injected with the $HT29^{lenti\text{-}ctrl}$ cell line, as determined by *ex-vivo* total hepatic luminescence (Fig. 5.4a,b). Furthermore, the livers of mice bearing $HT29^{MIFshRNA}$ metastases had fewer $CD45^{+}/CXCR2^{+}$ cells than those livers bearing $HT29^{lenti\text{-}ctrl}$ metastases. Although, there was no significant difference in the number of $CD45^{+}/CXCR2^{neg}$ cells between $HT29^{MIFshRNA}$ and $HT29^{lenti\text{-}ctrl}$ metastases (Fig. 5.4c-e), there was a trend towards fewer $CD45^{+}/CXCR2^{neg}$ cells in mice with $HT29^{MIFshRNA}$ tumours, suggesting that MIF inhibition may have had some effect on the recruitment of immune cell types other than neutrophils alone.

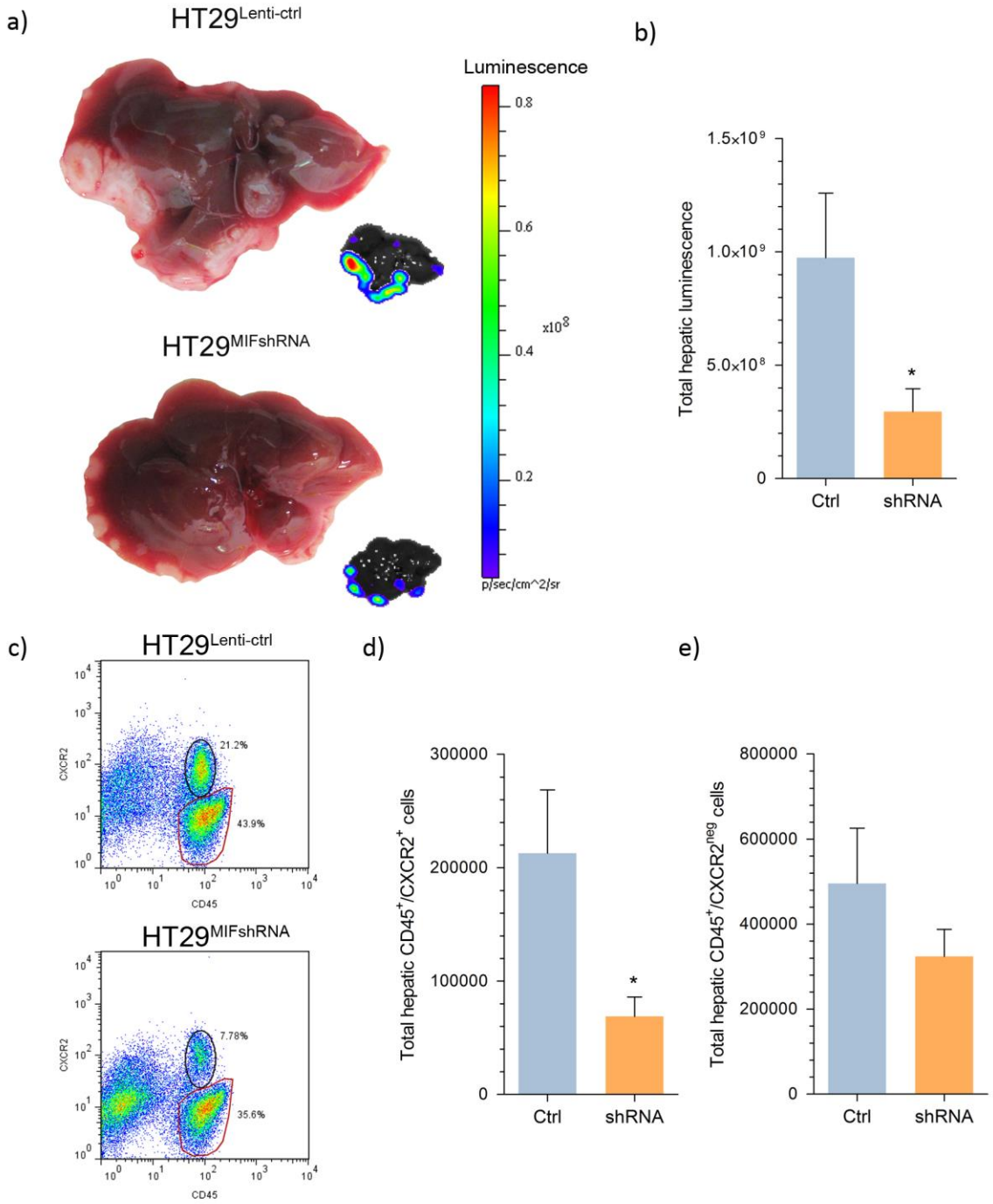

Figure 5.4 Inhibition of tumour-derived MIF delays hepatic metastasis formation

a) SCID mouse livers 8 weeks following intrasplenic injection of HT29$^{\text{Lenti-ctrl}}$ or HT29$^{\text{MIFshRNA}}$ cells.

b) Mean total hepatic luminescence in livers from mice injected with HT29$^{\text{Lenti-ctrl}}$ or HT29$^{\text{MIFshRNA}}$ cells.

c) CD45^{+}/CXCR2^{+} and CD45^{+}/CXCR2$^{\text{neg}}$ cell populations in the livers of mice inoculated with HT29$^{\text{Lenti-ctrl}}$ or HT29$^{\text{MIFshRNA}}$ cells.

d-e) Total hepatic CD45^{+}/CXCR2^{+} and CD45^{+}/CXCR2$^{\text{neg}}$ cell numbers in mice injected with HT29$^{\text{Lenti-ctrl}}$ or HT29$^{\text{MIFshRNA}}$ cells.

Data in (a) and (b) represent results from two experiments each with 6 mice per group. Data in (c), (d) and (e) represent results from two experiments each with 3 mice per group.

Whilst inhibition of MIF using shRNA is a useful proof-of-concept method, pharmacological inhibition of MIF activity is a method of greater clinical applicability. With this in mind, $HT29^{luc}$ tumour-bearing mice were treated with ISO-1 diluted in DMSO, or a concentration-matched DMSO control at day 10 following tumour cell inoculation. In previous work, ISO-1 inhibited the pro-inflammatory activity of MIF through antagonism of the intrinsic tautomerase activity of the chemokine (Lubetsky et al., 2002). ISO-1 also displays potent anti-inflammatory properties, being able to block MIF-driven TNF-α production by lipopolysaccharide-stimulated macrophages (Dabideen et al., 2007) as well as protect mice from the development of sepsis following caecal puncture (Al-Abed et al., 2005). We therefore wished to determine whether ISO-1 was capable of inhibiting tumour-associated neutrophil recruitment *in-vivo* and if so, whether this had an effect on metastatic growth.

By 5 weeks following intrasplenic HT29 injection, mice treated with ISO-1 had significantly reduced hepatic metastasis compared to those treated with the DMSO control (Fig. 5.5a,b). Surprisingly, there was no difference in the total hepatic neutrophil or $CD45^{+}/CXCR2^{neg}$ cell count between treatment groups suggesting that ISO-1 inhibited tumour growth through mechanisms independent of neutrophils recruitment (Fig. 5.5c-e).

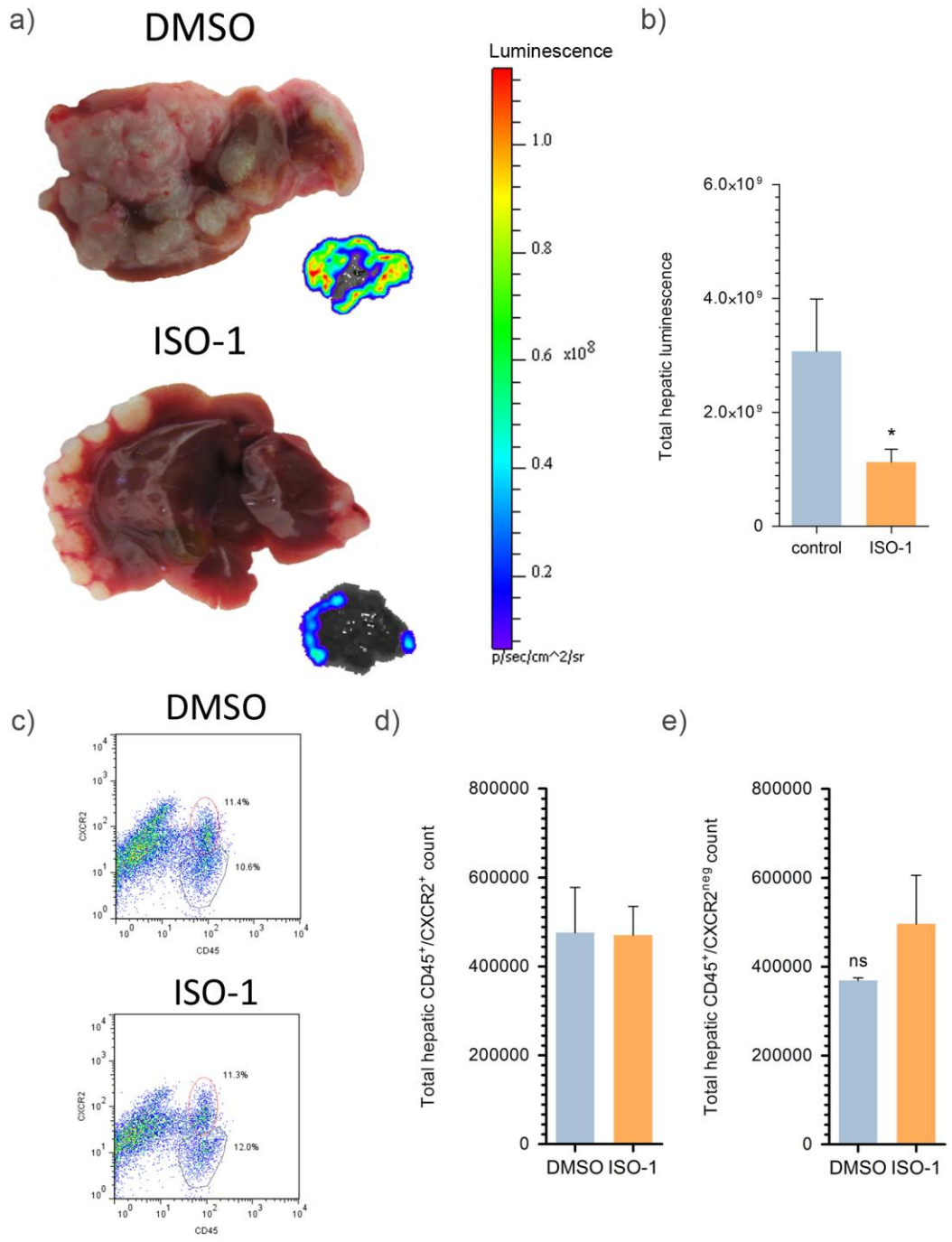

Figure 5.5 Pharmacological inhibition of MIF inhibits metastatic growth without affecting metastasis-asociated neutrophil count

a) HT29 hepatic metastases from mice treated with DMSO control or ISO-1.

b) Mean total hepatic luminescence in HT29 tumour-bearing livers from mice treated with DMSO control or ISO-1.

c) FACS plots from HT29 tumour-bearing mouse livers from mice treated with DMSO control or ISO-1.

d,e) Total hepatic $CD45^+/CXCR2^+$ and $CD45^+/CXCR2^{neg}$ cell numbers in HT29 hepatic metastases from mice treated with DMSO or ISO-1.

Data in (b) represent results from a single experiment of 8-9 mice per group. Data in (c), (d) and (e) represent results from a single experiment with 4 mice per group.

5.3.4 Depletion of neutrophils, or tumour-derived, but not systemic, MIF inhibition reduces metastatic angiogenesis

Given the significant research evidence linking neutrophils to the promotion of angiogenesis, we next questioned whether neutrophils promote vascular development in the hepatic metastatic microenvironment. We first examined whether blood vessel formation was inhibited by neutrophil absence by using our models of HT29 and HCT-116 hepatic metastasis in mice treated with anti-Ly6G or IgG2a. Blood vessels were identified in tissue sections of hepatic metastasis using antibodies targeting CD146 and CD31, both proteins expressed by endothelial cells. For this analysis, tumours from LoVo mice were not studied, as neutrophil depletion in these mice had such a profound effect on metastatic growth that tumours of sufficient size could not be obtained for analysis. Interestingly, for both HT29 and HCT-116 tumours, there was a significant reduction in metastatic vasculature in anti-Ly6G-treated mice compared to those administered IgG2a (Fig. 5.6a-d). A reduction in vascular density was also identified in mice bearing $HT29^{MIFshRNA}$ metastases compared to those with $HT29^{Lenti\text{-}ctrl}$ tumours (Fig. 5-7a and c), however no difference in vascular density was demonstrated for HT29 tumours in mice treated with ISO-1 compared to those administered the DMSO control (Fig. 5.7b and d).

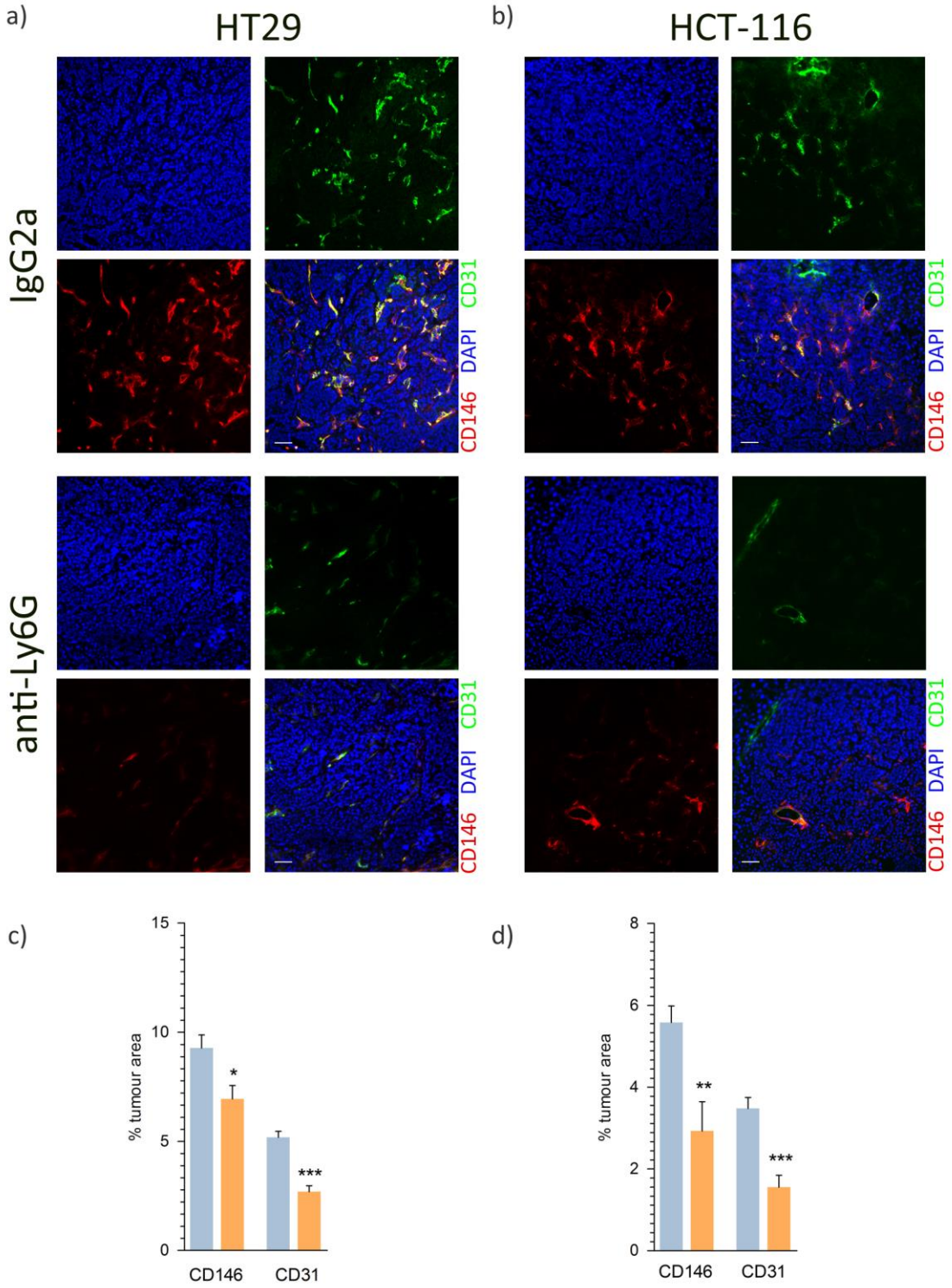

Figure 5.6 Neutrophil depletion is associated with reduced tumour vasculature

a-b) Immunohistochemical staining of HT29 and HCT116 hepatic metastases from IgG2a- or anti-Ly6G-treated mice. Blood vessels are stained with CD146 (red) and CD31 (green).

c-d) Bar graphs showing the percentage of tumour area staining positive for CD146 and CD31 in HT29 (c) and HCT-116 (d) hepatic metastases from IgG2a- and anti-Ly6G-treated mice (blue and orange bars respectively).

Data in (b) represents results from at least 5 metastases within the livers of up to 5 different mice per group.

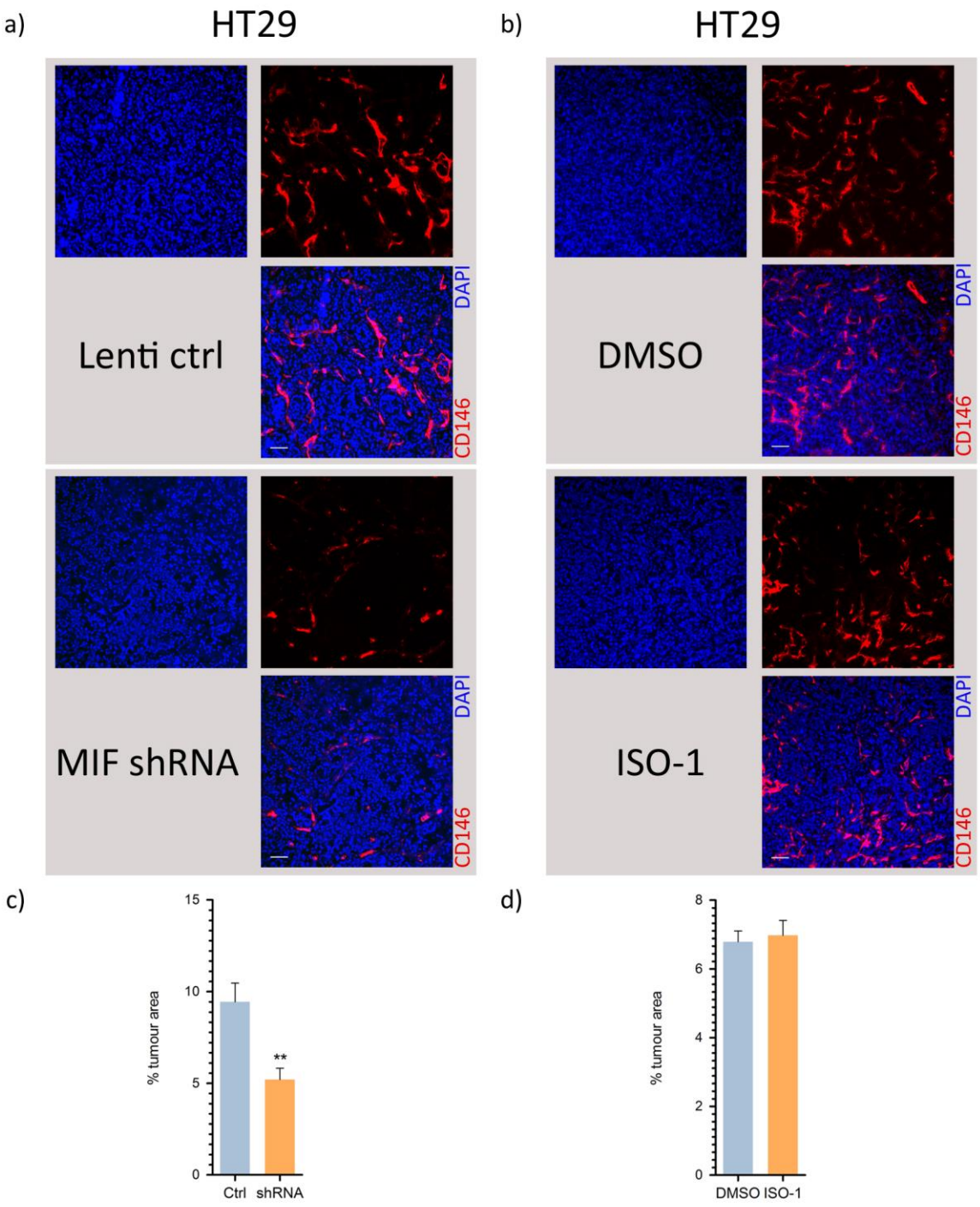

Figure 5.7 Inhibition of tumour-derived but not systemic MIF activity inhibits metastatic angiogenesis

a) HT29$^{\text{lenti ctrl}}$ and HT29$^{\text{MIFshRNA}}$ hepatic metastases stained for CD146^{+} vessels (red) with DAPI counterstaining (blue).

b) HT29 hepatic metastases in mice treated with the DMSO control or MIF inhibitor ISO-1 stained for CD146^{+} vessels (red) and DAPI (blue).

c and d) Quantification of the percentage of tumour areas showing CD146^{+} staining in the conditions stated in (a) and (b) respectively.

Data in (c) and (d) represent results from at least 5 metastases within the livers of up to 5 different mice per group.

5.3.5 Depletion of neutrophils or inhibition of tumour-derived and systemic MIF activity reduces metastatic proliferation

We next sought to determine the effect of neutrophil depletion, or MIF inhibition on the growth kinetics of hepatic metastases *in-vivo*. Proliferative HT29 and HCT-116 tumour cells in liver metastases were detected using antibodies targeting Ki67, a nuclear protein which is present only in actively dividing cells (Gerdes et al., 1984). Strikingly, neutrophil depletion significantly reduced the proportion of $Ki67^{+}$ cells within HT29 and HCT-116 metastases (Fig. 5.8a,b). Furthermore, proliferation was reduced in $HT29^{MIFshRNA}$ metastases compared to those developed using the $HT29^{Lenti\text{-}ctrl}$ cell line (Fig. 5.8c) and was also reduced in HT29 metastases from ISO-1-treated mice compared to those administered the DMSO control (Fig. 5.8d).

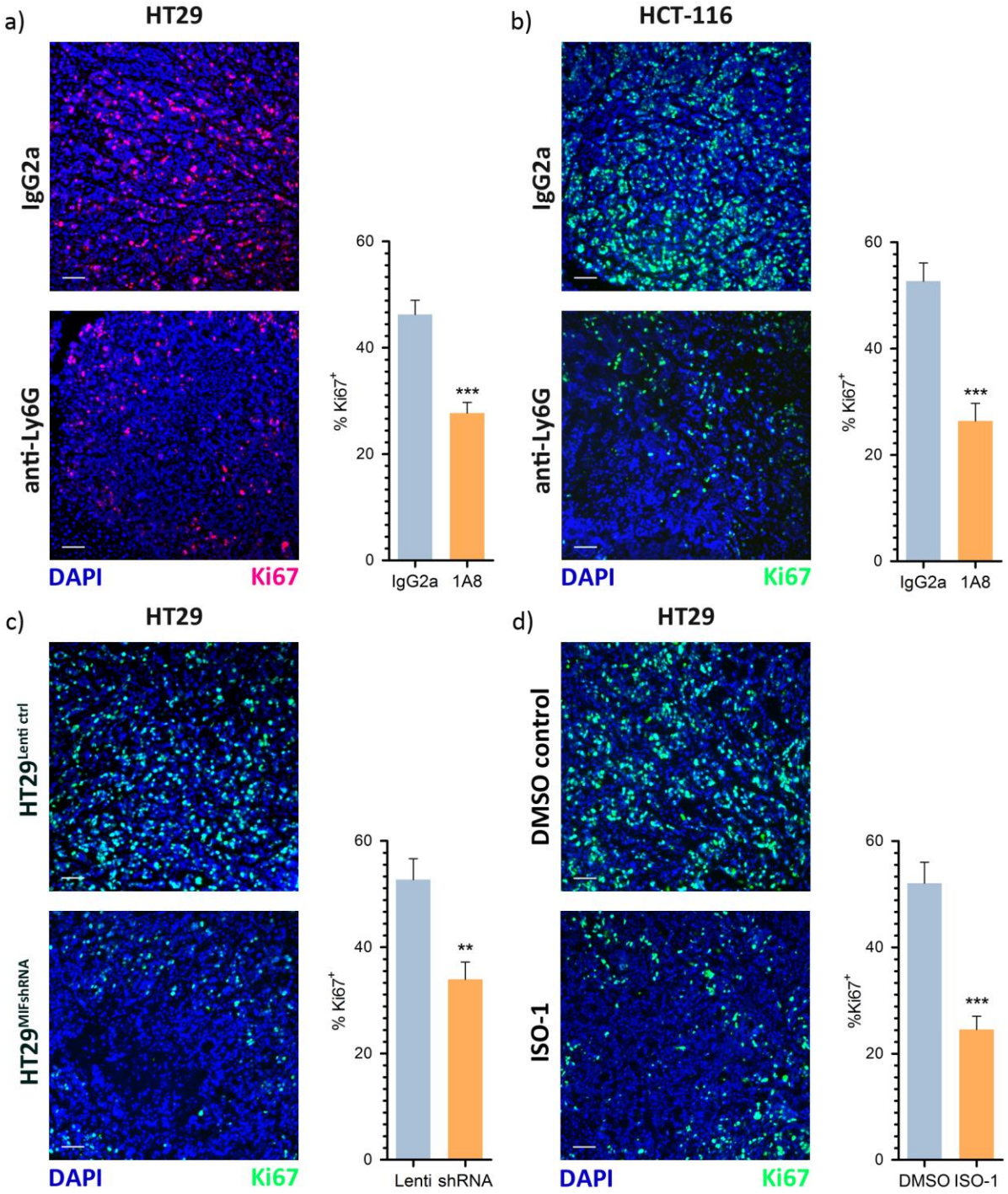

Figure 5.8 Neutrophil depletion and MIF inhibition decrease metastatic proliferation

a) HT29 metastases from IgG2a or anti-Ly6G treated mice stained with Ki67 (red) and couterstained with DAPI. Accompanying bar graph demonstrates results from multuiple tumours in several mice.

b) As for (a) but showing results for HCT-116 hepatic metastases with $Ki67^{+}$ cells in green.

c) As for (b) but showing results for mice injected with $HT29^{lenti\ ctrl}$ or $HT29^{MIFshRNA}$ cell lines.

d) As for (b) but showing results for HT29 tumour-bearing mice treated with DMSO or ISO-1.

Data presented in bar graphs represent the analysis of at least 5 tumours in up to 5 mice per group.

5.3.6 Inhibition of tumour-derived MIF, or systemic MIF inhibition has no effect on metastatic apoptosis

Next, the effect of tumour-derived and systemic MIF inhibition on apoptosis *in-vivo* was determined by immunohistochemical analysis of hepatic metastases from $HT29^{MIFshRNA}$, $HT29^{Lenti\ ctrl}$, or untransfected HT29 cells treated with ISO-1 or the DMSO control. Here, an immunofluorescence system was used to detect apoptotic cells by labeling and detection of DNA double strand breaks using the Terminal deoxynucleotidyle transferase dUTP Nick-End Labeling (TUNEL) method. In keeping with the findings for cultured cells, we found that MIF inhibition had no effect on the degree of apoptosis within metastatic deposits in either the MIFshRNA or ISO-1 experiments (Fig. 5.9). The effect of neutrophil depletion on intra-tumoural apoptosis has not yet been analysed.

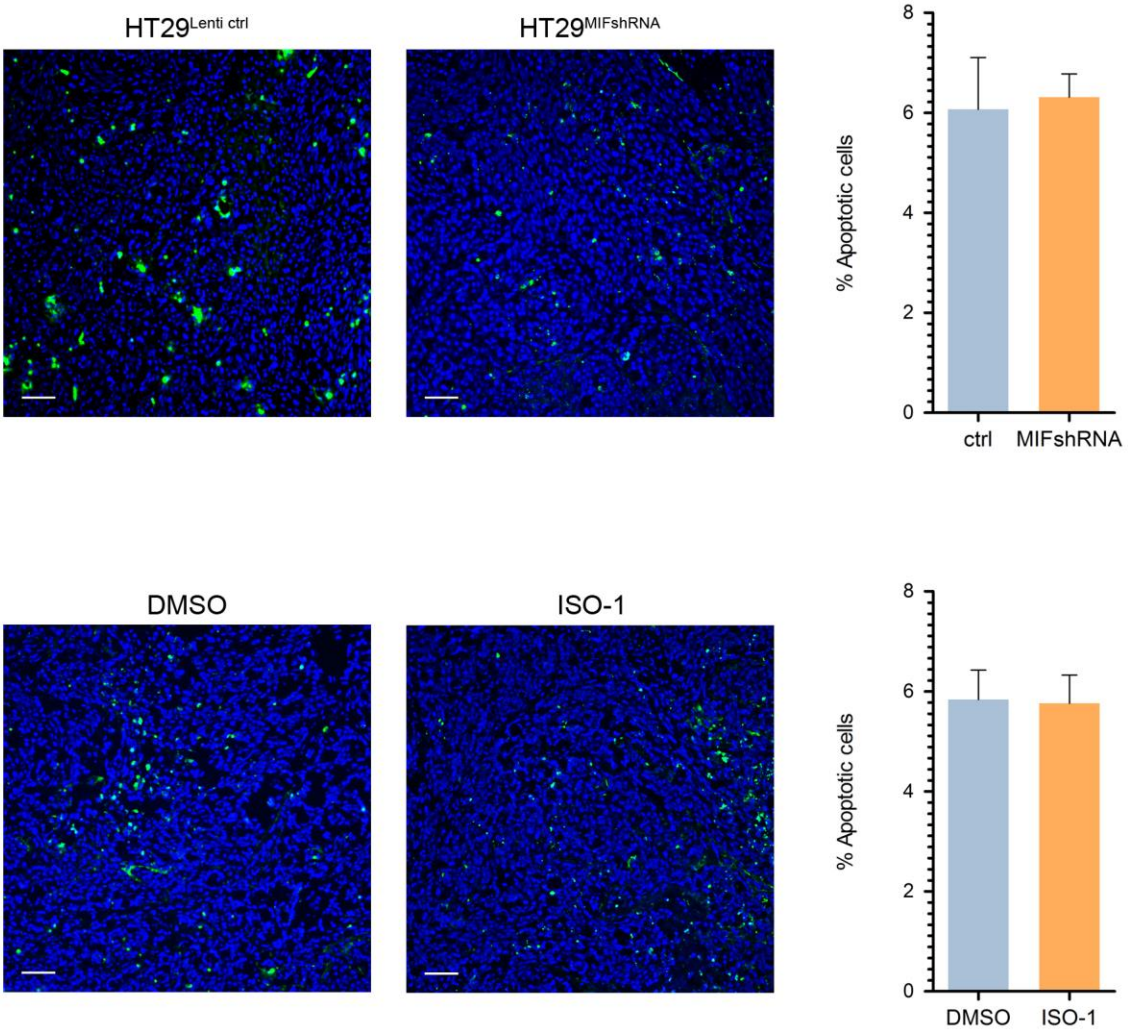

Figure 5.9 Effect of MIF inhibition on apoptosis rate in hepatic metastases

a) HT29$^{\text{Lenti ctrl}}$ and HT29$^{\text{MIFshRNA}}$ metastases stained with digoxigenin (green) to label apoptotic cells and couterstained with DAPI (blue). Accompanying bar graph demonstrates results from multiple tumours in several mice.

b) As for (a) but showing results for HT29 hepatic metastases treated with either DMSO alone or ISO-1 diluted in DMSO.

Data presented in bar graphs represent the analysis of at least 5 tumours in at least 3 mice per group.

5.3.7 Neutrophils are associated with tumour blood vessels and express pro-angiogenic factors

We had previously noted that both tumour blood vessels and neutrophils were present within channels formed between islands of metastatic colon cancer cells (Fig. 4.2 and 5.6a). Therefore, we next performed co-staining of CD146 and Ly6G in HT29, HCT-116 and LoVo hepatic metastases to determine the spatial relationship between developing tumour blood vessels and tumour-associated neutrophils. Interestingly, in numerous metastatic regions, neutrophils were found in close association with tumour blood vessels for all cell lines studied (Fig. 5.10a).

We next compared the mRNA expression of various angiogenic growth factors in $CD45^+/CXCR2^+$ neutrophils FACS sorted from the livers of naïve mice, to those from HT29, HCT-116 or LoVo hepatic metastases (Fig. 5.10b). Of note, various pro-angiogenic, secreted factors were commonly upregulated in tumour-associated neutrophils relative to those from naïve mice. Specifically, fibroblast growth factor-2 (FGF2), fibronectin and serine protease inhibitor E1 (SerpinE1) were upregulated at least 10-fold, in neutrophils from the hepatic metastases of all three cell lines relative to those from naïve livers. Multiple factors were upregulated to a lesser extent (at least 2-fold) in tumour-associated neutrophils, including angiopoietin-2, angiopoietin-like 3 and 4, granulin, heparanase, midkine, SerpinC1, SerpinF1, and TIMP- 3 (Fig. 5.9b).

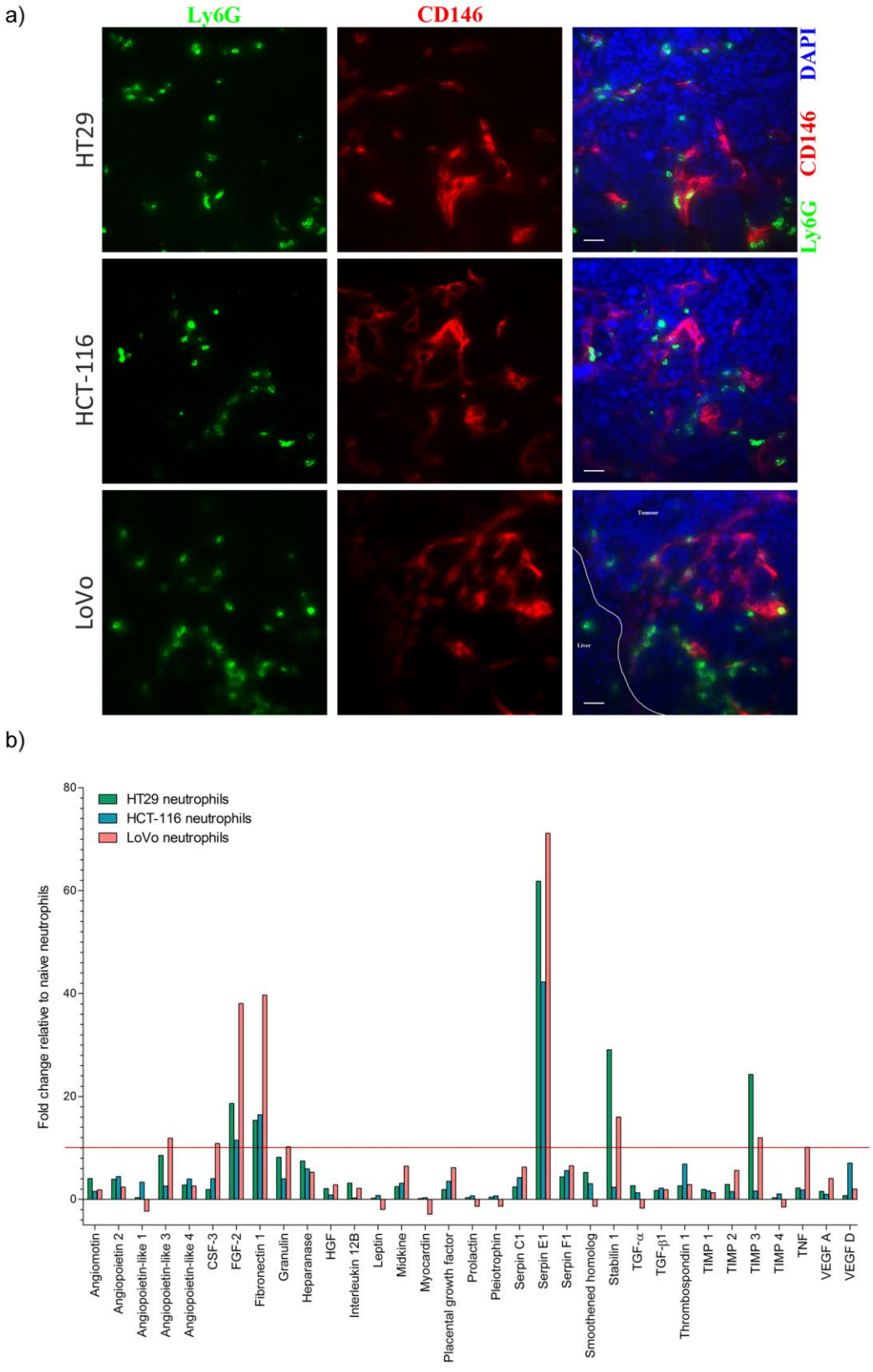

Figure 5.10 Tumour-associated neutrophils are are located near tumour vasculature and express pro-angiogenic factors

a) Immunohistochemical staining of neutrophils detected using anti-Ly6G (green) and vessels using anti-CD146 (red) in HT29, HCT-116 and LoVo hepatic metastases counterstained with DAPI

b) Gene array showing the fold change in angiogenic growth factor expression (RNA) in neutrophils FACS sorted from HT29, HCT-116 and LoVo hepatic metastases relative to those from naive mice. The red horizontal line indicates a 10 fold change for reference.

5.3.8 Patterns of FGF2 and Ly6G expression in murine hepatic metastasis

To confirm the gene array data demonstrating increased transcription of FGF2 in tumour-associated neutrophils relative to those from naïve liver and validate its expression at the protein level, immunohistochemical staining for FGF2 and Ly6G (neutrophils) was performed in HT29, HCT-116 and LoVo tumour-bearing and normal livers. Example images taken from this experiment are shown in figure 5.11 to demonstrate the various staining patterns identified. For each cell line, all of the staining patterns demonstrated in figure 5.11 were seen, although for simplicity, only a single example of each staining pattern is shown.

Ly6G positive neutrophils were seen in normal liver (Fig. 5.11a), however these cells were FGF2 negative, indicating that naïve neutrophils express very little FGF2. In contrast, we saw co-localisation of FGF2 and Ly6G in tumour tissues (Fig. 5.11b-d), indicating that tumour-associated neutrophils strongly express the FGF2 protein. Various patterns of FGF2 staining were seen in tumour-bearing livers. In regions of low tumour cell density, suggesting recent or active cell death (Fig. 5.11b), neutrophils strongly positive for FGF2 were seen, however no FGF could be seen in the ECM. Furthermore, in such areas, FGF2 expression was only seen in Ly6G positive cells, indicating that here, neutrophils are the primary source of FGF2 production within the tumour microenvironment. In more organised areas of metastasis without evidence of cell death (Fig. 5.11c and d), FGF2 positive neutrophils appeared within a mesh-work of FGF2 expression, which was present between islands of tumour cells in a pattern reminiscent of that seen for tumour-associated blood vessels (Fig 5.6a and b). This suggests that in such regions of the tumour FGF2 has been deposited in the ECM, potentially by FGF2-expressing neutrophils. Finally, in highly organised areas of metastasis (Fig. 5.11e), there were small areas of FGF2 positive staining lining islands of tumour cells, however neutrophils were not present.

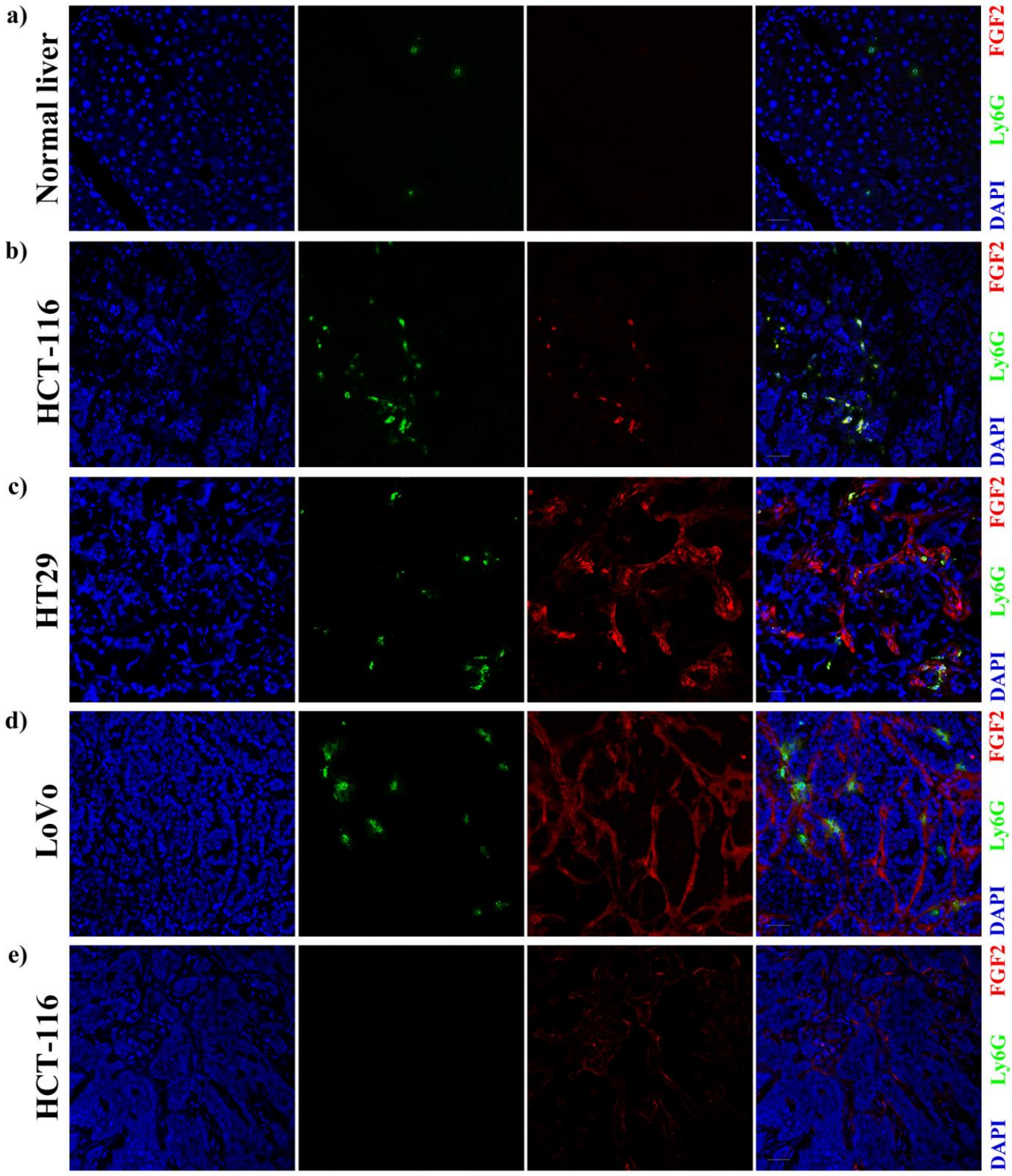

Figure 5.11 Patterns of FGF2 expression in hepatic metastases

Representative images from normal liver (a) and liver bearing hepatic metastases (b-e). Neutrophils are stained with anti-Ly6G (green), anti-FGF2 (red) and counterstaining with DAPI (blue).

For a detailed description of the findings presented in this figure see the text of section 5.3.8.

5.3.9 MIF is upregulated in patients with hepatic metastases

Elevated MIF expression has been demonstrated in patients with colon cancer relative to healthy controls and those patients with colonic adenoma (He et al., 2009)(Shkolnik et al., 1987), however, the relationship between MIF expression and hepatic metastasis formation in patients has not yet been studied. ELISA analysis of MIF expression in healthy volunteers, patients with primary colon cancer and those with hepatic metastasis demonstrated a step-wise increase in MIF expression with advancing disease (Fig. 5.12a). Furthermore, high MIF expression was demonstrated in hepatic colon cancer metastases compared to adjacent normal liver, with MIF expression detectable in 89% of 19 hepatic metastasis tissues studied (Fig. 5.12b). Interestingly, hepatic metastases also contained a significantly greater number of neutrophils compared to surrounding normal liver (Fig. 5.12c and d).

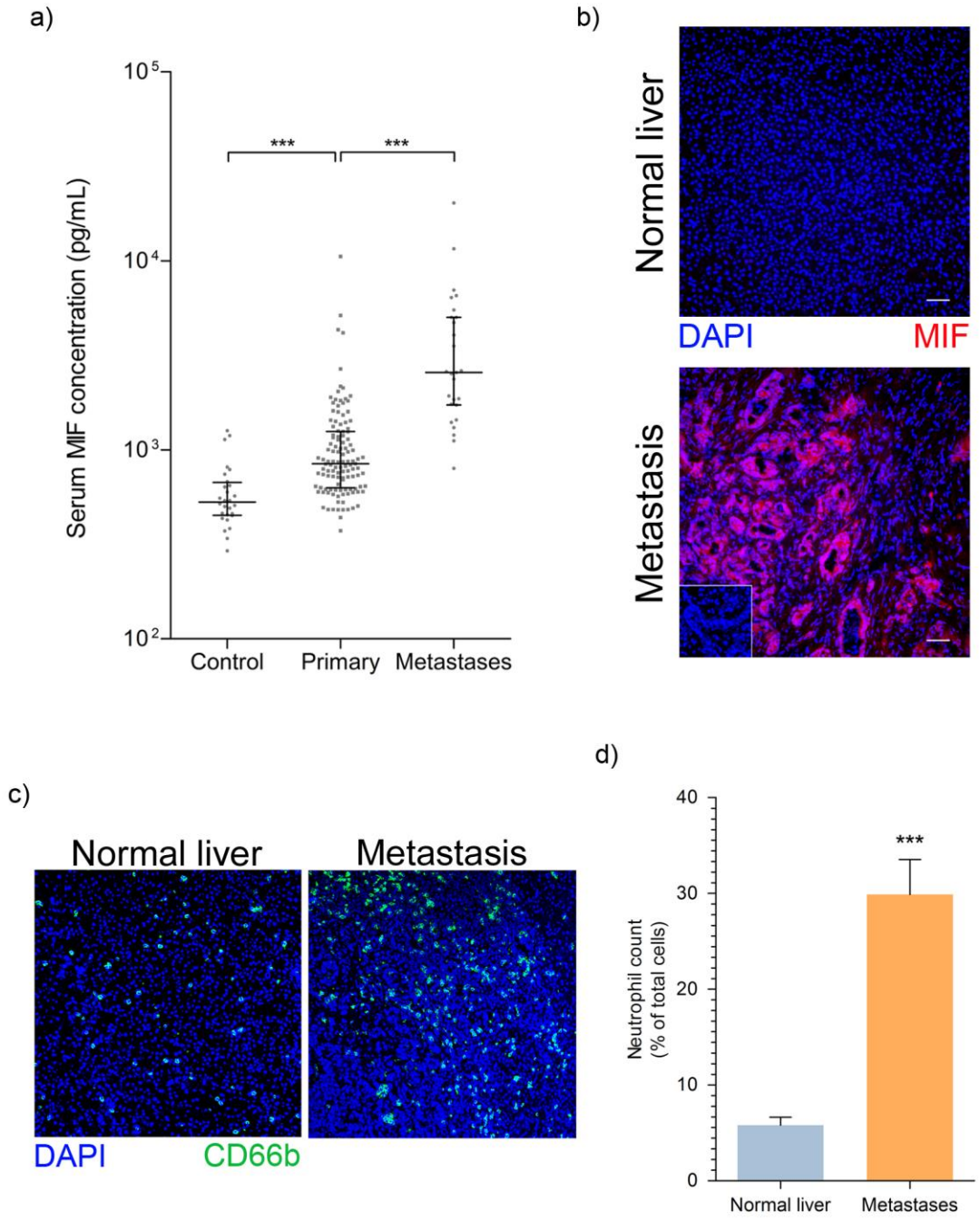

Figure 5.12 MIF expression and the presence of neutrophils in human hepatic metastases

a) Serum MIF concentration in 28 healthy control patients, 119 patients with primary colon cancer and 27 patients with colorectal hepatic metastases.

b) MIF expression in normal liver (top) adjacent to hepatic metastatic deposit (bottom) with isotype control (inset).

c) Neutrophils ($CD66b^+$ cells) identified in hepatic colorectal cancer metastases and adjacent normal liver.

d) Quantification of neutrophil count (as in (c)) in hepatic colorectal metastases and adjacent normal liver as determined by immunohistochemical staining.

In (a), median values and interquartile range are presented. P-values were determined using the Mann-Whitney U test. Data in (d) represents the analysis of at least 4 tumour areas in tissues taken from 10 patients per group.

5.4 Discussion

5.4.1 The role played by MIF in the recruitment of tumour-associated neutrophils

In this Chapter, we have demonstrated elevated expression of multiple human neutrophil chemoattractants in the serum of tumour-bearing mice relative to that from naïve animals. This indicates that the recruitment of neutrophils to the tumour microenvironment is an important feature of hepatic metastasis formation, a notion supported by the profound inhibitory effect of neutrophil depletion on metastatic growth (Chapter 4).

An indication that MIF is responsible for neutrophil recruitment by the colon cancer cell lines studied here comes from the observation that the livers bearing metastases from cell lines expressing high levels of MIF (HCT-116 and LoVo) contained a greater number of neutrophils than livers bearing metastases from cell lines expressing lower MIF levels (HT29) (c.f. Figs 4.4b and 5.2a). It is also notable that both LoVo and HCT-116 tumour-bearing mouse serum demonstrated elevated levels of various other neutrophil chemoattractants and so the elevated hepatic neutrophil count seen in association with hepatic metastases from these cell lines relative to HT29 metastases may result from the effect of chemokines other than MIF.

Nonetheless, the role played by MIF in the recruitment of neutrophils to HT29 hepatic metastases is clearly demonstrated, as tumour-specific MIF inhibition using MIFshRNA in HT29 cells, significantly reduced hepatic neutrophil infiltration. Notably, the effect of tumour-derived MIF inhibition was only tested in the HT29 cell line, as this was the only line that did not undergo significant apoptosis following lentiviral transfection. Given that other neutrophil chemoattractants were found in the serum of mice bearing LoVo and HCT-116 metastases (Fig.

5.1), it is possible that these tumours are capable of recruiting neutrophils even in the absence of MIF.

Interestingly, although MIF has been clearly demonstrated to act as a non-cognate ligand for CXCR2 (Bernhagen et al., 2007), only recently has its expression been linked to the recruitment of neutrophils in pathological settings such as cancer and inflammatory arthritis (Dumitru et al., 2011)(Santos et al., 2011). Furthermore, the study by Dumitru *et al*., did not include *in-vivo* work, relying instead solely on *in-vitro* analysis of the effect of MIF on neutrophil migration, as well as a correlative analysis of MIF expression and $CD66b^{+}$ neutrophil count in tissues taken from patients with head and neck cancer (Dumitru et al., 2011). Thus, ours are the first experiments linking MIF expression by cancer cell lines to the recruitment of pro-metastatic neutrophils. As such, we have demonstrated a previously unidentified mechanism through which MIF may promote hepatic metastasis formation.

5.4.2 Alternative roles for MIF in the hepatic metastatic microenvironment

Aside from chemotaxis, MIF has been demonstrated to possess other biological functions of potential importance to the progression of cancer. MIF inhibits the activity of p53 (Hudson et al., 1999), a protein that plays a key role in the induction of apoptosis in cells harboring DNA damage or oncogenic mutation (Lane, 1992). Indeed, treatment of both macrophages and fibroblasts with MIF overcame p53-dependent apoptosis, whilst MIF treatment bypassed p53-mediated growth arrest through the interference of p53-dependent transcription, as indicated by a reduction in p53 transcriptional targets p21 and Bax (Hudson et al., 1999). In support of these findings, cultured fibroblasts from $MIF^{-/-}$ mice displayed increased sensitivity to contact inhibition, entering a state of senescence sooner than fibroblasts from wild-type mice (Fingerle-Rowson et al., 2003)(Petrenko et al., 2003). This effect was

reversed upon simultaneous knockout of p53 in $MIF^{-/-}$ fibroblasts, directly implicating p53 in the inhibition of cell growth in $MIF^{-/-}$ cells. Finally, chemically induced fibrosarcomas in wild-type mice grew faster and with greater mitoses than those in $MIF^{-/-}$ mice (Fingerle-Rowson et al., 2003), indicating a direct link between MIF expression and tumour cell proliferation.

Interestingly, MIF also prevents apoptosis in cells by promoting the expression of oncogenes such as *ras* and *myc*, in a pathway involving members of the E2F protein family rather than p53 (Petrenko et al., 2003). Thus, *ras* and *myc* mutant cells co-expressing mutant p53 entered a state of growth arrest upon MIF inhibition, whilst those expressing wild-type p53 became apoptotic (Petrenko et al., 2003). This indicates that MIF's suppression of apoptosis in tumour cells, as well as in non-immortalised cells is p53 dependent.

Interestingly, $LoVo^{MIFshRNA}$ cells demonstrated an increase in the number of both early and late apoptotic cells relative to $LoVo^{Lenti\ ctrl}$ cells. Similarly, it proved impossible to culture $HCT\text{-}116^{MIFshRNA}$ cells, as although $HCT\text{-}116^{Lenti\ ctrl}$ cells were sufficiently resistant to the selection antibiotic, addition of a matched antibiotic concentration to the media of $HCT\text{-}116^{MIFshRNA}$ transfected cells resulted in rapid cell death, indicating that this cell line may be more sensitive to MIF inhibition. Both LoVo and HCT-116 cell lines are p53 wild-type, whereas HT29 – a cell line that did not appear to undergo significant apoptosis in response to MIF inhibition – is p53 mutant (Gayet et al., 2001)(Cottu et al., 1996). The *in-vitro* findings are further supported by the analysis of mouse livers following $HT29^{MIFshRNA}$ or $HT29^{Lenti\ ctrl}$ cell line injection; hepatic metastases from these cells demonstrated no difference in apoptosis, with similar findings for ISO-1 and DMSO-treated animals bearing HT29 hepatic metastases. It appears that HT29 cells may therefore be relatively protected from apoptosis caused by MIF inhibition due to their mutant p53 status, whereas this is not the case for LoVo or HCT116 cells. Our data is therefore

in keeping with the aforementioned studies demonstrating a relationship between the functions of MIF and p53.

MIF has also been demonstrated to promote the proliferation of a variety of cell types, through multiple means including activation of the ERK and STAT pathways (Ohta et al., 2012)(Lue et al., 2007). Furthermore, inhibition of endogenous MIF expression through lentiviral knockdown and exogenous MIF activity by ISO-1 treatment inhibited the proliferation of neural stem cells (Ohta et al., 2012), lung epithelia (Marsh et al., 2009), glioblastoma (Piette et al., 2009) and prostate cancer cells (Meyer-Siegler et al., 2006). We have yet to analyse the possible anti-proliferative effect of MIF inhibition *in-vitro*. However, both $HT29^{MIFshRNA}$ and ISO-1-treated HT29 metastases displayed a significant reduction in proliferation when compared with $HT29^{Lenti\ ctrl}$ or HT29-DMSO-treated metastases respectively, indicating that MIF may also promote the proliferation of tumour cells in the hepatic microenvironment.

Importantly, exogenous MIF activates cell signaling pathways involved in proliferation through interaction with the cell surface molecule CD74 (Lue et al., 2006), rather than through the CXC chemokine receptors responsible for its chemotactic activity. ISO-1, the small molecule inhibitor of MIF used in our experiments has been extensively reported in the research literature. It antagonises the intrinsic tautomerase activity of MIF and in doing so inhibits TNF secretion from macrophages and increases murine survival in sepsis models such as caecal ligation and puncture (Al-Abed et al., 2005)(Dabideen et al., 2007). Nonetheless, it is not clear whether ISO-1 inhibits the chemotactic activity of MIF for neutrophils. Interestingly, a recent analysis of several novel MIF inhibitors – the majority of which inhibited MIF tautomerase activity – demonstrated that all inhibitors produced a negative effect on cellular proliferation, however, only one of the molecules simultaneously inhibited the chemotactic effect of MIF

(Ouertatani-Sakouhi et al., 2010). Thus, MIF inhibitors may show selectivity with regards to the specific MIF function that they inhibit. In keeping with this observation, our data indicates that ISO-1 blocked MIF-dependent proliferation, but failed to inhibit chemotaxis of neutrophils to the metastatic niche, as HT29 tumours in ISO-1-treated mice displayed a similar neutrophil infiltrate to those treated with the DMSO control, despite significantly more proliferative tumour cells in the later.

5.4.3 A role for neutrophils in the promotion of hepatic metastatic angiogenesis

Several lines of evidence presented here link tumour-associated neutrophils to the promotion of metastatic angiogenesis. Initially, we identified a significant reduction in the percentage of tumour area staining positive for the vascular markers CD31 and CD146 in neutrophil-depleted HT29 and HCT-116 metastases compared to metastases in control mice. This indicates that blood vessel density is reduced in neutrophil-depleted tumours and that neutrophils may therefore contribute to angiogenesis in this setting. Strikingly, vasculature was also reduced in $HT29^{MIFshRNA}$ compared to $HT29^{Lenti\ ctrl}$ tumours, in keeping with reduced neutrophil infiltration in the former, whilst in ISO-1-treated HT29 tumours (which showed no reduction in neutrophil infiltration), there was no change in metastatic blood vessel density compared to mice given the DMSO control. Interestingly, HT29 and HCT-116 metastases devoid of neutrophils demonstrated reduced proliferation compared to metastases developed in control mice. This may be an indirect consequence of reduced tumour angiogenesis in the former, or because tumour-associated neutrophils have a direct growth promoting effect on tumour cells.

The research by others has demonstrated altered gene expression in neutrophils taken from the tumour microenvironment relative to those from normal tissue (Fridlender et al.,

2012)(Shojaei et al., 2007). We also performed gene expression analysis in naïve and tumour-associated neutrophils, but limited our analysis to genes involved in the regulation of blood vessel growth, given that neutrophil depletion inhibited tumour blood vessel formation and that tumour-associated neutrophils were found in close proximity to tumour blood vessels. Fascinatingly, neutrophils associated with hepatic metastases from all cell lines studied displayed elevated expression of several genes whose protein products have previously been shown to be involved in the promotion of angiogenesis relative to neutrophils from naïve mice.

One of the most highly up-regulated genes demonstrated in tumour-associated neutrophils was FGF2. The FGF2 protein is directly mitogenic for endothelial cells *in-vitro* (D'Amore and Smith, 1993), as well as being capable of promoting tumour vascularisation through synergistic activity with both platelet-derived growth factor (PDGF) (Cao et al., 2003)(Nissen et al., 2007) and VEGF (Asahara et al., 1995)(Kano et al., 2005). Interestingly, the murine FGF2 protein exists as three isoforms of varying molecular weight (18, 22 and 22.5 kD), with the smallest isoform being the only secreted form and therefore the only one capable of promoting angiogenesis (Liao et al., 2009). FGF2 signaling requires that FGF2 molecules bound to HSGAGs make contact with FGF-receptors, enabling receptor dimerisation with resultant trans-phosphorylation of intracellular tyrosine kinase domains and thereby signal transduction (Spivak-Kroizman et al., 1994)(Plotnikov et al., 1999). The binding of FGF2 to HSGAGs and thereby its deposition within the ECM are thus important for the pro-angiogenic function of FGF2.

Importantly, we have confirmed the presence of FGF2 expression at the protein level in tumour-associated neutrophils through immunohistochemical staining. Fascinatingly, we were also able to identify various patterns of FGF2 staining in relation to the presence of tumour-

associated neutrophils. It is difficult to draw any clear conclusions from the immunohistochemical analysis of hepatic metastasis tissues taken at a single time-point in the evolution of metastatic development. However, our data points to a specific sequence of events whereby neutrophils – recruited to the tumour in response to MIF – promote angiogenesis through deposition of FGF2 within the ECM. Thus, the immunohistochemistry images presented in figure 5.11 suggest that FGF2-expressing neutrophils may be preferentially recruited to sites of tumour cell death, as they appear at high frequency in such regions (Fig. 5.11b), as opposed to in regions where there is no evidence of cell death (Fig. 5.11e). We speculate that this may result from the release of inflammatory and perhaps hypoxic mediators in the wake of tumour cell death or hypoxia. Indeed, colon cancer cells grown in chronic hypoxic conditions express high levels of MIF (Yao et al., 2005) and it is therefore possible that the recruitment of FGF2-expressing neutrophils to the tumour microenvironment is directly linked to the expression of MIF by hypoxic tumour cells.

As well as demonstrating significant FGF2 expression within tumour-associated neutrophils, our immunohistochemical analysis showed that FGF2 is also expressed in a network pattern throughout tumours (Fig. 5.11c and d). Although we are yet to perform immunolabeling for CD31 and FGF2 concurrently, the FGF2 network is in a similar position within the tumour microenvironment to both developing blood vessels and ECM proteins such as collagen IV and laminin αV (my unpublished work from another project, Supplementary Fig. 1). This staining pattern has been previously demonstrated in studies of various epithelial tissues, which show FGF2 deposition within the basement membrane of the normal intestine, kidney and skin (Gonzalez et al., 1990) as well as that of blood vessels (Cordon-Cardo et al., 1990). In our study, FGF2 positive neutrophils were demonstrated within these FGF2 networks and neutrophils were also demonstrated in regions of developing tumour vasculature (Fig. 5.10a). Considering these findings together, it is possible that neutrophils secrete FGF2, which

is deposited within the tumour ECM in order to promote the migration and proliferation of endothelial cells within the tumour microenvironment and thereby drive angiogenesis.

Given the possibility that FGF2 deposition within the ECM is important for angiogenesis, it is interesting to consider that we have also demonstrated elevated expression of various genes involved in the regulation of ECM turnover in tumour-associated neutrophils. Neutrophils may therefore promote tumour angiogenesis in this setting directly through FGF2 production and through some indirect effect on the ECM. Indeed, SerpinE1, which was highly expressed by tumour-associated neutrophils promotes ECM deposition through inhibition of proteinases such as those of the MMP family (Oh et al., 2002)(Krag et al., 2005). Heparinase – an enzyme responsible for breakdown of HSGAGs commonly found in the ECM – was also expressed at high levels by tumour-associated neutrophils. At present, a potential relationship between serpinE1 and tumour angiogenesis has not been studied in the research literature. Heparinase, however, is a highly angiogenic protein of significant relevance to cancer progression. Transgenic mice over-expressing heparinase, for example displayed increased mammary vasculogenesis (Zcharia et al., 2004), whilst lymphoma cells transfected with a heparinase over-expression vector developed highly vascular, spontaneous hepatic metastases following subcutaneous tumour cell injection (Goldshmidt et al., 2002). Although it is not yet clear whether the pro-angiogenic function of heparinase results from its ability to release HSGAG-bound FGF2, it is notable that tumour-associated neutrophils express both the FGF2 protein and a gene in heparinase whose protein product potentially plays a role in FGF2 signaling. This suggests that promotion of FGF2 signaling is important for the pro-metastatic effect of tumour-associated neutrophils and it will therefore be interesting to analyse the effects of FGF2 inhibition on hepatic metastasis development in forthcoming experiments.

CHAPTER 6. Concluding Remarks

The aims of this research project were to identify immune cell populations recruited to the hepatic metastatic environment in response to tumour-derived chemokines and to determine whether such populations are capable of promoting metastatic growth. Throughout this thesis, we have presented significant experimental evidence demonstrating the recruitment of various immune cell subsets to the tumour-bearing liver. Importantly, the nature of the immune cell infiltrate appeared to be closely related to the tumour cell chemokine profile, suggesting that tumour-derived chemokines promoted the recruitment of specific immune cell subsets. Indeed, human colon cancer cell lines broadly expressed neutrophil chemoattractants and metastases developed using these lines were associated with neutrophil infiltration. Meanwhile, murine colon and lung cancer cell lines expressing CCL2 recruited $CCR2^{+}$ monocytes. This data was supported by the results of experiments in which inhibition of tumour-derived chemokines suppressed the recruitment of specific immune cell subsets and delayed metastatic progression. Although the work of others has linked MIF expression to the progression of colon cancer (He et al., 2009), ours is the first work to identify MIF as a tumour-derived chemokine responsible for metastatic development through the recruitment of neutrophils. We are also the first to demonstrate the importance of the CCL2/CCR2 axis in the recruitment of pro-metastatic monocytes to the hepatic metastatic microenvironment (Zhao et al., 2013).

Interestingly, cell types with significantly different immunological functions - such as the neutrophils and monocytes identified throughout our experiments - may promote metastatic progression through effects on the same process, namely angiogenesis. Thus, here we have demonstrated a reduction in hepatic tumour blood vessel density in mice depleted of neutrophils, as well as elevated expression of various pro-angiogenic genes in tumour-

associated neutrophils compared to those from naïve liver. Similarly, unpublished experiments performed in our lab have found that vessel density is significantly reduced in MC38 tumour-bearing CD11b-DTR mice treated with DT, compared to vehicle control-treated animals, indicating that tumour-associated monocytes also promote angiogenesis. The similar effect on angiogenesis for models in which different immune cell subsets are depleted could be explained by the ability of tumour-derived chemokines to polarise 'plastic' immune cell populations, as has been demonstrated for both macrophages (Mantovani et al., 2002) and neutrophils (Fridlender et al., 2009). In effect, the tumour may be indiscriminate about the cell type that is recruited to the metastatic microenvironment, as long as it can be polarised to a pro-angiogenic phenotype. Future work in our laboratory will attempt to characterise the microenvironmental factors that promote the pro-metastatic phenotype of various immune cell populations, in the hope of gaining a better understanding of this process as well as identifying new therapeutic targets.

6.1 Limitations of our research

Throughout the course of our experimentation, we modeled hepatic metastasis development by injecting tumour cells into the spleen prior to performing splenectomy. In this method, tumour cells enter the liver via the hepatic portal vein in a manner analogous to their presumed route from primary colon cancers in human pathology. Interestingly, although it is likely that hepatic metastases develop following migration of tumour cells via the hepatic portal vein in humans with gastrointestinal tumours, this is yet to be conclusively proven. Although this model has the advantage of generating reproducible metastatic disease within a short time frame, it has significant shortcomings, which may affect its relevance as a model for the development of metastasis in humans.

For example, the delivery of a concentrated bolus of tumour cells is likely to result in adverse haemodynamic and inflammatory effects within the liver and is unlikely to be in keeping with the way in which hepatic metastases develop in humans. In our experience, the few mice that became unwell within 48 hours of intrasplenic injection developed fulminant hepatic failure evidenced at post mortem examination. This suggests that the procedure has the potential to cause hepatic damage, which may affect the subsequent metastatic process. The fact that splenectomy is performed following tumour cell injection is also likely to have significant implications for murine immunity. The spleen is a potential site for extramedullary haematopoiesis of monocytes and neutrophils (Swirski et al., 2009)(Cortez-Retamozo et al., 2012) during times of pathological stress such as cancer development. Indeed, in a primary lung cancer model, splenectomy impaired the accumulation of tumour-associated macrophages and neutrophils and delayed tumour progression (Cortez-Retamozo et al., 2012). It is therefore possible that splenectomy has a negative effect on hepatic metastasis formation, an effect that cannot be taken into account by our model.

The tumour cell bolus effect and the issues caused by splenectomy could be avoided by using transgenic mouse models, or by orthotopically implanting colon cancer cells into the intestine. In such models, mice would have to develop spontaneous hepatic metastases to be of value for our research. Currently, there are no transgenic models of primary colon cancer that result in reliable hepatic metastasis formation (Taketo and Edelmann, 2009). Furthermore, despite the fact that other research groups have demonstrated spontaneous hepatic metastasis formation following the intracaecal implantation of various cancer cell lines (Zhang et al.)(Calon et al., 2012), in our hands the technique yielded only sporadic pulmonary and lymph node metastases, with little evidence of hepatic metastasis for MC38, HT29 and HCT-116 cell lines (results not shown).

Finally, the use of immunocompromised, SCID mice for an analysis of the relationship between the immune system and hepatic metastasis development is not ideal. The phenotype of the CB-17-SCID mice used in this study is of T- and B-cell absence, but normal NK cell function (Shultz et al., 2007). The use of this mouse strain enabled us to reproducibly develop hepatic metastases using human cell lines and in doing so study the role of cells of the innate immune system within the metastatic microenvironment. As such, we have obtained a better understanding of the biology of human colon cancer metastasis than the study of murine colon cancer cell lines alone would have allowed. However, the used of SCID mice ignores the effect that T-cell subsets may have on hepatic metastasis development, in terms of both their likely cytotoxicity towards tumour cells and their interaction with other cells within the tumour microenvironment.

It is therefore vital to support the data obtained from our animal models with an analysis of patient specimens, in order to ensure that our data is of clinical relevance. Where possible, we have attempted to do this. We have analysed human hepatic metastasis tissues for immune cell infiltration and have determined the chemokine concentration within serum samples from patients with primary and disseminated colon cancer. The concentration of both MIF and CCL2 were higher in the serum from patients with hepatic metastases compared to that from patients with primary cancer alone (Chapter 5 and (Zhao et al., 2013)). Furthermore, neutrophils were found to infiltrate hepatic metastases to a greater degree than the normal surrounding liver, potentially suggesting their active recruitment to the tumour microenvironment. Nonetheless, we are yet to perform experiments demonstrating a correlation between the infiltration of specific immune cell subsets within human metastases and the expression of various chemokines. Indeed, it will be important to demonstrate such links if we are to provide an argument for the inhibition of certain chemokines in order to impair the recruitment of pro-metastatic immune cell types in cancer patients.

6.2 The potential clinical relevance of our data

Whilst it would be naïve to believe that we can draw direct comparisons between the work presented here using animal models and clinical practice, it is important to consider whether our data has progressed the understanding of human cancer and whether in doing so we have identified any potential therapeutic targets. The data presented in Chapter 3 points to the importance of the CCL2-CCR2 signaling axis in the recruitment of pro-metastatic monocytes to the tumour microenvironment. Given these findings and that there is significant research evidence demonstrating a pro-metastatic role for tumour-associated monocytes/macrophages in other tumour types (Pollard, 2004)(Siveen and Kuttan, 2009)(Sica et al., 2008), it is possible that targeting such cells will be of clinical benefit to patients with colon cancer metastasis. However, the ideal methods of tumour-associated immune cell targeting are unclear.

Various potential methods include immune cell depletion, inhibition of chemokine/chemokine receptor signaling, re-education of pro-metastatic, polarised immune cells or targeting of the downstream effects of immune cells. Although in our models depletion of monocytes or neutrophils resulted in a significant inhibition of metastatic growth, it is unlikely that immune cell depletion will be a feasible option in humans, as such techniques are likely to put patients at risk of life-threatening infection. Re-education of immune cells and the targeting of their downstream effects have not been studied in this thesis, however these areas are currently under investigation in our laboratory. Our current research does, however indicate that inhibition of chemokine/chemokine receptor signaling could provide a growth-inhibitory effect in patients.

Our data suggests that targeting the CCL2/CCR2 receptor axis may provide a temporary, albeit limited metastasis-inhibitory effect. Nonetheless, data from the first trials targeting

CCL2/CCR2 in cancer patients using a monoclonal antibody to CCL2 (Carlumab) have demonstrated disappointing results (Pienta et al., 2013)(Sandhu et al., 2013). In the first trial, Carlumab transiently suppressed CCL2 concentration in patients with a variety of solid tumours, but levels rapidly succeeded the pre-treatment values once therapy was stopped (Sandhu et al., 2013), indicating that if it is to be effective, Carlumab will need to be administered on a long-term basis. In the second trial, Carlumab was well tolerated but provided no treatment benefit for patients with castrate-resistant prostate cancer (Pienta et al., 2013). The inherent redundancy of the chemokine-receptor network may underlie the failure of such agents that target single chemokines. As a case in point, in addition to CCL2, CCL7 and CCL8 are chemotactic ligands for the CCR2 receptor (Balkwill, 2004). Interestingly, CCL7 provided as equal a contribution to $CCR2^{+}$ inflammatory monocyte recruitment as CCL2 in the setting of bacterial infection (Jia et al., 2008) and is expressed at elevated levels in the hepatic metastases of colon cancer patients (Cho et al., 2012). Inhibition of CCL2 alone is therefore unlikely to reduce the recruitment of pro-metastatic $CCR2^{+}$ monocytes in patients whose tumours strongly express both CCL2 and CCL7.

We have also investigated the value of MIF inhibition as a treatment method for hepatic metastasis. Indeed, MIF inhibition successfully delayed the growth of HT29 metastases through a range of potential mechanisms including the inhibition of neutrophil recruitment, making it a promising potential therapeutic target. However, the fact that both HCT-116 and LoVo cells expressed potent neutrophil chemoattractants in addition to MIF, suggests redundancy in the human tumour-derived chemokine profile, indicating that these cell lines would be capable of neutrophil recruitment even if MIF were inhibited. This scenario appears similar to that described in the previous paragraph, again indicating significant redundancy in chemokine expression profile expression of cancer cells.

As well as demonstrating the expression of multiple chemokines with overlapping functions by single cell lines, our work with human colon cancer cells indicates that there is significant heterogeneity in chemokine expression between cell lines. This in turn suggests that there is likely to be significant heterogeneity in the chemokine expression profile of populations of cancer patients. Currently, no studies have analysed the expression of multiple chemokines in populations of patients with hepatic metastasis and so the degree of chemokine redundancy and heterogeneity in expression levels in such groups are unclear. Furthermore, there is no published evidence confirming the efficacy of MIF inhibition in cancer patients, although a monoclonal antibody to MIF is currently being trialed in patients with various solid tumours (www.clinicaltrials.gov NCT01765790).

In conclusion, our results indicate that immune cells of various lineages play a significant role in the development of hepatic metastasis for a range of different cell lines. To advance this work and determine its relevance to cancer patients, it will be important to gain a greater understanding of the interplay between cancer and immune cells in human hepatic metastases. Specifically, this will include acquiring an in depth knowledge of the various chemokine expression profiles displayed by cancer patients, as these molecules are the key regulators of tumour-associated immune cell recruitment and the variation in immune cell infiltrate seen between cancer patients. Indeed, our data suggests that the focus may need to move away from targeting single chemokines in populations of cancer patients and towards a patient-centered, individualised approach, in which serum is screened for various chemokines to enable selection of appropriate chemokine inhibitors.

Abdalla, E.K., Adam, R., Bilchik, A.J., Jaeck, D., Vauthey, J.-N., and Mahvi, D. (2006). Improving resectability of hepatic colorectal metastases: expert consensus statement. Ann. Surg. Oncol. *13*, 1271–1280.

Al-Abed, Y., Dabideen, D., Aljabari, B., Valster, A., Messmer, D., Ochani, M., Tanovic, M., Ochani, K., Bacher, M., Nicoletti, F., et al. (2005). ISO-1 Binding to the Tautomerase Active Site of MIF Inhibits Its Pro-inflammatory Activity and Increases Survival in Severe Sepsis. J. Biol. Chem. *280*, 36541–36544.

Adam, R., Laurent, A., Azoulay, D., Castaing, D., and Bismuth, H. (2000). Two-Stage Hepatectomy: A Planned Strategy to Treat Irresectable Liver Tumors. Ann. Surg. *232*, 777–785.

Adams, D.H., and Eksteen, B. (2006). Aberrant homing of mucosal T cells and extra-intestinal manifestations of inflammatory bowel disease. Nat. Rev. Immunol. *6*, 244–251.

Ahmed, D., Eide, P.W., Eilertsen, I.A., Danielsen, S.A., Eknæs, M., Hektoen, M., Lind, G.E., and Lothe, R.A. (2013). Epigenetic and genetic features of 24 colon cancer cell lines. Oncogenesis *2*, e71.

Allen, S.J., Crown, S.E., and Handel, T.M. (2007). Chemokine:Receptor Structure, Interactions, and Antagonism. Annu. Rev. Immunol. *25*, 787–820.

Alon, R., and Ley, K. (2008). Cells on the run: shear-regulated integrin activation in leukocyte rolling and arrest on endothelial cells. Curr. Opin. Cell Biol. *20*, 525–532.

Amann, T., Bataille, F., Spruss, T., Mühlbauer, M., Gäbele, E., Schölmerich, J., Kiefer, P., Bosserhoff, A.-K., and Hellerbrand, C. (2009). Activated hepatic stellate cells promote tumorigenicity of hepatocellular carcinoma. Cancer Sci. *100*, 646–653.

Anasagasti, M.J., Alvarez, A., Avivi, C., and Vidal-Vanaclocha, F. (1996). Interleukin-1-mediated H2O2 production by hepatic sinusoidal endothelium in response to B16 melanoma cell adhesion. J. Cell. Physiol. *167*, 314–323.

Ardi, V.C., Kupriyanova, T.A., Deryugina, E.I., and Quigley, J.P. (2007). Human neutrophils uniquely release TIMP-free MMP-9 to provide a potent catalytic stimulator of angiogenesis. Proc. Natl. Acad. Sci. U. S. A. *104*, 20262–20267.

Ardi, V.C., Van den Steen, P.E., Opdenakker, G., Schweighofer, B., Deryugina, E.I., and Quigley, J.P. (2009). Neutrophil MMP-9 proenzyme, unencumbered by TIMP-1, undergoes efficient activation in vivo and catalytically induces angiogenesis via a basic fibroblast growth factor (FGF-2)/FGFR-2 pathway. J. Biol. Chem. *284*, 25854–25866.

Arnold, S., Mira, E., Muneer, S., Korpanty, G., Beck, A.W., Holloway, S.E., Manes, S., and Brekken, R.A. (2008). Forced expression of MMP9 rescues the loss of angiogenesis and abrogates metastasis of pancreatic tumors triggered by the absence of host SPARC. Exp. Biol. Med. Maywood NJ *233*, 860–873.

Arnold, S.A., Rivera, L.B., Miller, A.F., Carbon, J.G., Dineen, S.P., Xie, Y., Castrillon, D.H., Sage, E.H., Puolakkainen, P., Bradshaw, A.D., et al. (2010). Lack of host SPARC enhances

vascular function and tumor spread in an orthotopic murine model of pancreatic carcinoma. Dis. Model. Mech. *3*, 57–72.

Arteta, B., Lasuen, N., Lopategi, A., Sveinbjörnsson, B., Smedsrød, B., and Vidal-Vanaclocha, F. (2010). Colon carcinoma cell interaction with liver sinusoidal endothelium inhibits organ-specific antitumor immunity through interleukin-1-induced mannose receptor in mice. Hepatol. Baltim. Md *51*, 2172–2182.

Asahara, T., Bauters, C., Zheng, L.P., Takeshita, S., Bunting, S., Ferrara, N., Symes, J.F., and Isner, J.M. (1995). Synergistic effect of vascular endothelial growth factor and basic fibroblast growth factor on angiogenesis in vivo. Circulation *92*, II365–371.

ATHENS, J.W., HAAB, O.P., RAAB, S.O., MAUER, A.M., ASHENBRUCKER, H., CARTWRIGHT, G.E., and WINTROBE, M.M. (1961). Leukokinetic studies. IV. The total blood, circulating and marginal granulocyte pools and the granulocyte turnover rate in normal subjects. J. Clin. Invest. *40*, 989–995.

Auffray, C., Fogg, D., Garfa, M., Elain, G., Join-Lambert, O., Kayal, S., Sarnacki, S., Cumano, A., Lauvau, G., and Geissmann, F. (2007). Monitoring of blood vessels and tissues by a population of monocytes with patrolling behavior. Science *317*, 666–670.

Auguste, P., Fallavollita, L., Wang, N., Burnier, J., Bikfalvi, A., and Brodt, P. (2007). The Host Inflammatory Response Promotes Liver Metastasis by Increasing Tumor Cell Arrest and Extravasation. Am. J. Pathol. *170*, 1781–1792.

Aune, D., Chan, D.S.M., Lau, R., Vieira, R., Greenwood, D.C., Kampman, E., and Norat, T. (2011). Dietary fibre, whole grains, and risk of colorectal cancer: systematic review and dose-response meta-analysis of prospective studies. BMJ *343*.

Balabanian, K., Lagane, B., Pablos, J.L., Laurent, L., Planchenault, T., Verola, O., Lebbe, C., Kerob, D., Dupuy, A., Hermine, O., et al. (2005). WHIM syndromes with different genetic anomalies are accounted for by impaired CXCR4 desensitization to CXCL12. Blood *105*, 2449–2457.

Bald, T., Quast, T., Landsberg, J., Rogava, M., Glodde, N., Lopez-Ramos, D., Kohlmeyer, J., Riesenberg, S., van den Boorn-Konijnenberg, D., Hömig-Hölzel, C., et al. (2014). Ultraviolet-radiation-induced inflammation promotes angiotropism and metastasis in melanoma. Nature *advance online publication*.

Balkwill, F. (2004). Cancer and the chemokine network. Nat. Rev. Cancer *4*, 540–550.

Ballas, Z.K., Buchta, C.M., Rosean, T.R., Heusel, J.W., and Shey, M.R. (2013). Role of NK Cell Subsets in Organ-Specific Murine Melanoma Metastasis. PLoS ONE *8*.

Barbera-Guillem, E., Smith, I., and Weiss, L. (1993). Cancer-cell traffic in the liver. II. Arrest, transit and death of B16F10 and M5076 cells in the sinusoids. Int. J. Cancer J. Int. Cancer *53*, 298–301.

Barone, C., Nuzzo, G., Cassano, A., Basso, M., Schinzari, G., Giuliante, F., D'Argento, E., Trigila, N., Astone, A., and Pozzo, C. (2007). Final analysis of colorectal cancer patients

treated with irinotecan and 5-fluorouracil plus folinic acid neoadjuvant chemotherapy for unresectable liver metastases. Br. J. Cancer *97*, 1035–1039.

Bashkin, P., Doctrow, S., Klagsbrun, M., Svahn, C.M., Folkman, J., and Vlodavsky, I. (1989). Basic fibroblast growth factor binds to subendothelial extracellular matrix and is released by heparitinase and heparin-like molecules. Biochemistry (Mosc.) *28*, 1737–1743.

Bataller, R., Ginès, P., Nicolás, J.M., Görbig, M.N., Garcia-Ramallo, E., Gasull, X., Bosch, J., Arroyo, V., and Rodés, J. (2000). Angiotensin II induces contraction and proliferation of human hepatic stellate cells. Gastroenterology *118*, 1149–1156.

Bayón, L.G., Izquierdo, M.A., Sirovich, I., van Rooijen, N., Beelen, R.H., and Meijer, S. (1996). Role of Kupffer cells in arresting circulating tumor cells and controlling metastatic growth in the liver. Hepatol. Baltim. Md *23*, 1224–1231.

Bazan, J.F., Bacon, K.B., Hardiman, G., Wang, W., Soo, K., Rossi, D., Greaves, D.R., Zlotnik, A., and Schall, T.J. (1997). A new class of membrane-bound chemokine with a CX3C motif. Nature *385*, 640–644.

Bekes, E.M., Schweighofer, B., Kupriyanova, T.A., Zajac, E., Ardi, V.C., Quigley, J.P., and Deryugina, E.I. (2011). Tumor-Recruited Neutrophils and Neutrophil TIMP-Free MMP-9 Regulate Coordinately the Levels of Tumor Angiogenesis and Efficiency of Malignant Cell Intravasation. Am. J. Pathol. *179*, 1455–1470.

Benseler, V., Warren, A., Vo, M., Holz, L.E., Tay, S.S., Le Couteur, D.G., Breen, E., Allison, A.C., van Rooijen, N., McGuffog, C., et al. (2011). Hepatocyte entry leads to degradation of autoreactive CD8 T cells. Proc. Natl. Acad. Sci. U. S. A. *108*, 16735–16740.

Bernhagen, J., Krohn, R., Lue, H., Gregory, J.L., Zernecke, A., Koenen, R.R., Dewor, M., Georgiev, I., Schober, A., Leng, L., et al. (2007). MIF is a noncognate ligand of CXC chemokine receptors in inflammatory and atherogenic cell recruitment. Nat. Med. *13*, 587–596.

Blanpain, C., Doranz, B.J., Bondue, A., Govaerts, C., De Leener, A., Vassart, G., Doms, R.W., Proudfoot, A., and Parmentier, M. (2003). The core domain of chemokines binds CCR5 extracellular domains while their amino terminus interacts with the transmembrane helix bundle. J. Biol. Chem. *278*, 5179–5187.

Boring, L., Gosling, J., Cleary, M., and Charo, I.F. (1998). Decreased lesion formation in CCR2-/- mice reveals a role for chemokines in the initiation of atherosclerosis. Nature *394*, 894–897.

Borrello, M.G., Alberti, L., Fischer, A., Degl'innocenti, D., Ferrario, C., Gariboldi, M., Marchesi, F., Allavena, P., Greco, A., Collini, P., et al. (2005). Induction of a proinflammatory program in normal human thyrocytes by the RET/PTC1 oncogene. Proc. Natl. Acad. Sci. U. S. A. *102*, 14825–14830.

Bos, P.D., Zhang, X.H.-F., Nadal, C., Shu, W., Gomis, R.R., Nguyen, D.X., Minn, A.J., van de Vijver, M.J., Gerald, W.L., Foekens, J.A., et al. (2009). Genes that mediate breast cancer metastasis to the brain. Nature *459*, 1005–1009.

Bouwens, L., Remels, L., Baekeland, M., Van Bossuyt, H., and Wisse, E. (1987). Large granular lymphocytes or “pit cells” from rat liver: isolation, ultrastructural characterization and natural killer activity. Eur. J. Immunol. *17*, 37–42.

Bozic, C.R., Gerard, N.P., von Uexkull-Guldenband, C., Kolakowski, L.F., Jr, Conklyn, M.J., Breslow, R., Showell, H.J., and Gerard, C. (1994). The murine interleukin 8 type B receptor homologue and its ligands. Expression and biological characterization. J. Biol. Chem. *269*, 29355–29358.

Brinkmann, V., Reichard, U., Goosmann, C., Fauler, B., Uhlemann, Y., Weiss, D.S., Weinrauch, Y., and Zychlinsky, A. (2004). Neutrophil Extracellular Traps Kill Bacteria. Science *303*, 1532–1535.

Brodt, P. (2013). Liver Metastasis: Biology and Clinical Management (Springer).

Brooks, P.C., Strömblad, S., Sanders, L.C., von Schalscha, T.L., Aimes, R.T., Stetler-Stevenson, W.G., Quigley, J.P., and Cheresh, D.A. (1996). Localization of Matrix Metalloproteinase MMP-2 to the Surface of Invasive Cells by Interaction with Integrin αvβ3. Cell *85*, 683–693.

Browse, D.J., Mathie, R.T., Benjamin, I.S., and Alexander, B. (2003). The role of ATP and adenosine in the control of hepatic blood flow in the rabbit liver in vivo. Comp. Hepatol. *2*, 9.

Bubendorf, L., Schöpfer, A., Wagner, U., Sauter, G., Moch, H., Willi, N., Gasser, T.C., and Mihatsch, M.J. (2000). Metastatic patterns of prostate cancer: an autopsy study of 1,589 patients. Hum. Pathol. *31*, 578–583.

Calon, A., Espinet, E., Palomo-Ponce, S., Tauriello, D.V.F., Iglesias, M., Céspedes, M.V., Sevillano, M., Nadal, C., Jung, P., Zhang, X.H.-F., et al. (2012). Dependency of colorectal cancer on a TGF-β-driven program in stromal cells for metastasis initiation. Cancer Cell *22*, 571–584.

Cao, R., Bråkenhielm, E., Pawliuk, R., Wariaro, D., Post, M.J., Wahlberg, E., Leboulch, P., and Cao, Y. (2003). Angiogenic synergism, vascular stability and improvement of hind-limb ischemia by a combination of PDGF-BB and FGF-2. Nat. Med. *9*, 604–613.

Carus, A., Ladekarl, M., Hager, H., Nedergaard, B.S., and Donskov, F. (2013). Tumour-associated CD66b+ neutrophil count is an independent prognostic factor for recurrence in localised cervical cancer. Br. J. Cancer *108*, 2116–2122.

Chambers, A.F., Groom, A.C., and MacDonald, I.C. (2002). Metastasis: Dissemination and growth of cancer cells in metastatic sites. Nat. Rev. Cancer *2*, 563–572.

Chan, D.S.M., Lau, R., Aune, D., Vieira, R., Greenwood, D.C., Kampman, E., and Norat, T. (2011). Red and processed meat and colorectal cancer incidence: meta-analysis of prospective studies. PloS One *6*, e20456.

Chen, W., Jin, W., Hardegen, N., Lei, K., Li, L., Marinos, N., McGrady, G., and Wahl, S.M. (2003). Conversion of Peripheral CD4+CD25− Naive T Cells to CD4+CD25+ Regulatory T Cells by TGF-β Induction of Transcription Factor Foxp3. J. Exp. Med. *198*, 1875–1886.

Cheng, W.-L., Wang, C.-S., Huang, Y.-H., Tsai, M.-M., Liang, Y., and Lin, K.-H. (2011). Overexpression of CXCL1 and its receptor CXCR2 promote tumor invasion in gastric cancer. Ann. Oncol. Off. J. Eur. Soc. Med. Oncol. ESMO *22*, 2267–2276.

Cheng, X.-S., Li, Y.-F., Tan, J., Sun, B., Xiao, Y.-C., Fang, X.-B., Zhang, X.-F., Li, Q., Dong, J.-H., Li, M., et al. (2014). CCL20 and CXCL8 synergize to promote progression and poor survival outcome in patients with colorectal cancer by collaborative induction of the epithelial-mesenchymal transition. Cancer Lett.

Cho, Y.B., Lee, W.Y., Choi, S.-J., Kim, J., Hong, H.K., Kim, S.-H., Choi, Y.-L., Kim, H.C., Yun, S.H., Chun, H.-K., et al. (2012). CC chemokine ligand 7 expression in liver metastasis of colorectal cancer. Oncol. Rep. *28*, 689–694.

Clark-Lewis, I., Schumacher, C., Baggiolini, M., and Moser, B. (1991). Structure-activity relationships of interleukin-8 determined using chemically synthesized analogs. Critical role of NH2-terminal residues and evidence for uncoupling of neutrophil chemotaxis, exocytosis, and receptor binding activities. J. Biol. Chem. *266*, 23128–23134.

Coca, S., Perez-Piqueras, J., Martinez, D., Colmenarejo, A., Saez, M.A., Vallejo, C., Martos, J.A., and Moreno, M. (1997). The prognostic significance of intratumoral natural killer cells in patients with colorectal carcinoma. Cancer *79*, 2320–2328.

Colotta, F., Re, F., Polentarutti, N., Sozzani, S., and Mantovani, A. (1992). Modulation of granulocyte survival and programmed cell death by cytokines and bacterial products. Blood *80*, 2012–2020.

Coman, D.R., deLONG, R.P., and McCutcheon, M. (1951). Studies on the mechanisms of metastasis; the distribution of tumors in various organs in relation to the distribution of arterial emboli. Cancer Res. *11*, 648–651.

Connolly, M.K., Clair, J.M.-S., Bedrosian, A.S., Malhotra, A., Vera, V., Ibrahim, J., Henning, J., Pachter, H.L., Bar-Sagi, D., Frey, A.B., et al. (2010). Distinct populations of metastases-enabling myeloid cells expand in the liver of mice harboring invasive and preinvasive intra-abdominal tumor. J. Leukoc. Biol. *87*, 713–725.

Cools-Lartigue, J., Spicer, J., McDonald, B., Gowing, S., Chow, S., Giannias, B., Bourdeau, F., Kubes, P., and Ferri, L. (2013). Neutrophil extracellular traps sequester circulating tumor cells and promote metastasis. J. Clin. Invest. *123*, 3446–3458.

Cordon-Cardo, C., Vlodavsky, I., Haimovitz-Friedman, A., Hicklin, D., and Fuks, Z. (1990). Expression of basic fibroblast growth factor in normal human tissues. Lab. Investig. J. Tech. Methods Pathol. *63*, 832–840.

Cortez-Retamozo, V., Etzrodt, M., Newton, A., Rauch, P.J., Chudnovskiy, A., Berger, C., Ryan, R.J.H., Iwamoto, Y., Marinelli, B., Gorbatov, R., et al. (2012). Origins of tumor-associated macrophages and neutrophils. Proc. Natl. Acad. Sci. U. S. A. *109*, 2491–2496.

Cotter, M.J., and Muruve, D.A. (2006). Isolation of neutrophils from mouse liver: A novel method to study effector leukocytes during inflammation. J. Immunol. Methods *312*, 68–78.

Cottu, P.H., Muzeau, F., Estreicher, A., Fléjou, J.F., Iggo, R., Thomas, G., and Hamelin, R. (1996). Inverse correlation between RER+ status and p53 mutation in colorectal cancer cell lines. Oncogene *13*, 2727–2730.

CRONKITE, E.P., and FLIEDNER, T.M. (1964). GRANULOCYTOPOIESIS. N. Engl. J. Med. *270*, 1347–1352 CONTD.

Cros, J., Cagnard, N., Woollard, K., Patey, N., Zhang, S.-Y., Senechal, B., Puel, A., Biswas, S.K., Moshous, D., Picard, C., et al. (2010). Human CD14dim monocytes patrol and sense nucleic acids and viruses via TLR7 and TLR8 receptors. Immunity *33*, 375–386.

Crosbie, O.M., Reynolds, M., McEntee, G., Traynor, O., Hegarty, J.E., and O'Farrelly, C. (1999). In vitro evidence for the presence of hematopoietic stem cells in the adult human liver. Hepatol. Baltim. Md *29*, 1193–1198.

Curiel, T.J., Coukos, G., Zou, L., Alvarez, X., Cheng, P., Mottram, P., Evdemon-Hogan, M., Conejo-Garcia, J.R., Zhang, L., Burow, M., et al. (2004). Specific recruitment of regulatory T cells in ovarian carcinoma fosters immune privilege and predicts reduced survival. Nat. Med. *10*, 942–949.

Van Cutsem, E., Köhne, C.-H., Hitre, E., Zaluski, J., Chang Chien, C.-R., Makhson, A., D'Haens, G., Pintér, T., Lim, R., Bodoky, G., et al. (2009). Cetuximab and chemotherapy as initial treatment for metastatic colorectal cancer. N. Engl. J. Med. *360*, 1408–1417.

D'Amore, P.A., and Smith, S.R. (1993). Growth factor effects on cells of the vascular wall: a survey. Growth Factors Chur Switz. *8*, 61–75.

Dabideen, D.R., Cheng, K.F., Aljabari, B., Miller, E.J., Pavlov, V.A., and Al-Abed, Y. (2007). Phenolic hydrazones are potent inhibitors of macrophage migration inhibitory factor proinflammatory activity and survival improving agents in sepsis. J. Med. Chem. *50*, 1993–1997.

Daley, J.M., Thomay, A.A., Connolly, M.D., Reichner, J.S., and Albina, J.E. (2008). Use of Ly6G-specific monoclonal antibody to deplete neutrophils in mice. J. Leukoc. Biol. *83*, 64–70.

Delaunoit, T., Alberts, S.R., Sargent, D.J., Green, E., Goldberg, R.M., Krook, J., Fuchs, C., Ramanathan, R.K., Williamson, S.K., Morton, R.F., et al. (2005). Chemotherapy permits resection of metastatic colorectal cancer: experience from Intergroup N9741. Ann. Oncol. Off. J. Eur. Soc. Med. Oncol. ESMO *16*, 425–429.

Diefenbach, A., Jensen, E.R., Jamieson, A.M., and Raulet, D.H. (2001). Rae1 and H60 ligands of the NKG2D receptor stimulate tumour immunity. Nature *413*, 165–171.

Divella, R., Daniele, A., Savino, E., Palma, F., Bellizzi, A., Giotta, F., Simone, G., Lioce, M., Quaranta, M., Paradiso, A., et al. (2013). Circulating levels of transforming growth factor-βeta (TGF-β) and chemokine (C-X-C motif) ligand-1 (CXCL1) as predictors of distant seeding of circulating tumor cells in patients with metastatic breast cancer. Anticancer Res. *33*, 1491–1497.

Dobbs, B.R., Rogers, G.W., Xing, H.Y., and Fraser, R. (1994). Endotoxin-induced defenestration of the hepatic sinusoidal endothelium: a factor in the pathogenesis of cirrhosis? Liver *14*, 230–233.

Doll, D., Keller, L., Maak, M., Boulesteix, A.-L., Siewert, J.R., Holzmann, B., and Janssen, K.-P. (2010). Differential expression of the chemokines GRO-2, GRO-3, and interleukin-8 in colon cancer and their impact on metastatic disease and survival. Int. J. Colorectal Dis. *25*, 573–581.

Duffield, J.S., Forbes, S.J., Constandinou, C.M., Clay, S., Partolina, M., Vuthoori, S., Wu, S., Lang, R., and Iredale, J.P. (2005). Selective depletion of macrophages reveals distinct, opposing roles during liver injury and repair. J. Clin. Invest. *115*, 56–65.

Dumitru, C.A., Gholaman, H., Trellakis, S., Bruderek, K., Dominas, N., Gu, X., Bankfalvi, A., Whiteside, T.L., Lang, S., and Brandau, S. (2011). Tumor-derived macrophage migration inhibitory factor modulates the biology of head and neck cancer cells via neutrophil activation. Int. J. Cancer J. Int. Cancer *129*, 859–869.

Eash, K.J., Greenbaum, A.M., Gopalan, P.K., and Link, D.C. (2010). CXCR2 and CXCR4 antagonistically regulate neutrophil trafficking from murine bone marrow. J. Clin. Invest. *120*, 2423–2431.

Eckmann, L., Jung, H.C., Schürer-Maly, C., Panja, A., Morzycka-Wroblewska, E., and Kagnoff, M.F. (1993). Differential cytokine expression by human intestinal epithelial cell lines: regulated expression of interleukin 8. Gastroenterology *105*, 1689–1697.

Ekbom, A., Helmick, C., Zack, M., and Adami, H.-O. (1990). Ulcerative Colitis and Colorectal Cancer. N. Engl. J. Med. *323*, 1228–1233.

Enzan, H., Himeno, H., Hiroi, M., Kiyoku, H., Saibara, T., and Onishi, S. (1997). Development of hepatic sinusoidal structure with special reference to the Ito cells. Microsc. Res. Tech. *39*, 336–349.

Erreni, M., Bianchi, P., Laghi, L., Mirolo, M., Fabbri, M., Locati, M., Mantovani, A., and Allavena, P. (2009). Expression of chemokines and chemokine receptors in human colon cancer. Methods Enzymol. *460*, 105–121.

Ewing, J. (1919). Neoplastic diseases (Philadelphia, and London: W.B. Saunders Company).

Ferlay, J., Parkin, D.M., and Steliarova-Foucher, E. (2010). Estimates of cancer incidence and mortality in Europe in 2008. Eur. J. Cancer *46*, 765–781.

Fingerle-Rowson, G., Petrenko, O., Metz, C.N., Forsthuber, T.G., Mitchell, R., Huss, R., Moll, U., Muller, W., and Bucala, R. (2003). The p53-dependent effects of macrophage migration inhibitory factor revealed by gene targeting. Proc. Natl. Acad. Sci. U. S. A. *100*, 9354–9359.

Flaumenhaft, R., Moscatelli, D., Saksela, O., and Rifkin, D.B. (1989). Role of extracellular matrix in the action of basic fibroblast growth factor: matrix as a source of growth factor

for long-term stimulation of plasminogen activator production and DNA synthesis. J. Cell. Physiol. *140*, 75–81.

Fleming, T.J., Fleming, M.L., and Malek, T.R. (1993). Selective expression of Ly-6G on myeloid lineage cells in mouse bone marrow. RB6-8C5 mAb to granulocyte-differentiation antigen (Gr-1) detects members of the Ly-6 family. J. Immunol. Baltim. Md 1950 *151*, 2399–2408.

Flossmann, E., and Rothwell, P.M. (2007). Effect of aspirin on long-term risk of colorectal cancer: consistent evidence from randomised and observational studies. The Lancet *369*, 1603–1613.

Fong, Y., Fortner, J., Sun, R.L., Brennan, M.F., and Blumgart, L.H. (1999). Clinical Score for Predicting Recurrence After Hepatic Resection for Metastatic Colorectal Cancer. Ann. Surg. *230*, 309.

Fridlender, Z.G., and Albelda, S.M. (2012). Tumor-associated neutrophils: friend or foe? Carcinogenesis *33*, 949–955.

Fridlender, Z.G., Sun, J., Kim, S., Kapoor, V., Cheng, G., Ling, L., Worthen, G.S., and Albelda, S.M. (2009). Polarization of Tumor-Associated Neutrophil Phenotype by TGF-β: "N1" versus "N2" TAN. Cancer Cell *16*, 183–194.

Fridlender, Z.G., Sun, J., Mishalian, I., Singhal, S., Cheng, G., Kapoor, V., Horng, W., Fridlender, G., Bayuh, R., Worthen, G.S., et al. (2012). Transcriptomic Analysis Comparing Tumor-Associated Neutrophils with Granulocytic Myeloid-Derived Suppressor Cells and Normal Neutrophils. PLoS ONE *7*, e31524.

Garden, O.J., Rees, M., Poston, G.J., Mirza, D., Saunders, M., Ledermann, J., Primrose, J.N., and Parks, R.W. (2006). Guidelines for resection of colorectal cancer liver metastases. Gut *55*, iii1–iii8.

Gayet, J., Zhou, X.P., Duval, A., Rolland, S., Hoang, J.M., Cottu, P., and Hamelin, R. (2001). Extensive characterization of genetic alterations in a series of human colorectal cancer cell lines. Oncogene *20*, 5025–5032.

Geissmann, F., Jung, S., and Littman, D.R. (2003). Blood Monocytes Consist of Two Principal Subsets with Distinct Migratory Properties. Immunity *19*, 71–82.

Génin, P., Algarté, M., Roof, P., Lin, R., and Hiscott, J. (2000). Regulation of RANTES Chemokine Gene Expression Requires Cooperativity Between NF-κB and IFN-Regulatory Factor Transcription Factors. J. Immunol. *164*, 5352–5361.

Gerber, N., Lowman, H., Artis, D.R., and Eigenbrot, C. (2000). Receptor-binding conformation of the "ELR" motif of IL-8: X-ray structure of the L5C/H33C variant at 2.35 A resolution. Proteins *38*, 361–367.

Gerdes, J., Lemke, H., Baisch, H., Wacker, H.H., Schwab, U., and Stein, H. (1984). Cell cycle analysis of a cell proliferation-associated human nuclear antigen defined by the monoclonal antibody Ki-67. J. Immunol. *133*, 1710–1715.

Germain, L., Blouin, M.J., and Marceau, N. (1988a). Biliary epithelial and hepatocytic cell lineage relationships in embryonic rat liver as determined by the differential expression of cytokeratins, alpha-fetoprotein, albumin, and cell surface-exposed components. Cancer Res. *48*, 4909–4918.

Germain, L., Noël, M., Gourdeau, H., and Marceau, N. (1988b). Promotion of growth and differentiation of rat ductular oval cells in primary culture. Cancer Res. *48*, 368–378.

Goldshmidt, O., Zcharia, E., Abramovitch, R., Metzger, S., Aingorn, H., Friedmann, Y., Schirrmacher, V., Mitrani, E., and Vlodavsky, I. (2002). Cell surface expression and secretion of heparanase markedly promote tumor angiogenesis and metastasis. Proc. Natl. Acad. Sci. U. S. A. *99*, 10031–10036.

Gong, J.H., and Clark-Lewis, I. (1995). Antagonists of monocyte chemoattractant protein 1 identified by modification of functionally critical NH2-terminal residues. J. Exp. Med. *181*, 631–640.

Gonzalez, A.M., Buscaglia, M., Ong, M., and Baird, A. (1990). Distribution of basic fibroblast growth factor in the 18-day rat fetus: localization in the basement membranes of diverse tissues. J. Cell Biol. *110*, 753–765.

Groh, V., Steinle, A., Bauer, S., and Spies, T. (1998). Recognition of stress-induced MHC molecules by intestinal epithelial gammadelta T cells. Science *279*, 1737–1740.

Gulubova, M.V. (2002). Expression of cell adhesion molecules, their ligands and tumour necrosis factor alpha in the liver of patients with metastatic gastrointestinal carcinomas. Histochem. J. *34*, 67–77.

Hackl, C., Gerken, M., Loss, M., Klinkhammer-Schalke, M., Piso, P., and Schlitt, H.J. (2011). A population-based analysis on the rate and surgical management of colorectal liver metastases in Southern Germany. Int. J. Colorectal Dis. *26*, 1475–1481.

Häger, M., Cowland, J.B., and Borregaard, N. (2010). Neutrophil granules in health and disease. J. Intern. Med. *268*, 25–34.

Halazun, K.J., Aldoori, A., Malik, H.Z., Al-Mukhtar, A., Prasad, K.R., Toogood, G.J., and Lodge, J.P.A. (2008). Elevated preoperative neutrophil to lymphocyte ratio predicts survival following hepatic resection for colorectal liver metastases. Eur. J. Surg. Oncol. J. Eur. Soc. Surg. Oncol. Br. Assoc. Surg. Oncol. *34*, 55–60.

Hamilton, T., Novotny, M., Pavicic, P.J., Herjan, T., Hartupee, J., Sun, D., Zhao, C., and Datta, S. (2010). Diversity in Post-Transcriptional Control of Neutrophil Chemoattractant Cytokine Gene Expression. Cytokine *52*, 116–122.

Hart, I.R., and Fidler, I.J. (1980). Role of organ selectivity in the determination of metastatic patterns of B16 melanoma. Cancer Res. *40*, 2281–2287.

He, X.-X., Chen, K., Yang, J., Li, X.-Y., Gan, H.-Y., Liu, C.-Y., Coleman, T.R., and Al-Abed, Y. (2009). Macrophage Migration Inhibitory Factor Promotes Colorectal Cancer. Mol. Med. *15*, 1–10.

Helicobacter and Cancer Collaborative Group (2001). Gastric cancer and Helicobacter pylori: a combined analysis of 12 case control studies nested within prospective cohorts. Gut *49*, 347–353.

Hellerbrand, C. (2013). Hepatic stellate cells--the pericytes in the liver. Pflüg. Arch. Eur. J. Physiol. *465*, 775–778.

Hemming, A.W., Reed, A.I., Howard, R.J., Fujita, S., Hochwald, S.N., Caridi, J.G., Hawkins, I.F., and Vauthey, J.-N. (2003). Preoperative Portal Vein Embolization for Extended Hepatectomy. Ann. Surg. *237*, 686–693.

Hendriks, H.F., Verhoofstad, W.A., Brouwer, A., de Leeuw, A.M., and Knook, D.L. (1985). Perisinusoidal fat-storing cells are the main vitamin A storage sites in rat liver. Exp. Cell Res. *160*, 138–149.

Herkel, J., Jagemann, B., Wiegard, C., Lazaro, J.F.G., Lueth, S., Kanzler, S., Blessing, M., Schmitt, E., and Lohse, A.W. (2003). MHC class II-expressing hepatocytes function as antigen-presenting cells and activate specific CD4 T lymphocyutes. Hepatol. Baltim. Md *37*, 1079–1085.

Hestdal, K., Ruscetti, F.W., Ihle, J.N., Jacobsen, S.E., Dubois, C.M., Kopp, W.C., Longo, D.L., and Keller, J.R. (1991). Characterization and regulation of RB6-8C5 antigen expression on murine bone marrow cells. J. Immunol. Baltim. Md 1950 *147*, 22–28.

Heuff, G., Oldenburg, H.S., Boutkan, H., Visser, J.J., Beelen, R.H., Van Rooijen, N., Dijkstra, C.D., and Meyer, S. (1993). Enhanced tumour growth in the rat liver after selective elimination of Kupffer cells. Cancer Immunol. Immunother. CII *37*, 125–130.

Hofmann, U.B., Westphal, J.R., Zendman, A.J., Becker, J.C., Ruiter, D.J., and van Muijen, G.N. (2000). Expression and activation of matrix metalloproteinase-2 (MMP-2) and its co-localization with membrane-type 1 matrix metalloproteinase (MT1-MMP) correlate with melanoma progression. J. Pathol. *191*, 245–256.

Holtmann, H., Winzen, R., Holland, P., Eickemeier, S., Hoffmann, E., Wallach, D., Malinin, N.L., Cooper, J.A., Resch, K., and Kracht, M. (1999). Induction of interleukin-8 synthesis integrates effects on transcription and mRNA degradation from at least three different cytokine- or stress-activated signal transduction pathways. Mol. Cell. Biol. *19*, 6742–6753.

Holz, L.E., Benseler, V., Bowen, D.G., Bouillet, P., Strasser, A., O'Reilly, L., d' Avigdor, W.M.H., Bishop, A.G., McCaughan, G.W., and Bertolino, P. (2008). Intrahepatic murine CD8 T-cell activation associates with a distinct phenotype leading to Bim-dependent death. Gastroenterology *135*, 989–997.

Houck, K.A., Ferrara, N., Winer, J., Cachianes, G., Li, B., and Leung, D.W. (1991). The vascular endothelial growth factor family: identification of a fourth molecular species and characterization of alternative splicing of RNA. Mol. Endocrinol. Baltim. Md *5*, 1806–1814.

Houck, K.A., Leung, D.W., Rowland, A.M., Winer, J., and Ferrara, N. (1992). Dual regulation of vascular endothelial growth factor bioavailability by genetic and proteolytic mechanisms. J. Biol. Chem. *267*, 26031–26037.

Huang, B., Lei, Z., Zhao, J., Gong, W., Liu, J., Chen, Z., Liu, Y., Li, D., Yuan, Y., Zhang, G.-M., et al. (2007). CCL2/CCR2 pathway mediates recruitment of myeloid suppressor cells to cancers. Cancer Lett. *252*, 86–92.

Huang, D.R., Wang, J., Kivisakk, P., Rollins, B.J., and Ransohoff, R.M. (2001). Absence of monocyte chemoattractant protein 1 in mice leads to decreased local macrophage recruitment and antigen-specific T helper cell type 1 immune response in experimental autoimmune encephalomyelitis. J. Exp. Med. *193*, 713–726.

Hudson, J.D., Shoaibi, M.A., Maestro, R., Carnero, A., Hannon, G.J., and Beach, D.H. (1999). A Proinflammatory Cytokine Inhibits P53 Tumor Suppressor Activity. J. Exp. Med. *190*, 1375–1382.

Huh, S.J., Liang, S., Sharma, A., Dong, C., and Robertson, G.P. (2010a). Transiently entrapped circulating tumor cells interact with neutrophils to facilitate lung metastasis development. Cancer Res. *70*, 6071–6082.

Huh, S.J., Liang, S., Sharma, A., Dong, C., and Robertson, G.P. (2010b). Transiently Entrapped Circulating Tumor Cells Interact with Neutrophils to Facilitate Lung Metastasis Development. Cancer Res. *70*, 6071–6082.

Hutti, J.E., Pfefferle, A.D., Russell, S.C., Sircar, M., Perou, C.M., and Baldwin, A.S. (2012). Oncogenic PI3K Mutations Lead to NF-κB–Dependent Cytokine Expression following Growth Factor Deprivation. Cancer Res. *72*, 3260–3269.

Ilie, M., Hofman, V., Ortholan, C., Bonnetaud, C., Coëlle, C., Mouroux, J., and Hofman, P. (2012). Predictive clinical outcome of the intratumoral CD66b-positive neutrophil-to-CD8-positive T-cell ratio in patients with resectable nonsmall cell lung cancer. Cancer *118*, 1726–1737.

Ilkovitch, D., and Lopez, D.M. (2009). The Liver Is a Site for Tumor-Induced Myeloid-Derived Suppressor Cell Accumulation and Immunosuppression. Cancer Res. *69*, 5514–5521.

Ilyas, M., Tomlinson, I.P.M., Rowan, A., Pignatelli, M., and Bodmer, W.F. (1997). ?-Catenin mutations in cell lines established from human colorectal cancers. Proc. Natl. Acad. Sci. U. S. A. *94*, 10330–10334.

Imai, K., Matsuyama, S., Miyake, S., Suga, K., and Nakachi, K. (2000). Natural cytotoxic activity of peripheral-blood lymphocytes and cancer incidence: an 11-year follow-up study of a general population. Lancet *356*, 1795–1799.

Iredale, J.P., Benyon, R.C., Pickering, J., McCullen, M., Northrop, M., Pawley, S., Hovell, C., and Arthur, M.J. (1998). Mechanisms of spontaneous resolution of rat liver fibrosis. Hepatic stellate cell apoptosis and reduced hepatic expression of metalloproteinase inhibitors. J. Clin. Invest. *102*, 538–549.

Ishai-Michaeli, R., Eldor, A., and Vlodavsky, I. (1990). Heparanase activity expressed by platelets, neutrophils, and lymphoma cells releases active fibroblast growth factor from extracellular matrix. Cell Regul. *1*, 833–842.

Ishak, K.G., Zimmerman, H.J., and Ray, M.B. (1991). Alcoholic liver disease: pathologic, pathogenetic and clinical aspects. Alcohol. Clin. Exp. Res. *15*, 45–66.

Itatani, Y., Kawada, K., Fujishita, T., Kakizaki, F., Hirai, H., Matsumoto, T., Iwamoto, M., Inamoto, S., Hatano, E., Hasegawa, S., et al. (2013). Loss of SMAD4 From Colorectal Cancer Cells Promotes CCL15 Expression to Recruit CCR1(+) Myeloid Cells and Facilitate Liver Metastasis. Gastroenterology *145*, 1064–1075.e11.

Ito, K., Govindarajan, A., Ito, H., and Fong, Y. (2010). Surgical treatment of hepatic colorectal metastasis: evolving role in the setting of improving systemic therapies and ablative treatments in the 21st century. Cancer J. Sudbury Mass *16*, 103–110.

Jablonska, J., Leschner, S., Westphal, K., Lienenklaus, S., and Weiss, S. (2010). Neutrophils responsive to endogenous IFN-beta regulate tumor angiogenesis and growth in a mouse tumor model. J. Clin. Invest. *120*, 1151–1164.

Jamieson, T., Clarke, M., Steele, C.W., Samuel, M.S., Neumann, J., Jung, A., Huels, D., Olson, M.F., Das, S., Nibbs, R.J.B., et al. (2012). Inhibition of CXCR2 profoundly suppresses inflammation-driven and spontaneous tumorigenesis. J. Clin. Invest. *122*, 3127–3144.

Jemal, A., Bray, F., Center, M.M., Ferlay, J., Ward, E., and Forman, D. (2011). Global cancer statistics. CA. Cancer J. Clin. *61*, 69–90.

Jia, T., Serbina, N.V., Brandl, K., Zhong, M.X., Leiner, I.M., Charo, I.F., and Pamer, E.G. (2008). Additive roles for MCP-1 and MCP-3 in CCR2-mediated recruitment of inflammatory monocytes during Listeria monocytogenes infection. J. Immunol. Baltim. Md 1950 *180*, 6846–6853.

Jones, S., Chen, W., Parmigiani, G., Diehl, F., Beerenwinkel, N., Antal, T., Traulsen, A., Nowak, M.A., Siegel, C., Velculescu, V.E., et al. (2008). Comparative lesion sequencing provides insights into tumor evolution. Proc. Natl. Acad. Sci. *105*, 4283–4288.

Ju, M.-J., Qiu, S.-J., Fan, J., Xiao, Y.-S., Gao, Q., Zhou, J., Li, Y.-W., and Tang, Z.-Y. (2009). Peritumoral activated hepatic stellate cells predict poor clinical outcome in hepatocellular carcinoma after curative resection. Am. J. Clin. Pathol. *131*, 498–510.

Kano, M.R., Morishita, Y., Iwata, C., Iwasaka, S., Watabe, T., Ouchi, Y., Miyazono, K., and Miyazawa, K. (2005). VEGF-A and FGF-2 synergistically promote neoangiogenesis through enhancement of endogenous PDGF-B–PDGFRβ signaling. J. Cell Sci. *118*, 3759–3768.

Kaplan, R.N., Riba, R.D., Zacharoulis, S., Bramley, A.H., Vincent, L., Costa, C., MacDonald, D.D., Jin, D.K., Shido, K., Kerns, S.A., et al. (2005). VEGFR1-positive haematopoietic bone marrow progenitors initiate the pre-metastatic niche. Nature *438*, 820–827.

Kärre, K., Ljunggren, H.G., Piontek, G., and Kiessling, R. (1986). Selective rejection of H-2-deficient lymphoma variants suggests alternative immune defence strategy. Nature *319*, 675–678.

Kasama, T., Kobayashi, K., Yajima, N., Shiozawa, F., Yoda, Y., Takeuchi, H.T., Mori, Y., Negishi, M., Ide, H., and Adachi, M. (2000). Expression of vascular endothelial growth factor by synovial fluid neutrophils in rheumatoid arthritis (RA). Clin. Exp. Immunol. *121*, 533–538.

Katoh, H., Wang, D., Daikoku, T., Sun, H., Dey, S.K., and DuBois, R.N. (2013). CXCR2-Expressing Myeloid-Derived Suppressor Cells Are Essential to Promote Colitis-Associated Tumorigenesis. Cancer Cell *24*, 631–644.

Katritch, V., Cherezov, V., and Stevens, R.C. (2012). Diversity and Modularity of G Protein-Coupled Receptor Structures. Trends Pharmacol. Sci. *33*, 17–27.

Kaufmann, A., Salentin, R., Gemsa, D., and Sprenger, H. (2001). Increase of CCR1 and CCR5 expression and enhanced functional response to MIP-1 alpha during differentiation of human monocytes to macrophages. J. Leukoc. Biol. *69*, 248–252.

Kelner, G.S., Kennedy, J., Bacon, K.B., Kleyensteuber, S., Largaespada, D.A., Jenkins, N.A., Copeland, N.G., Bazan, J.F., Moore, K.W., and Schall, T.J. (1994). Lymphotactin: a cytokine that represents a new class of chemokine. Science *266*, 1395–1399.

Khatib, A.-M., Fallavollita, L., Wancewicz, E.V., Monia, B.P., and Brodt, P. (2002). Inhibition of hepatic endothelial E-selectin expression by C-raf antisense oligonucleotides blocks colorectal carcinoma liver metastasis. Cancer Res. *62*, 5393–5398.

Khatib, A.-M., Auguste, P., Fallavollita, L., Wang, N., Samani, A., Kontogiannea, M., Meterissian, S., and Brodt, P. (2005). Characterization of the host proinflammatory response to tumor cells during the initial stages of liver metastasis. Am. J. Pathol. *167*, 749–759.

Kienast, Y., von Baumgarten, L., Fuhrmann, M., Klinkert, W.E.F., Goldbrunner, R., Herms, J., and Winkler, F. (2010). Real-time imaging reveals the single steps of brain metastasis formation. Nat. Med. *16*, 116–122.

Kim, H.K., De La Luz Sierra, M., Williams, C.K., Gulino, A.V., and Tosato, G. (2006). G-CSF down-regulation of CXCR4 expression identified as a mechanism for mobilization of myeloid cells. Blood *108*, 812–820.

Kinkel, K., Lu, Y., Both, M., Warren, R.S., and Thoeni, R.F. (2002). Detection of hepatic metastases from cancers of the gastrointestinal tract by using noninvasive imaging methods (US, CT, MR imaging, PET): a meta-analysis. Radiology *224*, 748–756.

Kinoshita, M., Uchida, T., Sato, A., Nakashima, M., Nakashima, H., Shono, S., Habu, Y., Miyazaki, H., Hiroi, S., and Seki, S. (2010). Characterization of two F4/80-positive Kupffer cell subsets by their function and phenotype in mice. J. Hepatol. *53*, 903–910.

Kitamura, T., Kometani, K., Hashida, H., Matsunaga, A., Miyoshi, H., Hosogi, H., Aoki, M., Oshima, M., Hattori, M., Takabayashi, A., et al. (2007). SMAD4-deficient intestinal tumors recruit CCR1+ myeloid cells that promote invasion. Nat. Genet. *39*, 467–475.

Kitamura, T., Fujishita, T., Loetscher, P., Revesz, L., Hashida, H., Kizaka-Kondoh, S., Aoki, M., and Taketo, M.M. (2010). Inactivation of chemokine (C-C motif) receptor 1 (CCR1) suppresses colon cancer liver metastasis by blocking accumulation of immature myeloid cells in a mouse model. Proc. Natl. Acad. Sci. *107*, 13063–13068.

Kleivi, K., Teixeira, M.R., Eknaes, M., Diep, C.B., Jakobsen, K.S., Hamelin, R., and Lothe, R.A. (2004). Genome signatures of colon carcinoma cell lines. Cancer Genet. Cytogenet. *155*, 119–131.

Kolaczkowska, E., and Kubes, P. (2013). Neutrophil recruitment and function in health and inflammation. Nat. Rev. Immunol. *13*, 159–175.

Kooby, D.A., Fong, Y., Suriawinata, A., Gonen, M., Allen, P.J., Klimstra, D.S., DeMatteo, R.P., D'Angelica, M., Blumgart, L.H., and Jarnagin, W.R. (2003). Impact of steatosis on perioperative outcome following hepatic resection. J. Gastrointest. Surg. Off. J. Soc. Surg. Aliment. Tract *7*, 1034–1044.

Kordes, C., Sawitza, I., Müller-Marbach, A., Ale-Agha, N., Keitel, V., Klonowski-Stumpe, H., and Häussinger, D. (2007). CD133+ hepatic stellate cells are progenitor cells. Biochem. Biophys. Res. Commun. *352*, 410–417.

Krag, S., Danielsen, C.C., Carmeliet, P., Nyengaard, J., and Wogensen, L. (2005). Plasminogen activator inhibitor-1 gene deficiency attenuates TGF-beta1-induced kidney disease. Kidney Int. *68*, 2651–2666.

Krzystek-Korpacka, M., Diakowska, D., Kapturkiewicz, B., Bębenek, M., and Gamian, A. (2013). Profiles of circulating inflammatory cytokines in colorectal cancer (CRC), high cancer risk conditions, and health are distinct. Possible implications for CRC screening and surveillance. Cancer Lett. *337*, 107–114.

Kuang, D.-M., Zhao, Q., Wu, Y., Peng, C., Wang, J., Xu, Z., Yin, X.-Y., and Zheng, L. (2011). Peritumoral neutrophils link inflammatory response to disease progression by fostering angiogenesis in hepatocellular carcinoma. J. Hepatol. *54*, 948–955.

Kuboki, S., Shin, T., Huber, N., Eismann, T., Galloway, E., Schuster, R., Blanchard, J., Edwards, M.J., and Lentsch, A.B. (2008). Hepatocyte signaling through CXC chemokine receptor-2 is detrimental to liver recovery after ischemia/reperfusion in mice. Hepatol. Baltim. Md *48*, 1213–1223.

Kumar, A., Sharma, P., and Sarin, S.K. (2008). Hepatic venous pressure gradient measurement: time to learn! Indian J. Gastroenterol. Off. J. Indian Soc. Gastroenterol. *27*, 74–80.

Kurihara, T., Warr, G., Loy, J., and Bravo, R. (1997). Defects in macrophage recruitment and host defense in mice lacking the CCR2 chemokine receptor. J. Exp. Med. *186*, 1757–1762.

Kusumanto, Y.H., Dam, W.A., Hospers, G.A.P., Meijer, C., and Mulder, N.H. (2003). Platelets and granulocytes, in particular the neutrophils, form important compartments for circulating vascular endothelial growth factor. Angiogenesis *6*, 283–287.

Lalor, P.F., Edwards, S., McNab, G., Salmi, M., Jalkanen, S., and Adams, D.H. (2002). Vascular adhesion protein-1 mediates adhesion and transmigration of lymphocytes on human hepatic endothelial cells. J. Immunol. Baltim. Md 1950 *169*, 983–992.

Lalor, P.F., Sun, P.J., Weston, C.J., Martin-Santos, A., Wakelam, M.J.O., and Adams, D.H. (2007). Activation of vascular adhesion protein-1 on liver endothelium results in an NF-kappaB-dependent increase in lymphocyte adhesion. Hepatol. Baltim. Md *45*, 465–474.

Lane, D.P. (1992). Cancer. p53, guardian of the genome. Nature *358*, 15–16.

Lautt, W. (2009). Hepatic Circulation: Physiology and Pathophysiology (Winnipeg: Morgan and Claypool Life Sciences).

Lee, B., Sharron, M., Montaner, L.J., Weissman, D., and Doms, R.W. (1999). Quantification of CD4, CCR5, and CXCR4 levels on lymphocyte subsets, dendritic cells, and differentially conditioned monocyte-derived macrophages. Proc. Natl. Acad. Sci. U. S. A. *96*, 5215–5220.

Lee, S., Jilani, S.M., Nikolova, G.V., Carpizo, D., and Iruela-Arispe, M.L. (2005). Processing of VEGF-A by matrix metalloproteinases regulates bioavailability and vascular patterning in tumors. J. Cell Biol. *169*, 681–691.

Levental, K.R., Yu, H., Kass, L., Lakins, J.N., Egeblad, M., Erler, J.T., Fong, S.F.T., Csiszar, K., Giaccia, A., Weninger, W., et al. (2009). Matrix Crosslinking Forces Tumor Progression by Enhancing Integrin Signaling. Cell *139*, 891–906.

Lévesque, J.-P., Hendy, J., Takamatsu, Y., Simmons, P.J., and Bendall, L.J. (2003). Disruption of the CXCR4/CXCL12 chemotactic interaction during hematopoietic stem cell mobilization induced by GCSF or cyclophosphamide. J. Clin. Invest. *111*, 187–196.

Liang, J., Piao, Y., Holmes, L., Fuller, G.N., Henry, V., Tiao, N., and Groot, J.F. de (2014). Neutrophils Promote the Malignant Glioma Phenotype through S100A4. Clin. Cancer Res. *20*, 187–198.

Liao, S., Bodmer, J., Pietras, D., Azhar, M., Doetschman, T., and Schultz, J.E.J. (2009). Biological Functions of the Low and High Molecular Weight Protein Isoforms of Fibroblast Growth Factor-2 in Cardiovascular Development and Disease. Dev. Dyn. Off. Publ. Am. Assoc. Anat. *238*, 249–264.

Lichtenstein, P., Holm, N.V., Verkasalo, P.K., Iliadou, A., Kaprio, J., Koskenvuo, M., Pukkala, E., Skytthe, A., and Hemminki, K. (2000). Environmental and heritable factors in the causation of cancer--analyses of cohorts of twins from Sweden, Denmark, and Finland. N. Engl. J. Med. *343*, 78–85.

Lin, E.Y., Nguyen, A.V., Russell, R.G., and Pollard, J.W. (2001). Colony-stimulating factor 1 promotes progression of mammary tumors to malignancy. J. Exp. Med. *193*, 727–740.

Liu, W., Tang, L., Zhang, G., Wei, H., Cui, Y., Guo, L., Gou, Z., Chen, X., Jiang, D., Zhu, Y., et al. (2004). Characterization of a novel C-type lectin-like gene, LSECtin: demonstration of carbohydrate binding and expression in sinusoidal endothelial cells of liver and lymph node. J. Biol. Chem. *279*, 18748–18758.

Loberg, R.D., Day, L.L., Harwood, J., Ying, C., St. John, L.N., Giles, R., Neeley, C.K., and Pienta, K.J. (2006). CCL2 is a Potent Regulator of Prostate Cancer Cell Migration and Proliferation. Neoplasia N. Y. N *8*, 578–586.

Loberg, R.D., Ying, C., Craig, M., Yan, L., Snyder, L.A., and Pienta, K.J. (2007). CCL2 as an Important Mediator of Prostate Cancer Growth In Vivo through the Regulation of Macrophage Infiltration. Neoplasia N. Y. N *9*, 556–562.

Lohse, A.W., Knolle, P.A., Bilo, K., Uhrig, A., Waldmann, C., Ibe, M., Schmitt, E., Gerken, G., and Meyer Zum Buschenfelde, K.H. (1996). Antigen-presenting function and B7 expression of murine sinusoidal endothelial cells and Kupffer cells. Gastroenterology *110*, 1175–1181.

Lu, R., Kujawski, M., Pan, H., and Shively, J.E. (2012). Tumor angiogenesis mediated by myeloid cells is negatively regulated by CEACAM1. Cancer Res. *72*, 2239–2250.

Lubetsky, J.B., Dios, A., Han, J., Aljabari, B., Ruzsicska, B., Mitchell, R., Lolis, E., and Al-Abed, Y. (2002). The tautomerase active site of macrophage migration inhibitory factor is a potential target for discovery of novel anti-inflammatory agents. J. Biol. Chem. *277*, 24976–24982.

Lue, H., Kapurniotu, A., Fingerle-Rowson, G., Roger, T., Leng, L., Thiele, M., Calandra, T., Bucala, R., and Bernhagen, J. (2006). Rapid and transient activation of the ERK MAPK signalling pathway by macrophage migration inhibitory factor (MIF) and dependence on JAB1/CSN5 and Src kinase activity. Cell. Signal. *18*, 688–703.

Lue, H., Thiele, M., Franz, J., Dahl, E., Speckgens, S., Leng, L., Fingerle-Rowson, G., Bucala, R., Lüscher, B., and Bernhagen, J. (2007). Macrophage migration inhibitory factor (MIF) promotes cell survival by activation of the Akt pathway and role for CSN5/JAB1 in the control of autocrine MIF activity. Oncogene *26*, 5046–5059.

Luo, J.-L., Maeda, S., Hsu, L.-C., Yagita, H., and Karin, M. (2004). Inhibition of NF-kappaB in cancer cells converts inflammation- induced tumor growth mediated by TNFalpha to TRAIL-mediated tumor regression. Cancer Cell *6*, 297–305.

Luzzi, K.J., MacDonald, I.C., Schmidt, E.E., Kerkvliet, N., Morris, V.L., Chambers, A.F., and Groom, A.C. (1998). Multistep Nature of Metastatic Inefficiency. Am. J. Pathol. *153*, 865–873.

Maccarana, M., Casu, B., and Lindahl, U. (1993). Minimal sequence in heparin/heparan sulfate required for binding of basic fibroblast growth factor. J. Biol. Chem. *268*, 23898–23905.

MacPhee, P.J., Schmidt, E.E., and Groom, A.C. (1995). Intermittence of blood flow in liver sinusoids, studied by high-resolution in vivo microscopy. Am. J. Physiol. *269*, G692–698.

Malka, D., Hammel, P., Maire, F., Rufat, P., Madeira, I., Pessione, F., Lévy, P., and Ruszniewski, P. (2002). Risk of pancreatic adenocarcinoma in chronic pancreatitis. Gut *51*, 849–852.

Malovic, I., Sørensen, K.K., Elvevold, K.H., Nedredal, G.I., Paulsen, S., Erofeev, A.V., Smedsrød, B.H., and McCourt, P.A.G. (2007). The mannose receptor on murine liver sinusoidal endothelial cells is the main denatured collagen clearance receptor. Hepatol. Baltim. Md *45*, 1454–1461.

Manfredi, S., Lepage, C., Hatem, C., Coatmeur, O., Faivre, J., and Bouvier, A.-M. (2006). Epidemiology and management of liver metastases from colorectal cancer. Ann. Surg. *244*, 254–259.

Mantke, R., Schmidt, U., Wolff, S., Kube, R., and Lippert, H. (2012). Incidence of synchronous liver metastases in patients with colorectal cancer in relationship to clinico-pathologic characteristics. Results of a German prospective multicentre observational study. Eur. J. Surg. Oncol. J. Eur. Soc. Surg. Oncol. Br. Assoc. Surg. Oncol. *38*, 259–265.

Mantovani, A., Sozzani, S., Locati, M., Allavena, P., and Sica, A. (2002). Macrophage polarization: tumor-associated macrophages as a paradigm for polarized M2 mononuclear phagocytes. Trends Immunol. *23*, 549–555.

Mantovani, A., Allavena, P., Sica, A., and Balkwill, F. (2008). Cancer-related inflammation. Nature *454*, 436–444.

Mantovani, A., Cassatella, M.A., Costantini, C., and Jaillon, S. (2011). Neutrophils in the activation and regulation of innate and adaptive immunity. Nat. Rev. Immunol. *11*, 519–531.

Marsh, L.M., Cakarova, L., Kwapiszewska, G., von Wulffen, W., Herold, S., Seeger, W., and Lohmeyer, J. (2009). Surface expression of CD74 by type II alveolar epithelial cells: a potential mechanism for macrophage migration inhibitory factor-induced epithelial repair. Am. J. Physiol. Lung Cell. Mol. Physiol. *296*, L442–452.

Martin, M.D., Kremers, G.-J., Short, K.W., Rocheleau, J.V., Xu, L., Piston, D.W., Matrisian, L.M., and Gorden, D.L. (2010). Rapid Extravasation and Establishment of Breast Cancer Micrometastases in the Liver Microenvironment. Mol. Cancer Res. *8*, 1319–1327.

Martín-Fontecha, A., Thomsen, L.L., Brett, S., Gerard, C., Lipp, M., Lanzavecchia, A., and Sallusto, F. (2004). Induced recruitment of NK cells to lymph nodes provides IFN-gamma for T(H)1 priming. Nat. Immunol. *5*, 1260–1265.

Martinez-Hernandez, A., and Martinez, J. (1991). The role of capillarization in hepatic failure: studies in carbon tetrachloride-induced cirrhosis. Hepatol. Baltim. Md *14*, 864–874.

Masi, G., Loupakis, F., Pollina, L., Vasile, E., Cupini, S., Ricci, S., Brunetti, I.M., Ferraldeschi, R., Naso, G., Filipponi, F., et al. (2009). Long-term outcome of initially unresectable metastatic colorectal cancer patients treated with 5-fluorouracil/leucovorin, oxaliplatin,

and irinotecan (FOLFOXIRI) followed by radical surgery of metastases. Ann. Surg. *249*, 420–425.

Matsushima, K., Larsen, C.G., DuBois, G.C., and Oppenheim, J.J. (1989). Purification and characterization of a novel monocyte chemotactic and activating factor produced by a human myelomonocytic cell line. J. Exp. Med. *169*, 1485–1490.

Matsusue, R., Kubo, H., Hisamori, S., Okoshi, K., Takagi, H., Hida, K., Nakano, K., Itami, A., Kawada, K., Nagayama, S., et al. (2009). Hepatic stellate cells promote liver metastasis of colon cancer cells by the action of SDF-1/CXCR4 axis. Ann. Surg. Oncol. *16*, 2645–2653.

Mauti, L.A., Le Bitoux, M.-A., Baumer, K., Stehle, J.-C., Golshayan, D., Provero, P., and Stamenkovic, I. (2011). Myeloid-derived suppressor cells are implicated in regulating permissiveness for tumor metastasis during mouse gestation. J. Clin. Invest. *121*, 2794–2807.

McCarty, S.M., and Percival, S.L. (2013). Proteases and Delayed Wound Healing. Adv. Wound Care *2*, 438–447.

McCourt, M., Wang, J.H., Sookhai, S., and Redmond, H.P. (1999). Proinflammatory mediators stimulate neutrophil-directed angiogenesis. Arch. Surg. Chic. Ill 1960 *134*, 1325–1331; discussion 1331–1332.

McMillan, R., and Scott, J.L. (1968). Leukocyte labeling with 51-Chromium. I. Technic and results in normal subjects. Blood *32*, 738–754.

Al-Mehdi, A.B., Tozawa, K., Fisher, A.B., Shientag, L., Lee, A., and Muschel, R.J. (2000). Intravascular origin of metastasis from the proliferation of endothelium-attached tumor cells: a new model for metastasis. Nat. Med. *6*, 100–102.

Mendoza, L., Olaso, E., Anasagasti, M.J., Fuentes, A.M., and Vidal-Vanaclocha, F. (1998). Mannose receptor-mediated endothelial cell activation contributes to B16 melanoma cell adhesion and metastasis in liver. J. Cell. Physiol. *174*, 322–330.

Mendoza, L., Carrascal, T., De Luca, M., Fuentes, A.M., Salado, C., Blanco, J., and Vidal-Vanaclocha, F. (2001). Hydrogen peroxide mediates vascular cell adhesion molecule-1 expression from interleukin-18–activated hepatic sinusoidal endothelium: Implications for circulating cancer cell arrest in the murine liver. Hepatology *34*, 298–310.

Mentzel, T., Brown, L.F., Dvorak, H.F., Kuhnen, C., Stiller, K.J., Katenkamp, D., and Fletcher, C.D. (2001). The association between tumour progression and vascularity in myxofibrosarcoma and myxoid/round cell liposarcoma. Virchows Arch. Int. J. Pathol. *438*, 13–22.

Mestdagt, M., Polette, M., Buttice, G., Noël, A., Ueda, A., Foidart, J.-M., and Gilles, C. (2006). Transactivation of MCP-1/CCL2 by beta-catenin/TCF-4 in human breast cancer cells. Int. J. Cancer J. Int. Cancer *118*, 35–42.

Meyer-Siegler, K.L., Iczkowski, K.A., Leng, L., Bucala, R., and Vera, P.L. (2006). Inhibition of macrophage migration inhibitory factor or its receptor (CD74) attenuates growth and invasion of DU-145 prostate cancer cells. J. Immunol. Baltim. Md 1950 *177*, 8730–8739.

Michaud, D.S. (2007). Chronic inflammation and bladder cancer. Urol. Oncol. *25*, 260–268.

Mitchell, R.A., Liao, H., Chesney, J., Fingerle-Rowson, G., Baugh, J., David, J., and Bucala, R. (2002). Macrophage migration inhibitory factor (MIF) sustains macrophage proinflammatory function by inhibiting p53: Regulatory role in the innate immune response. Proc. Natl. Acad. Sci. *99*, 345–350.

Moscatelli, D. (1987). High and low affinity binding sites for basic fibroblast growth factor on cultured cells: Absence of a role for low affinity binding in the stimulation of plasminogen activator production by bovine capillary endothelial cells. J. Cell. Physiol. *131*, 123–130.

Movahedi, K., Guilliams, M., Bossche, J.V. den, Bergh, R.V. den, Gysemans, C., Beschin, A., Baetselier, P.D., and Ginderachter, J.A.V. (2008). Identification of discrete tumor-induced myeloid-derived suppressor cell subpopulations with distinct T cell–suppressive activity. Blood *111*, 4233–4244.

Murdoch, C., Muthana, M., Coffelt, S.B., and Lewis, C.E. (2008). The role of myeloid cells in the promotion of tumour angiogenesis. Nat. Rev. Cancer *8*, 618–631.

Murphy, P.M., Baggiolini, M., Charo, I.F., Hébert, C.A., Horuk, R., Matsushima, K., Miller, L.H., Oppenheim, J.J., and Power, C.A. (2000). International Union of Pharmacology. XXII. Nomenclature for Chemokine Receptors. Pharmacol. Rev. *52*, 145–176.

Musso, O., Théret, N., Campion, J.P., Turlin, B., Milani, S., Grappone, C., and Clément, B. (1997). In situ detection of matrix metalloproteinase-2 (MMP2) and the metalloproteinase inhibitor TIMP2 transcripts in human primary hepatocellular carcinoma and in liver metastasis. J. Hepatol. *26*, 593–605.

Naglich, J.G., Metherall, J.E., Russell, D.W., and Eidels, L. (1992). Expression cloning of a diphtheria toxin receptor: identity with a heparin-binding EGF-like growth factor precursor. Cell *69*, 1051–1061.

Nielsen, B.S., Timshel, S., Kjeldsen, L., Sehested, M., Pyke, C., Borregaard, N., and Danø, K. (1996). 92 kDa type IV collagenase (MMP-9) is expressed in neutrophils and macrophages but not in malignant epithelial cells in human colon cancer. Int. J. Cancer J. Int. Cancer *65*, 57–62.

Niki, T., Pekny, M., Hellemans, K., Bleser, P.D., Berg, K.V., Vaeyens, F., Quartier, E., Schuit, F., and Geerts, A. (1999). Class VI intermediate filament protein nestin is induced during activation of rat hepatic stellate cells. Hepatol. Baltim. Md *29*, 520–527.

Nissen, L.J., Cao, R., Hedlund, E.-M., Wang, Z., Zhao, X., Wetterskog, D., Funa, K., Bråkenhielm, E., and Cao, Y. (2007). Angiogenic factors FGF2 and PDGF-BB synergistically promote murine tumor neovascularization and metastasis. J. Clin. Invest. *117*, 2766–2777.

Nozawa, H., Chiu, C., and Hanahan, D. (2006). Infiltrating neutrophils mediate the initial angiogenic switch in a mouse model of multistage carcinogenesis. Proc. Natl. Acad. Sci. U. S. A. *103*, 12493–12498.

Oh, C.K., Ariue, B., Alban, R.F., Shaw, B., and Cho, S.H. (2002). PAI-1 promotes extracellular matrix deposition in the airways of a murine asthma model. Biochem. Biophys. Res. Commun. *294*, 1155–1160.

Ohta, S., Misawa, A., Fukaya, R., Inoue, S., Kanemura, Y., Okano, H., Kawakami, Y., and Toda, M. (2012). Macrophage migration inhibitory factor (MIF) promotes cell survival and proliferation of neural stem/progenitor cells. J. Cell Sci. *125*, 3210–3220.

Okabe, H., Beppu, T., Hayashi, H., Ishiko, T., Masuda, T., Otao, R., Horlad, H., Jono, H., Ueda, M., Phd, S.S., et al. (2011). Hepatic stellate cells accelerate the malignant behavior of cholangiocarcinoma cells. Ann. Surg. Oncol. *18*, 1175–1184.

Okabe, H., Beppu, T., Ueda, M., Hayashi, H., Ishiko, T., Masuda, T., Otao, R., Horlad, H., Mima, K., Miyake, K., et al. (2012). Identification of CXCL5/ENA-78 as a factor involved in the interaction between cholangiocarcinoma cells and cancer-associated fibroblasts. Int. J. Cancer *131*, 2234–2241.

Olaso, E., Santisteban, A., Bidaurrazaga, J., Gressner, A.M., Rosenbaum, J., and Vidal-Vanaclocha, F. (1997). Tumor-dependent activation of rodent hepatic stellate cells during experimental melanoma metastasis. Hepatol. Baltim. Md *26*, 634–642.

Olaso, E., Salado, C., Egilegor, E., Gutierrez, V., Santisteban, A., Sancho-Bru, P., Friedman, S.L., and Vidal-Vanaclocha, F. (2003). Proangiogenic role of tumor-activated hepatic stellate cells in experimental melanoma metastasis. Hepatol. Baltim. Md *37*, 674–685.

Olson, T.S., and Ley, K. (2002). Chemokines and chemokine receptors in leukocyte trafficking. Am. J. Physiol. Regul. Integr. Comp. Physiol. *283*, R7–28.

Ouertatani-Sakouhi, H., El-Turk, F., Fauvet, B., Cho, M.-K., Pinar Karpinar, D., Le Roy, D., Dewor, M., Roger, T., Bernhagen, J., Calandra, T., et al. (2010). Identification and Characterization of Novel Classes of Macrophage Migration Inhibitory Factor (MIF) Inhibitors with Distinct Mechanisms of Action. J. Biol. Chem. *285*, 26581–26598.

Paget, S. (1889). THE DISTRIBUTION OF SECONDARY GROWTHS IN CANCER OF THE BREAST. The Lancet *133*, 571–573.

De Palma, M., Venneri, M.A., Galli, R., Sergi Sergi, L., Politi, L.S., Sampaolesi, M., and Naldini, L. (2005). Tie2 identifies a hematopoietic lineage of proangiogenic monocytes required for tumor vessel formation and a mesenchymal population of pericyte progenitors. Cancer Cell *8*, 211–226.

Park, J.E., Keller, G.A., and Ferrara, N. (1993). The vascular endothelial growth factor (VEGF) isoforms: differential deposition into the subepithelial extracellular matrix and bioactivity of extracellular matrix-bound VEGF. Mol. Biol. Cell *4*, 1317–1326.

Passlick, B., Flieger, D., and Ziegler-Heitbrock, H.W. (1989). Identification and characterization of a novel monocyte subpopulation in human peripheral blood. Blood *74*, 2527–2534.

Patel, D.D., Koopmann, W., Imai, T., Whichard, L.P., Yoshie, O., and Krangel, M.S. (2001). Chemokines have diverse abilities to form solid phase gradients. Clin. Immunol. Orlando Fla *99*, 43–52.

Pawlik, T.M., Olino, K., Gleisner, A.L., Torbenson, M., Schulick, R., and Choti, M.A. (2007). Preoperative chemotherapy for colorectal liver metastases: impact on hepatic histology and postoperative outcome. J. Gastrointest. Surg. Off. J. Soc. Surg. Aliment. Tract *11*, 860–868.

Pease, J.E., Wang, J., Ponath, P.D., and Murphy, P.M. (1998). The N-terminal extracellular segments of the chemokine receptors CCR1 and CCR3 are determinants for MIP-1alpha and eotaxin binding, respectively, but a second domain is essential for efficient receptor activation. J. Biol. Chem. *273*, 19972–19976.

Pedroza-Gonzalez, A., Verhoef, C., Ijzermans, J.N.M., Peppelenbosch, M.P., Kwekkeboom, J., Verheij, J., Janssen, H.L.A., and Sprengers, D. (2013). Activated tumor-infiltrating CD4+ regulatory T cells restrain antitumor immunity in patients with primary or metastatic liver cancer. Hepatol. Baltim. Md *57*, 183–194.

Penna, C., and Nordlinger, B. (2002). Surgery of liver metastases from colorectal cancer: new promises. Br. Med. Bull. *64*, 127–140.

Petrenko, O., Fingerle-Rowson, G., Peng, T., Mitchell, R.A., and Metz, C.N. (2003). MIF-deficiency is associated with altered cell growth and reduced susceptibility to Ras-mediated transformation. J. Biol. Chem.

Pienta, K.J., Machiels, J.-P., Schrijvers, D., Alekseev, B., Shkolnik, M., Crabb, S.J., Li, S., Seetharam, S., Puchalski, T.A., Takimoto, C., et al. (2013). Phase 2 study of carlumab (CNTO 888), a human monoclonal antibody against CC-chemokine ligand 2 (CCL2), in metastatic castration-resistant prostate cancer. Invest. New Drugs *31*, 760–768.

Piette, C., Deprez, M., Roger, T., Noël, A., Foidart, J.-M., and Munaut, C. (2009). The dexamethasone-induced inhibition of proliferation, migration, and invasion in glioma cell lines is antagonized by macrophage migration inhibitory factor (MIF) and can be enhanced by specific MIF inhibitors. J. Biol. Chem. *284*, 32483–32492.

Pinzani, M., Milani, S., De Franco, R., Grappone, C., Caligiuri, A., Gentilini, A., Tosti-Guerra, C., Maggi, M., Failli, P., Ruocco, C., et al. (1996). Endothelin 1 is overexpressed in human cirrhotic liver and exerts multiple effects on activated hepatic stellate cells. Gastroenterology *110*, 534–548.

Plotnikov, A.N., Schlessinger, J., Hubbard, S.R., and Mohammadi, M. (1999). Structural basis for FGF receptor dimerization and activation. Cell *98*, 641–650.

Pollard, J.W. (2004). Tumour-educated macrophages promote tumour progression and metastasis. Nat. Rev. Cancer *4*, 71–78.

Primrose, J.N. (2010). Surgery for colorectal liver metastases. Br. J. Cancer *102*, 1313–1318.

Proudfoot, A.E.I., Handel, T.M., Johnson, Z., Lau, E.K., LiWang, P., Clark-Lewis, I., Borlat, F., Wells, T.N.C., and Kosco-Vilbois, M.H. (2003). Glycosaminoglycan binding and oligomerization are essential for the in vivo activity of certain chemokines. Proc. Natl. Acad. Sci. *100*, 1885–1890.

Qian, B.-Z., Li, J., Zhang, H., Kitamura, T., Zhang, J., Campion, L.R., Kaiser, E.A., Snyder, L.A., and Pollard, J.W. (2011). CCL2 recruits inflammatory monocytes to facilitate breast tumor metastasis. Nature *475*, 222–225.

Randolph, G.J., Inaba, K., Robbiani, D.F., Steinman, R.M., and Muller, W.A. (1999). Differentiation of phagocytic monocytes into lymph node dendritic cells in vivo. Immunity *11*, 753–761.

Rao, H.-L., Chen, J.-W., Li, M., Xiao, Y.-B., Fu, J., Zeng, Y.-X., Cai, M.-Y., and Xie, D. (2012). Increased Intratumoral Neutrophil in Colorectal Carcinomas Correlates Closely with Malignant Phenotype and Predicts Patients' Adverse Prognosis. PLoS ONE *7*, e30806.

Rees, M., Tekkis, P.P., Welsh, F.K.S., O'Rourke, T., and John, T.G. (2008). Evaluation of Long-term Survival After Hepatic Resection for Metastatic Colorectal Cancer: A Multifactorial Model of 929 Patients. Ann. Surg. *247*, 125–135.

Reid, M.D., Basturk, O., Thirabanjasak, D., Hruban, R.H., Klimstra, D.S., Bagci, P., Altinel, D., and Adsay, V. (2011). Tumor-infiltrating neutrophils in pancreatic neoplasia. Mod. Pathol. Off. J. U. S. Can. Acad. Pathol. Inc *24*, 1612–1619.

Rodero, M.P., Auvynet, C., Poupel, L., Combadiere, B., and Combadiere, C. (2013). Control of Both Myeloid Cell Infiltration and Angiogenesis by CCR1 Promotes Liver Cancer Metastasis Development in Mice. Neoplasia N. Y. N *15*, 641–648.

Roomi, M.W., Monterrey, J.C., Kalinovsky, T., Rath, M., and Niedzwiecki, A. (2009). Patterns of MMP-2 and MMP-9 expression in human cancer cell lines. Oncol. Rep. *21*, 1323–1333.

Rushfeldt, C., Sveinbjørnsson, B., Seljelid, R., and Smedsrød, B. (1999). Early events of hepatic metastasis formation in mice: role of Kupffer and NK-cells in natural and interferon-gamma-stimulated defense. J. Surg. Res. *82*, 209–215.

Rutkauskas, S., Gedrimas, V., Pundzius, J., Barauskas, G., and Basevicius, A. (2006). Clinical and anatomical basis for the classification of the structural parts of liver. Med. Kaunas Lith. *42*, 98–106.

Ryan, G.R., Dai, X.M., Dominguez, M.G., Tong, W., Chuan, F., Chisholm, O., Russell, R.G., Pollard, J.W., and Stanley, E.R. (2001). Rescue of the colony-stimulating factor 1 (CSF-1)-nullizygous mouse (Csf1(op)/Csf1(op)) phenotype with a CSF-1 transgene and identification of sites of local CSF-1 synthesis. Blood *98*, 74–84.

Salcedo, R., Ponce, M.L., Young, H.A., Wasserman, K., Ward, J.M., Kleinman, H.K., Oppenheim, J.J., and Murphy, W.J. (2000). Human endothelial cells express CCR2 and respond to MCP-1: direct role of MCP-1 in angiogenesis and tumor progression. Blood *96*, 34–40.

Sandhu, S.K., Papadopoulos, K., Fong, P.C., Patnaik, A., Messiou, C., Olmos, D., Wang, G., Tromp, B.J., Puchalski, T.A., Balkwill, F., et al. (2013). A first-in-human, first-in-class, phase I study of carlumab (CNTO 888), a human monoclonal antibody against CC-chemokine ligand 2 in patients with solid tumors. Cancer Chemother. Pharmacol. *71*, 1041–1050.

Santos, L.L., Fan, H., Hall, P., Ngo, D., Mackay, C.R., Fingerle-Rowson, G., Bucala, R., Hickey, M.J., and Morand, E.F. (2011). Macrophage migration inhibitory factor regulates neutrophil chemotactic responses in inflammatory arthritis in mice. Arthritis Rheum. *63*, 960–970.

Sawitza, I., Kordes, C., Reister, S., and Häussinger, D. (2009). The niche of stellate cells within rat liver. Hepatol. Baltim. Md *50*, 1617–1624.

Scapini, P., Morini, M., Tecchio, C., Minghelli, S., Carlo, E.D., Tanghetti, E., Albini, A., Lowell, C., Berton, G., Noonan, D.M., et al. (2004). CXCL1/Macrophage Inflammatory Protein-2-Induced Angiogenesis In Vivo Is Mediated by Neutrophil-Derived Vascular Endothelial Growth Factor-A. J. Immunol. *172*, 5034–5040.

Scholten, D., Canals, M., Maussang, D., Roumen, L., Smit, M., Wijtmans, M., de Graaf, C., Vischer, H., and Leurs, R. (2012). Pharmacological modulation of chemokine receptor function. Br. J. Pharmacol. *165*, 1617–1643.

Scian, M.J., Stagliano, K.E.R., Anderson, M.A.E., Hassan, S., Bowman, M., Miles, M.F., Deb, S.P., and Deb, S. (2005). Tumor-derived p53 mutants induce NF-kappaB2 gene expression. Mol. Cell. Biol. *25*, 10097–10110.

Scoazec, J.Y., and Feldmann, G. (1991). In situ immunophenotyping study of endothelial cells of the human hepatic sinusoid: results and functional implications. Hepatol. Baltim. Md *14*, 789–797.

Serbina, N.V., and Pamer, E.G. (2006). Monocyte emigration from bone marrow during bacterial infection requires signals mediated by chemokine receptor CCR2. Nat. Immunol. *7*, 311–317.

Serbina, N.V., Jia, T., Hohl, T.M., and Pamer, E.G. (2008). Monocyte-mediated defense against microbial pathogens. Annu. Rev. Immunol. *26*, 421–452.

Shankaran, V., Ikeda, H., Bruce, A.T., White, J.M., Swanson, P.E., Old, L.J., and Schreiber, R.D. (2001). IFNgamma and lymphocytes prevent primary tumour development and shape tumour immunogenicity. Nature *410*, 1107–1111.

Shi, C., and Pamer, E.G. (2011). Monocyte recruitment during infection and inflammation. Nat. Rev. Immunol. *11*, 762–774.

Shimizu, S., Yamada, N., Sawada, T., Ikeda, K., Kawada, N., Seki, S., Kaneda, K., and Hirakawa, K. (2000). In vivo and in vitro interactions between human colon carcinoma cells and hepatic stellate cells. Jpn. J. Cancer Res. Gann *91*, 1285–1295.

Shkolnik, T., Livni, E., Reshef, R., Lachter, J., and Eidelman, S. (1987). Comparison of two lymphokines (macrophage migration inhibition, leukocyte adherence inhibition factors)

and carcinoembryonic antigen, in colorectal cancer and colonic premalignant lesions. Am. J. Gastroenterol. *82*, 1275–1278.

Shojaei, F., Wu, X., Malik, A.K., Zhong, C., Baldwin, M.E., Schanz, S., Fuh, G., Gerber, H.-P., and Ferrara, N. (2007). Tumor refractoriness to anti-VEGF treatment is mediated by CD11b+Gr1+ myeloid cells. Nat. Biotechnol. *25*, 911–920.

Shultz, L.D., Ishikawa, F., and Greiner, D.L. (2007). Humanized mice in translational biomedical research. Nat. Rev. Immunol. *7*, 118–130.

Sica, A., Larghi, P., Mancino, A., Rubino, L., Porta, C., Totaro, M.G., Rimoldi, M., Biswas, S.K., Allavena, P., and Mantovani, A. (2008a). Macrophage polarization in tumour progression. Semin. Cancer Biol. *18*, 349–355.

Sica, A., Larghi, P., Mancino, A., Rubino, L., Porta, C., Totaro, M.G., Rimoldi, M., Biswas, S.K., Allavena, P., and Mantovani, A. (2008b). Macrophage polarization in tumour progression. Semin. Cancer Biol. *18*, 349–355.

Siegel, R., DeSantis, C., Virgo, K., Stein, K., Mariotto, A., Smith, T., Cooper, D., Gansler, T., Lerro, C., Fedewa, S., et al. (2012). Cancer treatment and survivorship statistics, 2012. CA. Cancer J. Clin. *62*, 220–241.

Siveen, K.S., and Kuttan, G. (2009). Role of macrophages in tumour progression. Immunol. Lett. *123*, 97–102.

Smedsrød, B., De Bleser, P.J., Braet, F., Lovisetti, P., Vanderkerken, K., Wisse, E., and Geerts, A. (1994). Cell biology of liver endothelial and Kupffer cells. Gut *35*, 1509–1516.

Solaun, M.S., Mendoza, L., De Luca, M., Gutierrez, V., López, M.-P., Olaso, E., Lee Sim, B.K., and Vidal-Vanaclocha, F. (2002). Endostatin inhibits murine colon carcinoma sinusoidal-type metastases by preferential targeting of hepatic sinusoidal endothelium. Hepatol. Baltim. Md *35*, 1104–1116.

Sonoshita, M., Aoki, M., Fuwa, H., Aoki, K., Hosogi, H., Sakai, Y., Hashida, H., Takabayashi, A., Sasaki, M., Robine, S., et al. (2011). Suppression of colon cancer metastasis by Aes through inhibition of Notch signaling. Cancer Cell *19*, 125–137.

Sparmann, A., and Bar-Sagi, D. (2004). Ras-induced interleukin-8 expression plays a critical role in tumor growth and angiogenesis. Cancer Cell *6*, 447–458.

Spicer, J.D., McDonald, B., Cools-Lartigue, J.J., Chow, S.C., Giannias, B., Kubes, P., and Ferri, L.E. (2012). Neutrophils Promote Liver Metastasis via Mac-1–Mediated Interactions with Circulating Tumor Cells. Cancer Res. *72*, 3919–3927.

Spivak-Kroizman, T., Lemmon, M.A., Dikic, I., Ladbury, J.E., Pinchasi, D., Huang, J., Jaye, M., Crumley, G., Schlessinger, J., and Lax, I. (1994). Heparin-induced oligomerization of FGF molecules is responsible for FGF receptor dimerization, activation, and cell proliferation. Cell *79*, 1015–1024.

Stamatovic, S.M., Keep, R.F., Mostarica-Stojkovic, M., and Andjelkovic, A.V. (2006). CCL2 Regulates Angiogenesis via Activation of Ets-1 Transcription Factor. J. Immunol. *177*, 2651–2661.

Stangl, R., Altendorf-Hofmann, A., Charnley, R.M., and Scheele, J. (1994). Factors influencing the natural history of colorectal liver metastases. Lancet *343*, 1405–1410.

Starzl, T.E., Demetris, A.J., Trucco, M., Ramos, H., Zeevi, A., Rudert, W.A., Kocova, M., Ricordi, C., Ildstad, S., and Murase, N. (1992). Systemic chimerism in human female recipients of male livers. Lancet *340*, 876–877.

Steinbauer, M., Guba, M., Cernaianu, G., Köhl, G., Cetto, M., Kunz-Schughart, L.A., Geissler, E.K., Falk, W., and Jauch, K.-W. (2003). GFP-transfected tumor cells are useful in examining early metastasis in vivo, but immune reaction precludes long-term tumor development studies in immunocompetent mice. Clin. Exp. Metastasis *20*, 135–141.

Strieter, R.M., Polverini, P.J., Kunkel, S.L., Arenberg, D.A., Burdick, M.D., Kasper, J., Dzuiba, J., Damme, J.V., Walz, A., Marriott, D., et al. (1995). The Functional Role of the ELR Motif in CXC Chemokine-mediated Angiogenesis. J. Biol. Chem. *270*, 27348–27357.

Van Sweringen, H.L., Sakai, N., Quillin, R.C., Bailey, J., Schuster, R., Blanchard, J., Goetzman, H., Caldwell, C.C., Edwards, M.J., and Lentsch, A.B. (2013). Roles of hepatocyte and myeloid CXC chemokine receptor-2 in liver recovery and regeneration after ischemia/reperfusion in mice. Hepatol. Baltim. Md *57*, 331–338.

Swirski, F.K., Nahrendorf, M., Etzrodt, M., Wildgruber, M., Cortez-Retamozo, V., Panizzi, P., Figueiredo, J.-L., Kohler, R.H., Chudnovskiy, A., Waterman, P., et al. (2009). Identification of splenic reservoir monocytes and their deployment to inflammatory sites. Science *325*, 612–616.

Taichman, N.S., Young, S., Cruchley, A.T., Taylor, P., and Paleolog, E. (1997). Human neutrophils secrete vascular endothelial growth factor. J. Leukoc. Biol. *62*, 397–400.

Takada, A., Ohmori, K., Yoneda, T., Tsuyuoka, K., Hasegawa, A., Kiso, M., and Kannagi, R. (1993). Contribution of Carbohydrate Antigens Sialyl Lewis A and Sialyl Lewis X to Adhesion of Human Cancer Cells to Vascular Endothelium. Cancer Res. *53*, 354–361.

Takada, T., Toriyama, K., Muramatsu, H., Song, X.J., Torii, S., and Muramatsu, T. (1997). Midkine, a retinoic acid-inducible heparin-binding cytokine in inflammatory responses: chemotactic activity to neutrophils and association with inflammatory synovitis. J. Biochem. (Tokyo) *122*, 453–458.

Takeda, K., Hayakawa, Y., Smyth, M.J., Kayagaki, N., Yamaguchi, N., Kakuta, S., Iwakura, Y., Yagita, H., and Okumura, K. (2001). Involvement of tumor necrosis factor-related apoptosis-inducing ligand in surveillance of tumor metastasis by liver natural killer cells. Nat. Med. *7*, 94–100.

Taketo, M.M., and Edelmann, W. (2009). Mouse Models of Colon Cancer. Gastroenterology *136*, 780–798.

Tashiro, Y., Nishida, C., Sato-Kusubata, K., Ohki-Koizumi, M., Ishihara, M., Sato, A., Gritli, I., Komiyama, H., Sato, Y., Dan, T., et al. (2012). Inhibition of PAI-1 induces neutrophil-driven neoangiogenesis and promotes tissue regeneration via production of angiocrine factors in mice. Blood *119*, 6382–6393.

Tazzyman, S., Barry, S.T., Ashton, S., Wood, P., Blakey, D., Lewis, C.E., and Murdoch, C. (2011). Inhibition of neutrophil infiltration into A549 lung tumors in vitro and in vivo using a CXCR2-specific antagonist is associated with reduced tumor growth. Int. J. Cancer J. Int. Cancer *129*, 847–858.

Tazzyman, S., Niaz, H., and Murdoch, C. (2013). Neutrophil-mediated tumour angiogenesis: Subversion of immune responses to promote tumour growth. Semin. Cancer Biol. *23*, 149–158.

Theodoratou, E., Farrington, S.M., Tenesa, A., McNeill, G., Cetnarskyj, R., Korakakis, E., Din, F.V.N., Porteous, M.E., Dunlop, M.G., and Campbell, H. (2013). Associations between dietary and lifestyle risk factors and colorectal cancer in the Scottish population. Eur. J. Cancer Prev. Off. J. Eur. Cancer Prev. Organ. ECP.

Thomas, M.L. (1989). The Leukocyte Common Antigen Family. Annu. Rev. Immunol. *7*, 339–369.

Thomas, K.M., Taylor, L., and Navarro, J. (1991). The interleukin-8 receptor is encoded by a neutrophil-specific cDNA clone, F3R. J. Biol. Chem. *266*, 14839–14841.

Timmers, M., Vekemans, K., Vermijlen, D., Asosingh, K., Kuppen, P., Bouwens, L., Wisse, E., and Braet, F. (2004). Interactions between rat colon carcinoma cells and Kupffer cells during the onset of hepatic metastasis. Int. J. Cancer J. Int. Cancer *112*, 793–802.

Toh, B., Wang, X., Keeble, J., Sim, W.J., Khoo, K., Wong, W.-C., Kato, M., Prevost-Blondel, A., Thiery, J.-P., and Abastado, J.-P. (2011). Mesenchymal transition and dissemination of cancer cells is driven by myeloid-derived suppressor cells infiltrating the primary tumor. PLoS Biol. *9*, e1001162.

Tremblay, P.-L., Auger, F.A., and Huot, J. (2006). Regulation of transendothelial migration of colon cancer cells by E-selectin-mediated activation of p38 and ERK MAP kinases. Oncogene *25*, 6563–6573.

Tremblay, P.-L., Huot, J., and Auger, F.A. (2008). Mechanisms by which E-Selectin Regulates Diapedesis of Colon Cancer Cells under Flow Conditions. Cancer Res. *68*, 5167–5176.

Tsuji, K., Yamauchi, K., Yang, M., Jiang, P., Bouvet, M., Endo, H., Kanai, Y., Yamashita, K., Moossa, A.R., and Hoffman, R.M. (2006). Dual-color imaging of nuclear-cytoplasmic dynamics, viability, and proliferation of cancer cells in the portal vein area. Cancer Res. *66*, 303–306.

Ueda, A., Okuda, K., Ohno, S., Shirai, A., Igarashi, T., Matsunaga, K., Fukushima, J., Kawamoto, S., Ishigatsubo, Y., and Okubo, T. (1994). NF-kappa B and Sp1 regulate transcription of the human monocyte chemoattractant protein-1 gene. J. Immunol. *153*, 2052–2063.

Ugel, S., Peranzoni, E., Desantis, G., Chioda, M., Walter, S., Weinschenk, T., Ochando, J.C., Cabrelle, A., Mandruzzato, S., and Bronte, V. (2012). Immune tolerance to tumor antigens occurs in a specialized environment of the spleen. Cell Rep. *2*, 628–639.

University of Utah (2014). Liver Histology.

Vermeulen, P.B., Colpaert, C., Salgado, R., Royers, R., Hellemans, H., Van Den Heuvel, E., Goovaerts, G., Dirix, L.Y., and Van Marck, E. (2001). Liver metastases from colorectal adenocarcinomas grow in three patterns with different angiogenesis and desmoplasia. J. Pathol. *195*, 336–342.

Vidal-Vanaclocha, F. (2008). The Prometastatic Microenvironment of the Liver. Cancer Microenviron. *1*, 113–129.

Vidal-Vanaclocha, F., Alonso-Varona, A., Ayala, R., and Barberá-Guillem, E. (1990). Functional variations in liver tissue during the implantation process of metastatic tumour cells. Virchows Arch. A Pathol. Anat. Histopathol. *416*, 189–195.

Vidal-Vanaclocha, F., Fantuzzi, G., Mendoza, L., Fuentes, A.M., Anasagasti, M.J., Martín, J., Carrascal, T., Walsh, P., Reznikov, L.L., Kim, S.H., et al. (2000). IL-18 regulates IL-1beta-dependent hepatic melanoma metastasis via vascular cell adhesion molecule-1. Proc. Natl. Acad. Sci. U. S. A. *97*, 734–739.

Vlodavsky, I., Korner, G., Ishai-Michaeli, R., Bashkin, P., Bar-Shavit, R., and Fuks, Z. (1990). Extracellular matrix-resident growth factors and enzymes: possible involvement in tumor metastasis and angiogenesis. Cancer Metastasis Rev. *9*, 203–226.

Vollmar, B., and Menger, M.D. (2009). The hepatic microcirculation: mechanistic contributions and therapeutic targets in liver injury and repair. Physiol. Rev. *89*, 1269–1339.

Voskoboinik, I., Smyth, M.J., and Trapani, J.A. (2006). Perforin-mediated target-cell death and immune homeostasis. Nat. Rev. Immunol. *6*, 940–952.

Walsh, S.R., Cook, E.J., Goulder, F., Justin, T.A., and Keeling, N.J. (2005). Neutrophil-lymphocyte ratio as a prognostic factor in colorectal cancer. J. Surg. Oncol. *91*, 181–184.

Wang, H.H., McIntosh, A.R., Hasinoff, B.B., Rector, E.S., Ahmed, N., Nance, D.M., and Orr, F.W. (2000). B16 Melanoma Cell Arrest in the Mouse Liver Induces Nitric Oxide Release and Sinusoidal Cytotoxicity: A Natural Hepatic Defense against Metastasis. Cancer Res. *60*, 5862–5869.

Warren, A., Le Couteur, D.G., Fraser, R., Bowen, D.G., McCaughan, G.W., and Bertolino, P. (2006). T lymphocytes interact with hepatocytes through fenestrations in murine liver sinusoidal endothelial cells. Hepatol. Baltim. Md *44*, 1182–1190.

Watanabe, H., Miki, C., Okugawa, Y., Toiyama, Y., Inoue, Y., and Kusunoki, M. (2008). Decreased expression of monocyte chemoattractant protein-1 predicts poor prognosis following curative resection of colorectal cancer. Dis. Colon Rectum *51*, 1800–1805.

Webb, N.J., Myers, C.R., Watson, C.J., Bottomley, M.J., and Brenchley, P.E. (1998). Activated human neutrophils express vascular endothelial growth factor (VEGF). Cytokine *10*, 254–257.

Wein, A., Riedel, C., Köckerling, F., Martus, P., Baum, U., Brueckl, W.M., Reck, T., Ott, R., Hänsler, J., Bernatik, T., et al. (2001). Impact of surgery on survival in palliative patients with metastatic colorectal cancer after first line treatment with weekly 24-hour infusion of high-dose 5-fluorouracil and folinic acid. Ann. Oncol. Off. J. Eur. Soc. Med. Oncol. ESMO *12*, 1721–1727.

Wiegard, C., Wolint, P., Frenzel, C., Cheruti, U., Schmitt, E., Oxenius, A., Lohse, A.W., and Herkel, J. (2007). Defective T helper response of hepatocyte-stimulated CD4 T cells impairs antiviral CD8 response and viral clearance. Gastroenterology *133*, 2010–2018.

Wiktor-Jedrzejczak, W., and Gordon, S. (1996). Cytokine regulation of the macrophage (M phi) system studied using the colony stimulating factor-1-deficient op/op mouse. Physiol. Rev. *76*, 927–947.

Williams, D.L., Sherwood, E.R., McNamee, R.B., Jones, E.L., and Di Luzio, N.R. (1985). Therapeutic efficacy of glucan in a murine model of hepatic metastatic disease. Hepatol. Baltim. Md *5*, 198–206.

Wirtz, D., Konstantopoulos, K., and Searson, P.C. (2011). The physics of cancer: the role of physical interactions and mechanical forces in metastasis. Nat. Rev. Cancer *11*, 512–522.

Wisse, E. (1970). An electron microscopic study of the fenestrated endothelial lining of rat liver sinusoids. J. Ultrastruct. Res. *31*, 125–150.

Wisse, E., De Zanger, R.B., Jacobs, R., and McCuskey, R.S. (1983). Scanning electron microscope observations on the structure of portal veins, sinusoids and central veins in rat liver. Scan. Electron Microsc. 1441–1452.

Wolf, M.J., Hoos, A., Bauer, J., Boettcher, S., Knust, M., Weber, A., Simonavicius, N., Schneider, C., Lang, M., Stürzl, M., et al. (2012). Endothelial CCR2 signaling induced by colon carcinoma cells enables extravasation via the JAK2-Stat5 and p38MAPK pathway. Cancer Cell *22*, 91–105.

Wyckoff, J.B., Jones, J.G., Condeelis, J.S., and Segall, J.E. (2000). A Critical Step in Metastasis: In Vivo Analysis of Intravasation at the Primary Tumor. Cancer Res. *60*, 2504–2511.

Xiao, W.-K., Chen, D., Li, S.-Q., Fu, S.-J., Peng, B.-G., and Liang, L.-J. (2014). Prognostic significance of neutrophil-lymphocyte ratio in hepatocellular carcinoma: a meta-analysis. BMC Cancer *14*, 117.

Xu, L.-H., Cai, S.-J., Cai, G.-X., and Peng, W.-J. (2011). Imaging diagnosis of colorectal liver metastases. World J. Gastroenterol. WJG *17*, 4654–4659.

Xue, C., Wyckoff, J., Liang, F., Sidani, M., Violini, S., Tsai, K.-L., Zhang, Z.-Y., Sahai, E., Condeelis, J., and Segall, J.E. (2006). Epidermal Growth Factor Receptor Overexpression

Results in Increased Tumor Cell Motility In vivo Coordinately with Enhanced Intravasation and Metastasis. Cancer Res. *66*, 192–197.

Yan, Y., Rubinchik, S., Wood, A.L., Gillanders, W.E., Dong, J., Watson, D.K., and Cole, D.J. (2006). Bystander Effect Contributes to the Antitumor Efficacy of CaSm Antisense Gene Therapy in a Preclinical Model of Advanced Pancreatic Cancer. Mol. Ther. *13*, 357–365.

Yang, L., DeBusk, L.M., Fukuda, K., Fingleton, B., Green-Jarvis, B., Shyr, Y., Matrisian, L.M., Carbone, D.P., and Lin, P.C. (2004). Expansion of myeloid immune suppressor Gr+CD11b+ cells in tumor-bearing host directly promotes tumor angiogenesis. Cancer Cell *6*, 409–421.

Yang, L., Jung, Y., Omenetti, A., Witek, R.P., Choi, S., Vandongen, H.M., Huang, J., Alpini, G.D., and Diehl, A.M. (2008). Fate-mapping evidence that hepatic stellate cells are epithelial progenitors in adult mouse livers. Stem Cells Dayt. Ohio *26*, 2104–2113.

Yao, K., Shida, S., Selvakumaran, M., Zimmerman, R., Simon, E., Schick, J., Haas, N.B., Balke, M., Ross, H., Johnson, S.W., et al. (2005). Macrophage migration inhibitory factor is a determinant of hypoxia-induced apoptosis in colon cancer cell lines. Clin. Cancer Res. Off. J. Am. Assoc. Cancer Res. *11*, 7264–7272.

Yeudall, W.A., Vaughan, C.A., Miyazaki, H., Ramamoorthy, M., Choi, M.-Y., Chapman, C.G., Wang, H., Black, E., Bulysheva, A.A., Deb, S.P., et al. (2012). Gain-of-function mutant p53 upregulates CXC chemokines and enhances cell migration. Carcinogenesis *33*, 442–451.

Yoshidome, H., Kohno, H., Shida, T., Kimura, F., Shimizu, H., Ohtsuka, M., Nakatani, Y., and Miyazaki, M. (2009). Significance of monocyte chemoattractant protein-1 in angiogenesis and survival in colorectal liver metastases. Int. J. Oncol. *34*, 923–930.

Yoshimura, T., Matsushima, K., Tanaka, S., Robinson, E.A., Appella, E., Oppenheim, J.J., and Leonard, E.J. (1987). Purification of a human monocyte-derived neutrophil chemotactic factor that has peptide sequence similarity to other host defense cytokines. Proc. Natl. Acad. Sci. U. S. A. *84*, 9233–9237.

Zajac, E., Schweighofer, B., Kupriyanova, T.A., Juncker-Jensen, A., Minder, P., Quigley, J.P., and Deryugina, E.I. (2013). Angiogenic capacity of M1- and M2-polarized macrophages is determined by the levels of TIMP-1 complexed with their secreted proMMP-9. Blood *122*, 4054–4067.

Zamai, L., Ahmad, M., Bennett, I.M., Azzoni, L., Alnemri, E.S., and Perussia, B. (1998). Natural killer (NK) cell-mediated cytotoxicity: differential use of TRAIL and Fas ligand by immature and mature primary human NK cells. J. Exp. Med. *188*, 2375–2380.

Zcharia, E., Metzger, S., Chajek-Shaul, T., Aingorn, H., Elkin, M., Friedmann, Y., Weinstein, T., Li, J.-P., Lindahl, U., and Vlodavsky, I. (2004). Transgenic expression of mammalian heparanase uncovers physiological functions of heparan sulfate in tissue morphogenesis, vascularization, and feeding behavior. FASEB J. *18*, 252–263.

Zhang, Y., Davis, C., Ryan, J., Janney, C., and Peña, M.M.O. Development and characterization of a reliable mouse model of colorectal cancer metastasis to the liver. Clin. Exp. Metastasis 1–16.

Zhao, L., Lim, S.Y., Gordon-Weeks, A.N., Tapmeier, T.T., Im, J.H., Cao, Y., Beech, J., Allen, D., Smart, S., and Muschel, R.J. (2013). Recruitment of a myeloid cell subset (CD11b/Gr1 mid) via CCL2/CCR2 promotes the development of colorectal cancer liver metastasis. Hepatol. Baltim. Md *57*, 829–839.

Zhou, L.J., and Tedder, T.F. (1996). CD14+ blood monocytes can differentiate into functionally mature CD83+ dendritic cells. Proc. Natl. Acad. Sci. U. S. A. *93*, 2588–2592.

Zhou, S.-L., Dai, Z., Zhou, Z.-J., Wang, X.-Y., Yang, G.-H., Wang, Z., Huang, X.-W., Fan, J., and Zhou, J. (2012). Overexpression of CXCL5 mediates neutrophil infiltration and indicates poor prognosis for hepatocellular carcinoma. Hepatol. Baltim. Md *56*, 2242–2254.

Ziegler-Heitbrock, L., Ancuta, P., Crowe, S., Dalod, M., Grau, V., Hart, D.N., Leenen, P.J.M., Liu, Y.-J., MacPherson, G., Randolph, G.J., et al. (2010). Nomenclature of monocytes and dendritic cells in blood. Blood *116*, e74–80.

Zlotnik, A., and Yoshie, O. (2012). The Chemokine Superfamily Revisited. Immunity *36*, 705–716.

Zuo, Y., Ren, S., Wang, M., Liu, B., Yang, J., Kuai, X., Lin, C., Zhao, D., Tang, L., and He, F. (2013). Novel roles of liver sinusoidal endothelial cell lectin in colon carcinoma cell adhesion, migration and in-vivo metastasis to the liver. Gut *62*, 1169–1178.

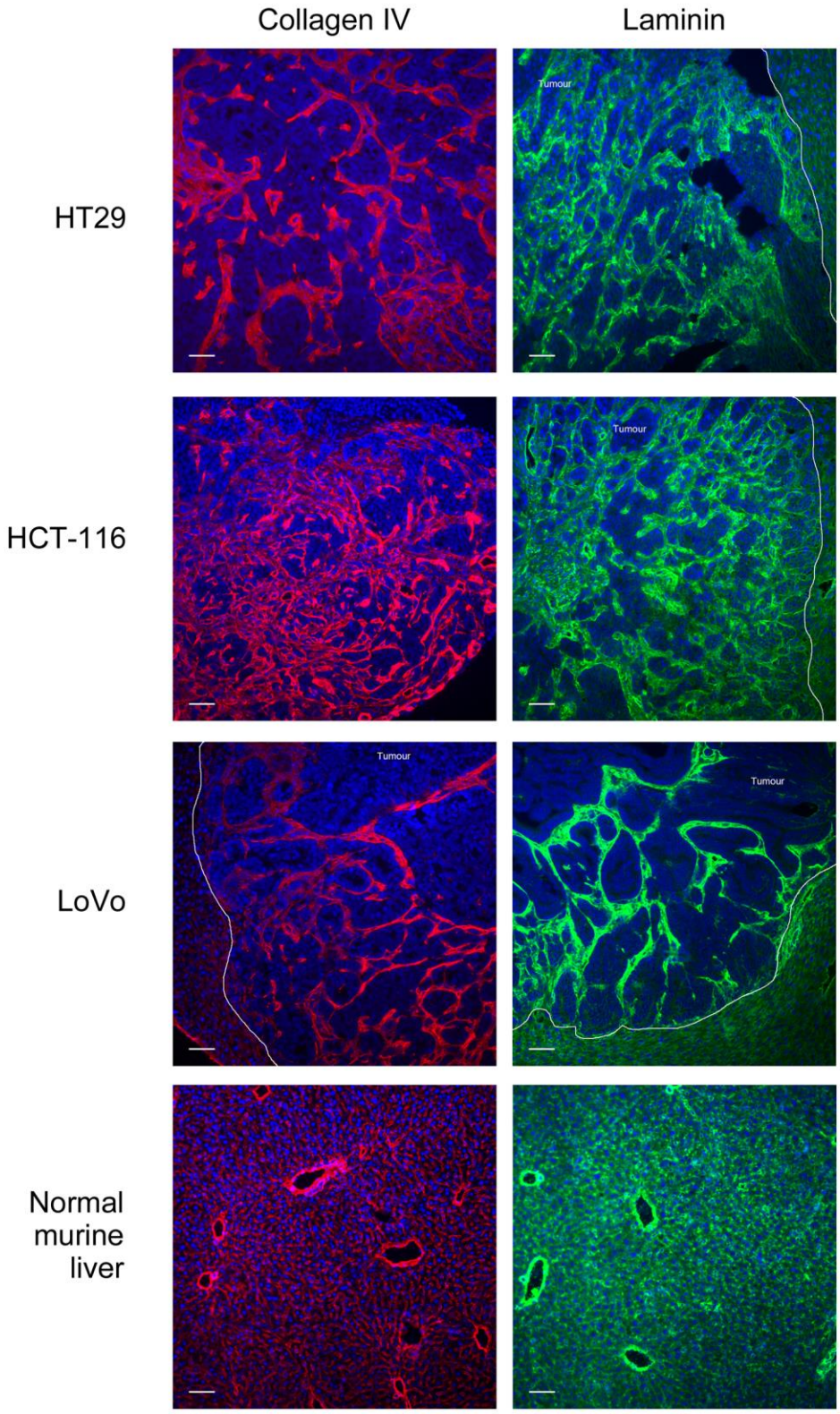

Supplementary Figure 5.11 ECM staining patterns in murine hepatic metastases

Immunolabeling performed for collagen IV (red) and laminin (green) with DAPI counterstaining in HT29, HCT-116 and LoVo metastases as well as normal SCID mouse liver.

The patterns demonstrated are similar to that shown for FGF2 staining in Fig. 5.11 suggesting that FGF2 resides in close association with key ECM proteins found within the tumour.